



Fell, Kate Charlotte (2022) Enhancing pharmaceutical micropollutant identification in biosolids through derivatisation and advanced chromatographic techniques. PhD thesis.

<https://theses.gla.ac.uk/83054/>

Copyright and moral rights for this work are retained by the author

A copy can be downloaded for personal non-commercial research or study, without prior permission or charge

This work cannot be reproduced or quoted extensively from without first obtaining permission in writing from the author

The content must not be changed in any way or sold commercially in any format or medium without the formal permission of the author

When referring to this work, full bibliographic details including the author, title, awarding institution and date of the thesis must be given

Enlighten: Theses

<https://theses.gla.ac.uk/>
research-enlighten@glasgow.ac.uk

ENHANCING PHARMACEUTICAL MICROPOLLUTANT IDENTIFICATION IN BIOSOLIDS THROUGH DERIVATISATION AND ADVANCED CHROMATOGRAPHIC TECHNIQUES

Kate Charlotte Fell

BSc Glasgow Caledonian University

MSc University of Strathclyde

SUBMITTED IN FULFILMENT OF THE REQUIREMENTS FOR THE DEGREE OF

Doctor of Philosophy

James Watt School of Engineering

College of Science and Engineering

University of Glasgow

SUBMITTED: FEBRUARY 2022

© Kate C. Fell 2022

Abstract

Pharmaceutical products (PhCs) are used to remedy illness, though the environmental impact of these PhCs after excretion, is something which many do not take into consideration. Wastewater treatment plants (WWTPs) were not designed to remove complex compounds like PhCs, and so PhCs are routinely detected in WWTP effluent, including sludge and biosolids. These are often applied to agricultural land to improve soil quality - introducing a diffuse route for PhCs into the environment – which has detrimental consequences on aquatic life. Thus, monitoring the PhC levels is advisable. This thesis describes the development of a suitable analysis method for detection of PhCs in complex biosolid matrices, which adheres to principles of Green Chemistry. Qualitative characterisation of non-spiked biosolid samples was implemented through ultrasound assisted sample preparation and gas chromatographic techniques. This research combines ultrasound assisted extraction and derivatisation with two-dimensional gas chromatography time of flight mass spectrometry (GCxGC-TOFMS). Optimisation of PhC derivatisation progressed through evaluation of the primary reaction mechanism in silylation: a nucleophilic substitution of the second order (S_N2) and applying the knowledge to experimental design. Silylation using 50 μ L of N-trimethylsilyl-N-methyltrifluoroacetamide (MSTFA), heated to 50°C for 40 mins was successful for derivatisation of several PhC compounds including carbamazepine and warfarin. Efficacy of silylation was dependant on the molar ratio of the reaction, with an increase in molar ratio increasing the desired derivative response (Le Chatelier's principle was observed). Competing reactions, when PhCs were derivatised in a mixture, was found to have a negative effect on derivative response. Implementation of ultrasound via a sonotrode was optimised using design of experiment and was found to significantly reduce extraction (5 mins) and derivatisation time (30s), reducing overall sample preparation time by 37%. A significant reduction (97%) in solvent consumption was observed in comparison to traditional methods though an increase in %RSD was observed, due to issues stability of TMS derivatives. The application of GCxGC for analysis of biosolid samples overcame issues with sensitivity and co-elution observed with one-dimensional GC, and matrix effects observed with LC-MS/MS. Derivatives of carbamazepine, ibuprofen, paracetamol, salicylic acid were detected in the non-spiked biosolid samples using GCxGC-TOFMS and LC-MS/MS, though triclosan was also detected when using the GC method. The optimised UAE-UAD-GCxGC-TOFMS and associated data processing was evaluated for the non-targeted characterisation of biosolid samples. The data processing method was deemed sufficient in terms of repeatability, robustness, and selectivity, though issues with sensitivity were observed. Regardless, differences between the three biosolid samples and between pellets of the same biosolid were observed. The optimised method aligns with Green Chemistry principles 'Prevention', 'Atom Economy', 'Safer Solvents and Auxiliaries' and 'Design for Energy Efficiency', making it a sustainable alternative to traditional analysis methods.

Table of Contents

| | |
|--|----|
| Abstract..... | 2 |
| Table of Contents..... | 3 |
| List of Tables..... | 7 |
| List of Figures..... | 9 |
| Acknowledgements..... | 16 |
| Declaration of originality..... | 17 |
| Abbreviations..... | 18 |
| Chapter 1: Introduction..... | 19 |
| 1.1 Background..... | 19 |
| 1.2 Research Aims and Objectives..... | 20 |
| 1.3 Thesis outline..... | 20 |
| Chapter 2: Literature Review..... | 22 |
| 2.1 Introduction..... | 22 |
| 2.2 Pharmaceutical Compounds..... | 22 |
| 2.2.1 Background..... | 22 |
| 2.2.2 Environmental Sources..... | 26 |
| 2.2.2.1 Point Sources..... | 26 |
| 2.2.2.2 Diffuse Sources..... | 28 |
| 2.2.3 Consequences..... | 28 |
| 2.2.4 Wastewater Treatment Plants (WWTPs)..... | 29 |
| 2.3 Analysis methods..... | 33 |
| 2.3.1 Targeted and Non-targeted..... | 33 |
| 2.3.2 Extraction Methods..... | 34 |
| 2.3.3 Separation Methods..... | 36 |
| 2.4 Derivatisation..... | 40 |
| 2.4.1 Methods..... | 40 |
| 2.5 Green Chemistry..... | 43 |
| 2.6 Conclusion..... | 45 |
| Chapter 3: Instrumental and Analytical Techniques..... | 46 |
| 3.1 Introduction..... | 46 |
| 3.2 Sample Preparation Techniques..... | 46 |
| 3.2.1 Ultrasonication (Sonication)..... | 46 |
| 3.2.2 Derivatisation..... | 50 |
| 3.3 Design of Experiments (DOE)..... | 61 |
| 3.3.1 Screening Test..... | 62 |

| | |
|--|-----|
| 3.3.2 Factorial Designs..... | 62 |
| 3.3.3 Response Surface Regression Design | 63 |
| 3.3.4 DOE Outputs..... | 64 |
| 3.3 Chromatographic Techniques | 67 |
| 3.3.1 Capillary Column Gas Chromatography..... | 68 |
| 3.3.2 Two-dimensional Comprehensive Gas Chromatography | 70 |
| 3.3.3 Liquid Chromatography | 74 |
| 3.3.4 Column Theory | 77 |
| 3.4 Mass Spectrometry Techniques | 82 |
| 3.4.1 Types of Ionisation..... | 82 |
| 3.4.2 Types of Mass Analyser..... | 87 |
| Chapter 4: Understanding and optimising conventional silylation for exhaustive derivatisation of pharmaceutical compounds..... | 92 |
| 4.1 Introduction..... | 92 |
| 4.1.1 Derivatisation of PhCs | 92 |
| 4.1.2 Silylation | 92 |
| 4.2 Methods..... | 96 |
| 4.2.1 Reagents | 96 |
| 4.2.2 Pharmaceutical Compound Selection | 96 |
| 4.2.3 Derivatisation..... | 97 |
| 4.2.4 Optimisation of Derivatisation..... | 98 |
| 4.2.5 Response Measurements for TMS derivatives..... | 100 |
| 4.2.6 GC-MS Analysis | 101 |
| 4.2.7 Software | 102 |
| 4.2.8 Statistics | 102 |
| 4.3 Results and Discussion | 103 |
| 4.3.1 Derivatisation..... | 103 |
| 4.3.2 Optimisation of Derivatisation..... | 106 |
| 4.4 Conclusions..... | 125 |
| Chapter 5: Investigation into the use of ultrasonication for the extraction and derivatisation of pharmaceutical compounds from biosolid samples | 127 |
| 5.1 Introduction..... | 127 |
| 5.1.1 Sonochemistry and Green Chemistry | 127 |
| 5.1.2 Optimised UAE methods for PhCs | 128 |
| 5.2 Methods..... | 130 |
| 5.2.1 Reagents | 130 |
| 5.2.2 Stock Solution Preparation..... | 130 |
| 5.2.3 Biosolid Sample Collection and Preparation | 130 |

| | |
|---|-----|
| 5.2.4 Sonotrode Device | 131 |
| 5.2.5 GC-MS Analysis | 132 |
| 5.2.6 Software | 133 |
| 5.2.7 Ultrasonic Assisted Extraction (UAE) Method Development | 133 |
| 5.2.8 Ultrasonic Assisted Derivatisation (UAD)..... | 136 |
| 5.2.9 Application to Biosolid Samples..... | 139 |
| 5.3. Results and Discussion | 140 |
| 5.3.1 Ultrasonic Assisted Extraction (UAE) Method Development | 140 |
| 5.3.2 Ultrasonic Assisted Derivatisation (UAD)..... | 146 |
| 5.3.3 Applicability to biosolid samples..... | 151 |
| 5.4 Conclusions..... | 154 |
| Chapter 6: Application of advanced chromatographic techniques in the non-targeted analysis of pharmaceutical compounds in biosolid samples | 156 |
| 6.1 Introduction..... | 156 |
| 6.1.1 Analysis Methods..... | 156 |
| 6.1.2 Data Processing Workflow | 157 |
| 6.2 Methods..... | 161 |
| 6.2.1 Reagents | 161 |
| 6.2.2 Stock Solution Preparation..... | 161 |
| 6.2.3 Biosolid Sample Collection and Preparation | 161 |
| 6.2.4 Extraction Procedure..... | 162 |
| 6.2.5 Derivatisation Procedure..... | 163 |
| 6.2.6 Pellets..... | 163 |
| 6.2.7 Analysis Methods..... | 163 |
| 6.2.8 Software | 165 |
| 6.3 Results and Discussion | 166 |
| 6.3.1 Comparison to Gold Standard (LC-MS/MS) method | 166 |
| 6.3.2 Translation from GC-MS to GCxGC-TOFMS | 168 |
| 6.3.3 Comparison of GCxGC-TOFMS vs LC-MS/MS | 172 |
| 6.4 Conclusion | 190 |
| Chapter 7: Conclusions and recommendations | 191 |
| 7.1 Restatement of Research Objectives..... | 191 |
| 7.1.1 Research Aims and Objectives | 191 |
| 7.2 Summary Details of Key Findings for Chapter 4 to Chapter 6..... | 191 |
| 7.2.1 Understanding and optimising conventional silylation for exhaustive derivatisation of pharmaceutical compounds..... | 191 |
| 7.2.2 Investigation into the use of ultrasonication for the extraction and derivatisation of pharmaceutical compounds from biosolid samples | 192 |

| | |
|---|-----|
| 7.2.3 Application of advanced chromatographic techniques in the non-targeted analysis of pharmaceutical compounds in biosolid samples | 192 |
| 7.3 Conclusions and Recommendations for Future Work | 192 |
| Appendix A – Chapter 3 | 196 |
| Appendix B – Chapter 4 | 197 |
| Appendix C – Chapter 5 | 202 |
| Appendix D – Chapter 6 | 204 |
| References..... | 209 |

List of Tables

| | |
|---|-----|
| Table 2-1: Pharmaceuticals grouped by Anatomical Therapeutic Class (ATC) 1st and 2nd Tier Classification defined by the World Health Organisation (WHO) (World Health Organisation, 2020) with examples. | 24 |
| Table 2-2: Derivatisation techniques: Acylation, Alkylation and Silylation: derivatisable functional groups and reagent examples | 42 |
| Table 2-3: Common mass spectral fragments after silylation, including diagnostic fragment ions, neutral losses and typical ion ratios by functional group (Lai & Fiehn, 2018)..... | 43 |
| Table 2-4: Anastas and Warner's 12 Principles of Green Chemistry (Anastas & Warner, 1998)..... | 44 |
| Table 3-1: Resolution Equation Terms: methods to increase resolution in LC and GC..... | 79 |
| Table 4-1: Optimal Derivatisation Temperatures and Times for the silylation of various PhCs found in literature. Optimal reagent indicated by an Asterix (*)..... | 94 |
| Table 4-2: Pharmaceutical compounds for spiked solutions: information on LogP, MW, and labile hydrogens..... | 97 |
| Table 4-3: Sample preparation and derivatisation procedure for all experimental work conducted in Chapter 4. Details include PhCs analysed, calculated millimolar concentrations for PhCs, derivatisation reagent volume and corresponding calculated molar ratio, and derivatisation protocol. Millimolar concentrations were calculated using JChem for excel. | 99 |
| Table 4-4: Determination of a statistically significant plateau for full paracetamol silylation: BSTFA + 1% TMCS and MSTFA (ANOVA analysis). All data satisfied all ANOVA criteria (see Appendix) | 109 |
| Table 4-5: Calculated molar ratios for MSTFA and BSTFA + 1% TMCS of four independent studies which compared silylation efficiencies of MSTFA and BSTFA + 1% TMCS on silylation of various of PhCs. Each study did not vary the volume of reagent used..... | 111 |
| Table 4-6: Average Rf responses (n=3) for five PhCs when silylated using the optimised DOE derivatisation method (50°C for 40mins). Comparison of individual PhCs vs PhCs in a mixture. %RSD highlighted in brackets..... | 125 |
| Table 5-1: DOE Fractional Factorial Design: Sonication Parameters (Pulse, Amplitude and Time) for optimisation of extraction. Each run represents a unique combination of factor levels. | 136 |
| Table 5-2: Definitive Screening Design for Ultrasonic Assisted Derivatization. Each run represents a unique combination of factor levels..... | 138 |
| Table 5-3: Face-centred (a=1) central composite design (CCD) parameters for response optimisation of the silylation of carbamazepine. | 139 |
| Table 5-4: Response factors for PhC peaks after each extraction stage (1-3). Response factors (Rf) declined rapidly with each extraction step. Overall percentage decrease for all PhCs was >79% which suggests that the PhC has nearly been fully extracted. | 142 |
| Table 5-5: Relative Extraction Recoveries for 5 PhCs extracted from 0.1 g, 0.5 g and 1 g ground biosolid samples. Recoveries calculated by spiking before and after extraction, and comparing. Average recoveries (n=6) detailed. RSD ranges calculated from SBE and SAE samples to give RSD range..... | 145 |
| Table 5-6: Absolutely recovery values for GC-MS method. Recovery calculated by dividing the SBE samples, by the PhC mix Standard and multiplying by 100. Lower recoveries suggest interference from matrix components..... | 146 |
| Table 6-1: Inclusion List: Retention times (mins), precursor and product ions (m/z) for the spiked PhCs – LC-MS/MS analysis | 164 |
| Table 6-2: PhCs detected by targeted LC-MS/MS in non-spiked and spiked biosolid samples. Dapsone was the only PhC not detected in the spiked samples. Those highlighted green are identified in the corresponding sample, and those highlighted red are not. Bio1 and Bio2 refer to the Biosolid | |

| | |
|---|-----|
| sample. NS = non-spiked, S = spiked with PhC mixture. PhC Std. refers to the standard mixture of PhCs. | 166 |
| Table 6-3: Calculated matrix effects for LC-MS/MS analysis of biosolids..... | 168 |
| Table 6-4: Comparison of analysis methods for identification of PhCs in non-spiked biosolid samples | 172 |
| Table 6-5: F-ratio threshold determination: Number of detected features and identified PhC features at varying F-ratio thresholds. | 176 |
| Table 6-6: Sensitivity analysis of ChromaTOF Tile software: non-spiked vs spiked biosolid samples | 183 |
| Table S8-1: Common loss fragments from a molecular ion - electron impact ionisation..... | 196 |
| Table S8-2: Common observed additions to molecular ions, forming adducts in ESI | 196 |
| Table S9-1: Calculation of dilution factor - worked example..... | 198 |
| Table S11-1: List of samples analysed in batch. Samples and order randomised on Minitab. | |
| Randomisation used to prevent bias. All samples analysed in duplicate. | 206 |

List of Figures

| | |
|---|----|
| Figure 2.1: Routes of PhCs into the environment – point sources and diffuse sources..... | 26 |
| Figure 2.2: Wastewater Treatment Plant Processes: From Raw Sewage to Discharge and Biosolid Formation. Adapted from (Britannica Encyclopedia, n.d.; Scottish Government, 2021)..... | 30 |
| Figure 2.3: Wastewater Treatment Plant Processes: From Sludge to Biosolids. Adapted from (Britannica Encyclopedia, n.d.; Scottish Government, 2021)..... | 31 |
| Figure 2.4: Oasis HLB sorbent (Waters Oasis Sample Extraction SPE Products : Waters, n.d.) used in extraction of PhCs from wastewater. The hydrophilic area retains polar analytes, and the lipophilic retains non-polar analytes, which increases the scope of the analysis (targeted analytes can differ in physicochemical properties) | 35 |
| Figure 2.5: Chromatographic methods for analysis of pharmaceutical compounds. Adapted from (Fatta et al., 2007; Kostopoulou & Nikolaou, 2008)..... | 40 |
| Figure 3.1: Cavitation process during ultrasonication: formation and growth of bubbles through compression and rarefaction cycles; before implosion. Adapted from (Hielscher, 2020b)..... | 47 |
| Figure 3.2: Instruments used to apply ultrasound to samples: a) sonication bath (Ultrasonic Baths, Elmasonic P Series, n.d.) b) probe (Hielscher, 2020c) c) sonotrode (Hielscher, 2020d)..... | 50 |
| Figure 3.3: Acylation Reaction mechanism, where Y = hetero atom (i.e., OH, NH, or SH), X = leaving group (CH ₃ etc.) and R = aliphatic or aromatic side group. | 51 |
| Figure 3.4: Alkylation Reaction Mechanism: Nucleophilic displacement (Knapp, 1979), where X is a halogen or good other leaving group and R and R1 are different aliphatic or aromatic side groups. A base catalyst is added to facilitate the reaction. | 52 |
| Figure 3.5: Esterification Reaction Mechanism adapted from (Halket & Zaikin, 2004), where R and R1 are different aliphatic or aromatic side groups. H ⁺ ions generated from a volatile acidic catalyst such as hydrochloric acid (HCl)..... | 53 |
| Figure 3.6: General single-step S _N 2-Si reaction mechanism for Silylation of compounds. Intermediate states (indicated by square brackets) for illustrative purposes only..... | 54 |
| Figure 3.7: Formation of the penta-covalent binds through p -> d bonding in the unoccupied 3d orbitals of the Si atom. The O atom of the nucleophile can be replaced with a N atom. Adapted from Pierce, 1968 (Pierce, 1968)..... | 54 |
| Figure 3.8: Silylation reaction mechanisms for a) examples for i) alcohols ii) carboxylic acids iii) primary amines iv) secondary amines and v) amide N vi) amide O, Y= sample, X = leaving group for example, Cl for trimethylchlorosilane (TMCS). Intermediates are for illustration only. Each reaction shows an S _N 2 backside attack of the TMCS by the functional group. Ease of silylation decreases from top to bottom. Adapted from (Knapp, 1979). | 55 |
| Figure 3.9: Stability of the carbocation. Stability increases with additional 'R' groups – from methyl group, to primary, secondary, and tertiary carbocations. Ease of silylation decreases from primary to tertiary groups, due to increased stability. | 56 |
| Figure 3.10: Silylation Reagent Structures: 1- HMDS, 2- TMCS, 3-TMSI, 4- BSA, 5- BSTFA, 6- MSTFA, 7- MTBSTFA | 57 |
| Figure 3.11: Resonance Structures: a) Amide - electrons oscillate between the nitrogen and oxygen atoms b) Carboxylic Acid – electrons oscillate between the two oxygen atoms c) Phenol – electrons oscillate between the oxygen and benzene ring | 58 |
| Figure 3.12: Effect of Steric Hindrance on nucleophilic attack of an electrophile. The same phenomenon is observed when the sterically hindered groups are attached to the nucleophile. | 59 |
| Figure 3.13: Factorial Designs where A, B and C are different factors. a) Two-factor design with two levels, b) Three-factor design with two levels c) Three-factor fractional factorial design (1/2) with 2 levels | 63 |

| | |
|---|----|
| Figure 3.14: Response Surface Regression Design a) Central Composite Design (CCD) points b) Face-centred CCD c) Box-Behnken design (BBD). Black = factorial points, red = axial points, green = mid-points and blue = centre points..... | 64 |
| Figure 3.15: Design of Experiment output: Example of a Pareto Chart (Minitab Inc, 2022). Factors are displayed as blue bars on the chart. Any factor which has a statistically significant effect (95% confidence limit) on the response (strength) will cross the red dashed line. In this example, each individual factor is significant, however the interactions between the factors are not. | 65 |
| Figure 3.16: Design of Experiment output: Example of an interaction plot. Interaction between oven temperature and oven time is observed. A lower % moisture is observed at 135°C when baked for 30 mins, instead of 60 mins. Although baking for 90 mins produced the lowest moisture content at all temperatures. Interaction was only visible between values for 30 and 60 mins. | 65 |
| Figure 3.17: Design of Experiment output: Example of a contour plot (Minitab Inc, 2019). Curved contours indicate statistically significant quadratic terms in the model. The response increases with increasing concentration and ratio, with the highest response indicated by the dark green colour. | 66 |
| Figure 3.18: Design of Experiment output: Example of an optimisation plot (Minitab Inc, 2021b). Flexibility and Strength are maximised with factor settings of Press: 95, Sealant = 75 and Machine = 2 – all are the high settings of the factors. | 67 |
| Figure 3.19: a) Basic schematic of a one-dimensional gas chromatography (GC) system b) schematic of a cross section of a capillary column phase to show the multiple coatings. Adapted from (de Zeeuw, 2017). Polyamide outer coating allows for column flexibility, with the stationary phase coated to the fused silica layer. c) column composition for a DB-5 column – (5%-phenyl)-methylpolysiloxane – change in percentage = different column stationary phase..... | 70 |
| Figure 3.20: Logical order of elution Reversed Phase GCxGC column set-up. For Normal Phase elution order, replace low with high etc..... | 71 |
| Figure 3.21: a) Basic GCxGC Set-up and illustration of the peak separation achieved by GCxGC. Adapted from (SepSolve Analytical, 2016) b) two-dimensional surface plot c) three-dimensional contour plot for b). | 72 |
| Figure 3.22: Modulation Process detailing the cryofocussing process a) Analyte (green) through the column b) Hot/cold node processes, blue represents cold pulse, and red, hot pulse..... | 73 |
| Figure 3.23: a) Schematic of a sorbent coated silica particle b) the basic structure of a siloxane group where the stationary phase will bond to and c) common R groups include cyano, C18 and diol used as the stationary phase - dependant on the column and analyte compound. | 75 |
| Figure 3.24: a) Resolution and Peak Separation (Shimadzu, 2020) b) Resolution Factor Plot (Sigma-Aldrich, 2007)..... | 78 |
| Figure 3.25: Combined Van Deemter Plots: a) Column Contributions b) Carrier Gas for GC where H = plate height and v = linear velocity of mobile phase (cm/sec) | 81 |
| Figure 3.26: Annotated Gas Chromatography Chromatogram Example. The chromatograms produced using LC are similar, as analytes will elute in order of affinity for the stationary phase, producing peaks. Column bleed is not as prevalent in LC. | 81 |
| Figure 3.27: Schematic of electron impact (EI) ionisation. Adapted from (Electron Impact - an Overview ScienceDirect Topics, n.d.) . Green balls represent the sample, blue balls represent electrons, and the red balls represent generated ions. The sample passes through the electron beam, where ions are generated..... | 83 |
| Figure 3.28: Electron Impact Ionisation - production of molecular ions, cations, and radicals..... | 83 |
| Figure 3.29: Ketoprofen a) NIST Library EI Mass Spectra b) Fragmentation of ketoprofen to produce the most abundant m/z ions depicted in the EI mass spectra | 85 |
| Figure 3.30: Schematic of an electrospray ionisation source; eluent enters the MS system through a capillary needle, where negative ions are trapped, and positive ions in solution create a Taylor cone at the tip of the needle, due to reduction in surface tension. The droplets reduce in size due to internal coulombic repulsion and evaporation until singular | 86 |

| | |
|--|-----|
| Figure 3.31: Schematic of Quadrupole Mass Analysers a) Single Quadrupole (adapted from (Argoti, 2008)) b) Triple Quadrupole running in SIM mode | 88 |
| Figure 3.32: Basic Schematic of Time of Flight (TOF) Mass Spectral Detector, adapted from LECO (Joseph, n.d.). Eluate is bombarded with electrons, forming ions which are pushed into the flight tube in packets by the push pulse plate. Ions drift through the tube at varying rates dependant on the kinetic energy and molecular size. Larger ions take longer to reach the detector. | 90 |
| Figure 3.33: Schematic of a Q-Exactive Orbitrap Mass Spectrometer. Adapted from (Thermo Fisher Scientific, 2016). | 91 |
| Figure 4.1: Chemical structure of the chosen compounds. 1: metronidazole, 2: sotalol, 3: atenolol, 4: paracetamol, 5: dapson, 6: salicylic acid, 7: warfarin, 8: carbamazepine, 9: clofibrilic acid, 10: ketoprofen, 11: ibuprofen, 12: diclofenac, 13: triclosan, 14: fluvastatin | 97 |
| Figure 4.2: Comparison of response factors (n=3) for each identified PhC (0.5 mg/mL) in three reconstitution solvents: ethyl acetate, dichloromethane, and acetonitrile. Generally, Rfs were lower for dichloromethane, whilst ethyl acetate and acetonitrile were similar. | 104 |
| Figure 4.3: Derivatised PhC Mix in EA (0.5 mg/mL) and Derivatised Sotalol in EA (0.5 mg/mL) chromatogram. Phenanthrene (0.05 mg/mL) used as the internal standard (RT – 15.782). Scouting method used to determine GC method and to ensure all PhCs were detected on the chromatogram in their derivatised form. Fluvastatin is the only compound not detected. | 106 |
| Figure 4.4: Silylation of Paracetamol by X-TMS. The phenol group undergoes silylation first, producing paracetamol mono-TMS. This molecule reacts with another X-TMS group, where the amide group is silylated on the oxygen atom, forming paracetamol di-TMS. Mono- and di-TMS mass spectra and fragmentation patterns are located in the Appendix. | 107 |
| Figure 4.5: Silylation of paracetamol to its mono- and di-TMS derivatives. Average log-transformed PAs of mono- and di-TMS derivatives by molar ratio of BSTFA + 1% TMCS and ratio of MSTFA: PhC active sites (0-1000:1). | 108 |
| Figure 4.6: Silylation of carbamazepine-to-carbamazepine mono-TMS. The addition of the TMS group causes steric hindrance which prevents a second reaction on the remaining labile hydrogen. Thus, no carbamazepine di-TMS can be formed. | 113 |
| Figure 4.7: Silylation of carbamazepine: Effect of varying Molar ratio (MSTFA: PhC active sites) on silylation of carbamazepine-to-carbamazepine mono-TMS. a) 1-10 μ L (32:1 – 317:1) Results for 32:1 are not shown, as carbamazepine mono-TMS was not produced. b) 10-120 μ L (317:1-3799:1). Results are shown in separate plots as preparation and analysis was conducted months apart – which may explain variance in response. | 114 |
| Figure 4.8: Boxplot of Molar Ratio vs Plateau Response (PA*DF) for 10-120 μ L (317-3979) MSTFA. – a difference in response is observed at the statistically significant plateau (P = 0.05) for the different molar ratios suggesting the silylation reaction has reached an equilibrium. Plateau responses were calculated from 5-35 mins for all molar ratios, except from 633 (20 μ L – 10-35 mins) and 1583 (50 μ L – 15-35 mins). | 116 |
| Figure 4.9: Example of competing reactions - all PhCs compete to react with MSTFA, to form different TMS derivatives | 117 |
| Figure 4.10: Example of competitive first order parallel reaction rates, where P, Q and R are PhCs and A, B and C are their respective TMS derivatives. | 117 |
| Figure 4.11: Parallel reaction: plot of [MSTFA], [A], [B] and [C] over time (s). Reaction P + MSTFA \rightarrow [A] is seen as the main reaction whilst Q + MSTFA \rightarrow [B] and R + MSTFA \rightarrow [C] as side reactions. | 118 |
| Figure 4.12: Effect of varying molar ratio (MSTFA: PhC*active sites) on a pharmaceutical mixture a) kinetics over time i) paracetamol di-TMS ii) carbamazepine mono-TMS iii) diclofenac mono-TMS iv) atenolol di-TMS. PAs were normalised by dividing by the dilution factor. | 119 |
| Figure 4.13: Boxplots highlighting the average PA*DF for each derivatised compound over a 90-minute time period with varying molar ratios. Paracetamol di-TMS, carbamazepine mono-TMS, diclofenac mono-TMS and atenolol di-TMS. | 120 |

| | |
|--|-----|
| Figure 4.14: Design of Experiment, Initial Factorial Design Results. Pareto Charts a) carbamazepine and b) carbamazepine mono-TMS. Addition of pyridine (μL) and silylation time (mins) are considered significant parameters in this reaction. Associated Main Effects Plots c) carbamazepine d) carbamazepine mono-TMS. Increasing all parameters was shown to increase carbamazepine mono-TMS response and decrease carbamazepine response. | 122 |
| Figure 4.15: Response optimisation of conventional parameters for the carbamazepine silylation reaction. Contour plots of a) CBZ and b) CBZ-TMS. Interaction plots of c) CB and d) CBZ-TMS. Response optimisation of both time and temperature. | 123 |
| Figure 4.16: Average Rf responses (n=3) for five PhCs silylated both individually and in a mixture using optimised method (40°C for 50 mins). | 125 |
| Figure 5.1: Martin et al. (Martín et al., 2010), HPLC-DAD chromatogram of a spiked compost sample. PhCs spiked at a concentration level of $300 \mu\text{g}/\text{kg}$. Although matrix effects were not discussed, it seems that matrix effects are likely to contribute. | 129 |
| Figure 5.2: UP200St Ultrasonic Probe VialTweeter and VialPress attachments: Vial positioned in the VialPress. a) sonication set-up, $300 \mu\text{L}$ glass crimp seal vial with large plastic adapter b) extraction set-up, 10 mL glass crimp seal vial, with fine plastic adapter | 132 |
| Figure 5.3: Optimisation of the Ultrasonic Assisted Extraction method. A flow chart highlighting the parameters which were optimised for efficient PhC extraction from biosolid samples using a UAE sonotrode device. | 134 |
| Figure 5.4: Flow chart for optimisation of UAD silylation using the sonicator. Parameter's amplitude, pulse and time optimised using design of experiment (DOE). | 137 |
| Figure 5.5: Flow chart of the optimised extraction and derivatisation method applied to biosolid samples. More details of volumes and sonication and centrifugation parameters can be found in section 5.2.3 Biosolid Sample Collection and Preparation. | 140 |
| Figure 5.6: Comparison of 1st to 3rd extracts to determine number of cycles. Chromatogram shown from 6.6 to 8.3 mins to highlight the derivatised PhC peaks in this region (salicylic acid di-TMS, clofibric acid mono-TMS, ibuprofen mono-TMS, and paracetamol di-TMS). Peak areas for 4 th extract were determined to be too small to justify another extraction step. Red = 1 st extract, Green = 2 nd extract, Blue = 3 rd extract. | 142 |
| Figure 5.7: DOE response interaction plots for responses a) ibuprofen mono-TMS b) triclosan mono-TMS and c) carbamazepine mono-TMS. Parameters analysed: pulse (40, 60, 80%), amplitude (40, 60, 80%) and time (5.0, 7.5, 10.0 mins). The slope of each line indicates the effect of the parameter on the response. A larger gradient suggests a greater response. Parallel lines suggest no interaction. | 143 |
| Figure 5.8: DOE response optimisation for UAE. Response of ibuprofen mono-TMS, Triclosan mono-TMS and carbamazepine mono-TMS. Optimal parameters determined to be 40% pulse, 80% amplitude for a 5-minute time-period. Composite desirability = 0.9743 suggesting the responses for all compounds have been maximised. | 144 |
| Figure 5.9: Pareto Charts for the standardised effects of the Definitive Screening Design of sonication parameters for the silylation of carbamazepine-to-carbamazepine mono-TMS. a) carbamazepine b) carbamazepine mono-TMS. The red line indicates the statistical significance threshold (p-value = 0.05). Statistically significant factors include the addition of pyridine (both) and the amplitude of the sonication wave (carbamazepine only). | 147 |
| Figure 5.10: Contour plot for Carbamazepine mono-TMS for the face-centred (a=1) central composite design. All parameters (pulse, amplitude, and time) are shown. Dark green areas show greatest Rf, which is optimal. | 148 |
| Figure 5.11: Response optimisation chart for the face-centred (a=1) central composite design. Carbamazepine mono-TMS response maximised, and carbamazepine response minimised. Optimal parameters are 60% amplitude, 40% pulse for 30 seconds. | 149 |
| Figure 5.12: Total ion chromatogram (TIC) overlay of non-spiked biosolid samples extracted using the optimised method from 1.0g of ground biosolids. A) ibuprofen mono-TMS, salicylic acid di-TMS, | |

| | |
|--|-----|
| and paracetamol di-TMS detected in all samples (n=3) B) carbamazepine mono-TMS peak identified in all samples..... | 152 |
| Figure 6.1: ChromaTOF Tile software: How it works a) Formation of Tiles on reference chromatogram, b) Tiles applied to all Chromatograms and compared. For the purpose of illustration, Tile sizes are much larger than appropriate for the chromatogram. Adapted from (LECO, 2020). ... | 158 |
| Figure 6.2: Feature intensity vs sample number at differing F-ratios. a) High F-ratio – large differences between classes b) small differences between classes c) Low F-ratio: small difference between class d) large difference between samples of same class. Adapted from (LECO, 2020). | 160 |
| Figure 6.3: Biosolid 1, Biosolid 2 and Biosolid 3 Pellets as collected. | 162 |
| Figure 6.4: Excluded Areas form Tile Analysis - D1:2600-4000, D2: 0-1.2s – highlighted by red area on the chromatogram. Exclusions prevent solvent peaks being included in the analysis. All targeted PhCs eluted within this time frame. | 165 |
| Figure 6.5: Heatmap of LC-MS/MS analysed non-spiked samples (n=6). Blank vs Biosolid 1 vs Biosolid 2. Colour indicates PhC peak detection, where dark green & red indicates increased detection. Sample blanks show no detected peaks, suggesting less contamination, in comparison to the Biosolid samples. Initial observations: Biosolid 2 is has less detected peaks than Biosolid 1. | 167 |
| Figure 6.6: Annotated GCxGC Chromatogram for derivatised PhC Standard in ethyl acetate. Detected derivatised PhC peaks numbered and identified using mass spectra. 1 – Salicylic acid di-TMS (1296, 1.815); 2- Clofibric acid mono-TMS (1428, 1.805); 3 – Paracetamol di-TMS (1436, 1.910); 4 – Ibuprofen mono-TMS (1468, 1.835); 5 – Metronidazole mono-TMS (1656, 1.615); 6 – Triclosan mono-TMS (2204, 1.795); 7 – Ketoprofen mono-TMS (2360, 1.680); 8 – Diclofenac mono-TMS (2460, 1.715); 9- carbamazepine mono-TMS (2536, 1.590); 10 – Phenanthrene (1984, 1.585). | 169 |
| Figure 6.7: Two-dimensional gas chromatogram illustrating the ‘roof-tile’ structured elution of siloxanes and fatty acids; and the separation of peaks which co-elute on one-dimensional GC. The second-dimension separation prevents co-elution of metronidazole mono-TMS and ketoprofen mono-TMS with dodecanoic acid mono-TMS and sebacic acid di-TMS, respectively..... | 170 |
| Figure 6.8: Comparison of spiked and non-spiked chromatograms for all biosolids – a) Biosolid 1 b) Biosolid 2 and c) Biosolid 3. Comparison made on total ion chromatogram (TIC) with the z-axis set to 100,000. | 171 |
| Figure 6.9: Comparison of spiked vs non-spiked Biosolid 1 samples for PhCs using extracted ion chromatograms (EIC) a) Ketoprofen mono-TMS (m/z 73) b) Diclofenac mono-TMS (m/z 367) and c) Salicylic acid di-TMS (m/z 267). Ions chosen from mass spectra (inset- NIST mass spectral database). | 171 |
| Figure 6.10: Phenanthrene peaks for three concentrations of PhC standards – little intra-class and inter-class difference. X = feature area and Y = sample number (2 replicates per sample) Tile parameters = F-ratio threshold 10; S/N threshold = 10, Tile Size = 3, 20. | 176 |
| Figure 6.11: Comparison of Pharmaceutical standards at three different concentrations - multivariate analysis and inter and intra-sample variation analysis. Tile Size = 3, 20, S/N ratio = 10, Fischer Ratio = 20. a) Scores plot b) loadings plot c) bar chart of all PhCs | 178 |
| Figure 6.12: Contour plots highlighting carbamazepine mono-TMS peaks (m/z 193) in all three PhC concentrations | 179 |
| Figure 6.13: Bar charts illustrating feature areas for features over an F-ratio range of 20-81. Differences in feature areas within samples from the same batch suggest variance is intra-batch and not inter-batch. Batch 1 = yellow, batch 2 = blue, batch 4 = red and batch 5 = green..... | 180 |
| Figure 6.14: Multivariate analysis of samples from different batches. Batch 1 is represented in yellow, batch 2 in blue, batch 4 in red and batch 5 in green. Principal component analysis (PCA) applied to log-transformed data with interferent features removed. Features with F-ratio threshold of 20. a) scores plot of all features b) loadings plot of all features | 181 |
| Figure 6.15: Partial least squares discriminant analysis (PLSDA) of log transformed Batch data. F-ratio threshold = 20. Interferent compounds removed. Batch 1 is represented in blue, batch 2 in orange, batch 4 in grey and batch 5 in green. | 182 |

| | |
|--|-----|
| Figure 6.16: PCA analysis for non-spiked vs spiked Biosolid 1 samples a) scores plot for F-ratio threshold 5 b) scores plot for F-ratio threshold 1. No grouping suggests little variance between the samples..... | 184 |
| Figure 6.17: Comparison of non-spiked (blue) and spiked (brown) samples for Identified PhCs in a) Biosolid 1 b) Biosolid 2 c) Biosolid 3 and d) Random Features from Biosolid 1, 2 and 3. F-ratio threshold of 1. Charts suggest intrasample variation attributes to the variance more than inter-sample variance..... | 185 |
| Figure 6.18: Homogeneity of Pellets - Biosolid 1: a) sPLSDA scores plot b) sPLSDA loadings plot | 186 |
| Figure 6.19: Homogeneity of Pellets – Biosolid 1: Bar charts describe inter-pellet variance. | 187 |
| Figure 6.20: Comparison of pellets from 3 different biosolid samples (n=6). sPLSDA score plot suggests variance between the Biosolid samples, and between pellets of the same sample..... | 188 |
| Figure 6.21: Comparison of Biosolids (Biosolid 1, 2 and 3) a) scores plot from PCA b) scores plot from sPLSDA c) bar charts for Feature 04871 (individual F-ratio = 29). | 189 |
| Figure S9.1: Vials used for GC derivatisation. a) 2ml GC vial b) 200µl vial insert and c) 300µl sonication vial (Thermo Fischer Scientific Inc., 2022)..... | 197 |
| Figure S9.2: Comparison of reconstitution solvents, with identified PhCs and RTs. A) full chromatogram, b) magnified chromatogram showing RT 9.5 to 18 mins. Ethyl acetate and dichloromethane had comparable results, whereas acetonitrile had consistently lower peak area ratios and incomplete silylation of diclofenac. Ethyl acetate was chosen as the reconstitution solvent, due to its increased performance and decreased toxicity when compared to dichloromethane..... | 198 |
| Figure S9.3: Peak areas for a) phenanthrene and b) paracetamol mono- and di-TMS derivatives for MSTFA vs BSTFA + 1% TMCS prior to log transformation. Peak areas were significantly lower for all peaks for BSTFA + 1% TMCS..... | 198 |
| Figure S9.4: Peak areas for a) phenanthrene and b) paracetamol mono- and di-TMS derivatives for MSTFA vs BSTFA + 1% TMCS after log transformation. Peak areas were similar and more appropriate for comparison. | 199 |
| Figure S9.5: Observed mass spectra and related fragmentation patterns for paracetamol a) mono-TMS and b) di-TMS. Fragmentation patterns determined by the mass spectrums. Beta-fragmentation for di-TMS suggesting silylation of the oxygen on the amide group, as reported by Caban and Stepnowski (Caban & Stepnowski, 2018). Characteristic ion at m/z 73 is highlighted in a) which corresponds to the trimethylsilyl (TMS) group. | 199 |
| Figure S9.6: Interval plot for ANOVA analysis of a) MSTFA and b) BSTFA + 1% TMCS. ANOVA concluded that a plateau was formed from 20µl for MSTFA and 150µl for BSTFA + 1% TMCS (n=3, p-value = 0.05)..... | 199 |
| Figure S9.7: Effect of pyridine on average PA for carbamazepine mono-TMS. 2-sample t-test (p-value = 0.000, n=6). W Pyr = with pyridine and wo Pyr = without pyridine. A clear statistically significant difference is observed between the two samples. | 200 |
| Figure S9.8: Warfarin mono-TMS. Chromatogram and MS (inset) for warfarin when analysed individually. Warfarin mono-silylates on the oxygen atom of the COOH. | 200 |
| Figure S9.9: Response Optimisation Chart for carbamazepine silylation. Software is programmed to generate the exact parameters (time and temperature) where the CBZ response is minimised and CBZ-TMS response is maximised. Optimal responses are 50oC for 39.39 mins..... | 201 |
| Figure S10.1: Biosolid Samples – top: biosolid pre- and post-grinding. bottom: L-R whole, partially ground and completely ground sample with apparatus (mortar and pestle) | 202 |
| Figure S10.2: Biosolid samples - extraction and reconstitution with optimised method. Reconstitution in 1ml of Ethyl Acetate..... | 202 |
| Figure S10.3: Sonotrode set-up. Top: Sonotrode operated in soundproof box, placed in a fume hood. Fume hood sash was fully down whilst in operation. Sonotrode controlled by the control panel (silver device to the LHS of photo). Bottom: Sonotrode device with a 10ml headspace vial attached in the VialPress. | 203 |

| | |
|--|-----|
| Figure S10.4: Two-sample t-test output for the comparison of optimised conventional oven and sonication methods. p-value = 0.262. No statistically significant difference observed. | 203 |
| Figure S11.1: Plot illustrating the multi-step gradient for LC-MS/MS analysis. Reversed phase analysis mode. A = acetonitrile and B = 10mmol ammonium formate adjusted to pH 3.5 with formic acid. | 204 |
| Figure S11.2: Total Ion Chromatograms and Extracted ion chromatograms (m/z 73) for blank ethyl acetate analysed before sample (left), and blank ethyl acetate analysed after a short (5 min) blank sample – analysed immediately after a biosolid sample (right). This shows that no carryover from the biosolid sample occurred, and that the short blank method was sufficient for between samples. | 204 |
| Figure S11.3: Measurement of first- and second-dimension peak width for optimal tile size calculation. Carbamazepine mono-TMS peak (2536s, 1.580s). | 205 |
| Figure 11.4: Ibuprofen mono-TMS in PhC standards. a) Feature area decreases from 1000-40 ug/L. b) MS for identified feature (top) which matches MS from NIST database (bottom) | 205 |
| Figure S11.5: MS obtained for the four features which PC1 and PC2 are based. | 207 |
| Figure S11.6: PCA scores plots for a) Biopellets 2 and b) Biopellets 3 – a clear difference is observed between biopellets of the same biosolid sample. This suggests pellets are not homogenous – thus it is recommended to combine numerous pellets and grind before extraction. | 208 |

Acknowledgements

First and foremost, I would like to express my deepest gratitude to my supervisor, Dr. Caroline Gauchotte-Lindsay, for her unwavering encouragement and support throughout my PhD. Her knowledge and guidance have been invaluable and paramount to the completion of this thesis. For this, I am eternally grateful.

I would also like to thank Dr. Ioannis Sampsonidis, Dr. Joanne Roberts, Dr. Mark Stillings and Dr. Laurie Savage for their time, expertise and help with this project. I gratefully acknowledge the EPSRC for funding this project, allowing me the opportunity to conduct this research. I give special thanks to Anne McGarrity, Julie Russell and technicians for their lab assistance and technical knowledge.

To my fellow PhD students, Celeste Felion, Anca Amariei, Melissa Moore and Dominic Quinn – thank you for the encouragement, help, support, and laughter. Without you all, I would have not made it this far. Sincerest thanks to Alexander Hamilton for his continuous advice, support, and encouragement, and for making my PhD journey an unforgettable and enjoyable experience.

This PhD would not have been possible without the help and support of so many people – to those I have not named individually, please know I am extremely grateful for your contributions to my achievements and research.

Finally, I am completely indebted to my family and friends for their unconditional love, support, patience, and encouragement throughout my studies. To my parents and grandparents, know all my achievements have been for you.

Declaration of originality

I certify that the thesis presented here for examination for a PhD degree of the University of Glasgow is solely my own work other than where I have clearly indicated that it is the work of others (in which case the extent of any work carried out jointly by me and any other person is clearly identified in it) and that the thesis has not been edited by a third party beyond what is permitted by the University's PGR Code of Practice.

The copyright of this thesis rests with the author. No quotation from it is permitted without full acknowledgement.

I declare that this thesis does not include work forming part of a these presented successfully for another degree.

I declare that this thesis has been produced in accordance with the University of Glasgow's Code of Good Practice in Research.

I acknowledge that if any issues are raised regarding good research practice based on review of this thesis, the examination may be postponed pending the outcome of any investigation of the issues.

Name: Kate Charlotte Fell

Registration Number: 2024026

Abbreviations

| <u>Instruments</u> | | <u>Theory</u> | |
|--------------------|---|---------------------|---------------------------------------|
| FID | Flame Ionisation Detector/Detection | ArOH | Aromatic Hydroxyl (Phenol) |
| GC | Gas Chromatography | CONH | Amide |
| GCxGC | 2D Comprehensive Gas Chromatography | COOH | Carboxylic acid |
| HLB | Hydrophilic-Lipophilic Balance | NH | Amine |
| HPLC | High Performance Liquid Chromatography | NSAIDs | Non-steroidal anti-inflammatory drugs |
| LC | Liquid Chromatography | OH | Hydroxyl |
| MCX | Strong Cation Exchange | PhC | Pharmaceutical Compound |
| MAX | Strong Anion Exchange | WWTPs | Wastewater Treatment Plants |
| MS | Mass Spectrometry | 1° | Primary |
| MS/MS | Tandem Mass Spectrometry | 2° | Secondary |
| SIM | Single Ion Monitoring | 3° | Tertiary |
| SPE | Solid Phase Extraction | | |
| TIC | Total Ion Chromatogram | | |
| TOF | Time of Flight | | |
| UAD | Ultrasonic Assisted Derivatisation | | |
| UAE | Ultrasonic Assisted Extraction | | |
| <u>Analysis</u> | | <u>Measurements</u> | |
| bis-TMS | two TMS groups added | a.m.u. | Atomic Mass Units |
| BSTFA | N, O-Bistrifluoroacetamide | b.p. | Boiling Point (°C) |
| CBE | Combined Before Extraction | Da | Daltons |
| di-TMS | two TMS groups added | F-ratio | Fischer Ratio |
| DCM | Dichloromethane | h | hours |
| DOE | Design of Experiments | i.d. | Internal Diameter |
| EA | Ethyl Acetate | kg | Kilogram |
| EC | Emerging Contaminants | L | Litre |
| EDTA | Ethylenediaminetetraacetic acid | LOD | Limit of Detection |
| HMDS | Hexamethyldisilazane | LOQ | Limit of Quantification |
| MeOH | Methanol | M | Molar/moles |
| MeCN | Acetonitrile | mg | Milligram |
| mono-TMS | one TMS group added | ml | Millilitre |
| MSTFA | N-methyl-N-(trimethylsilyl)trifluoroacetamide | mM | Millimolar/millimoles |
| PCA | Principal Component Analysis | MW | Molecular Weight |
| PLSDA | Partial Least Squares Discriminant Analysis | m/z | Mass to Charge ratio |
| Pyr | Pyridine | ng | Nanogram |
| tetra-TMS | four TMS groups added | RRF | Relative Response Factor |
| THF | Tetrahydrofuran | RT | Retention Time |
| TMCS | Trimethylchlorosilane | S/N | Signal to Noise Ratio |
| TMS | trimethylsilyl | µg | Microgram |
| tri-TMS | three TMS groups added | µl | Microlitre |

Chapter 1: Introduction

1.1 Background

Emerging pharmaceuticals (PhCs) are of particular concern to environmental scientists around the globe. The recalcitrant nature of PhCs, and the inadequate wastewater treatment plant processes, almost guarantees the presence of PhCs in treated wastewater and sludge. Biosolids are a product of sludge treatment, and pellets are often applied to land as an environmentally friendly alternative to fertiliser; thus, providing a route into the environment. The presence of PhCs in the environment has been attributed to detrimental consequences – including an increase in antimicrobial resistance - though, no regulations governing the release of PhCs into the environment have been imposed.

Robust and sensitive analytical methods are required to observe and identify PhCs in environmental matrices such as biosolids. Though many applied techniques generate high energy and solvent consumption, which does not align with the principles of Green Chemistry. The majority of studies apply a targeted approach to analysis, only identifying certain PhCs, and thus the full pharmaceutical load of the sample is not known.

To fully characterise environmental samples, the application of non-targeted analysis is required. Although studies have identified several pharmaceuticals in biosolids and sludge, the overall pharmaceutical load is unknown. The complex matrix contains a vast number of pharmaceuticals, coupled with the potentially toxic metabolites, transformation products and degradation compounds, which all contribute to environmental pollution, though may be missed with targeted analysis. In order to increase the removal efficacy of wastewater treatment plants (WWTPs), we must fully understand which PhCs remain after treatment. It is only then that the environmental impact of PhCs can be reduced. Therefore, an analysis method which can simultaneously extract and detect all potential problematic compounds is required. These findings would allow environmental analytical chemists to monitor the presence of PhCs in the environment and regulatory bodies (such as the Scottish Environmental Protection Agency) to regulate their release into the environment.

Due to the advancements in analytical instrumentation, and the recent increased interest in environmental conservation, the updated analytical method should fully characterise environmental samples, whilst additionally adhering to Green Chemistry principles. The development of such a method would advance the analysis of complex environmental matrices and reduce the environmental impact of the analyses.

The application of ultrasound has proven successful in a variety of sample preparation techniques, though the full capability of the technique has yet to be explored – particularly the use of a sonotrode device for ultrasound assisted extraction and derivatisation. The use of such techniques could potentially

overcome issues with energy and solvent consumption. For example, ultrasound facilitates inter-particle collisions, allowing for an increased rate of reaction. Additionally, the application of two-dimensional gas chromatography (GCxGC) coupled to time-of-flight mass spectrometry (TOFMS) for non-targeted analysis has been proven to be successful in a number of scientific fields including analysis of counterfeit food and drink, biomarker discovery and pesticide analysis. The use of this technique may overcome issues with sensitivity and co-elution found with traditional techniques. Indeed, GCxGC provides an increased peak capacity and resolving power compared to traditional GC methods allowing enhanced separation of complex mixtures such as coal tar.

Thus, the potential of these techniques will be measured through analysis of biosolid samples. Due to the complex matrix and the vast range of pharmaceutical compounds found in such samples, they are the ideal choice for testing the capabilities of the novel analytical methodology.

1.2 Research Aims and Objectives

The aim of this research is to investigate the use of ultrasonic assisted techniques and a two-dimensional gas chromatography method in the non-targeted characterisation of pharmaceuticals in biosolids, with respect to Green Chemistry principles. To achieve the aims of this project, the following objectives were identified:

- To evaluate and optimise a derivatisation method suitable for a range of pharmaceutical compounds.
- To develop and evaluate the novel use of a sonotrode device for optimal ultrasonic assisted extraction and derivatisation of pharmaceutical compounds in biosolid samples.
- To evaluate the use of a two-dimensional gas chromatography method compared with the ‘gold standard’ liquid chromatography method for analysis of pharmaceutical compounds in biosolids.
- To investigate the use of two-dimensional gas chromatography method with an associated data processing workflow for non-targeted characterisation of pharmaceuticals in biosolid samples.

1.3 Thesis outline

This thesis details the development of a novel analytical procedure for non-targeted analysis of pharmaceuticals in biosolid samples.

Chapter 2 introduces emerging environmental contaminants and the analytical methods used in their identification. Chapter 2 also presents a review of literature surrounding emerging pharmaceuticals in the environment. Lastly, an introduction to the 12 Principles of Green Chemistry is included.

Chapter 3 explains the theory behind the analytical techniques used in this thesis. The principles of sonication, derivatisation, gas chromatography, two-dimensional gas chromatography, liquid chromatography, and mass spectrometry are described in detail.

Chapter 4 presents the study of silylation of pharmaceutical compounds by one-dimensional gas chromatography analysis. The development and optimisation of an adequate derivatisation method for a range of pharmaceuticals is described and evaluated in terms of Green Chemistry and non-targeted analysis.

Chapter 5 presents the study of the ultrasonic assisted techniques in the extraction and derivatisation of pharmaceuticals from biosolid samples. The development and optimisation of a novel sample preparation method using a sonotrode device is detailed and evaluated.

Chapter 6 presents the validation of two-dimensional gas chromatography in the non-targeted characterisation of biosolid samples. A comparison is drawn between results obtained via one-dimensional gas chromatography, two-dimensional gas chromatography and liquid chromatography analysis, for the identification of targeted pharmaceuticals in the biosolid samples.

Finally, Chapter 7 summarises the major findings of this research, and highlights recommendations for further investigation.

Chapter 2: Literature Review

2.1 Introduction

Environmental pollution has been a problem since the industrial revolution. Contamination of air, water, and soil through urbanisation, exploration and population growth has produced a plethora of harmful effects (Ukaogo et al., 2020). Pollution is an ongoing world-wide problem; however, the adverse effects have reached the point at which pollution can no longer be ignored. This has inspired a global revolution – with activists such as Greta Thunberg and Extinction Rebellion leading the way. A war on environmental pollution has been triggered, with the intention to highlight the problem, overturn the effects, and generate legislature as a preventative measure. Pollution is often illustrated as clouds of smoke billowing from factories, large oil spills in oceans or rubbish lining seas and rural areas. Though not all pollution is visible to the naked eye – many environmental pollutants are small molecules, classed as emerging contaminants.

Emerging contaminants (ECs), or contaminants of emerging concern, are defined as naturally occurring or synthetic chemicals (Rosenfeld & Feng, 2011) which have the potential of entering the environment, causing known or suspected environmental damage, and detrimental ecological and human health effects (Dey et al., 2019). Despite the potential environmental harm, the majority of these compounds are not widely monitored at present. No regulations are imposed which govern their release into the environment. Studies have shown that ECs are persistent within the environment (Caban et al., 2015; Fatta et al., 2007; Huggett et al., 2003; Petrović et al., 2003; Prebihalo et al., 2015; Xu et al., 2015), leading to bioaccumulation and harmful environmental and health consequences (Frédéric & Yves, 2014). Over the last decade, many scientific studies have focussed on emerging contaminants, such as microplastics (Blair et al., 2019), personal care products (PCPs) (Biel-Maeso et al., 2019; Díaz & Peña-Alvarez, 2017; Li et al., 2021), and pharmaceutical compounds (Daughton & Ternes, 1999; McClellan & Halden, 2010; Rogowska et al., 2020; Walters et al., 2010), with regard to their prevalence within, and their impact on the environment. This thesis focuses on the pharmaceutical compounds, and thus, these will be described in more depth.

In this chapter, the route of pharmaceuticals into the environment, the consequences, and the previous research into emerging pharmaceuticals in wastewater, sludge and biosolid samples will be reviewed.

2.2 Pharmaceutical Compounds

2.2.1 Background

Natural sources including plants, herbs and fungi, were amongst the first source of therapeutic medication used to relieve pain prior to the production of the first synthetic drug (chloral hydrate) in the mid-nineteenth century (Jones, 2011). The word ‘drug’ itself is thought to be from the old French

word ‘*drouge*’ or Dutch word ‘*droog*’ – both referring to a barrel containing herbs (Jones, 2011). From the initial production of chloral hydrate for medicinal use in 1869 (Encyclopedia Britannica, 2020), the drug discovery, development and production of medicinal pharmaceuticals has rapidly increased into a billion dollar industry (Mikulic, 2021). Pharmaceutical drugs (PhCs) prescribed today have often been derived from natural sources, for example morphine from the opium poppy, quinine from the cinchona tree, digoxin from foxglove plants and aspirin from willow bark (Jones, 2011; Weatherall, 1990). Around 20,000 approved PhCs are available (U.S. Food and Drug Administration, 2021), though this number is ever-rising with over 3,000 new patented pharmaceuticals each year in the EU (Statista, 2022).

Today’s society generally relies on synthetic drugs to treat and/or cure ailments within the human body, yet do not think of the possible environmental consequences associated with their use. As PhCs were originally derived from natural sources, there may still be new drugs yet to be discovered. Therefore, it would seem counterproductive to allow the PhCs to cause harm to the very source from which they originated.

Therapeutic Classes

Pharmaceutical compounds are used to treat specific ailments dependant on their location within the body and thus PhCs can be split into different therapeutic classes. Each therapeutic class contains several individual compounds, which act to treat ailments within each class. Some PhCs can be found in more than one class, for example, aspirin is considered as an analgesic but also as an antiplatelet (NHS Digital, 2018) and prednisolone is considered an anti-inflammatory agent, an anti-hemorrhoidal, a corticosteroid, a dermatological, a decongestant, an ophthalmological, and an ontological drug (World Health Organisation, 2018). The number of therapeutic classes varies dependent on the governing body. The World Health Organization (WHO) use a classification system known as the Anatomical Therapeutic Chemical (ATC) classification system, which first classifies PhCs by 14 main anatomical or pharmacological groups (see Table 2-1), and then further by therapeutic and pharmacological subgroups (World Health Organisation, 2020).

Table 2-1: Pharmaceuticals grouped by Anatomical Therapeutic Class (ATC) 1st and 2nd Tier Classification defined by the World Health Organisation (WHO) (World Health Organisation, 2020) with examples.

| Group | ATC 1st Level Classification | Common Tier 2 Therapeutic Classes | Example |
|--------------|--|--|---|
| A | Alimentary tract and metabolism | Drugs for Acid Related Disorders Drugs used in constipation Drugs for Functional Gastrointestinal Disorders Drugs used in Diabetes Antiemetics and antinauseants Antidiarrheals, intestinal anti-inflammatory/anti-infective agents Vitamins | Famotidine Bisacodyl Metoclopramide Metformin Ondansetron Sulfasalazine Ascorbic Acid (Vitamin C) |
| B | Blood and blood forming organs | Antithrombotic Agents | Warfarin |
| C | Cardiovascular system | Cardiac Therapy Antihypertensives Diuretics Peripheral Vasodilators Beta blocking agents Calcium channel blockers Agents acting on the renin-angiotensin system Lipid Modifying Agents | Adenosine Doxazosin Torasemide Pentoxifylline Nadolol Verapamil Lisinopril Gemfibrozil |
| D | Dermatologicals | Antifungals for dermatological use Anti-acne preparations | Salicylic Acid Sulfacetamide |
| G | Genito urinary system and sex hormones | Sex hormones and modulators of the genital system Urologicals | Estrone Tamsulosin |
| H | Systemic hormonal preparations, excluding sex hormones and insulin | Corticosteroids for systemic use | Prednisolone |
| J | Anti-infective for systemic use | Anti-bacterials for systemic use | Cloxacillin |
| L | Antineoplastic and immunomodulating agents | Anti-mycobacterials Antineoplastic agents | Dapsone Ifosfamide |
| M | Musculo-skeletal system | Endocrine therapy Anti-inflammatory and antirheumatic products Drugs for treatment of bone diseases | Tamoxifen Ibuprofen Alendronic Acid |
| N | Nervous system | Anaesthetics Analgesics Antiepileptics Psycholeptics Psychoanaleptics | Lidocaine Acetaminophen Carbamazepine Lorazepam Fluoxetine |
| P | Antiparasitic products, insecticides, and repellents | Antiprotozoals | Metronidazole |
| R | Respiratory system | Anthelmintics Drugs for obstructive airway diseases Antihistamines for systemic use Nasal Preparations | Levamisole Clenbuterol Loratadine Pseudoephedrine |
| S | Sensory organs | Ophthalmologicals | Idoxuridine |
| V | Various | Contrast Media Diagnostic Agents | Iopromide Folic Acid |

Dosage, metabolism, and excretion

Pharmaceuticals are taken in everyday life to treat a variety of ailments and to prevent diseases. Dosage is dependent on the PhC drug, and the severity of the illness, with over-the-counter medication generally less potent than prescribed medication. Analgesics paracetamol and ibuprofen are routinely administered to treat mild headaches or symptoms of a common cold. An average dose for an adult is 1000 mg paracetamol (NHS Inform, 2021b) and 400 mg ibuprofen (NHS Inform, 2021a), taken up to 4 times a day. Administered orally, the active pharmaceutical ingredients (APIs) in both paracetamol and ibuprofen are thought to inhibit cyclooxygenase (COX) pathways (Gerriets et al., 2021; Rao & Knaus, 2008), reducing pain before undergoing metabolism for excretion. Metabolism aids in excretion by converting the APIs to the more hydrophilic metabolites through various metabolic pathways, which are more easily excreted. PhCs are generally excreted as metabolites in faeces and urine, however a portion is excreted unchanged, as the parent PhC. The proportion excreted in faeces and urine is PhC compound dependant. Only 15% of an average dose of ibuprofen is excreted as the unchanged API, with the remainder excreted as various metabolites (Farré et al., 2008). Similarly, around 95% of a paracetamol dose is excreted as metabolites (Meredith & Goulding, 1980). In contrast, beta-blockers atenolol and sotalol are excreted mostly as the API. Atenolol undergoes very little metabolism with 90% of an average dose excreted as the parent compound, around 50% of this excreted in faeces (Drugbank, 2005a; Kirch & Görg, 1982). Sotalol is excreted entirely as the parent compound primarily in urine (Bayer HealthCare Pharmaceuticals Inc., 2011; Drugbank, 2005b), as no metabolism takes place. The mass use of pharmaceuticals coupled with the incomplete human metabolism is thought to contribute to the abundance of PhCs and their metabolites in wastewater (Kummerer, 2010; Li, 2014).

Pharmaceutical Physicochemical Properties

Excretion is highly dependent on the physicochemical properties of the PhC. Molecular weight (MW), structure and number of ionisable functional groups all contribute, though polarity has the greatest influence on the route of excretion.

Polarity in the context of the thesis refers to the lipophilic or hydrophilic nature of a PhC compound; and is defined by the partition co-efficient. The partition coefficient (P) describes the distribution of a solute in a system with two immiscible solvents (Bannan et al., 2016), an organic phase (generally 1-octanol) and an aqueous phase (Tetko & Livingstone, 2007). The ratio (P) is calculated using equation (I-1) though is generally reported as the logarithm of the ratio (LogP).

$$P = \frac{[solute]_{ORGANIC}}{[solute]_{AQUEOUS}} \quad (I-1)$$

A high LogP indicates a more lipophilic (non-polar) compound, and a low LogP indicates a more hydrophilic (polar) compound. Pharmaceutical compounds tend to be more hydrophilic in nature, as most oral drugs are designed to be excreted through urine (abiding by Lipinski's rule of 5) (Leeson,

2016). Lipinski states that a partition coefficient (LogP) <5 is required to aid in absorption (Lipinski et al., 1997), and can influence the route of excretion (Leeson, 2016).

Additionally, the LogP influences the distribution of PhCs in wastewater treatment plants (WWTPs) (see 2.2.4 Wastewater Treatment Plants (WWTPs)). PhCs with a LogP of 2.5 or greater tend to bind to sediment, whereas those with a $\text{LogP} <2.5$ are likely to remain in the wastewater (Li, 2014). For example, acidic non-steroidal anti-inflammatory drugs (NSAIDs, e.g., paracetamol, $\text{LogP} = 0.91$) are highly polar, mostly remaining in the water media (Kuster et al., 2008), whereas more basic PhCs such as antiepileptics (e.g., carbamazepine, $\text{LogP} = 2.77$) have a higher organic content and are more likely to sorb to organic matter (Fatta et al., 2007).

The polarity of compounds is a major concern in drug discovery and the environment but also poses problems when considering analytical analysis techniques. Those with high polarity or high MW can be challenging to analyse and thus care must be taken to choose a suitable analytical technique for identification and quantification of the compounds (see 2.3 Analysis methods & Chapter 3).

2.2.2 Environmental Sources

Emerging pharmaceutical compounds enter the environment through many routes, at either point source locations, where a singular area can be pin-pointed, or diffusely, over a larger geographical area. A brief review of each is detailed below.

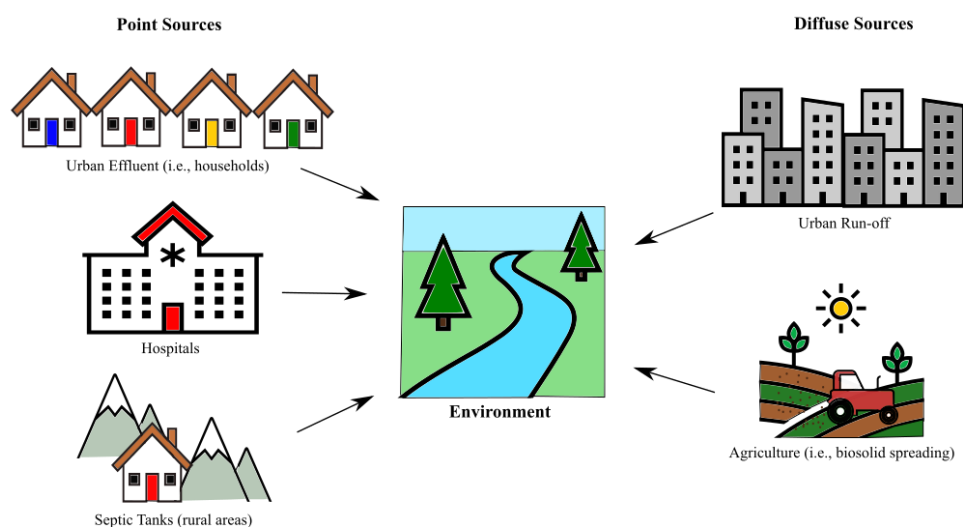


Figure 2.1: Routes of PhCs into the environment – point sources and diffuse sources.

2.2.2.1 Point Sources

The main route of PhCs into the environment is through human consumption; where PhCs and metabolites are excreted almost exclusively in faeces and urine (Barreto et al., 2021). Therefore, point source locations often are attributed to human waste disposal including urban wastewater (i.e.,

households) (Bound & Voulvoulis, 2005; Preisner et al., 2021), hospitals (Santos et al., 2013; Verlicchi et al., 2012), and septic tanks (Li, 2014; Yang et al., 2017).

Urban wastewater

Wastewater generated from urban areas, including from households, schools or businesses, is classed as urban wastewater (UWW) (Eriksson et al., 2002). UWW contains many toxic chemicals, pathogenic bacteria and viruses (Speight, 2020), registering it as a hazardous material, which requires purification. The PhC load of UWW is compiled mainly from excreted PhCs, though an additional contribution from improperly discarded medication (toilet/sink) is also noted (Bound & Voulvoulis, 2005). Raw wastewater travels from households and other urban buildings through a network of sewers to municipal WWTPs, where water is purified before release in the environment. However, municipal WWTPs are not designed to remove complex compounds such as pharmaceuticals (Petrović et al., 2003) and therefore these compounds are not fully eliminated, remaining in the WWTP effluent and sludge (the semi-solid organic residual of WWTP processes) (Deblonde et al., 2011; Jelic et al., 2011; Pereira et al., 2011; Rodriguez-Mozaz et al., 2015). Treated UWW has shown to contribute to antibiotic resistance (Goñi-Urriza et al., 2000; Rodriguez-Mozaz et al., 2015) and eutrophication of rivers and surface waters (Preisner et al., 2021).

Hospitals

Hospitals are considered as an intensive point source location, with consumption of large quantities of often high strength PhCs, leading to a release of highly concentrated PhC effluent (Verlicchi et al., 2012). The pharmaceutical load of the hospital effluent can vary, dependent on the number of hospital beds; hospital age; number and type of wards; cultural and geographical location; and seasonal weather changes (Santos et al., 2013; Verlicchi et al., 2012). Regardless of the high concentrations, no pre-treatment is received prior to reaching municipal WWTPs, where insufficient removal leads to a high influx of PhCs into the environment. This is of particular concern for hospitals situated in remote locations such as the Scottish Highlands (Marsik et al., 2017). Due to the smaller intake of the WWTP in less densely populated locations, the PhC load in the wastewater will be at an increased level (higher percentage in comparison to urban WW); as the in-sewer dilution is far lower (Nebot et al., 2015).

Septic Tanks

Septic tanks are often installed in rural areas, due to a lack of established sewer networks, providing waste collection/treatment to around 4% of the UK population (DEFRA, 2012). Septic tanks collect waste from one household or business, before dispersing into soil via a network of drain fields (trenches) for further treatment (Yang et al., 2016). As with hospitals in remote locations, septic tanks are smaller vessels which hold a smaller volume of wastewater and thus the PhC load will be more concentrated. The differences in concentration are likely to be dependent on the use and dosage of the PhCs prior to excretion (Yang et al., 2016). Septic tanks introduce PhCs into the environment mainly through soil

filtration (Phillips et al., 2015), though additional PhC release is attributed to the increased likelihood of leakage in comparison to WWTPs (Li, 2014).

2.2.2.2 Diffuse Sources

The spreading of treated sewage sludge (also known as biosolids) in agricultural settings is the primary diffuse route of contamination. Urban run-off (due to heavy rainfall) is another, though somewhat lesser, contributor (Li, 2014).

Biosolids

Biosolids are often applied to agricultural land to improve soil quality (Li, 2014). Produced from treated sewage sludge, biosolids are rich in nutrients (McClellan & Halden, 2010) and are often used as a cheaper, greener alternative to traditional fertilisers (US EPA, 2016). It is widely acknowledged that PhCs will sorb to sludge during WWTPs, resulting in insufficient removal (see 2.2.4.1 Wastewater Treatment Plant Processes). Sorbed PhCs then migrate into surface water, ground water and soil, through leachate, when biosolids are applied to land (McClellan & Halden, 2010). Over 500 pollutants have been found in biosolids since 1993 (US EPA, 2016). With over 50,000 tonnes (dry weight) of biosolids applied to agricultural land each year in Scotland (Scottish Government, 2021) and an estimated 4 million metric tonnes (dry weight) of biosolids applied within the EU (Macherius et al., 2012), there arises a potential for a large amount of PhCs to enter the environment through this pathway.

Urban run-off

Urban run-off is defined as water flow generated from increased rainfall and impermeable or saturated surfaces such as roads, rooftops and other man-made surfaces found in urban areas (US EPA, 2003). The impervious surfaces transport environmental contaminants from WWTPs, water storage tanks, landfills, lagoons and storm drains (Valett & Sheibley, 2009). Though little research has been undertaken, urban run-off has shown to play a role in the dissemination of antibiotics, which merits further research (Almakki et al., 2019).

2.2.3 Consequences

Each individual EC poses a potential risk to the environment - residues can be toxic to aquatic life (Frédéric & Yves, 2014), and potentially harmful to human life (Anand et al., 2021). An increase in frequency of endocrine related diseases in humans, such as declining male fertility (Fatta-Kassinos et al., 2011) has increased the awareness to a potential problem. Some argue that the detected concentrations of PhCs are far below the derived safe limits (Schulman et al., 2002; Zenker et al., 2014), however the vast majority of the scientific community argue that there is overwhelming evidence of environmental damage, particularly to aquatic life, and thus it is widely accepted that PhCs are environmental pollutants which must be removed.

Many PhCs including ibuprofen, sulfasalazine, diclofenac and carbamazepine are known to adversely affect algae, through mutations in the chloroplast proteome (Li, 2014; Vannini et al., 2011); with diclofenac also inducing kidney necrosis, or hyperplasia in fish (Mehinto et al., 2010). Estrogens have been shown to cause endocrine disruption in fish (Pawlowski et al., 2004), negatively affecting their reproductive system. The synthetic estrogen, 17 α -ethinylestradiol (EE2), the main API in the contraceptive pill, was shown to increase the female population of fish at concentrations above 1 ng/L (Pawlowski et al., 2004), completely feminising the population with concentrations above 3.5 ng/L (Li, 2014). With 29% of the UK female population taking the contraceptive pill in 2018 (Stewart, 2021), there is a possibility of a potentially environmentally endangering concentration entering the environment.

Emerging antibiotics are also of profound concern, as the presence of these compounds in the environment may cause an increase in the occurrence of antibiotic resistant bacteria (Daughton & Ternes, 1999) and antibiotic resistant genes (Verlicchi et al., 2015). Ding *et al.* concluded that chronic exposure to low levels of antibiotics may be the root of the development of antibiotic resistant bacterial strains in the environment (Ding et al., 2011); which raises concerns of an increase in more resistant bacterial strains like the prominent medical example of methicillin-resistant *Staphylococcus aureus* (MRSA) (Kummerer, 2004). Additionally, increasing antimicrobial resistance entails an increase in medical costs, prolonged hospital stays and higher mortality (Lima et al., 2020).

Additional concerns have arisen concerning possible uptake of PhCs into food crops, as biosolids are regularly used to fertilise agricultural land (McClellan & Halden, 2010). Though the uptake of certain PhCs (e.g., carbamazepine) has been established (Zheng et al., 2014), the adverse effects are not fully known at this stage, and further investigation is required (Jayampathi et al., 2019).

The consequences will not diminish without proper regulations in place, thus the conclusions drawn from these studies motivates the need to investigate remediation of PhCs in wastewater and sludge.

2.2.4 Wastewater Treatment Plants (WWTPs)

As mentioned, PhCs and metabolites are excreted almost exclusively in faeces and urine (Barreto et al., 2021); thus the main route of PhCs into the environment is through treated wastewater and sludge. Wastewater undergoes several treatments at WWTPs prior to release, though it is widely accepted that these processes do not sufficiently remove complex compounds such as PhCs (Felis et al., 2020). A brief description of the processes and the efficacy of PhC removal are described in this section.

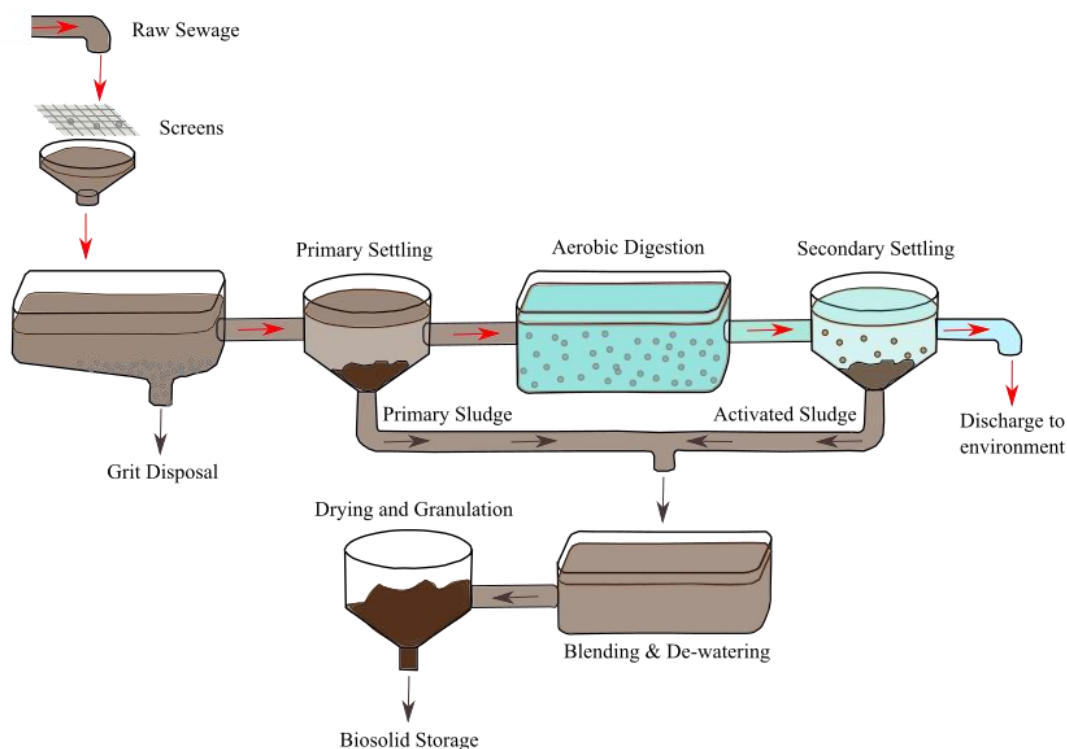


Figure 2.2: Wastewater Treatment Plant Processes: From Raw Sewage to Discharge and Biosolid Formation. Adapted from (Britannica Encyclopedia, n.d.; Scottish Government, 2021)

2.2.4.1 Wastewater Treatment Plant Processes

Wastewater

In Scotland, wastewater is purified through a five-stage process. Initially the wastewater is filtered through a series of screens, to remove any interferents such as rubbish, stones, or grit. The filtered wastewater is left to rest, where gravity forms two separate layers – primary sludge and clarified wastewater, in a process known as ‘settling’ (Scottish Government, 2021). At this point, the water and sludge processes separate, with sludge removed for further treatment. The wastewater then undergoes aerobic ‘digestion’, where micro-organisms remove nutrients through consumption. A secondary ‘settling’ stage is applied to remove the suspended microorganisms, producing activated sludge. Treated wastewater is then released into the environment (see Figure 2.2).

Sludge

Primary and activated sludge produced in the WWTP is processed separate from the wastewater. The processing method for sludge is slightly different. Anaerobic digestion (AD) is often applied to both primary and activated sludge to break down organic matter. AD degrades and stabilises sludge using a variety of microbes, under anaerobic conditions (Chen et al., 2008). It is sometimes pre-treated with thermal hydrolysis (THP), to reduce sludge viscosity, and improve the anaerobic digestion performance, reducing treatment times (Scottish Government, 2021). The THP process involves heating dewatered sludge to 160-180 °C for 30 mins, under pressure, which causes cell lysis upon pressure release (Barber,

2016) (Figure 2.3). Additionally, thermal drying (TD) can be applied to raw or treated sludge, to significantly reduce the volume, through the removal of water. Temperatures of up to 450 °C achieved during the process, provide adequate pathogen removal, though the method is extremely energy intensive, which can be costly (Scottish Government, 2021). Further processes such as lime treatment (or liming) can be applied to treated sludge, increasing the pH to over 12, helping to reduce pathogens and sludge associated odours (Wong & Fang, 2000).

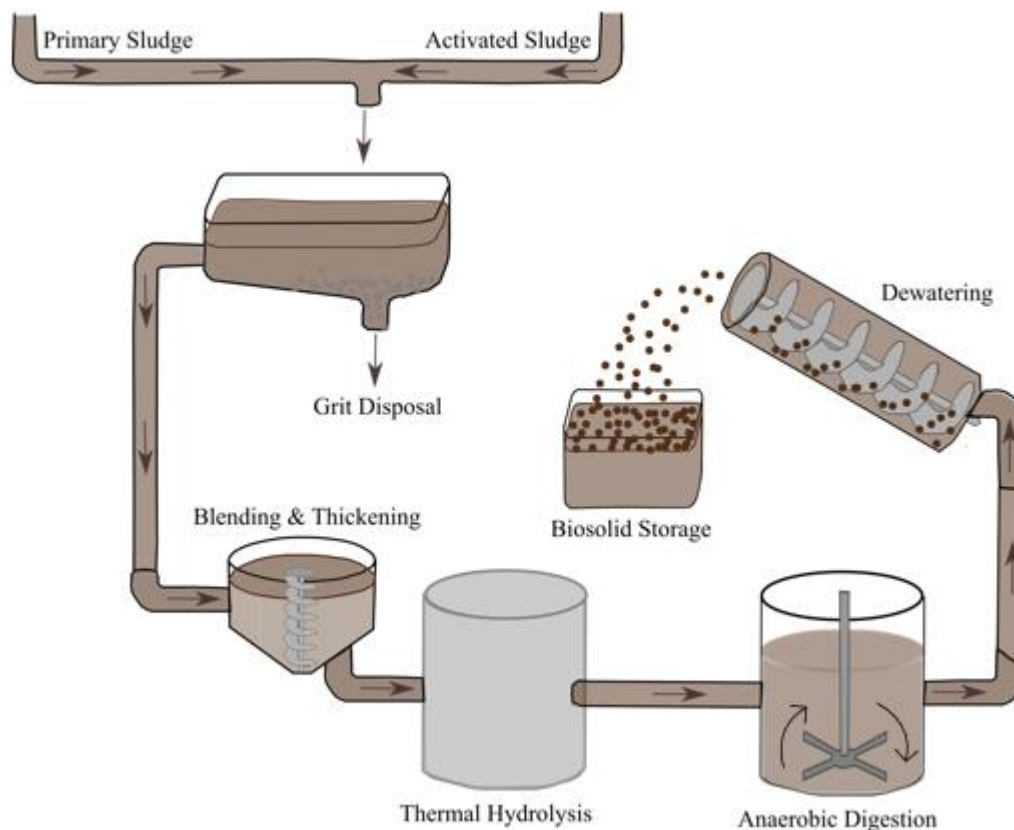


Figure 2.3: Wastewater Treatment Plant Processes: From Sludge to Biosolids. Adapted from (Britannica Encyclopedia, n.d.; Scottish Government, 2021).

Sludge is applied to agricultural land as either biosolid cake, or biosolid pellets. Biosolid pellets tend to have around 95% dry matter, whereas this is reduced to 25-40 % for biosolid cakes (Scottish Government, 2021). In Scotland, the majority of biosolids are created from dried sludge which has undergone no further treatment, such as digestion or stabilisation (Scottish Government, 2021) (see Figure 2.2). Therefore, PhCs are likely to remain in the sludge.

2.2.4.2 Removal Efficacy

The removal efficacy of PhCs through WWTPs has been explored by many. Jelic *et al.* studied the presence of 43 PhCs (from 12 therapeutic classes) in influent and effluent of 3 WWTPs. They detected 32 PhCs in WWTP influent, 29 PhCs in wastewater effluent and 21 PhCs in treated sludge; suggesting less than 10% of the targeted PhCs were removed by the WWTP (Jelic *et al.*, 2011). Deblonde *et al.*

reviewed over 40 publications for the removal rates of 50 target PhCs. They concluded that overall removal rates (calculated using equation (1-2)) ranged from 0 % for iodinated X-ray contrast media, to 97 % for the psychostimulant caffeine; with commonly used analgesics, anti-inflammatories, and beta-blockers in the region of 30-40 % (Deblonde et al., 2011).

$$\text{Removal Rate} = \left(\frac{\text{Influent Concentration} - \text{Effluent Concentration}}{\text{Influent Concentration}} \right) * 100 \quad (1-2)$$

Estrogens (estrone, estradiol, estriol, and synthetic estrogen 17 α -ethinylestradiol) have also been identified in WWTP effluent at similar concentrations to WWTP influent (1-100 ng/L) throughout literature (Pereira et al., 2011) suggesting the hormones are not removed by the WWTP processes. The removal rates of 14 antibiotics (including chloramphenicol and gentamycin) in 4 WWTPs ranged from 14-100 %, though the average removal rate was 59 % (Tahrani et al., 2015). Felis *et al.* reviewed over 30 peer reviewed articles concluding that 23 common antibiotics (including amoxicillin and trimethoprim) have been identified in treated wastewater in low to high ng/L concentrations (Felis et al., 2020). During the WWTP, some PhCs are likely to bind to organic matter (dependent on LogP); and thus are not removed fully, but instead present in the collected sludge. Gago-Ferrero *et al.* detected 35 PhCs and illicit drugs in low to high $\mu\text{g}/\text{kg}$ concentrations in treated sludge (Gago-Ferrero et al., 2015). Samaras *et al.* also detected 6 PhCs and endocrine disrupting compounds at similar concentrations ($\mu\text{g}/\text{kg}$) with WWTP removal rates ranging from 20-85 % (V. G. Samaras et al., 2013). A similar range in removal rates (20-70%) was identified by Carballa *et al.*, though no removal of carbamazepine was observed, even after anaerobic digestion (Carballa et al., 2006).

The insufficient removal of PhCs by the WWTP processes has given rise to the routine detection of antibiotics and other PhCs in biosolid samples. McClellan and Halden identified 38 targeted PhCs, including commonly used medications ibuprofen, metformin and triclosan in over 80 % of analysed biosolids samples (McClellan & Halden, 2010). Ding *et al.* detected 14 targeted PhCs in treated biosolid samples collected from 6 WWTPs with concentrations ranging widely from 2.6 to 743.6 $\mu\text{g}/\text{kg}$ (Ding et al., 2011) with antibiotics oxytetracycline and chlortetracycline present in the largest concentrations (>250 $\mu\text{g}/\text{kg}$). This is of particular concern, as tetracyclines have been shown to accumulate in soil, quantified in concentrations of (>100 $\mu\text{g}/\text{kg}$) several months after initial application (Hamscher et al., 2002). Albero *et al.* identified 11 PhCs in biosolid samples, with NSAIDs ibuprofen and paracetamol detected in 100 % of analysed samples (Albero et al., 2014). Carbamazepine and triclosan were amongst the PhCs regularly detected in digested sludge (Barron et al., 2008); which is additional concern as these PhCs have shown great resistance to natural attenuation (Chenxi et al., 2008b).

The incomplete removal of PhCs at wastewater treatment plants (WWTPs) and recalcitrant nature of PhCs has ensured their persistence in soils for 5 years after biosolid application (Gravert et al., 2021; Walters et al., 2010). The concentrations of PhCs in sludge and biosolids vary, though are generally

found at trace levels (Fatta et al., 2007). The complex matrix and low concentrations provide challenges in analysis. Thus, suitable analysis methods are required to identify and quantify PhC concentrations.

2.3 Analysis methods

2.3.1 Targeted and Non-targeted

Targeted analysis (or suspect screening) refers to analyses where the studied compounds are known prior to analysis (Ballin & Laursen, 2019); whereas non-targeted analysis refers to analyses in which analytes are unknown and are not limited in number or origin (Milman & Zhurkovich, 2017). Targeted methods focus only on a selective set of known compounds - thus the physicochemical properties of each are known and the behaviour of the compounds can be predicted. This allows a sample preparation method, which will enhance the detection of these compounds, to be developed and used. Non-targeted analysis is far more challenging. The aim is to simultaneously detect as many compounds as possible. This includes both 'Known Unknowns' – compounds are known to the analyst (i.e. some of the target compounds) and 'Unknown Unknowns' - analytes which are unknown in literature and to the analyst (Milman & Zhurkovich, 2017) which poses challenges in both sample preparation and identification.

Targeted methods are generally quantitative and provide greater sensitivity and selectivity than non-targeted methods (Ballin & Laursen, 2019). However, they provide limited information about a sample, only presenting data on specified compounds. Thus, there is the possibility of missing other analytes of interest. Non-targeted analysis gives a more in-depth characterisation of samples, as no pre-defined analytes are targeted. Methods are more qualitative, than quantitative – though provide information relating to the sample as a whole. The output is often referred to as a 'fingerprint', though can contain over 10,000 peaks, which leads to time consuming and challenging data processing. Samples are compared to reference standards or each other to elucidate small changes in sample composition. These changes are converted to valuable information through multi-variate analysis, such as principal component analysis (PCA) or partial least squares discriminant analysis (PLSDA); which illustrates visually differences and similarities between samples. Newly developed software, including ChromaTOF Tile (see Chapter 6) has been developed to reduce the data processing time, and easily elucidate inter-sample variance.

The application of a non-targeted method would be beneficial in the analysis of ECs in environmental samples such as biosolids. The land application of biosolid is an identified route of PhCs into the environment. Though with the large number of PhCs available, it is unknown exactly which compounds are not removed in WWTPs and thus released into the environment. Furthermore, the PhCs may undergo transformation or degradation, with the possibility of increased toxicity of these newly formed and unknown products (Li et al., 2014). Therefore, to properly assess the extent of the problem and provide possible solutions, the PhC load of the biosolid must first be fully characterised.

Non-targeted analysis has been used successfully in many different fields including: identification of food contaminants (Kunzelmann et al., 2018); biomarkers for disease (Tao et al., 2020; Zhang et al., 2016); performance enhancing drugs (de Albuquerque Cavalcanti et al., 2018) and counterfeit Scotch Whisky (Stupak et al., 2018). Although the benefits of non-targeted analysis in environmental matrices are known, the majority of studies which analyse emerging PhCs still only target groups of compounds - either belonging to the same therapeutic class (Antonić & Heath, 2007; González et al., 2015; Logarinho et al., 2016; Marsik et al., 2017; Rodriguez-Mozaz et al., 2015; Samaras et al., 2010; Sebök et al., 2008), multiple therapeutic classes (Gago-Ferrero et al., 2015; Guerra et al., 2014; Kumirska et al., 2019; Martín et al., 2010; Migowska et al., 2012; Peysson & Vulliet, 2013; Verlicchi et al., 2012), or PhCs which contain the same functional groups (e.g., acidic compounds) (Lacina et al., 2013; Öllers et al., 2001; Samaras et al., 2011). Few studies utilise non-targeted analysis methods (Blum et al., 2017; Gravert et al., 2021; Müller et al., 2011; Veenaas et al., 2018; Veenaas & Haglund, 2017), due to the challenges associated with sample preparation.

PhCs differ in physicochemical properties such as polarity, solubility, volatility, and molecular weight which all influence the required extraction and analysis method (see below). The application of multiple sample preparation or analysis stages has been used to analyse multiple PhCs in various studies (Albero et al., 2014; Carballa et al., 2004; Löffler & Ternes, 2003; Migowska et al., 2012; Ternes et al., 2005), though doing so, increases solvent and energy consumption, bias and overall analysis time. Whereas other studies have been able to analyse multiple PhCs with one extraction and analysis step (Gago-Ferrero et al., 2015). Therefore, a novel non-targeted analytical method which could characterise the PhC micropollutant load without intensive sample preparation, would transform the way contaminants are detected and identified.

2.3.2 Extraction Methods

Extraction is a key sample processing step on which the success of the overall analysis depends. For non-targeted analysis, an extraction step which extracts as many analytes as possible (in this case PhCs) is desired. Extraction and clean-up methods which increase selectivity should be avoided, to prevent bias of extracted analytes (for example, targeting only acidic compounds). Common extraction methods used in analysis of PhCs in wastewater, sludge and biosolids are discussed in relation to their applicability to non-targeted analysis.

2.3.2.1 Solid Phase Extraction (SPE)

SPE is a powerful extraction technique which has been applied in the extraction of pharmaceuticals from wastewater (Jelic et al., 2011; Lavén et al., 2009; Söregård et al., 2019; Yu & Wu, 2011) and biosolid/sludge (Barron et al., 2008; Guerra et al., 2014; Huber et al., 2016; US EPA, 2007; Yu & Wu, 2012) matrices in a variety of studies. The choice of sorbent is imperative to the success of the extraction - most studies successfully apply mixed mode cartridge Oasis HLB (hydrophilic-lipophilic balance)

(Figure 2.4): either individually (Barron et al., 2008; Bisceglia et al., 2010; Guerra et al., 2014; Jelic et al., 2011; Lacina et al., 2013; McClellan & Halden, 2010; Pérez-Lemus et al., 2019; Santos et al., 2013; Söregård et al., 2019; US EPA, 2007; Xiang et al., 2018), or in tandem with another cartridge (primarily Oasis MCX) (Gros et al., 2009; Lavén et al., 2009). SPE with a single cartridge is preferred, due to the increased number of SPE cartridges and delicate set-up required for tandem SPE.

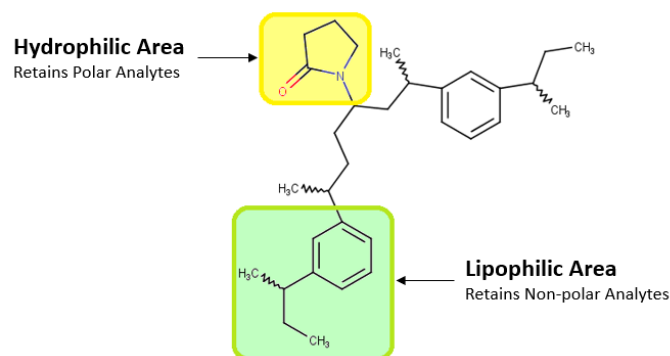


Figure 2.4: Oasis HLB sorbent (Waters Oasis Sample Extraction SPE Products : Waters, *n.d.*) used in extraction of PhCs from wastewater. The hydrophilic area retains polar analytes, and the lipophilic retains non-polar analytes, which increases the scope of the analysis (targeted analytes can differ in physicochemical properties)

SPE can be applied as the primary extraction method (Gros et al., 2010; Huber et al., 2016; Jelic et al., 2011; Santos et al., 2013; Söregård et al., 2019; Verlicchi et al., 2012), though is more often used as a clean-up stage after extraction (Barron et al., 2008; Guerra et al., 2014; Jelic et al., 2011; McClellan & Halden, 2010; Radjenović et al., 2009; US EPA, 2007; Walters et al., 2010). SPE consists of 4 stages: cartridge conditioning, sample load, sample wash, and analyte elution. During the wash stage, a solvent is used to elute impurities and interferents, yet allow the analyte compounds to be retained on the SPE sorbent. However, analyte retention depends on the physicochemical properties of the analyte; and no SPE sorbent can cover the entire range of PhCs. Thus, in non-targeted analysis, some analytes may be lost at this stage (Hajeb et al., 2022).

2.3.2.2 Pressurised Liquid Extraction (PLE)

PLE, also referred to as accelerated solvent extraction (ASE), has been used for extraction of PhCs primarily from solid matrices including sludge/biosolids (Barron et al., 2008; Ding et al., 2011; Jelic et al., 2011; Radjenović et al., 2009), sediment (Antonić & Heath, 2007; H. Langford et al., 2011) and soils (Biel-Maeso et al., 2019). Operating under high temperatures and pressures, solvent physicochemical properties are altered (e.g., a reduction in surface tension and viscosity), increasing the ease with which the solvent can penetrate the solid matrix, and extract the analytes (Alvarez-Rivera et al., 2020). The technique has shown fast and efficient extraction of pharmaceuticals (Barron et al., 2008; Biel-Maeso et al., 2019; Ding et al., 2011; Radjenović et al., 2009), with the automated procedure allowing for simultaneous extraction of multiple samples (Ding et al., 2011). Improvements in extraction yields, reproducibility, and extraction time are observed in comparison to other traditional

extraction techniques (Alvarez-Rivera et al., 2020; Pérez-Lemus et al., 2019). Used as the primary extraction technique, often SPE is applied after as a clean-up stage, to remove interferences, or as an analyte concentration step (Barron et al., 2008; Ding et al., 2011; Jelic et al., 2011; Pérez-Lemus et al., 2019). This additional step can impart selectivity to the analysis, as described above.

2.3.2.3 Ultrasonic Assisted Extraction (UAE)

A rise in UAE for extraction of PhCs from solid matrices has been observed over the last 10 years, making it one of the most popular extraction techniques at present (Pérez-Lemus et al., 2019). The simple and effective technique uses relatively small volumes of organic solvents and can be applied using common laboratory equipment (e.g., ultrasonic bath), making it a more affordable and ‘Greener’ alternative to Soxhlet and other extraction techniques (Pérez-Lemus et al., 2019). Although, akin to PLE, UAE is often followed by SPE, as the extraction is never completely selective.

Over 10 studies use UAE methods to accelerate extraction of PhCs from biosolid samples (Chenxi et al., 2008b; Gago-Ferrero et al., 2015; Guerra et al., 2014; Martín et al., 2010; McClellan & Halden, 2010; US EPA, 2007; Walters et al., 2010; Yu & Wu, 2012), though most follow the method developed by the United States Environmental Protection Agency (US EPA) for analysis of PhCs and PCPs in water, soil, sediment and biosolids, known as Method 1694 (US EPA, 2007). This method applies UAE for simultaneous extraction of PhCs from solid samples, including biosolids. An acidic and basic fraction are produced through two extraction methods (extraction solvents are phosphate buffer/acetonitrile and ammonium hydroxide/acetonitrile respectively), prior to SPE clean up with Oasis HLB cartridges. This method has been successfully used by multiple other studies (Guerra et al., 2014; McClellan & Halden, 2010; Walters et al., 2010) when analysing over 50 PhCs in sludge and biosolid samples.

All methods referenced have been targeted methods, though have successfully extracted up to 150 target PhCs ranging many therapeutic classes, and a wide variety of functional groups. Therefore, it is hypothesised that a similar extraction method could be applied in a non-targeted method, to elucidate further PhCs. Of the described methods, SPE imparts some selectivity to the extraction step, and thus must be avoided as both the primary extraction method, and as a clean-up stage. PLE and UAE have both been used successfully in the extraction of numerous PhCs. Either method would be suitable for the non-targeted analysis, though the additional benefits of low energy and solvent consumption associated with UAE make it the optimal choice in this study.

2.3.3 Separation Methods

Chromatography methods coupled with mass spectrometry (MS) remain the most common methods for analysis and identification of pharmaceutical residues in environmental samples. Although liquid chromatography (LC) is most commonly used for quantification, gas chromatography (GC) has been utilised for the identification and quantification of many PhCs (see Figure 2.5).

2.3.3.1 Liquid Chromatography (LC)

Reversed-phase LC (see Chapter 3) is the most common method of analysis for PhCs in environmental samples, including WWTP effluent (Kovalova et al., 2012; Rodriguez-Mozaz et al., 2015; Samaras et al., 2011; Verlicchi et al., 2012; Xu et al., 2015), and sludge/biosolids (Albero et al., 2014; Ding et al., 2011; Gago-Ferrero et al., 2015; Huber et al., 2016). It is the preferred chromatographic technique due to the low volatility and polar nature of the PhC compounds – with the majority of pharmaceutical analysis studies being conducted on LC (Nikolin et al., 2004) (see Figure 2.5).

LC coupled with tandem MS (LC-MS/MS) is the most prevalent analysis technique for PhCs in biosolid samples (Albero et al., 2014; Barron et al., 2008; Chenxi et al., 2008a; Ding et al., 2011; Gago-Ferrero et al., 2015; Guerra et al., 2014; Huber et al., 2016; McClellan & Halden, 2010; Radjenović et al., 2009; Walters et al., 2010), though LC-MS (Gros et al., 2009, 2010) and LC-DAD (diode array detection) (Martín et al., 2010) have also been used. Tandem MS improves sensitivity and specificity of analyses (Fatta et al., 2007; Pitt, 2009), through use of specified precursor and product ions (see Chapter 3). However, this requires knowledge of possible analytes, and is therefore used primarily in targeted, or semi-targeted analysis.

LC-MS/MS analysis has some disadvantages - interferents from complex matrices have shown to increase ion suppression and enhancement (Petrović et al., 2003; Radjenović et al., 2009; Samaras et al., 2011), causing issues with identification and quantification of analytes (Ternes, 2001). A clean-up stage (i.e. SPE) is often added to remove interferents (Fatta et al., 2007), though Radjenović *et al.* observed signal suppression and enhancement in all 31 PhCs studied, ranging from -94.2 % to 694.3 % (Radjenović et al., 2009), when analysing sludge samples, despite post extraction SPE. This step also increases sample preparation time and solvent consumption. Additionally, LC-MS/MS must be undertaken in both positive and negative ion mode (particularly for non-targeted analysis); which doubles analysis time and solvent consumption. Both are known limitations with electrospray ionisation (ESI) techniques used in LC analysis (see Chapter 3); though are not as prevalent when electron impact (EI) ionisation is used. Therefore, GC techniques are sometimes utilised when analysing complex matrices to overcome these issues.

2.3.3.2 Gas Chromatography (GC)

Although not as prevalent, GC has become more widely used for wastewater analysis in the last decade due to the increased sensitivity (Ohoru et al., 2019), greater separation efficiency (Lacina et al., 2013; Marsik et al., 2017), increased sustainability (Albero et al., 2014) and decreased cost (Filigenzi, 2017) of the technique, in comparison to LC methods.

Though some limitations to GC analysis exist. To analyse polar compounds, sample preparation must include a derivatisation step, to increase compatibility with GC. PhCs are polar compounds with low volatility; thus, must be derivatised to increase compatibility with GC analysis, increasing sample

preparation time (Fatta et al., 2007). Derivatisation is discussed below (see Section 2.4 Derivatisation). Furthermore, high MW compounds such as macrolide antibiotics (azithromycin, MW = 749.0 g/mol) or X-ray contrast agents (iopamidol, MW = 777.09 g/mol) have very low volatility which cannot be increased by derivatisation. Thus, these PhCs must be analysed via LC (Carballa et al., 2004; Rodriguez-Mozaz et al., 2015; Xu et al., 2017).

One-dimensional GC has been used for analyses of PhCs (as derivatives) in various environmental matrices including river, pond and tap water (Jux et al., 2002), drinking water (Azzouz & Ballesteros, 2013; Caban et al., 2015), soils (Biel-Maeso et al., 2019; Kumirska et al., 2019; J. Xu et al., 2008), sludge (Albero et al., 2014; Samaras et al., 2011; Yu & Wu, 2012) and wastewater effluent (González et al., 2015; Huggett et al., 2003; Samaras et al., 2010). Targeted therapeutic classes analysed in wastewater and sludge include anti-psychotics (Logarinho et al., 2016), β -blockers (Huggett et al., 2003; Kumirska et al., 2019), estrogens (González et al., 2015), and NSAIDs (Migowska et al., 2012), with other studies targeting PhCs from a number of therapeutic classes (Albero et al., 2014; Migowska et al., 2012; Ternes, 2001).

Akin to LC, mass spectrometry is the most prevalent detection method in wastewater and sludge analysis. GC-MS has been used in both scan and SIM (selected ion monitoring) modes (see Chapter 3), for identification and quantitation respectively (Caban et al., 2015; González et al., 2015; Kumirska et al., 2019). Additionally, tandem MS has been used to increase sensitivity in targeted methods (Albero et al., 2014; Biel-Maeso et al., 2019; Ternes, 2001) through specified precursor and product ions.

Ternes (2001) compared LC-MS/MS with GC-MS for analysis of PhCs in wastewater, concluding that GC-MS was sufficient for acidic PhCs, achieving limits of quantification (LOQs) as low as 10 ng/L, decreasing to 1 ng/L if tandem MS was applied (GC-MS/MS) (Ternes, 2001). Gonzalez *et al.* concluded that GC-MS was applicable to estrogenic compounds, with good precision, accuracy, and recovery; highlighting GC-MS as the preferred technique (over LC) for simultaneous separation of synthetic and natural estrogens (González et al., 2015). Though derivatisation is required, Migowska *et al.* stated that the low cost, superior resolution and reduction in matrix effects, made GC techniques more suited to complex matrices such as wastewater and sludge samples (Migowska et al., 2012). This was supported by Kumirska *et al.* and Albero *et al.* whom used GC-MS methods for the analysis of >15 PhCs, from a range of therapeutic classes (Albero et al., 2014; Kumirska et al., 2019).

2.3.3.3 Two-dimensional Gas Chromatography (GCxGC)

In the last twenty years, 2D comprehensive gas chromatography (GCxGC) has been used in the analysis of emerging contaminants - including pesticides and organohalogens (Prebihalo et al., 2015), drug residues (Lacina et al., 2013; Matamoros et al., 2010; Song et al., 2004) (including NSAIDs (Marsik et al., 2017), steroids (Kopperi et al., 2013), PhC by-products (Beldean-Galea et al., 2014)) and domestic contaminants (Blum et al., 2017) - in water and wastewater matrices.

This powerful technique overcomes issues with co-elution and hidden peaks, often observed in one dimensional analysis, through the addition of a secondary column. The second dimension separation increases peak capacity (Lacina et al., 2013) and separation efficiency, making it a suitable technique for complex samples and non-targeted methods. Additionally, GCxGC minimises matrix effects of complex samples: decreasing background noise (Lacina et al., 2013), improving mass spectral quality (Song et al., 2004), and increasing reliable identification and quantification of analytes (Kopperi et al., 2013). Though the two-dimensional separation requires a fast acquisition, thus high-resolution mass spectrometers, such as time-of-flight (TOF) detectors are required (SepSolve Analytical, 2016) (see Chapter 3).

Few studies have analysed wastewater or sludge samples by GCxGC; however, have applied the method to other complex matrices. Matamoros *et al.* successfully demonstrated the use of a GCxGC-TOFMS method for the analysis of 73 ECs (including 13 PhCs) in river water at trace concentrations (Matamoros et al., 2010). Marsik *et al.* also successfully detected all targeted NSAIDs in rivers and tributaries, identifying their presence in all samples at low $\mu\text{g/L}$ levels (Marsik et al., 2017). In terms of wastewater, Kopperi *et al.* successfully quantified several steroidal compounds using GCxGC (Kopperi et al., 2013), and Lacina *et al.* concluded that the separation efficiency of a GCxGC method is superior to all common chromatography methods (LC, GC or HPLC); with increased sensitivity achieved for acidic PhCs in wastewater samples (Lacina et al., 2013). Although all methods described are targeted methods, it suggests that GCxGC shows great potential for screening unknown contaminants in complex matrices (Kopperi et al., 2013).

Veenaas *et al.* used a non-targeted GCxGC approach to successfully screen contaminants in sewage sludge (Veenaas et al., 2018). Using PLE (n-hexane: dichloromethane (80:20)) for extraction, gel permeation chromatography (GPC) for sample clean-up, and a normal phase column set-up; with over 10,000 peaks were detected in each sample. Through various data processing stages (peak alignment, blank removal etc.), the number of peaks was reduced to <1,500. Of these peaks, 192 compounds from seven categories (plastic additives, surface active compounds, flavours, fragrances, food constituents, personal care products, and miscellaneous) were identified. No pharmaceutical compounds were identified in the sewage sludge, though this may be attributed to the polarity of the extraction solvent. The extraction solvent is made primarily of n-hexane, which is a non-polar solvent – which will lessen the extraction of polar analytes, like PhCs. Altering the extraction method and removing the clean-up stage may increase the likelihood of PhC identification. However, the vast range of detected compounds by this method, suggests that an altered GCxGC method would be ideal for non-targeted analysis of biosolid compounds.

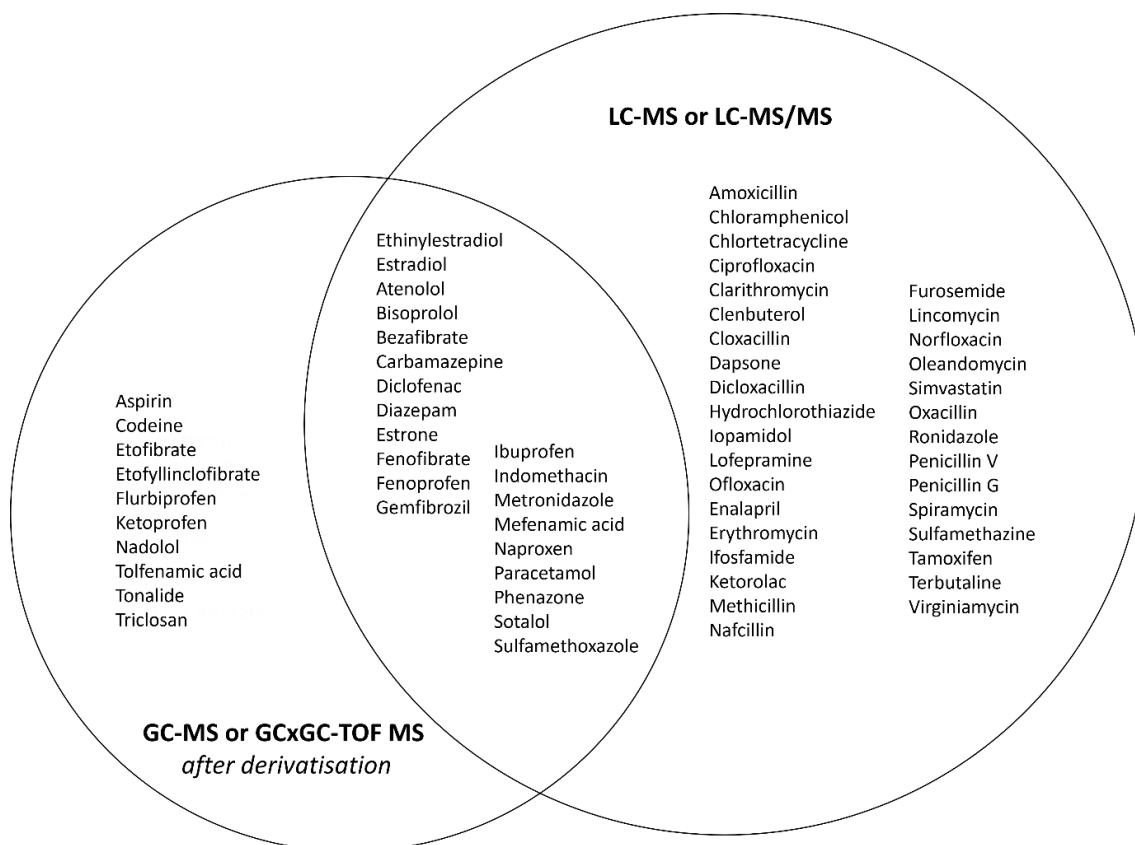


Figure 2.5: Chromatographic methods for analysis of pharmaceutical compounds. Adapted from (Fatta et al., 2007; Kostopoulou & Nikolaou, 2008).

2.4 Derivatisation

2.4.1 Methods

Derivatisation of PhCs is required prior to GC analysis, to increase compatibility with the technique. Derivatisation increases volatility and thermal stability of PhCs, reducing compound polarity. There are three common types of derivatisation methods: alkylation, acylation and silylation, though only two are applied to PhCs (alkylation and silylation). Reaction mechanisms and common reagents are detailed in Chapter 3.

The choice of derivatisation process is analyte dependant; with multiple derivatisation steps not uncommon for PhCs (Huggett et al., 2003; Ternes, 2001). Alkylation (or methylation) has been used to derivatise acidic (Farré et al., 2001; Marsik et al., 2017; Sacher et al., 2001; Verenitch et al., 2006) and neutral pharmaceutical compounds (Andreozzi et al., 2003) in various water matrices; though reagents are generally toxic chemicals, i.e. diazoalkanes (Orata, 2012), which can negatively impact the environment.

Silylation is the most common derivatisation technique for PhCs. Silylation has been applied to PhCs from various therapeutic classes including NSAIDs (Caban et al., 2014; Lacina et al., 2013; Samaras et

al., 2010; Sebök et al., 2008), estrogens (Caban et al., 2013; González et al., 2015; Vallejo et al., 2010), anti-psychotics (Logarinho et al., 2016), β -blockers (Caban et al., 2013; Huggett et al., 2003; Yilmaz & Arslan, 2009) and diuretics (Brunelli et al., 2006). Various silylation reagents are used, dependant on the analytes, including N, O-Bis(trimethylsilyl)trifluoroacetamide (BSTFA), N-Methyl-N-(trimethylsilyl)trifluoroacetamide (MSTFA) and N-(tert-Butyldimethylsilyl)-N-methyltrifluoroacetamide (MTBSTFA). Catalysts trimethylchlorosilane (TMCS) and pyridine are often added to facilitate the reaction (Blau & King, 1978). Silylation parameters including reagent (Caban et al., 2011; Caban & Stepnowski, 2018; Kumirska et al., 2013), reagent volume (Samaras et al., 2010), reaction time (Caban et al., 2011; Samaras et al., 2011; Sebök et al., 2008) and reaction temperature (Kumirska et al., 2019; Lacina et al., 2013; Migowska et al., 2012; Yilmaz & Arslan, 2009) are optimised for each individual analysis, though results differ from study to study.

For example, Samaras *et al.* used GC-MS to analyse four common NSAIDs (ibuprofen, diclofenac, naproxen and ketoprofen) in wastewater and sewage sludge after silylation and found that 50 μ l BSTFA+1% TMCS and 10 μ l pyridine, heated to 70 °C for 20 mins, were the optimum silylation conditions, with the addition of a small volume of pyridine greatly improving sensitivity (RSD <9%) (Samaras et al., 2011). However, Sebök *et al.* concluded that the optimum silylation conditions utilised 225 μ L of HDMS + 25 μ L of TFAA as the reagent, and heated to 70 °C for 90 mins for the same compounds (Sebök et al., 2008). This was similar to the method of Lacina *et al.* who concluded that 70°C for 90 mins was optimal for the silylation of 10 NSAIDs (including ibuprofen, diclofenac, naproxen and ketoprofen), though used 200 μ L of MSTFA + 200 μ L of pyridine as the reagent (Lacina et al., 2013). Which again differs from that optimised by Albero *et al.*, who used 50 μ L of MTBSTFA, heated to 70 °C for 60 mins, to derivatise 16 PhCs (including ibuprofen, diclofenac, naproxen and ketoprofen).

Although heating is the most common mode for facilitating derivatisation, new techniques are becoming more prominent including ultrasonic assisted derivatisation (UAD) (Fiamegos et al., 2004; Luque de Castro et al., 2011; Orozco-Solano et al., 2010; Pietrogrande et al., 2017; Seidi & Yamini, 2012; Vallejo et al., 2010) and microwave assisted derivatisation (MAD) (Amendola et al., 2003; Casals et al., 2014; Deng et al., 2005; Söderholm et al., 2010). Both methods have been used to drastically shorten derivatisation times of sterols (Orozco-Solano et al., 2010), carboxylic acids (Pietrogrande et al., 2017), and amino acids (Deng et al., 2005; Fiamegos et al., 2004). Though, few studies have applied MAD to PhCs (Amendola et al., 2003; Casals et al., 2014; Zuo et al., 2007), with even less applying UAD (Kotowska et al., 2014; Vallejo et al., 2010). Though UAD has shown to reduce the derivatisation time by up to 50 % in comparison to MAD (Luque de Castro et al., 2011). Therefore, this coupled with the Green benefits of reduced solvent and energy consumption; suggests ultrasound would be a desirable technique for this study.

Table 2-2: Derivatisation techniques: Acylation, Alkylation and Silylation: derivatisable functional groups and reagent examples

| Derivatisation Method | Functional Group | Common Reagents |
|-----------------------|---------------------------|--|
| Acylation | OH, SH, NH | Trifluoroacetic Anhydride (TFAA) Pentafluoropropionic Anhydride (PFPA) Heptafluorobutyric Anhydride (HFBA) Pentafluorobenzyl Chloride (PFBCl) Pentafluoropropanol (PFPOH) |
| Alkylation | COOH, OH, SH, NH | Diazoalkanes Dialkylacetals Pentafluorobenzyl bromide (PFBBR) Boron trifluoride (BF ₃) Tetrabutylammonium hydroxide (TBH) |
| Silylation | COOH, OH, SH, NH, CONH | Trimethylchlorosilane (TMCS) Trimethylsilylimidazole (TMSI) Bistrimethylsilyltrifluoroacetamide (BSTFA) N-methyl-trimethylsilyltrifluoroacetamide (MSTFA) N-methyl-N-t-butyltrimethylsilyltrifluoroacetamide (MTBSTFA) |

2.4.1.1 Mass Spectral Patterns for TMS derivatives

An advantage of silylation is the unique fragmentation patterns created by the addition of the trimethylsilyl (TMS) group which can be used to identify compounds in MS more efficiently. Common ions on a silylated mass spectrum include m/z 73 (MW of TMS group), and a loss of 15 amu from the molecular ion peak $[M-15]^+$, corresponding with an α -cleavage of a methyl (CH₃) radical from the TMS group (Harvey & Vouros, 2020). Lai and Fiehn (Lai & Fiehn, 2018) studied the fragmentation patterns of TMS silylated small molecules, elucidating that different functional groups produce different fragmentation patterns in MS. A list of the fragment ions can be found in Table 2-3.

Molecular ions are of low abundance for primary alcohols, where the major ion corresponds to the $[M-15]^+$, which is further fragmented by transfer of hydrogen atom to an oxygen atom, producing the $[HO-Si(CH_3)_2]^+$ ion with m/z 75. Secondary and tertiary alcohols also produce the $[M-15]^+$ ion peak, yet at a lower abundance, with the base peak more likely to be the product of an α -cleavage, with m/z 117 (Harvey & Vouros, 2020). Thiols produce sulphur equivalents of many of the TMS alcohol peaks, such as m/z 91, and m/z 163, equivalent to m/z 75 and m/z 117 for OH groups, respectively. Fragmentation of primary amines is also similar to alcohols: with α -cleavages forming product ions m/z 102 and m/z 174 for mono- and di-silylated compounds, respectively (Harvey & Vouros, 2020; Lai & Fiehn, 2018).

Table 2-3: Common mass spectral fragments after silylation, including diagnostic fragment ions, neutral losses and typical ion ratios by functional group (Lai & Fiehn, 2018)

| Functional Group | Common TMS Fragment Ions (m/z) |
|-------------------------|---|
| OH (aliphatic) | 75, 89, 103, 117, 129, 131, 145, 147, 189, 217, 219 |
| OH (aromatic) | 135, 151, 165 |
| OH (complex) | 237, 267 |
| COOH (mono) (aliphatic) | 103, 117, 129, 132, 145 |
| COOH (di) (aliphatic) | 147, 204, 217, [M-31], [M-105] |
| COOH (poly) (aliphatic) | [M-15], [M-43], [M-87], [M-105], [M-133] |
| COOH (mono) (aromatic) | 135, 151, 166, [M-15], [M-133] |
| NHs (1°) | 146, 174, 188 |
| NHs (2°) | 86, 100, 102, 116, 130 |
| NHs (OH or COOH) | 147 |
| Steroids | 117, 129 |
| Thiols | 91, 163, 178 |
| Phosphates (inorganic) | 299, 314, 211, 227, 243, 387 |
| Phosphates (organic) | 299, 315, 211, 227, 243, 387 |

2.5 Green Chemistry

Sustainable chemistry, often referred to as ‘Green Chemistry’, is defined as “*the design of chemical products and processes which reduce or eliminate the use or generation of hazardous substances... across the life cycle of a chemical product, including design, manufacture, use and ultimate disposal*” (US EPA, 2013). Green chemistry has become more prevalent within the science sector, as society looks for alternative and more sustainable resources; in order to reduce global pollution and prevent harm to the planet and its population.

However, this is not a new idea, the concept of Green Chemistry originates in the 1990s (Zuin et al., 2021), and is seen as the natural progression for the science industry. In 1998, Anastas and Warner published the ‘12 principles of Green Chemistry’ based on a collation of ideas and suggestions from previous studies conducted by bodies such as the US Environmental Protection Agency (EPA) and the European Union (EU) (Anastas & Warner, 1998). The twelve principles are outlined in Table 2-4.

Table 2-4: Anastas and Warner's 12 Principles of Green Chemistry (Anastas & Warner, 1998)

| 12 Principles of Green Chemistry | | |
|---|--|--|
| 1 | Prevention | Preventing the production of waste, is better than treating already produced waste. |
| 2 | Atom Economy | Synthetic methods should be designed to maximise use of all materials in the process into the final product to minimise waste. |
| 3 | Less Hazardous Chemical Synthesis | Synthetic methods should be designed to use and generate harmless substances, with less toxicity to human and environmental health, where possible. |
| 4 | Designing safer chemicals | The design of new chemicals should aim to preserve function efficacy yet reduce toxicity. |
| 5 | Safer Solvents and Auxiliaries | Use of auxiliary substances (solvents, separation agents etc.) should be made unnecessary wherever possible, and harmless when used. |
| 6 | Design for Energy Efficiency | The environmental and economic impacts should be considered when designing new protocols and chemicals. Impacts should be minimised with ambient parameters (e.g., temperatures and pressures) used. |
| 7 | Use of Renewable Feedstocks | Feedstocks or raw materials should be renewable where feasible. |
| 8 | Reduce Derivatives | Unnecessary derivatisation should be minimised or avoided, if possible, as extra reagents are required and can generate more waste. |
| 9 | Catalysis | Use of selective catalysts is better than stoichiometric reagents. |
| 10 | Design for Degradation | Degradation products of new chemicals should be designed to not persist in the environment, and breakdown into harmless compounds |
| 11 | Real-time analysis for Pollution Prevention | Analysis in 'real-time' to allow in-process monitoring and control of possible formation of hazardous compounds, should be a main consideration when developing new analytical methods. |
| 12 | Inherently Safer Chemistry for accident prevention | Chemicals, and compounds which form these substances should be chosen to minimise potential for chemical accidents – including releases, explosions, and fires. |

The fundamental element of the principles – to make chemistry 'benign by design' (Sheldon & Norton, 2020), focussing on prevention rather than remediation (Sheldon, 2017). Scientists and engineers are asked to apply the principles when designing novel chemicals, processes and products with the intention of avoiding the creation of harmful or toxic waste products (American Chemical Society, 2022).

The uptake of the principles over the last two decades was reviewed by Erythropel *et al.*, who noted significant progress in various Principles including 1, 6 and 9 (Prevention, Design for Energy Efficiency and Catalysis, respectively). However, they noted that Principle 4 (Designing safer chemicals), is one of the least developed principles (Erythropel *et al.*, 2018); attributing this to the lack of toxicity data readily available on potential effective and safe alternatives to hazardous compounds (Zimmerman & Anastas, 2015). Whereas, for other Principles, previously collected data has been used to develop guides which allow for easier adherence to Green Chemistry. For example, Principle 5 – Safer Solvent and Auxiliaries, states that solvent use should be minimised, and where possible, less harmful solvents should be substituted for more harmful solvents. To aid in selection, a solvent-risk rating has been developed, by reinterpreting many solvent selection guidelines (SSGs). The risk rating of over 150 traditional solvents used in analytical chemistry, were calculated by using an algorithm developed specifically for this purpose (E. Yilmaz & Soylak, 2020). Many physicochemical properties were taken into consideration including LogP, boiling point (°C), and viscosity (cP) of the solvent; and environmental factors such as the lethal water concentration for half the fish population (fish LC₅₀), the

photochemical tropospheric potential (POCP) and the half-life for biodegradation ($BOD_{1/2}$) (Gałuszka et al., 2013; Kokosa, 2019; E. Yilmaz & Soylak, 2020). Water has a risk rating of 1.0000 as it is considered innocuous; a reduction in risk rating indicates a potential environmental risk. The lower the calculated risk rating, the more harmful the solvent (e.g., ethanol has a risk rating of 0.9300, hexane a rating of 0.7057 and benzene a rating of 0.6098) (E. Yilmaz & Soylak, 2020).

Therefore, it is crucial that development and implementation of these guidelines continues throughout chemistry and other sciences. Though the underlying basis of Green Chemistry should be extrapolated to other areas, including the prescription of medications. Provided the therapeutic effect is equivalent, substitution of persistent, bio-accumulative and toxic compounds with alternative compounds which possess less harmful or hazardous profiles is of importance (Brooks, 2019). With respect to PhCs, an example would be replacing diclofenac sodium, an anti-inflammatory which is notoriously persistent in the environment (European Commission, 2014), with naproxen or ibuprofen - less harmful alternatives.

With the concept of green chemistry more widely acknowledged and implemented in all scientific industries, a sample preparation method for analysis of PhCs in biosolids and sludge, which meets the sustainable requirements is highly desirable.

2.6 Conclusion

In this chapter, the route of PhCs into the environment were presented and correlated with the adverse effects on the environment. The physicochemical properties of the PhCs, including LogP and MW affect the route of excretion, and distribution in WWTPs. The concentration of excreted PhCs is based on the location and population density.

The existing methods of analysing PhCs in complex matrices was reviewed. Extraction and analysis methods were evaluated on applicability to non-targeted analysis and alignment with Green Chemistry principles. It was demonstrated that a GCxGC method was suited for non-targeted analysis in many complex matrices, and thus could be applied to biosolid samples.

In the following Chapter, the instrumental and analytical techniques used for this research are discussed in detail.

Chapter 3: Instrumental and Analytical Techniques

3.1 Introduction

Several analytical techniques were used in this study. It is for this reason that a chapter which describes the principles of the analytical instrumentation used within the project has been included. The specific instrumentation and parameters are discussed in each research chapter.

3.2 Sample Preparation Techniques

The main techniques used in this study to improve sample preparations are ultrasonication – the application of ultrasound to chemical applications to facilitate reactions; and derivatisation – the changing of a compound to facilitate analysis. Ultrasonication is used to facilitate both liquid-liquid extraction and silylation derivatisation of pharmaceuticals from biosolids. Each technique is described in further detail, including the underlying processes and parameters.

3.2.1 Ultrasonication (Sonication)

Acoustics is known as the study of sound; defined by the waves, which create the sound. Ultrasound is defined as waves which operate at a different wave frequency to sound waves. Audible sound waves lie within the frequency of 10 Hz - 20 kHz, whereas ultrasonic waves have frequencies of greater than 20 kHz (Tiwari, 2015). Therefore, ultrasound is simply sound waves, which are pitched above human hearing. The waves can be transmitted through any solid, liquid or gas which possesses elastic properties (Luque de Castro et al., 2011); making it ideal for chemical applications, including extraction and derivatisation. When used in chemical applications, such as these techniques, the process is referred to as 'sonochemistry'.

Ultrasound used in sonochemistry can be classed into two main groups: low intensity (<1 W/cm²) and high intensity (10-1000 W/cm²) sonication. Low intensity sonication is defined as a non-destructive technique, used in quality assurance, particularly for the analysing the physicochemical properties of compounds. Conversely, high intensity sonication has destructive tendencies, commonly used in processing applications, and more notably, extraction (Tiwari, 2015).

Ultrasonication is an easy to use, versatile technique which aligns with green chemistry objectives and requires a low investment – thus is ideal for novel analytical methods. This study applies ultrasound to facilitate extraction and derivatisation processes. Although the process/reactions of each technique may differ, the underlying process remains the same.

3.2.1.1 Cavitation

The underlying process which drives extraction and derivatisation in sonication is cavitation. This process involves alternating between expansion and compression cycles in the liquid medium generated by high energetic ultrasonic waves, creating voids in the liquid, which are seen as bubbles (Hielscher, 2020b; Luque de Castro et al., 2011; Pérez-Lemus et al., 2019). Expansion produces negative pressure which pulls molecules away from each other, creating the cavities (bubbles) which grow, before imploding when the cavity can no longer absorb energy efficiently and so, collapse violently (during high pressure cycle) (Luque de Castro et al., 2011) (See Figure 3.1). The size of the bubble depends highly on the ultrasonic frequency and intensity (Seidi & Yamini, 2012).

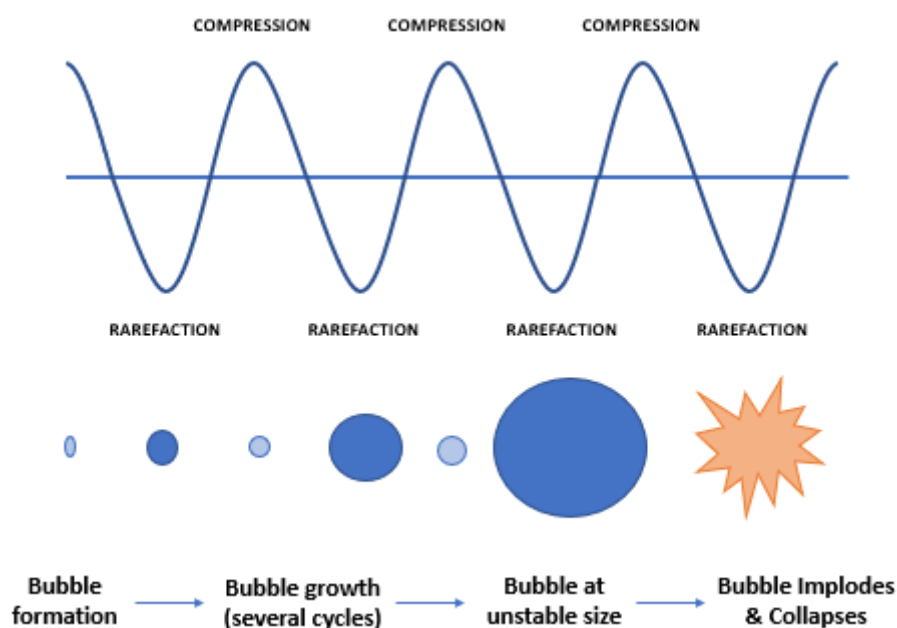


Figure 3.1: Cavitation process during ultrasonication: formation and growth of bubbles through compression and rarefaction cycles; before implosion. Adapted from (Hielscher, 2020b).

Cavitation bubbles can be divided into two types: transient and stable. Transient cavities exist for a very short period, often less than one compression and rarefaction cycle, before collapsing violently, whilst stable cavities are relatively long lived and exist for more than one cycle (Tiwari, 2015). When cavitation bubbles implode, several physical effects are produced, including shock waves, microjets and turbulence, which all influence the reaction taking place. Additionally, extremely high temperatures and pressures are reached locally (Hielscher, 2020a) during implosion, which are generally accepted as “the origin of the chemical effects” (Fiamegos et al., 2004). Estimated temperatures of about 4500-5000 K (Hielscher, 2020a) and pressures of 1000 -1700 atm (Cravotto & Cintas, 2006; Santos & Capelo, 2007) are reached, at a miniscule level (Tiwari, 2015).

The collapse of the cavitation bubble also produces free radicals and various other species (Cravotto & Cintas, 2006; Luque de Castro et al., 2011). When water is used as the solvent, highly reactive $H\cdot$ and

OH[•] radicals are produced through the dissociation of water. The radicals induce a variety of reactions, including silylation (Orozco-Solano et al., 2010), oxidation (Santos & Capelo, 2007), and degradation (Tiwari, 2015).

3.2.1.2 Factors which affect cavitation

The cavitation process is highly influenced by several factors. The operating parameters (frequency power or intensity and duration) of the ultrasound application (Pérez-Lemus et al., 2019); the solvent properties (type, ratio, viscosity, volatility and surface tension) (Cravotto & Cintas, 2006); and the temperature and pressure conditions of the reaction all have an effect on the cavitation process/ultrasonic methods (Tiwari, 2015).

Operating parameters

Ultrasonic power, intensity, or acoustic energy density (all which account for the energy entering the system), are the main design parameters when developing US methods. Intensity is proportional to amplitude; thus, intensity will increase if amplitude increases. A high amplitude enhances agitation, however, reduces levels of cavitation and so does not necessarily improve extraction efficacy (Tiwari, 2015). High amplitude can cause issues with probe erosion, which can contaminate samples with metal ions, particularly if a metal probe is used (Betts et al., 2013; Ong et al., 2016). Increased intensity can also promote degradation of analyte compounds; therefore, it is necessary to optimise the amplitude prior to sonication. Frequency will also influence the cavitation process. Most US systems operate at a given frequency, often in a low frequency range of 20-40 kHz (Tiwari, 2015). The sonotrode used in this study operating at 26 kHz (Hielscher, 2020c). Bubble lifetimes vary between 100-350 μ s (around 70-100 acoustic cycles) dependant on the applied frequency (Sunartio et al., 2007). Ultrasound applied in a continuous mode is thought to increase extraction yields (Pan et al., 2012), with similar mass transfer to ultrasound applied in pulsed mode (short bursts of sonication). However, pulsed mode will reduce energy consumption and increase the lifetime of the instrument (Tiwari, 2015).

Solvent Properties

Solvent choice has a large effect on the extraction process. The polarity of the solvent, and the solubility of the target analyte in the solvent are two major considerations in the extraction process. The chemical reactivity of the solvent influences the order in which chemical reactions will occur (primary or secondary etc.) (Tiwari, 2015). Therefore, solvent properties must also be taken into consideration prior to extraction. Viscous solvents reduce cavitation, whilst volatile solvents may evaporate during sonication, particularly if high temperatures are obtained. Solvent vapour pressure has a large effect on the intensity of the implosion, whilst surface tension (and viscosity) control the transient threshold of the cavitation bubbles (Tiwari, 2015).

Matrix properties

Matrix particle size has a large effect on sonication, with particular respect to extraction methods. Reducing particle size of the matrix, and increasing surface area by grinding samples for example, will increase the efficiency of the extraction. Application of ultrasound facilitates matrix swelling, which will also aid in diffusion and mass transfer, as pores of the matrix are enlarged by the process (Tiwari, 2015). Solvent to matrix ratio has a large influence on the extraction process - a smaller ratio is thought to decrease the extraction efficacy.

Reaction conditions

The changes in temperature and pressure help to facilitate both the derivatisation and extraction processes. Shear disruption associated with the changes create small pores on the matrix surface, which enhances solvent penetration and mass transfer of target compounds into the solvent through increased permeation (Tiwari, 2015). However, higher temperatures negatively affect cavitation, as solvent vapour can fill the cavities, preventing violent collapse (Tiwari, 2015). Implosion also causes microscopic turbulence, which accelerates diffusion through agitation and high velocity interparticle collisions (Tiwari, 2015). The intense mixing of samples influences the number of high velocity collisions between the analyte compound and the derivatisation reagent or extraction solvent. An increase in number of collisions, increases the overall reaction rate: with a decrease in derivatisation and extraction time being observed (Yebra, 2012).

3.2.1.3 Types of US instruments

There are three main types of instruments used to apply ultrasound to samples: ultrasonic baths, sonication probes, or sonoreactors (including sonotrodes) (see Figure 3.2). Sonication baths are common laboratory equipment; and thus, are relatively inexpensive. However, many limitations are associated with the baths. Baths are not powerful tools ($1-5 \text{ W/cm}^2$); and lack in uniformity of the ultrasound transmission (Delgado-Povedano & Luque de Castro, 2013) – the intensity of the ultrasound can differ at different locations in the bath (Santos & Capelo, 2007), which may negatively affect results (robustness). The loss of the ultrasonic energy originates from indirect sonication when using a bath as waves travel through the medium which surrounds the sample vial. Conversely, sonication probes are generally immersed into the sample medium, directly transmitting the high intensity energy for quick sample processing, with minimal energy loss (Tiwari, 2015). Generally, sonication probes are preferred over sonication baths due to their increased extraction efficiency and yield, and relatively short extraction times (Tiwari, 2015). Sonication probes generate around $\times 100$ greater power than sonication baths, with the added advantage of ultrasound parameter control (amplitude and pulse). However, probes are easily degraded and increase the possibility of cross- contamination between samples (Santos & Capelo, 2007). High-intensity probes can also raise the temperature of the medium to $85 \text{ }^\circ\text{C}$, which can lead to analyte degradation, or evaporation of the solvent medium (Santos & Capelo, 2007; Tiwari, 2015).

Sonoreactors (including the sonotrode) offer similarities to both the ultrasonic bath, and the sonication probe, by applying intense indirect sonication, without possibility of sample loss or contamination (Hielscher, 2020d). Ultrasound application using a sonotrode is generally x50 more intense than a bath (Tiwari, 2015), though less intense than a probe (probe>sonotrode>bath). Samples can be processed in sealed vials, which eliminates the possibility of sample loss via evaporation, or cross contamination.

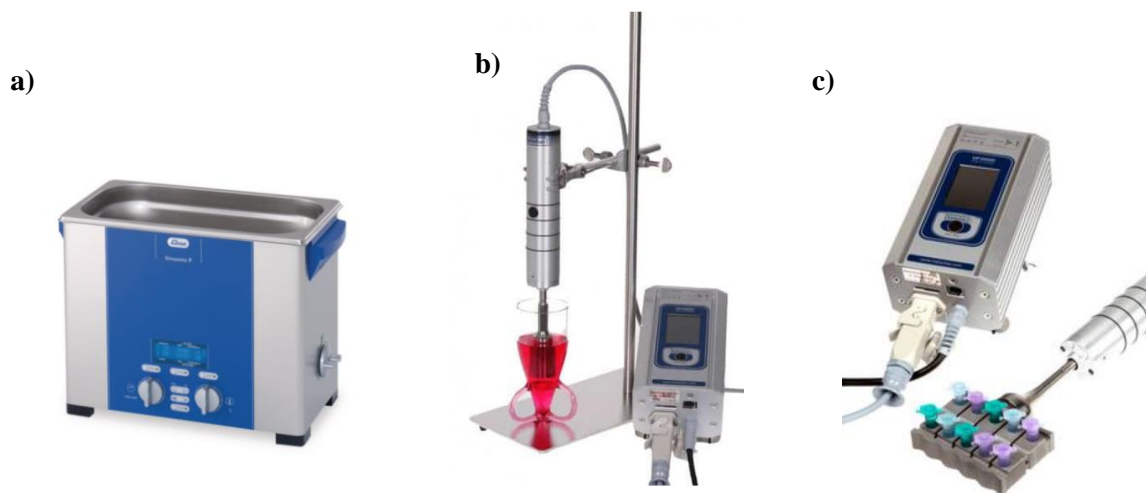


Figure 3.2: Instruments used to apply ultrasound to samples: a) sonication bath (Ultrasonic Baths, Elmasonic P Series, *n.d.*) b) probe (Hielscher, 2020c) c) sonotrode (Hielscher, 2020d)

3.2.2 Derivatisation

Derivatisation is the process of chemically transforming an analyte compound to increase its suitability for analysis by a specific analytical technique. Generally, derivatisation is applied to an analyte to increase the thermal stability and volatility of the compound, whilst simultaneously reducing its polarity for compatibility with gas chromatography (GC). Derivatisation improves the chromatographic performance (e.g., peak shape and separation) and detectability, whilst reducing thermal decomposition in the mass spectrum (Knapp, 1979).

Derivatisation of pharmaceutical compounds (PhCs) prior to GC analysis will enhance detection, improve peak shape, and provide a more sensitive technique in comparison to LC analysis, primarily due to the reduction in matrix effects (Kermia et al., 2016). Therefore, there is a real requirement for a derivatisation procedure which encapsulates as many PhCs as possible - to ensure that minimal compound selectivity is introduced for non-targeted analysis. This study aims to optimise silylation parameters for post-extraction derivatisation and analysis of PhCs in biosolid samples.

3.2.2.1 Derivatisation Methods

There are three main types of derivatisation reactions: acylation, alkylation and silylation; each replacing a labile (active) hydrogen (OH, NH, or SH) with an acyl, alkyl, or silyl group, respectively (Knapp, 1979). The choice of derivatisation depends on the analyte compound, with the processes applied either individually or in tandem to derivatise specific groups on the analyte, creating more

compatible derivatives. Reagents of varying strength can be applied to analyte mixtures, with catalysts and heating applied to facilitate the reaction.

Each of the derivatisation methods are described briefly, however, silylation is described in more depth as this technique was used throughout the study. A focus on optimisation of silylation for pharmaceutical compounds is detailed in Chapter 4.

Acylation

Acylation involves the replacement of a labile hydrogen, with an acyl (R-C=O-) group. The mechanism (see Figure 3.3) is a substitution reaction of the active hydrogen, and involves either nucleophilic, electrophilic, or free radical displacement of the leaving group on the acylating reagent.

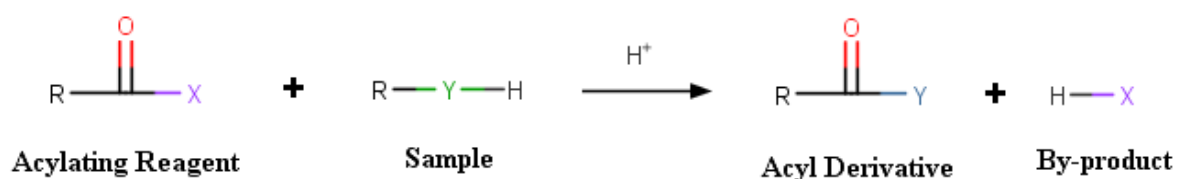


Figure 3.3: Acylation Reaction mechanism, where Y = hetero atom (i.e., OH, NH, or SH), X = leaving group (CH₃ etc.) and R = aliphatic or aromatic side group.

Acylation is commonly used to derivatise compounds with an active hydrogen, such as hydroxyl, thiol, and amino groups, converting them to esters, thioesters, and amides, respectively. Less commonly, acylation can also be used to derivatise unsaturated compounds (C=C) and aromatic rings (Blau & King, 1978; Sigma Aldrich, 2011). However, to the author's knowledge, acylation is not capable of derivatising carboxylic acids.

Possible reagents include acid anhydrides, acid halides, or acylated imidazoles, amides or phenols. However, the acidic by-products formed in the reaction with anhydride reagents must be removed prior to GC-MS analysis, otherwise will pose a degradation risk to the column (Knapp, 1979). Therefore, this is often not chosen as a derivatisation method for GC analysis.

Alkylation

Alkylation is described as the replacement of an active hydrogen with an aliphatic or aliphatic-aromatic alkyl group and is often used as a first step when derivatising. The principal reaction mechanism driving the reaction is referred to as nucleophilic displacement, shown in Figure 3.4 (Knapp, 1979). Generally used to derivatise carboxylic acids (in particular, converting fatty acids to their methyl esters or FAMES), alkylation is also capable of derivatising alcohols, thiols, amines, and amides, producing the respective esters, ethers, thioethers, N-alkylamines and N-alkylamides and sulphonamides.

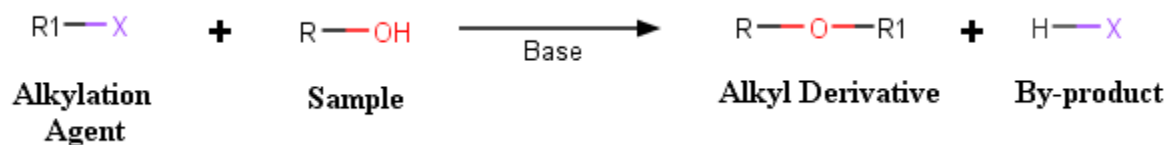


Figure 3.4: Alkylation Reaction Mechanism: Nucleophilic displacement (Knapp, 1979), where X is a halogen or good other leaving group and R and R1 are different aliphatic or aromatic side groups. A base catalyst is added to facilitate the reaction.

The reaction occurs in the presence of a basic catalyst. The strength of the catalyst depends on the strength of the acidic groups on the analyte. Weak acidic groups (e.g., hydroxyls) require strong basic catalysts, and stronger acidic groups (e.g., phenols or carboxylic acids) require weak basic catalysts.

Common alkylation reagents employed for this derivatisation include alkyl halides, nitro-substituted chlorobenzenes or fluorobenzenes, diazoalkanes, dimethylformamide dialkylacetals and tetraalkylammonium hydroxides.

Most alkylation reagents, (with particular regards to diazoalkanes), are considered as potential mutagens and carcinogens (Bloom, 2019). As this research is heavily focussed on Green Chemistry and environmental pollutants, the use of a potential mutagen or carcinogen as a reagent which will be heavily used in the study was counterintuitive. The risk of the agent entering the environment and the green chemistry mantra of making reactions ‘benign by design’, coupled with the plethora of literature studies successfully using silylation methods, the decision to use silylation as the derivatisation method was justified.

Esterification

Esterification is a type of alkylation but also can be considered as a stand-alone mechanism. The esterification process is shown in Figure 3.5; where an alcoholic reagent is used with a volatile acidic catalyst (e.g., HCl). The acidic group on the analyte takes a proton from the acidic catalyst, forming a positive oxygen group on the carbonyl in the acid (C-O+). The carboxyl group is condensed in the acid, and the OH group in the alcoholic reagent, eliminating water; and forming an ester derivative. A product of the reaction is water, which would need to be removed prior to GC analysis, akin to the acidic by-products of acylation.

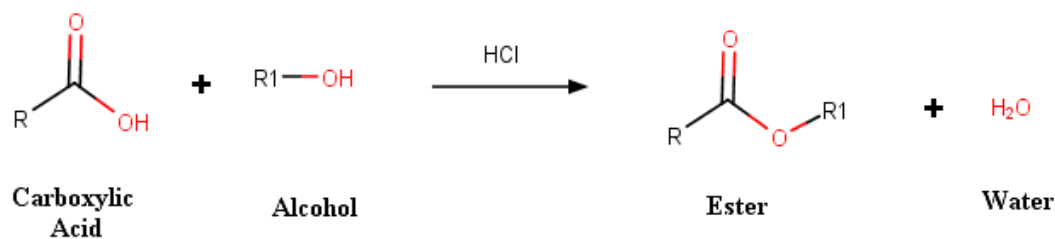


Figure 3.5: Esterification Reaction Mechanism adapted from (Halket & Zaikin, 2004), where R and R1 are different aliphatic or aromatic side groups. H^+ ions generated from a volatile acidic catalyst such as hydrochloric acid (HCl).

Although alkylation, esterification and acylation are all capable derivatising agents, silylation is the most widely used technique for derivatisation (Orata, 2012). This is echoed in studies which derivatise pharmaceutical compounds in environmental matrices, where alkylation methods are second to silylation (Caban & Stepnowski, 2018; Jux et al., 2002; Kumirska et al., 2019; Logarinho et al., 2016; Marsik et al., 2017; Sacher et al., 2001; Ternes, 2001), and acylation rarely used. As PhCs are the target of this study, silylation derivatisation was chosen as the derivatisation method and so is discussed in further detail.

3.2.3.1 Silylation

Akin to acylation and alkylation, silylation refers to the replacement of a labile hydrogen with a silyl group, most commonly a trimethylsilyl group (TMS) unless stated otherwise. Silylation reagents have the ability to react with a wide range of functional groups (alcohols, carboxylic acids, amines, and amides), readily volatilising samples and is therefore the most widely used technique for non-volatile samples (Orata, 2012), including PhCs. As silylation was the chosen derivatisation method in this study, the mechanism and other attributes will be detailed in this section.

Reaction Mechanism

Silylation follows the mechanism of a second order nucleophilic substitution reaction ($\text{S}_{\text{N}}2$) (Orata, 2012). The mechanism consists of a reaction between an electrophile and a nucleophile to form a derivative. An electrophile is an electron acceptor and a nucleophile an electron donor (has one or more lone pairs of electrons), which react to form a covalent bond. In general $\text{S}_{\text{N}}2$ reactions, a carbon atom on the electrophile is attacked by the labile hydrogen group on the nucleophile, however in the case of silylation, a silicon atom is attacked instead, and so is often denoted as $\text{S}_{\text{N}}2\text{-Si}$ in literature (Moldoveanu and David, 2014; Pierce, 1968).

In the reaction, the labile hydrogen group on the nucleophile (generally an OH or NH group) attacks the Si atom of the electrophile in a ‘backside attack’ (Orata, 2012; Serre, 1984). The attack forces the leaving group (e.g., chlorine) to leave, producing the silyl derivative. The single step process does not form any intermediate stages; however, these are included in Figure 3.6 to illustrate the reaction mechanism.

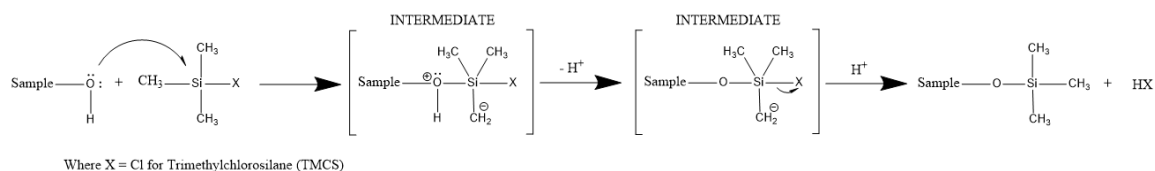


Figure 3.6: General single-step S_N2 -Si reaction mechanism for Silylation of compounds. Intermediate states (indicated by square brackets) for illustrative purposes only.

The S_N2 -Si reaction differs from a general S_N2 reaction as the silicon atom harbours unoccupied and accessible 3d orbitals, which allows for additional bonding (Pierce, 1968) (Figure 3.7). With reference to the silylation of a hydroxyl or carboxyl group, a lone pair of electrons on the oxygen atom is shared by the d orbital on the silicon atom of the electrophile (silylation reagent), creating a ($d\pi - p\pi$) dative bond, which allows for the formation of the penta-covalent intermediate stages (Pierce, 1968). Only one lone pair interacts and thus, nitrogen also shares this dative bonding phenomenon allowing for the silylation of amines. Initially the nucleophile (PhC) attacks the silicon to form the first penta-coordinated silicon intermediate; a loss of a proton alters the structure to the second penta-coordinated intermediate. The leaving group then leaves as an anion, which is protonated forming HX (Knapp, 1979) (Figure 3.6).

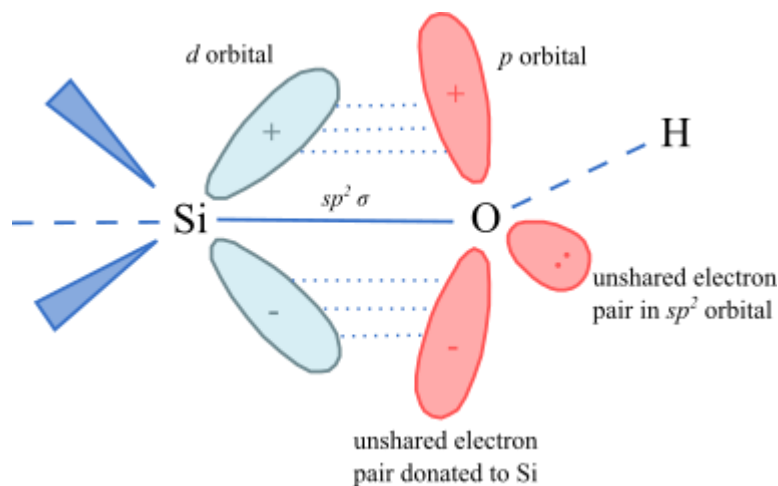


Figure 3.7: Formation of the penta-covalent binds through $p \rightarrow d$ bonding in the unoccupied 3d orbitals of the Si atom. The O atom of the nucleophile can be replaced with a N atom. Adapted from Pierce, 1968 (Pierce, 1968).

Ease of Silylation

The strength of both the electrophiles and nucleophiles present in the reaction have a large influence on the silylation reaction. Ease of silylation is known to decrease from hydroxyls (OH) > phenols (ArOH) > carboxylic acids (COOH) > amines (NH) > amides (CONH); with ease decreasing from primary (1°) to tertiary (3°) alcohols and from primary (1°) to secondary (2°) for amines (see Figure 3.8) (Moldoveanu and David, 2014; Orata, 2012; Pierce, 1968), in relation to the stability of the carbocation (see Figure 3.9). The decrease in ease of silylation can be described by a number of molecular factors.

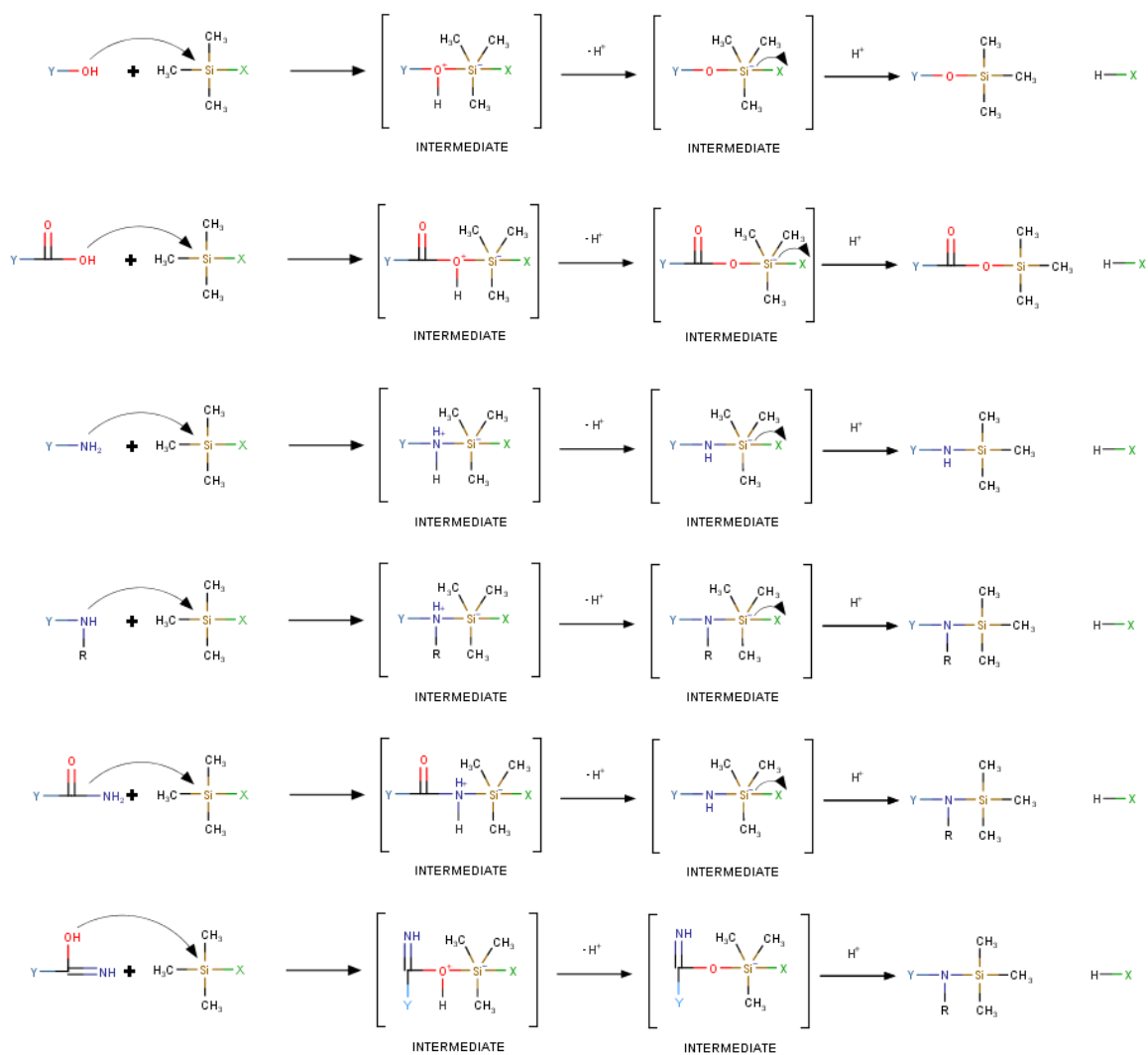


Figure 3.8: Silylation reaction mechanisms for a) examples for i) alcohols ii) carboxylic acids iii) primary amines iv) secondary amines and v) amide N vi) amide O, Y= sample, X = leaving group for example, Cl for trimethylchlorosilane (TMCS). Intermediates are for illustration only. Each reaction shows an S_N2 backside attack of the TMCS by the functional group. Ease of silylation decreases from top to bottom. Adapted from (Knapp, 1979).

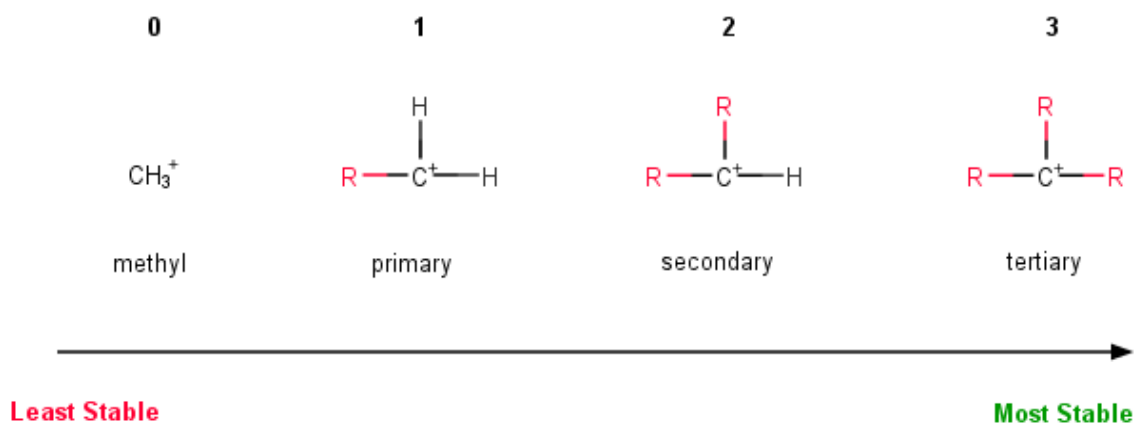
Number of R groups attached to the carbocation:

Figure 3.9: Stability of the carbocation. Stability increases with additional 'R' groups – from methyl group, to primary, secondary, and tertiary carbocations. Ease of silylation decreases from primary to tertiary groups, due to increased stability.

1. Electrophilicity

Silylation is highly dependent on the strength of the electrophile's leaving group. A strong leaving group is one which can accommodate a negative charge easily (Knapp, 1979) and has little to no $p \rightarrow d$ π bonding with the Si atom (Pierce, 1968); weak bases such as electronegative atoms (e.g. chlorine, fluorine) are ideal. The electrophile in the derivatisation reaction is the silylation reagent.

Many silylation reagents are available with varying silylation potentials including hexamethyldisilazane (HMDS), trimethylchlorosilane (TMCS), trimethylsilylimidazole (TMSI), bistrimethylsilylacetamide (BSA), bistrimethylsilylfluoroacetamide (BSTFA), N-methyl-trimethylsilylfluoroacetamide (MSTFA) and N-methyl-N-t-butyltrimethylsilyltrifluoroacetamide (MTBSTFA) (Figure 3.10). Increasing silyl donor ability will increase the strength of the bond being formed, and thus increase stability of the derivative (Parkinson, 2012). Silyl reagents are influenced by both the sample solvent and the addition of a catalyst (see below). Order of silyl donor ability often varies, however, it is widely considered that (without addition of a catalyst) HMDS is the weakest silyl donor, and BSTFA and MSTFA are strong silyl donors (Blau & King, 1978; Knapp, 1979; Moldoveanu and David, 2014; Parkinson, 2012).

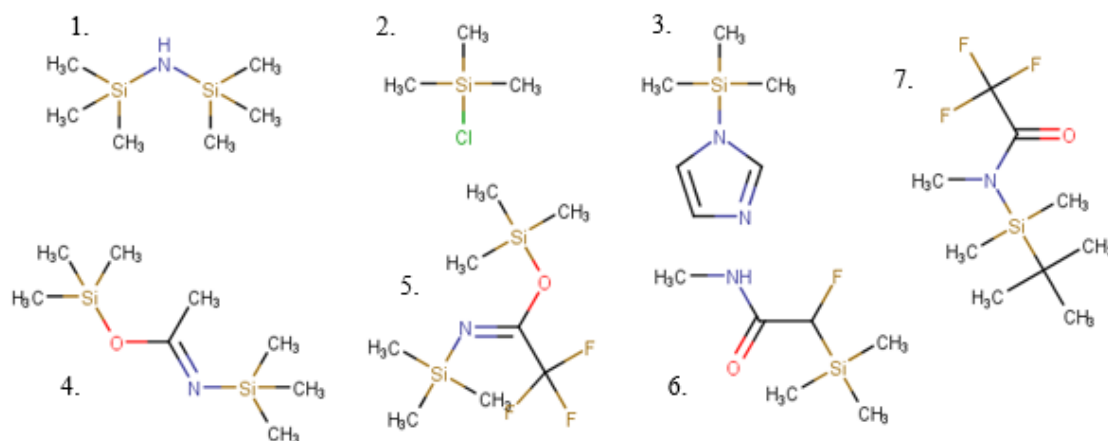


Figure 3.10: Silylation Reagent Structures: 1- HMDS, 2- TMCS, 3-TMSI, 4- BSA, 5- BSTFA, 6-MSTFA, 7- MTBSTFA

Silylation reagents, MSTFA and BSTFA + 1%TMCS are often used in the derivatisation of polar pharmaceuticals (Blau & Halket, 1993; Drewes, 2007; Migowska et al., 2012). BSTFA and MSTFA are widely considered to be strong silyl donors of similar silylation potential (Kumirska et al., 2013; Sigma Aldrich, 2018) and thus choice of reagent is theoretically interchangeable for the two reagents, however BSTFA remains the most common. MSTFA is the more volatile of the two, with by-products tending to elute with the solvent peak due to a lower boiling point of the by-products. Due to the increased volatility of the by-products, MSTFA is suitable for volatile trace analysis (Sigma Aldrich, 2011); and thus, when looking for non-targeted analysis of pharmaceuticals, often at trace concentrations, this is beneficial to prevent coelution with a target analyte.

2. Nucleophilicity

Likewise, a strong nucleophile is also required for silylation. Stronger nucleophiles increase the rate of reaction. Hydroxyls are the strongest nucleophilic group, and the easiest to silylate. Oxygen atoms bear two lone pairs of electrons, which are more sterically available than the unique lone pair on a nitrogenous compound: therefore, increasing the donation ability of the compound. An increase in nucleophilicity is also observed with increasing electron density, and therefore conjugate bases of acidic functional groups are easier to silylate. In the deprotonated form (O^- or COO^-), hydroxyls have an additional lone pair of electrons, which increase the number of electron pairs able to be donated from two to three. Amines and amide groups are considered weaker nucleophiles; both are considered weak acids, and thus removal of a proton is harder to facilitate. In the derivatisation reaction in this study, the pharmaceutical compound is the nucleophile. Altering the pH of the solvent, can ensure analytes are in the ionised form to facilitate the reaction.

3. Electron withdrawing effects

Electron withdrawing effects within analyte compounds can hinder the silylation reaction. Conjugation found in double bonds or benzene rings, decreases the donation ability (Moldoveanu and David, 2014),

as electrons are part of an electron cloud, and thus harder to remove. Therefore, ArOHs are harder to silylate than OH groups due to conjugation in the benzene ring. Other electronegative atoms close to the nucleophilic group, will also have withdrawing effects. The addition of a second oxygen group, coupled with a double bond in a carboxylic acid, decreases the ease of silylation, and thus are harder to silylate than OH or ArOHs (Figure 3.11b).

Resonance and tautomerisation created by electron-withdrawing effects, have cast speculation to the location of the silylation reaction for amide groups. The silylation reaction is theorised to take place at the nitrogen atom, as this has the labile hydrogen; however, it is also theorised that due to the ability of the electrons in the amide group to shift between the nitrogen and oxygen atoms (Figure 3.11a); the reaction instead occurs on the oxygen atom (Caban & Stepnowski, 2018).

Oxygen has a higher affinity for the silicon atom, therefore, a Si-O bond would be favoured for greater thermal stability than a Si-N bond (Pierce, 1968). Caban & Stepnowski, 2018 favour O-silylation of the amide group in their work with acetaminophen. This is reiterated by Pierce, 1968 who theorised that resonance contributions of a phenyl group will stabilise an O-silylated compound (paracetamol contains a phenol group). However, Pierce also suggests that the O-silylation occurs first with a rapid tautomeric shift to the N-TMS-amide, as this is, in general, more stable. Little theorised that both N-silyl and O-silyl tautomers can be formed (Little, 1999).

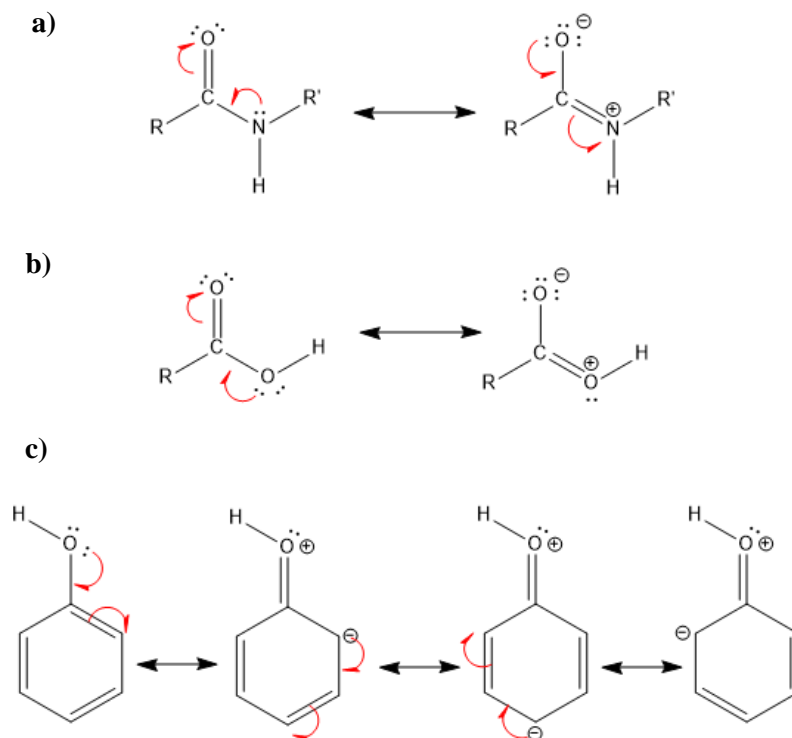


Figure 3.11: Resonance Structures: a) Amide - electrons oscillate between the nitrogen and oxygen atoms b) Carboxylic Acid - electrons oscillate between the two oxygen atoms c) Phenol - electrons oscillate between the oxygen and benzene ring

4. Steric Hindrance

The ability of a nucleophile attacking an electrophile is heavily influenced by steric hindrance on both counterparts. As the functional groups adjacent to the silicon atom (electrophile) increase in size (from $H > CH_3$ etc.), the nucleophile's ability to access the Si atom is severely impeded, resulting in a slow reaction, or no reaction at all (Blau & King, 1978) (Figure 3.12). Smaller groups are therefore advantageous. This is observed on the nucleophile also, where large, bulky groups adjacent to the active hydrogen containing group, create a larger steric effect, impeding the ability of the nucleophile from accessing the electrophile, hindering the reaction (Moldoveanu and David, 2014). Thus, describing the reduction in ease of silylation from a primary to secondary amine and primary to tertiary alcohol.

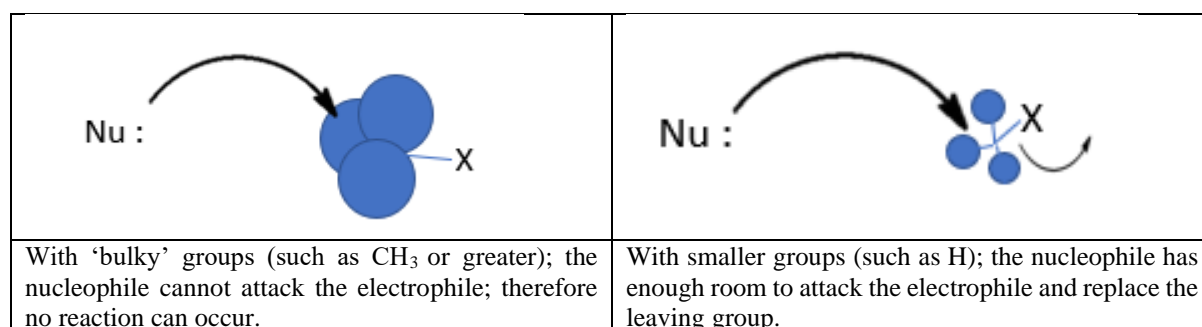


Figure 3.12: Effect of Steric Hindrance on nucleophilic attack of an electrophile. The same phenomenon is observed when the sterically hindered groups are attached to the nucleophile.

5. Catalyst

Reaction rates can be increased by the addition of a catalyst, such as pyridine or trimethylchlorosilane (TMCS) (Blau & King, 1978). Basic catalysts (pyridine) are added as acid scavengers (Orata, 2012), aiding in the removal of protons from the solution. TMCS is generally added to stronger silylating agents such as MSTFA or BSTFA to facilitate a reaction by increasing the silyl donor strength (Knapp, 1979). TMCS is itself, a TMS containing electrophile with a strong leaving group (Cl), which will react with any nucleophilic groups. Due to the smaller structure of the TMCS, compared with larger silylating groups (MSTFA or BSTFA), less steric effects will be observed, and thus TMCS may silylate more sterically hindered groups on the analyte. Some postulate that when used together, pyridine and TMCS form a complex (Pierce, 1968), which then reacts with the analyte, however to the author's knowledge, this has never been proven.

Reaction Time and Temperature

Reaction time is compound dependant and thus varies widely. Many compounds are completely derivatised upon dissolution in the silylation reagent (Blau & King, 1978), however sterically hindered and difficult to silylate compounds may require a longer silylation period to reach complete derivatisation (Pierce, 2004). Reaction time can be decreased by increasing the kinetic energy of the

reaction, by either increasing temperature (Li, 2017), applying ultrasound (Cohen et al., 2018), or using a catalyst (Blau & King, 1978).

Applying heat has been shown to facilitate the silylation reaction, whilst also encouraging silylation of hindered, or difficult to silylate groups (Blau & King, 1978). However, care must be taken to avoid thermal degradation of compounds, prior to their complete derivatisation (Sigma Aldrich, 2011). Typical procedures require heating to between 60-80 °C for upwards of 20 minutes; with some compounds in extreme cases requiring up to 16 hours to ensure complete derivatisation (Sigma Aldrich, 1997). On occurrence, temperatures of up to 150 °C are required (Pierce, 1968). Unhindered primary alcohols often fully derivatise immediately at room temperature and thus require no heating (Pierce, 2004). As temperature is thought to have an influence on the reaction time, these parameters are often considered together when optimising silylation reactions.

Additionally, increasing the volume of the silylation reagent will reduce the reaction time, as the second order rate reaction is transformed into a pseudo-first order reaction (see Rate of Silylation and Molar Ratio).

Rate of Silylation and Molar Ratio

The rate determining step in a silylation reaction is bimolecular, i.e. there are two reactants, the pharmaceutical compound and the derivatisation reagent, and thus the rate depends on concentrations of both (Ouellette & Rawn, 2015). The rate (v) of S_N2 reactions are considered overall to be second order, first order in the electrophile (derivatisation reagent) and first order in the nucleophile (analyte) (Ouellette & Rawn, 2015), suggesting that if the concentration of one is doubled, the rate of reaction will double.

$$v = k[Der. Agent]^1[analyte]^1 \quad (3-1)$$

Where v = rate of reaction ($M s^{-1}$), k = rate constant (s^{-1}), $[Der. Agent]$ = concentration of derivatisation agent (M) and $[analyte]$ = analyte concentration (M).

However, S_N2 reactions have extensively been studied under pseudo-first order reaction conditions (Seoud et al., 2016) due to one reactant being present in a large excess (Latham & Burgess, 1977; Orata, 2012). From literature, it is stated that a minimum excess of 2:1 (molar ratio = Der. Agent: labile hydrogen) is required for derivatisation to occur, therefore the analyte (nucleophile) is the limiting reagent in the reaction. Generally a far higher ratio is undertaken (>100:1), to ensure the silylation reagent is in excess and thus the application of pseudo first order conditions is applicable (Seoud et al., 2016). When one reactant is in a large excess ($[Der. Agent] \gg [analyte]$), the amount of Der. Agent consumed is negligible, and thus the rate is mainly dependent on the $[analyte]$, thus a pseudo-first order reaction is given for the disappearance of the analyte:

$$v_{\text{analyte}} = k_{\text{obs}}[\text{analyte}]^1 \quad (3-2)$$

Where v_{analyte} = rate of reaction of analyte ($M s^{-1}$), k_{obs} = observed rate constant ($M^{-1}s^{-1}$) and $[\text{analyte}]$ = analyte concentration.

The proportionality factor (k_{obs}) deduced from an experiment is known as the observed rate constant, and is related to k by:

$$k_{\text{obs}} = k[\text{Der. Agent}]^1 \quad (3-3)$$

PhCs can contain multiple functional groups at which the derivatisation reaction can occur. Each labile hydrogen will compete for the derivatisation reagent and should be considered as competitive reactions with different rates. This will have an effect on the overall reaction rate. Therefore, the number of active sites (labile hydrogens) on the analyte molecule must be taken into consideration when calculating the molar ratio. The molar ratio of the reaction will influence the reaction rate and can be increased with increasing volume of silylation reagent. However, it would seem that most studies do not calculate the molar ratio, with many choosing a reagent and volume which are in a large molar excess with no optimisation (Blau & King, 1978; Kumirska et al., 2019; Migowska et al., 2012). Others optimise silylation by opting for a volume of reagent and varying all other parameters (reagent, heating, shaking) (Caban & Stepnowski, 2018; Kumirska et al., 2013; Lacina et al., 2013; Sebök et al., 2008) or choosing one reagent and varying the volume used (Samaras et al., 2011; Wu et al., 2009).

3.3 Design of Experiments (DOE)

Development and optimisation of novel analytical methods is a lengthy and costly process. The response of an experiment relies on many different factors, all of which can potentially facilitate or hinder the reaction in question. Changing one factor at a time may seem the most intuitive and logical approach to increasing response of the reaction, however, requires numerous experiments which is time consuming, and solvent and energy heavy. To overcome this, design of experiment (DOE) techniques are implemented.

DOE is a systematic approach to problem solving (National Institute of Standards and Technology, 2012a), used to investigate the process/reaction and understand how experimental factors influence the overall response (Wagner et al., 2014). Factors (or input variables) are defined as variables which are likely to affect the process – i.e., time, amplitude, and pulse for ultrasonication reactions used in this study. Factors can be divided into different levels, for example the ‘volume of MSTFA added’ could be divided into two levels of 25 μL and 100 μL or 4 levels of 25 μL , 50 μL , 75 μL , and 100 μL . For factors which have infinite values (i.e., time), high and low levels are identified (i.e., 1 and 10 mins), ensuring the experimental range of values is covered.

DOE can be applied to experiments to solve numerous problems (National Institute of Standards and Technology, 2012a):

- a) To decipher whether a single factor has resulted in a change in the overall process
- b) To understand which factor(s) influence the process (ranked from most important to least important)
- c) To model the process with a high predictive power
- d) To optimise the process response

Used prior to data collection (experimental design stage), DOE constructs a set of representative experiments (Sartorius, 2020), which will vary all factors at once, avoiding numerous unnecessary experiments (National Institute of Standards and Technology, 2012b). The number of input factors is not limited by DOE, therefore numerous input factors can be narrowed down to a critical few throughout the DOE process. DOE rationally connects experiments, to estimate the influence of each factor on the overall response (Sartorius, 2020). The response (output variable) is defined by the user.

Experimental software (i.e., Minitab) can be used to create, randomise, and analyse the DOE. The run order of the experiments is randomised to prevent bias on the response variable. There are many ways in which DOE processes can be implemented to optimise an experiment. Three DOE processes were utilised in this study, each is outlined below.

3.3.1 Screening Test

To determine the most important input factors from a large number of potential factors, a screening test is applied (National Institute of Standards and Technology, 2013). Factors with little effect on the response are eliminated. Fractional factorial (resolution III) and Plackett-Burman designs can have up to 15 and 47 factors (input variables), respectively (Minitab Inc., 2017; National Institute of Standards and Technology, 2012b). These designs are used to screen linear terms, which allow for a low number of experimental runs. However, both are classed as 2-level designs (see below) and so cannot estimate squared terms or curvature in response. Definitive screening designs (DSDs) are classed as resolution IV designs and tend to have greater than four factors and include linear and square terms.

3.3.2 Factorial Designs

A factorial design is used to determine the effects of multiple factors on an experimental response. Multiple factors are studied simultaneously, which reduces the number of experiments. To determine interaction effects, each factor is studied at more than one level. Generally, each factor is studied at two coded levels; high (+) and low (-) and an optimal factor level, to evaluate the robustness in both directions. Coded factor levels are chosen by the operator and should be within a reasonable distance from the optimal factor.

The effect of each factor on the chosen response factor is calculated by subtracting the average response at the low (-) variable from the average response at the high (+) variable. A comparison of the effect indicates the factor with the most influence on the response. This is often illustrated in a Pareto Chart (see 3.3.4 DOE Outputs). Therefore, important factors (those which cause an effect on response) can be distinguished from less important factors.

DOE can be used to determine factor interactions which influence the response variable, something which cannot be determined using a one-factor-at-a-time approach. Coded values for interaction effects are calculated by the multiplication of the single effect (A, B or C). For example, the interaction effect of factors A and B would be AB. However, the levels must also be included, and thus the overall effect can be calculated as follows: $A(+)*B(+)=AB(+)$, $A(+)*B(-)=AB(-)$, $A(-)*B(+)=AB(-)$ or $A(-)*B(-)=AB(+)$. The interaction effects are calculated in the same way as for individual effects and are generally illustrated with an interaction plot or contour plot (see 3.3.4 DOE Outputs). It is assumed that the importance of interactions will decrease with increasing factor levels, and thus it is unlikely that there will be significant interactions with more than two factors (Lechner, 2021).

Full factorial designs measure the response at all combinations of the factor levels. The number of experiments to run (n) is determined by the number of factors (k), where $n = 2^k$. A 2-level design with 3 factors, results in 8 experimental runs; 4 factors result in 16 runs etc. All combinations of factor levels are included in the experimental runs. As k increases, n increases rapidly and thus a fractional factorial design could be applied.

Fractional factorial designs only analyse a selected ‘fraction’ of the full factorial design (see Figure 3.13). This is often applied where resources or time are limited, or when the design includes a large number of factors, to reduce the number of experimental runs. However, as this is only a ‘fraction’ of the full factorial design, some factors and interactions may be confounded.

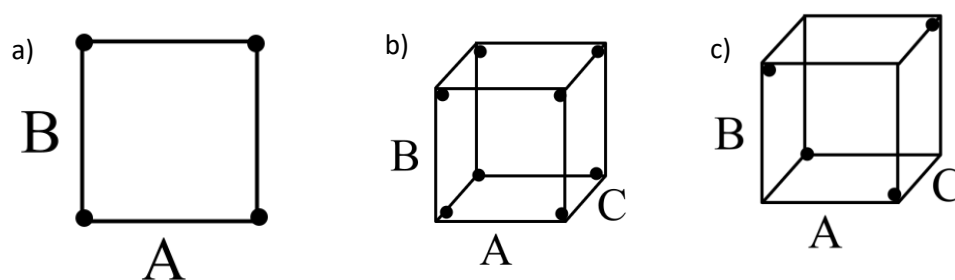


Figure 3.13: Factorial Designs where A, B and C are different factors. a) Two-factor design with two levels, b) Three-factor design with two levels c) Three-factor fractional factorial design (1/2) with 2 levels

3.3.3 Response Surface Regression Design

Once important factors have been determined using the screening or factorial designs, response surface design can be used to refine the model and optimise the response factor. Response surface designs

differ from factorial designs, as curvature in the response can be modelled. There are two types of response surface designs – central composite (CCD) or Box-Behnken (BBD). CCD can fit a full quadratic model, whereas BBD have fewer points which generates a lower number of runs, with the same number of factors. BBD have 3-levels per factor, whereas CCD can have up to 5 factors. CCD include all factor settings, including extreme settings (all low/high settings); whereas BBD do not.

CCD are the most commonly used response surface designs. The designs are similar of that to full or fractional factorial designs, with additional centre and axial points (Figure 3.14a). These additional points allow for curvature modelling. Curvature is detected when the mean response of the centre point is significantly greater or less than the mean response of the factors at their low or high levels (Minitab Inc., 2017). However, centre points alone do not have enough information to model curvature and thus a face-centered central composite design (CCD) is applied.

In face-centered designs, axial points are located at the centre of each face (Figure 3.14b). The face-centered CCD encompasses the required quadratic terms (square terms), adding more points to the design. The model described linear main effects, 2-factor interactions, and square terms for all continuous factors, which allows for a quadratic model to be fitted.

BBDs are independent quadratic designs, where points are located at the midpoints of the edges and at the centre. The main advantage of this design is the lower number of experimental runs; however, issues with regions of poor predictability (missing corners) gives rise to potential losses in data. Therefore, face-centered CCD designs were used in this study.

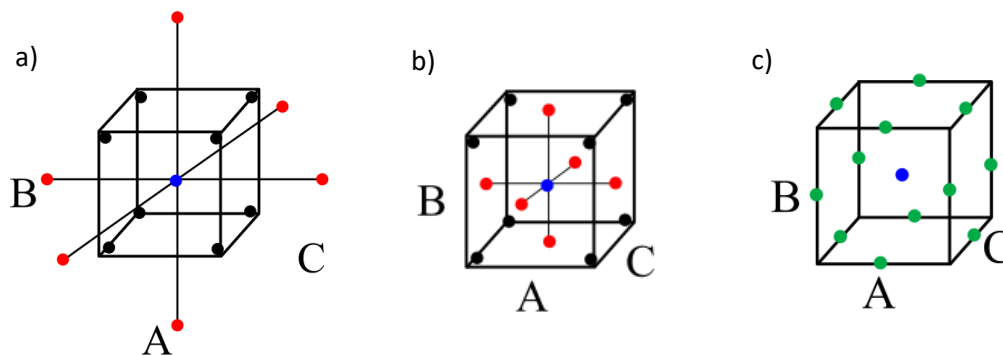


Figure 3.14: Response Surface Regression Design a) Central Composite Design (CCD) points b) Face-centred CCD c) Box-Behnken design (BBD). Black = factorial points, red = axial points, green = mid-points and blue = centre points.

3.3.4 DOE Outputs

3.3.4.1 Pareto Charts

A pareto chart defines the statistically significant factors which effect the response and is an output of a screening or factorial design. The chart allows for comparison between the relative magnitude of the standardised effect of each factor, as both main and interaction effects. Factors are displayed as bars on the chart – any bar which crosses the red dashed line, indicates a statistically significant factor (p-value

= 0.05) (Minitab Inc, 2022). Although significant factors are identified, the effect of the factors on the response (increase/decrease) cannot be determined at this stage (Minitab Inc., 2020).

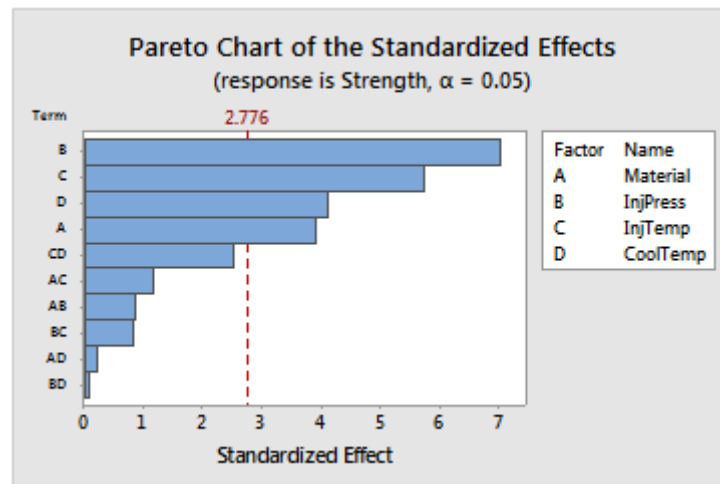


Figure 3.15: Design of Experiment output: Example of a Pareto Chart (Minitab Inc, 2022). Factors are displayed as blue bars on the chart. Any factor which has a statistically significant effect (95% confidence limit) on the response (strength) will cross the red dashed line. In this example, each individual factor is significant, however the interactions between the factors are not.

3.3.4.2 Interaction Plots

Interaction plots are an output of a factorial design and illustrate possible interactions between different factors. Factors with considerably different slopes (i.e., large variation in gradients) between the line of each factor, indicate a higher degree of interaction. However, statistically significant interactions cannot be drawn from the plot. Parallel lines indicate no interaction.

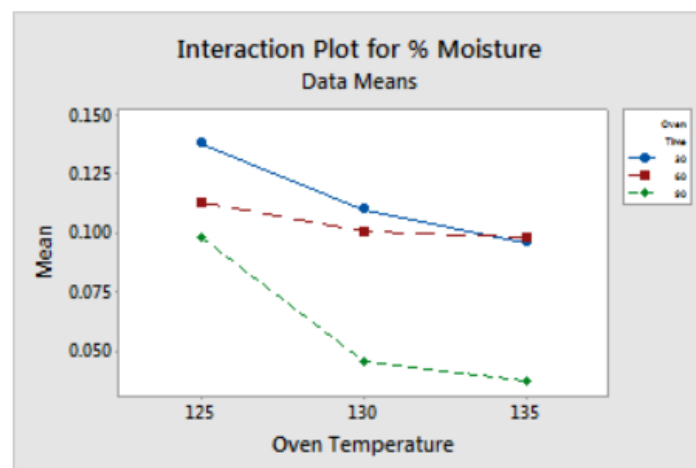


Figure 3.16: Design of Experiment output: Example of an interaction plot. Interaction between oven temperature and oven time is observed. A lower % moisture is observed at 135°C when baked for 30 mins, instead of 60 mins. Although baking for 90 mins produced the lowest moisture content at all temperatures. Interaction was only visible between values for 30 and 60 mins.

3.3.4.3 Contour Plots

Contour plots are used to plot the relationship between two important continuous factors and a fitted response. These plots can be an output of a screening, factorial, or response surface design. The plots are used to determine settings which will maximise (or minimise – depending on the desired analysis) the response variable. Points which have the same response value are connected, to produce contour lines (Minitab Inc., 2021a). Colours represent different contours, thus indicating differences and similarities in response.

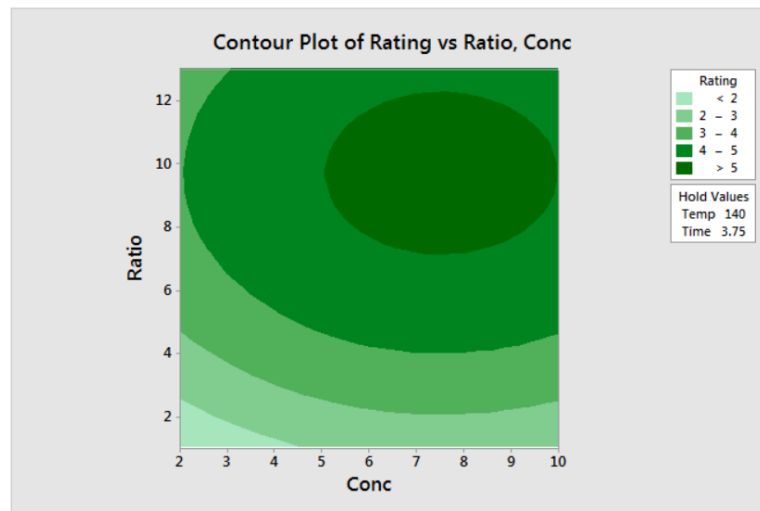


Figure 3.17: Design of Experiment output: Example of a contour plot (Minitab Inc, 2019). Curved contours indicate statistically significant quadratic terms in the model. The response increases with increasing concentration and ratio, with the highest response indicated by the dark green colour.

3.3.4.4 Optimisation Plots

Optimisation plots are used to identify the optimal settings of input variables (factors) required to produce a given response (or responses). These plots are an output of a screening, factorial, or response surface design. In this study, it is an output of the response surface design. The user indicates which response is to be optimised in the optimisation settings, prior to production of the plot. Factor settings (high and low) are described at the top in black, with the optimal setting for each described in red. Response variables are on the left-hand side of the chart, with the optimised response labelled (maximum or minimum). The blue dashed line on the plot represents the response for the current factor level and the red line represents the current factor level. The composite desirability (D) and desirability of each response (d) should be as close to 1 as possible – this indicates the desired response is optimised. If two responses were to be optimised, one response maximised and one minimised, D would indicate the overall ability of the model to optimise both responses. A low composite desirability (D) may indicate one response is optimised, though the other is not.



Figure 3.18: Design of Experiment output: Example of an optimisation plot (Minitab Inc, 2021b). Flexibility and Strength are maximised with factor settings of Press: 95, Sealant = 75 and Machine = 2 – all are the high settings of the factors.

3.3 Chromatographic Techniques

Chromatography is an invaluable tool in today's laboratory, for separating and identifying compounds in a sample. Sometimes referred to as the 'separation science', chromatography derives from the Greek words '*chroma*' and '*graphien*' translating to 'writing with colour' (Bergslien, 2012). Chromatography is defined as a 'physical method of separation in which the components to be separated are distributed between two phases, one of which is stationary, the other moves in a definitive direction' (Lewis, 2009). Whether thin layer chromatography (TLC), liquid chromatography (LC) or gas chromatography (GC), the mobile phase and stationary phase are two of the main components required for the separation. The mobile phase, is the phase which moves, often denoted by the primary word in the chromatography name, gas in **GC** and liquid in **LC**. The stationary phase remains constant, a sorbent, chosen with reference to the targeted analytes of one's analysis. Analyte compounds will partition between the stationary phase and the mobile phase, dependent on affinity, and thus separation occurs.

Paper (planar) chromatography is the simplest version of the technique: a piece of filter paper bearing a dot of ink, is placed in a small volume of solvent, ensuring the dot remains above the solvent level. The solvent will progress through the filter paper by capillary action and break down the ink dot into smaller components. The solvent will continue to travel up the filter paper, with some soluble components travelling further than others, dependant on their affinity for the solvent. Components will eventually resolve, and the distance travelled can be used to identify them.

This mechanism is emulated in slightly different ways throughout the chromatography techniques, but the basis remains the same. Both LC and GC techniques were employed in this study and are described in further detail.

3.3.1 Capillary Column Gas Chromatography

Gas chromatography (GC) is a chromatographic technique widely used in pharmaceutical and environmental analysis. As the name suggests, gas is used as the mobile phase, either nitrogen (N₂), hydrogen (H₂) or mostly commonly Helium (He), and thus analytes must be in the gaseous phase for this analysis and so must be relatively volatile.

Separation of compounds is based primarily on boiling point (b.p.), with secondary influence of the polarity of the compound and its affinity for the stationary phase. Volatility is a main factor which affects separation in GC: in general, the lower the boiling point, the less retained the analyte is within the GC column; thus, solvents with low b.p. are often used (dichloromethane, ethyl acetate, methanol etc.), to ensure little to no interference with analyte compounds.

Physicochemical properties of the analyte will influence its volatility. Larger compounds (such as macrolide antibiotics) by nature have a relatively high molecular weight, which increases the boiling point of the compound. This introduces limitations to the analysis, as compounds with a MW of > 400 a.m.u. have little to no volatility, and thus are incapable of being analysed using GC. Analytes with an increased number of halogen atoms (N, O, Cl etc.) have both increased polarity and molecular weight. The higher MW atoms coupled with the increased energy required to break the strong intermolecular bonds, increase the boiling point of the analyte which creates issues with GC analysis. To reduce the polarity and increase the volatility and thermal stability of the analyte compounds, derivatisation is applied in the sample preparation stage (see 3.2.2 Derivatisation).

One dimensional GC set-up

In one-dimensional chromatography, the sample is injected into the instrument where it travels through the capillary column in the mobile phase, eluting to the detector in order of affinity for the stationary phase of the column. Traditionally GC instruments are coupled to flame ionisation (FID), electrochemical (ECD) or mass spectrometer (MS) detectors, depending on which detector best suits the analysis in question. All detectors used in this study were variants of mass spectral detectors and described in the section titled “3.4 Mass Spectrometry Techniques”.

Injection

Small volumes (0.5-2 µL) of sample are injected into the GC via syringe either through manual injection, or automatic injection. Automatic injection ensures that the injection is repeatable and reproducible, generally producing better results in terms of reproducibility. Manual injection can introduce human error, particularly with small injection volumes, however this can generally be accounted for by the inclusion of an internal standard.

There are two possible injection modes in GC: split or splitless. Splitless injection ensures all sample injected transfers to the column, whereas split injection transfers only a specified fraction (i.e., a split

ratio of 10:1 = 10%) of the sample to the column. Split injection is therefore generally used for highly concentrated samples, to avoid overload and contamination of the column, and splitless is used for trace analysis. Samples with challenging matrices such as wastewater can be analysed using splitless mode, post-sample preparation (including sample clean-up).

Inlet/Oven

The transition of the compound from liquid to gaseous phase is a major factor in GC analysis and is controlled by the inlet and oven temperatures. High inlet temperatures ensure that the sample is converted to the gaseous phase, whereas the temperature programme (within the GC oven) controls the partitioning of the analyte into the stationary phase. Isocratic elution is obtained by constant oven temperature, whereas temperature programmes start at a low temperature (often 40 °C), and gradually increase throughout the run at a specified rate, which allows for a range of analytes (with a range of volatilities) to be separated in one injection, within a reasonable timeframe. Generally, a scouting method will be applied in the first instance to determine whether an isocratic or gradient temperature programme is required.

Columns

The polarity of the compound and the analyte's affinity for the stationary phase is another factor which attributes to well performed GC analysis. In capillary columns (more widely used than packed columns), the stationary phase is located in the column in the inner walls (see Figure 3.19). The stationary phase is chosen dependant on the polarity of the target analyte compounds. Non-polar stationary phases will retain non-polar analytes for longer, eluting polar analytes first, and vice versa for polar columns. Capillary GC has been utilised for many years due to the high plate numbers (100 K+) generated, which provides powerful separations with high efficiency. As the mobile phase cannot be changed, the selectivity is obtained from the column stationary phase (see 3.3.4 Column Theory for further detail).

Columns are typically 30-60 m long, with a film thickness of between 0.1 and 10 µm and an internal diameter between 0.25 µm and 0.5 µm. Due to the nature of GC, thermal stability to at least 325 °C is common for capillary columns, allowing for separation of higher MW compounds; however, columns designed specifically for the analysis of high MW compounds are available (higher maximum temperature). The stationary phase is the main component of the columns, with the polarity of the stationary phase is indicated by an OV- number, the higher the number, the more polar the phase. Different manufacturers may change the OV- (Ohio Valley) to DB- (Agilent), HP- (Agilent) or Rtx- (Restek), however the principal remains the same. For example, a DB-5 column is routinely used non-polar column, with a stationary phase consisting of (5%-phenyl)-methylpolysiloxane, whereas a DB-17 column is a mid-polar column consisting of (50%-phenyl)-methylpolysiloxane. The DB-5 is equivalent to HP-5 and DB-17 to HP-17 etc. Generally, a stationary phase thickness of 0.25 µm is used, however

the thickness can vary on the analysis. An increasing stationary phase thickness will increase retention of volatile compounds, as the analyte can diffuse further into the phase, and so is retained for longer, whereas thin films are used for high MW compounds (de Zeeuw, 2017).

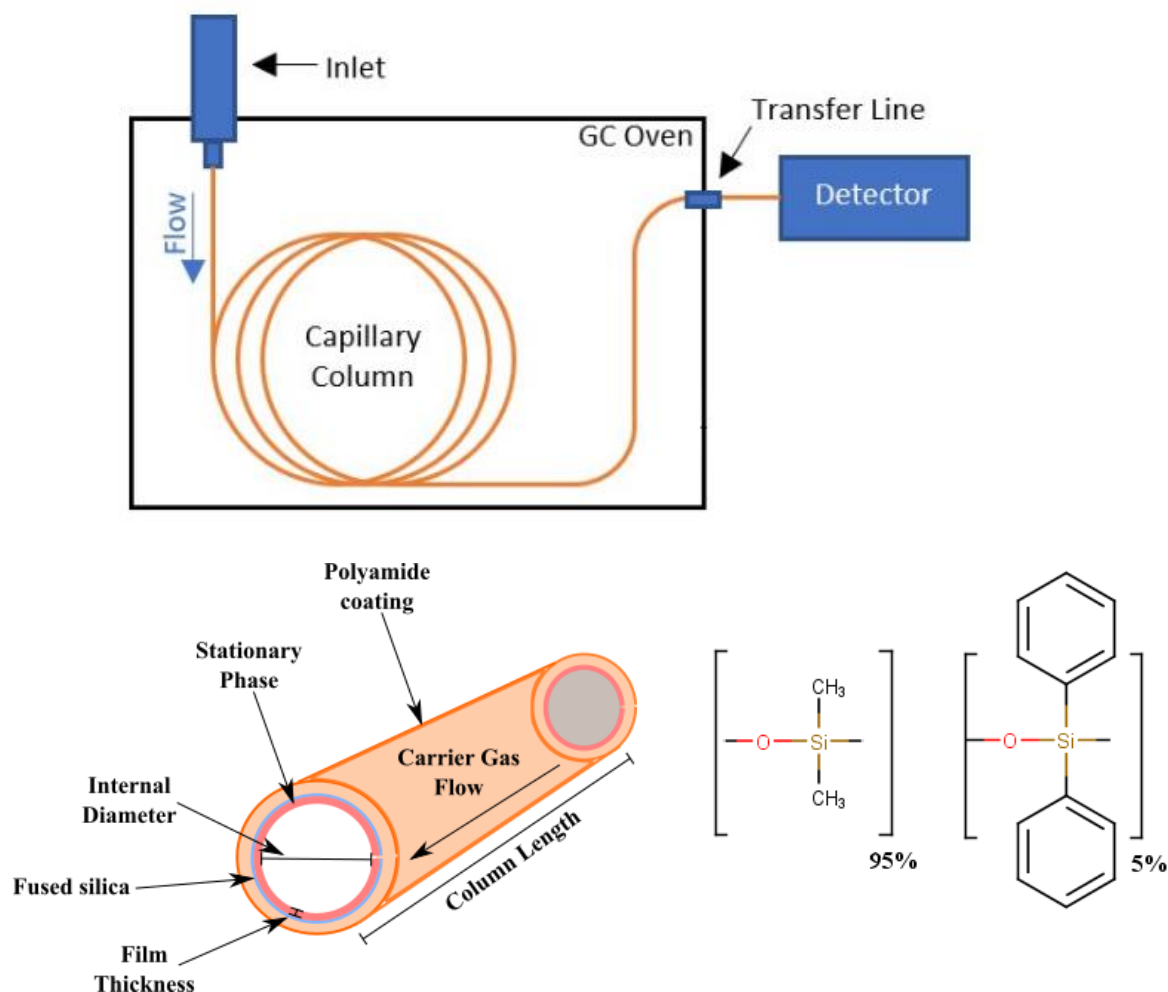


Figure 3.19: a) Basic schematic of a one-dimensional gas chromatography (GC) system b) schematic of a cross section of a capillary column phase to show the multiple coatings. Adapted from (de Zeeuw, 2017). Polyamide outer coating allows for column flexibility, with the stationary phase coated to the fused silica layer. c) column composition for a DB-5 column – (5%-phenyl)-methylpolysiloxane – change in percentage = different column stationary phase.

3.3.2 Two-dimensional Comprehensive Gas Chromatography

Two-dimensional comprehensive gas chromatography (GCxGC) is an advanced separation technique used to enhance the separation of analytes in complex matrices, providing greater analyte identifications. Generally utilised to separate co-eluting peaks, the heightened separation efficiency of the instrument, is ideal for separation of complex mixtures including environmental analyses. The increased peak capacity and identification makes it a powerful technique ideal for non-targeted analysis.

The GCxGC set-up is fairly similar to one-dimensional GC, however, as the name suggests, two orthogonal capillary columns of different length are installed, coupled by a modulator (see Figure 3.21a). The primary column (1°) separates analytes based primarily on volatility, and is the longer of

the two columns, generally 30-60 m. The secondary column (2°) is far shorter, around 1-2 m long, to provide a rapid separation, based predominantly on polarity. Reverse phase GCxGC is obtained through a polar 1° column, and a non-polar 2° column (see Figure 3.20), whilst normal phase is obtained through a non-polar 1° column, and a polar 2° column. Resulting chromatograms (Figure 3.21b) are two-dimensional and have the additional advantage of allowing for identification of peaks that are hidden by co-elution on singular GC-MS, allowing for a broader identification of compounds within the sample.

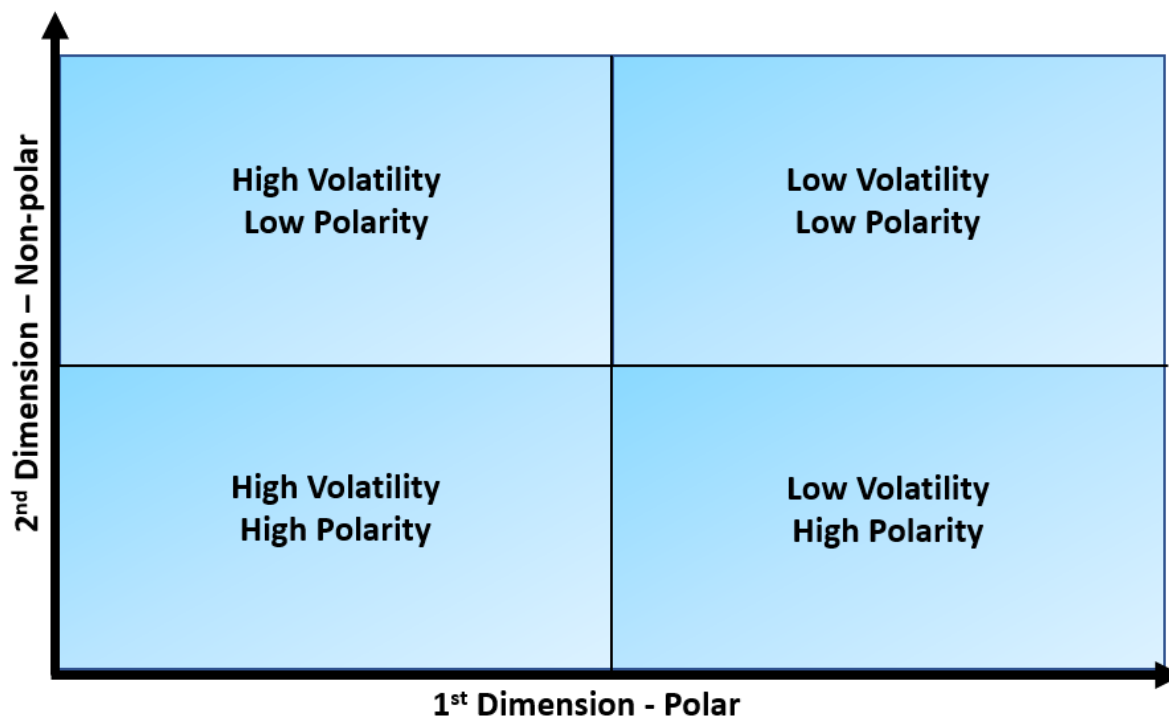


Figure 3.20: Logical order of elution Reversed Phase GCxGC column set-up. For Normal Phase elution order, replace low with high etc.

The parameters of a GCxGC are similar to that of one-dimensional GC. The samples can be injected in split or splitless mode, the inlet temperature and oven temperature are optimised to suit the analysis. Other than column length, the column characteristics (stationary phase composition and thickness and internal diameter) do not differ to the columns used in one-dimensional GC. The column and set-up are selected to suit the required analysis. An additional oven is required to house the secondary column and is located within the primary oven. The temperature of this oven can also be controlled and is usually set to a fixed temperature above the primary oven (e.g., + 15°C to primary oven temperature).

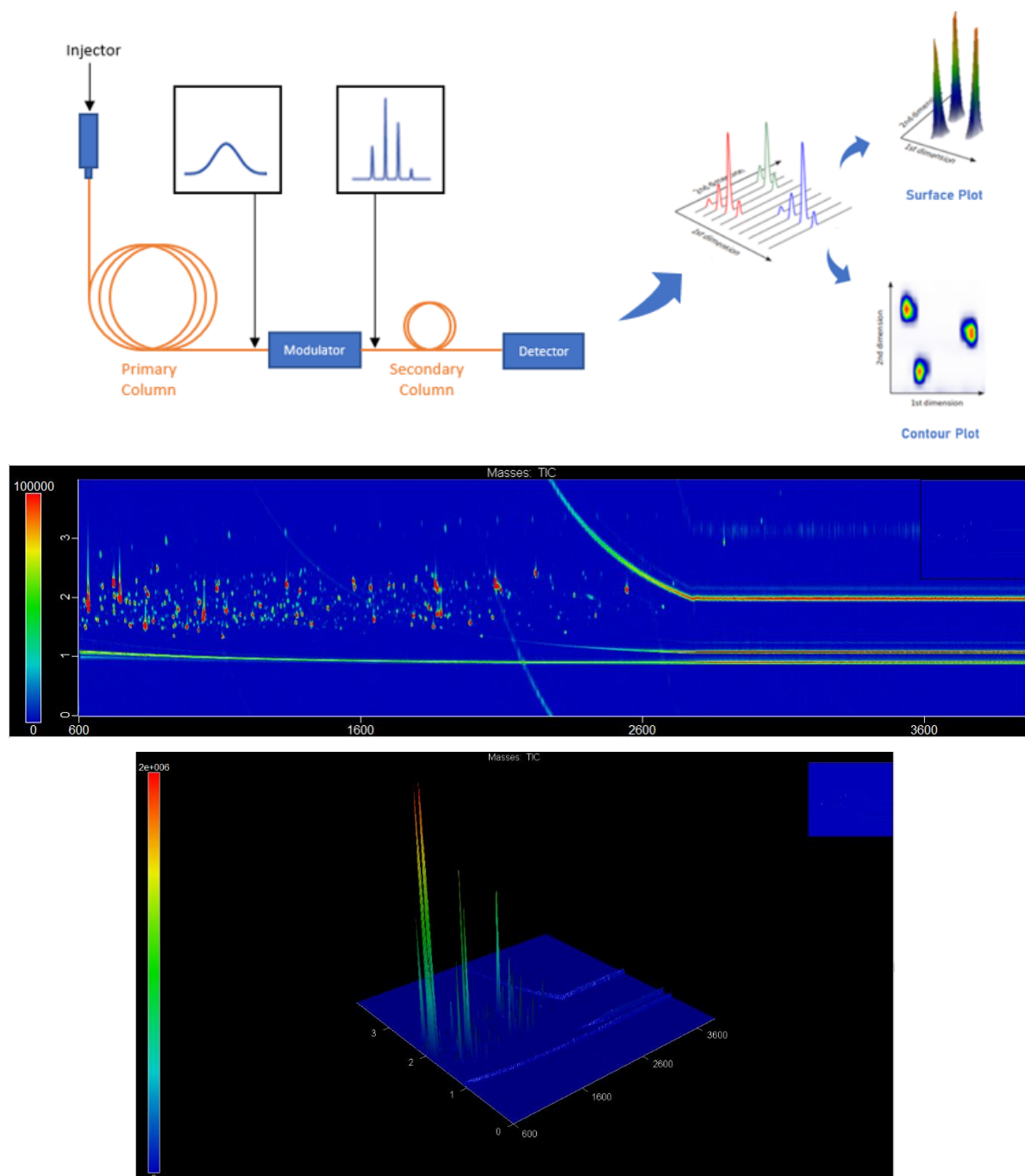


Figure 3.21: a) Basic GCxGC Set-up and illustration of the peak separation achieved by GCxGC. Adapted from (*SepSolve Analytical*, 2016) b) two-dimensional surface plot c) three-dimensional contour plot for b).

The role of the modulator is significant in GCxGC analysis. The modulator is located between the two ovens where it traps, focuses, and re-injects 1^o column eluate into the 2^o column in discrete packages/narrow chromatographic bands. Akin to the secondary oven, the modulator is set to a fixed temperature above the primary oven (e.g., 20°C). There are two types of modulators: a flow modulator or a thermal modulator. Flow modulators are robust and cheap however, thermal modulators offer superior resolution for complex matrices (JSB International, 2015). A thermal modulator was used in this study and is described in more detail.

The thermal modulator has quad jets, two cold nodes positioned above the column, and two hot nodes below. Cold nodes release N_2 gas (cooled by liquid nitrogen) and hot nodes release heated air onto the outside of the column. The gases are pulsed, switching on and off, to trap and release the sample at allocated times. Eluate from the 1^o column is halted by the first cold node, trapping and focussing of the sample into a narrow band, before switching to the hot node where the analytes desorb from the stationary phase. This focussing process repeats on the second set of nodes, before re-injecting into the 2^o column (see Figure 3.22). Narrow bandwidths provide increased method sensitivity (SepSolve Analytical, 2016) and thus modulation periods (set prior to analysis) generally last around 5 s. Increasing the modulation period prevents strongly retained 1st dimension compounds from the ‘wrap-around’ phenomenon, although decreases the number of bands taken from the 1st dimension peak. Thermal modulation improves the peak separation, resolution, and capacity (Lacina et al., 2013), and also obtains lower limits of detection due to the cryo-focussing stage.

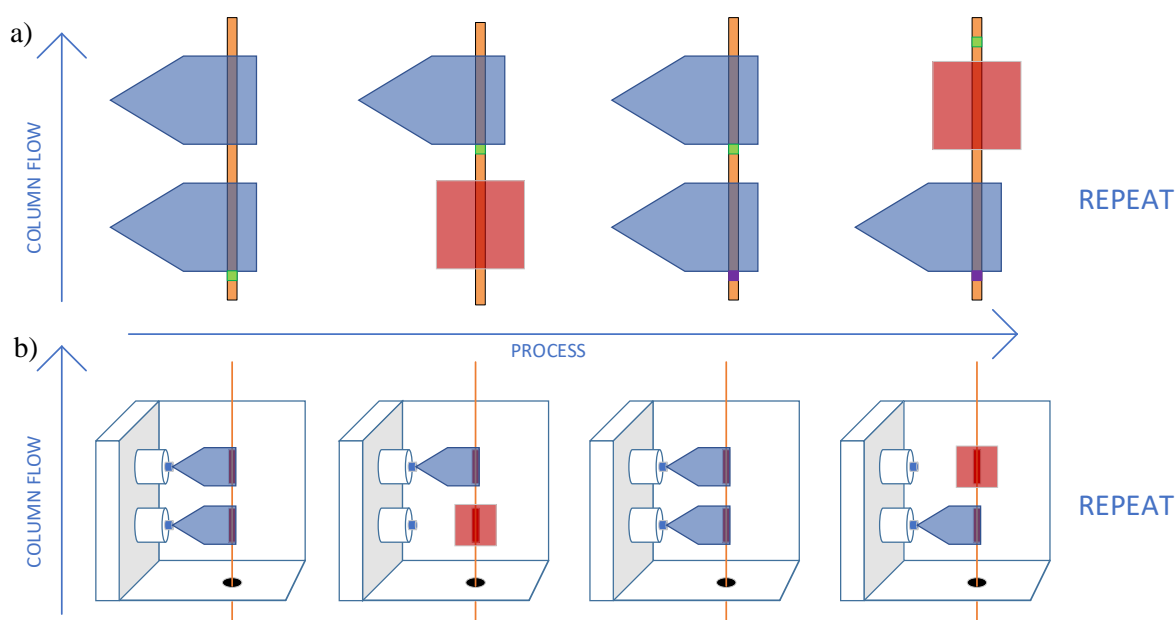


Figure 3.22: Modulation Process detailing the cryofocussing process a) Analyte (green) through the column b) Hot/cold node processes, blue represents cold pulse, and red, hot pulse.

Advantages to GCxGC include control of temperature in both 1^o and 2^o ovens, and therefore retention times in the 2nd dimension can be reduced by use of temperature offsets. Increased peak capacity and resolution are also obtained on GCxGC without having to increase chromatographic runtime, due to the information produced in the 2nd dimension. The use of orthogonal columns in GCxGC also allows for an increased use of chromatographic space. However, this powerful technique has above average costs due to the sensitivity of the technique; and produces a large volume of data and therefore a high-resolution mass spectral detector which is capable of acquiring the data at fast scan rates is required (e.g., time of flight (TOF)).

Narrow peaks are generated in the second dimension, and thus a detector with a high acquisition rate, generally 30-200 Hz, is generally used. The most common detection method is high performance mass spectrometry, such as time of flight, however flame ionisation detection (FID), electron capture detection (ECD) and sulphur chemiluminescence detection (SCD) have also been used, amongst others (SepSolve Analytical, 2016). By stacking the modulated linear outputs from the second-dimension side by side, a three-dimensional surface plot is obtained; however, sample comparison is often done in the two-dimensional contour plot (see Figure 3.21a+b). In both plots, the first-dimension retention time is plotted against the second-dimension retention time (x vs y); with the colour gradient illustrating the intensity of the peak (also shown by the z-axis in the surface plot).

3.3.3 Liquid Chromatography

Liquid chromatography is the most commonly used analysis method for the analysis of PhCs in a plethora of environmental matrices, including drinking water, wastewater, soil, and sludge. The name is derived from the liquid mobile phase, which has a large bearing on the selectivity of the method. Liquid chromatography is a robust analysis method which does not require any prior derivatisation, though sample clean-up is essential to prevent column blockage.

The LC set-up consists of a liquid mobile phase and a liquid coated solid stationary phase. Compounds are separated most notably on their affinity for the stationary phase sorbent. A solid stationary phase particle (silica gel) is coated with a polar or non-polar 'liquid' stationary phase, depending on the intended LC set-up. The particles are packed into the chromatography column, with the size of the particles influencing the efficiency of the method.

The analytes will partition into the pores on the particles, with compounds with affinity for the stationary phase retained within the stationary phase. Compounds with weak affinity for the stationary phase will not partition into the pores, remaining in the mobile phase, and will elute first. As the composition of the mobile phase changes (the percentage organic increases or decreases), the retained compounds will partition back into the mobile phase and elute to the detector. The more affinity a compound has for the stationary phase, the longer it will be retained.

Injection

In LC analysis, slightly higher volumes of sample are injected onto the column (10-50 μL) via syringe either through manual injection, or automatic injection, dependant on column dimensions. Automatic injection is the most common in industrial applications, with manual injection used primarily in teaching laboratories. In contrast to GC, all of the injected sample is carried onto the LC column by the constant flow of the mobile phase. Therefore, injection volume must be optimal to prevent sample overload and band broadening. Samples should be injected in the same solvent composition as the mobile phase to prevent peak distortion and poor sensitivity.

Columns

Polarity of the compound and its affinity for the stationary phase is the main attributing factor to successful LC analysis. Akin to GC columns, stationary phases can be non-polar or polar. The stationary phase is bonded to small porous (or superficially porous) silica particles. The silica particles have a diameter of around 3 to 10 μm , and react with the bond-phase coating, commonly siloxanes. The stationary phase bonds to the siloxane groups (see Figure 3.23); with common R groups being diol, amino, cyano, C_8 , C_{18} or any hydrocarbon, dependant on the phase of the chromatography.

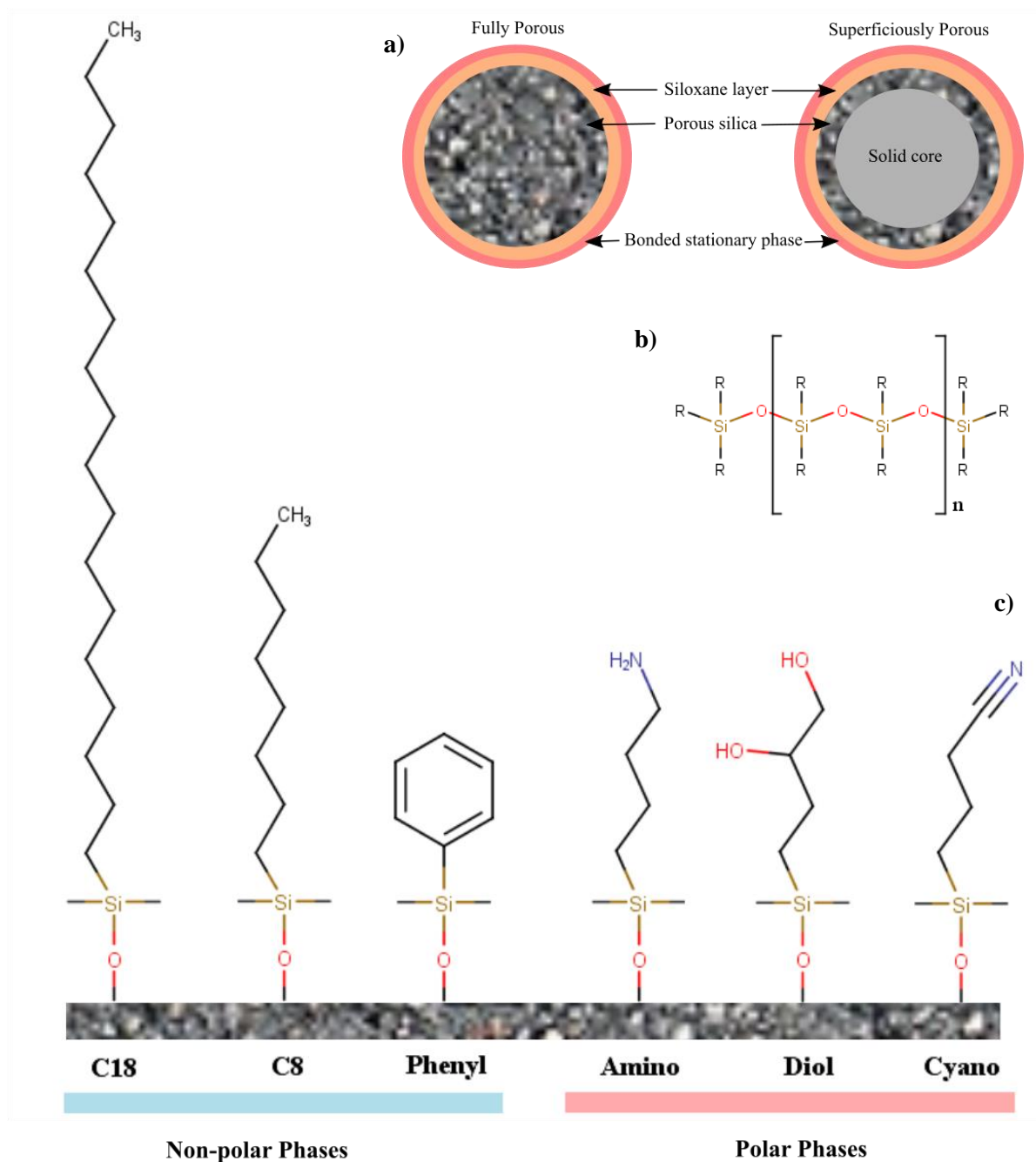


Figure 3.23: a) Schematic of a sorbent coated silica particle b) the basic structure of a siloxane group where the stationary phase will bond to and c) common R groups include cyano, C_{18} and diol used as the stationary phase - dependant on the column and analyte compound.

The stationary phase is the main component of the columns, with the polarity of the stationary phase indicated in the column name (e.g., Water's AccQ.Tag Ultra C18). The stationary phase is chosen dependant on the polarity of the target analyte compounds. When the stationary phase is a polar sorbent (i.e., a cyano phase) and the mobile phase is a non-polar solvent (i.e., hexane), the process is known as normal-phase chromatography. When the mobile phase is more polar (i.e., acetonitrile) and the stationary phase non-polar (i.e., C18 phase); the process is referred to as reversed phase chromatography. Reversed phase is the most commonly used LC set-up in environmental analysis, and in general due to the less harmful polar mobile phase (water can be used).

Columns are typically 15-30 cm long, with an internal diameter between 3.9 and 4.6 mm, or 2 and 3 mm for narrow bore columns and particle sizes of around 1.7 to 5 μm (diameter). Due to the nature of the columns, flow rates are kept between 1 to 2 mL/min and 200 to 300 $\mu\text{L}/\text{min}$ respectively, to prevent band broadening of peaks and high pressure in the instrument (Waters Corporation, 2003).

Mobile Phase

Mobile phase composition has a large effect on the elution of the analytes. The mobile phase composition is changed to alter the elution order or decrease the run time of the sample. Akin to temperature in GC, isocratic or gradient elution can be applied. The mobile phase composition remains constant in isocratic runs (e.g., water: acetonitrile 30:70) whilst the mobile phase composition changes to pre-set values in gradient runs (e.g., water: acetonitrile 30:70 for 5 mins, then increase acetonitrile to 10:90 on a linear gradient). Gradient elution reduces peak width and increases resolution, increasing peak capacity.

Mobile phases are made with solvents of HPLC grade quality, to prevent column and instrument degradation. Mobile phases are degassed and often filtered prior to use to prevent bubbles, contamination, and bacterial growth.

Matrix effects

The matrix of a sample is defined as all other components in the sample which are not the analyte. The matrix can vary depending on the analysis – from blood to urine and in this case faeces in the form of treated biosolids. Matrix effects are encountered when a matrix component (e.g., a fatty acid) co-elutes with the analyte, causing either ion suppression or enhancement of the signal when using electrospray ionisation (see 3.4.1.2 Electrospray Ionisation (ESI)), in comparison to the analyte eluting individually (Hall et al., 2012). Suppression and enhancement result in decreased and increased signals respectively, which lead to errors in quantification. The physicochemical properties of the analyte compound can have an influence the degree of the enhancement or suppression, with more polar compounds affected to a higher degree than less polar compounds, thought to be due to co-elution with other polar components in the matrix (Babushok, 2015).

Environmental samples (including biosolid samples) have complex matrices, thus, pose challenges in sample analysis. Sample clean-up stages can be used to reduce matrix effects by removal of the interfering components. Clean-up steps include SPE (solid phase extraction) or QuEChERS (quick, easy, cheap, effective, rugged and safe) in which the sample is passed through a cartridge containing a sorbent, which separates analytes from interferents based on their affinity for the sorbent. This is commonly used in wastewater analysis with an Oasis HLB (hydrophilic-lipophilic balance) sorbent used to remove contaminants. However, SPE can introduce a level of selectivity to the analysis as only analytes which favour the sorbent will be retained. This is detrimental to a non-targeted screening as some “unknown unknowns” (potential analytes) may be removed during the SPE process. Increased sample preparation time and solvent consumption is also expected with SPE or QuEChERS.

Adding chelating agents such as ethylenediaminetetraacetic acid (EDTA) is a common practice when analysing environmental samples. EDTA binds to minerals and metals preventing further reaction with analyte compounds in turn reducing or preventing matrix effects. Sample dilution in a suitable medium is another option to reduce matrix effects, however it will also reduce the signal of the analyte peak, with the possibility of the analyte concentration being below the LOD.

3.3.4 Column Theory

3.3.4.1 Peak Resolution

Resolution is a major aspect of chromatography, represented as a numerical value, it defines the separation between two peaks, with a $R_s > 1.5$ desired. Many factors contribute to resolution and are defined by the resolution equation (see equation (3-4)).

$$R_S = \left(\frac{\sqrt{N}}{4}\right) \left(\frac{\alpha-1}{\alpha}\right) \left(\frac{k_B}{1+k_B}\right) \quad (3-4)$$

Where:

- N = measurement of efficiency ($N = 5.54 (t_R'/W_{0.5})$)
- α = measurement of selectivity ($\alpha = (k_2/k_1)$)
- k = retention measurement ($k = (t_R - t_0)/t_0$)
 - t_R = retention time (mins)
 - t_0 = void retention time (mins)
 - t_R' = adjusted retention time (mins)
 - $W_{0.5}$ = peak width at half height
 - N = number of theoretical plates

Each bracket in (3-4) pertains to one aspect of separation: **efficiency**, **selectivity**, and **retention**. Resolution is highly dependent on selectivity (see Figure 3.24b), thus the choice of appropriate stationary phase (both phase and thickness) is essential for adequate resolution, otherwise overlapping

of peaks may occur. Separation also depends on the retention, which is highly influenced by temperature in GC analysis, and mobile phase composition in LC analysis, with small changes having a large influence on resolution. Column characteristics including column length and flow rate, have a large effect on the efficiency; if the number of theoretical plates is too low, the chromatogram will include broad peaks which will not be baseline separated.

Altering each term in the resolution equation, by altering the column characteristics and chromatographic method, will have varying effects on the resolution. Methods to alter the terms in both LC and GC are defined in Table 3-1. However, it must be noted that some parameters are inversely proportional, and so altering a column parameter to increase one factor of resolution, may have detrimental effects on another factor. For example, reducing the particle size to increase efficiency in LC, will also increase the pressure within the system. Therefore, this must be taken into consideration prior to analysis.

To ensure sufficient resolution, N is required to be as large as possible, α must be greater than 1.5 (baseline separation) and k must be between 2 and 10 (reversed phase analysis). Selectivity has the largest effect on resolution, however at low resolution, retention factor is most important (see Figure 3.24b).

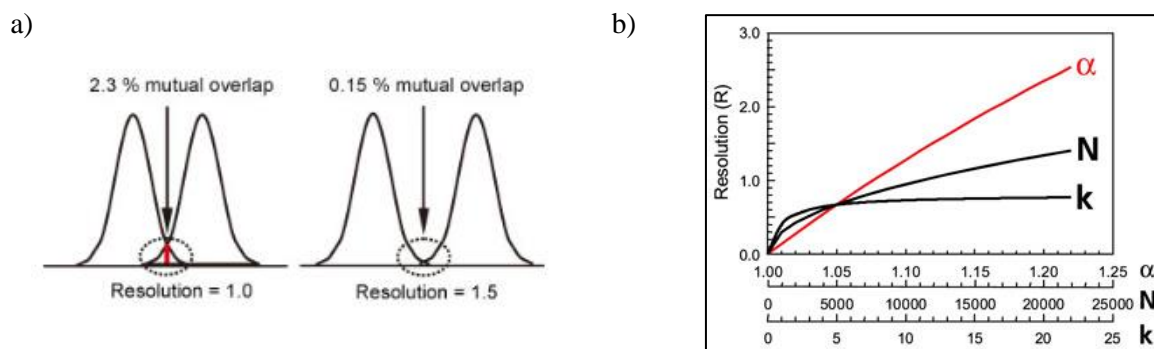


Figure 3.24: a) Resolution and Peak Separation (Shimadzu, 2020) b) Resolution Factor Plot (Sigma-Aldrich, 2007)

The efficiency term plays a significant role in the separation of peaks, which can lead to broad peaks and can be explained by the Van Deemter equation and plot (see 3.3.4.2 Peak (Band) Broadening).

Table 3-1: Resolution Equation Terms: methods to increase resolution in LC and GC

| Resolution Equation Term | Effect of changes on Rs | To increase resolution in LC | To increase resolution in GC |
|--------------------------|--|--|---|
| Efficiency | Large INCREASE in N, small INCREASE in Rs | Reduce flow rate Reduce column length Reduce particle size Reduce column load | Reduce flow rate Alter column length |
| Selectivity | Small CHANGES in α , large EFFECT on Rs | Increase temperature Alter mobile phase composition Alter stationary phase Alter pH of mobile phase | Alter stationary phase of the column |
| Retention | Small CHANGES in k, large INCREASE in Rs | Alter the mobile phase composition: reduce % ORGANIC by 10% = 3x INCREASE in k | Alter the temperature during the run (gradient temperature programming) |

3.3.4.2 Peak (Band) Broadening

Band broadening is a term used to describe the width of a peak increasing over the chromatographic run. Molecules of a singular compound will elute from the column at slightly different rates, with the retention time given to the time it takes the ‘average’ molecule to elute. This phenomenon results in a Gaussian shaped peak which is highly desirable; however, broadening can also be detrimental, if the peak width is too large, overlapping peaks can occur. Band broadening, with respect to column contributions, can be described by the Van Deemter equation (equation (3-5)). If a peak broadens too quickly, efficiency is severely reduced.

$$H = A + \frac{B}{\mu} + C\mu \quad (3-5)$$

Where:

- H = measure of efficiency (plate height)
- A = Eddy Diffusion Co-efficient
- B = Longitudinal diffusion term
- C = Mass transfer (diffusion of analyte in liquid and gas phases)
- μ = carrier gas velocity

$$H = \lambda d_p + 2\gamma \frac{D_m}{v} + \kappa \frac{d_p^2}{D_m} v \quad (3-6)$$

Where:

- H = measure of efficiency (plate height)
- λ = factor relating to size and distribution of channels between particles, and uniformity of packing
- d_p = particle size
- v = linear velocity of mobile phase
- γ = obstruction factor due to column packing – does not affect GC analysis
- D_m = diffusion coefficient of analyte in mobile phase
- K = factor relating to pore size on stationary phase

Eddy diffusion (**A**) relates to the how well a column is packed and is directly proportional to the particle size. Due to the wall coated capillary columns in GC; Eddy diffusion (**A**) is eliminated from the equation, as there is no packing within the column. However, this term is important for LC – where packed columns introduce various pathways in which the analyte can travel. The paths may differ in length which means the analyte will elute from the column at different times. Smaller particle sizes will reduce the **A** term, preventing negative effects such as peak tailing and band broadening.

Longitudinal diffusion (**B**) relates to the movement of the analyte molecules through the column, and thus is affected by the mobile phase or carrier gas flow (LC and GC, respectively), which has a large effect on band broadening. Analyte molecules are constantly moving from areas of high concentration to low concentration, which creates a “band” of sample – the farther the sample must travel, the larger the band is. Generally, in GC analysis, **B** reduces with increasing MW of the carrier gas (see Figure 3.25b). Although nitrogen gas seems to be the optimum carrier for GC analysis (see Figure 3.25b) it has a much narrower velocity range than helium or hydrogen; as such, efficiency reduces substantially at higher flow rates. Therefore, helium is regularly chosen over nitrogen gas. Hydrogen is not as commonly used due to the increased flammability of the gas. In LC, **B** is directly proportional to the solvent diffusion coefficient (D_m), or rate of analyte diffusion into the mobile phase and can have a significant impact at low flow rates. Altering the mobile phase, to a solvent with a low viscosity will increase the analyte diffusion – increasing the temperature will also decrease the viscosity of the solvent but may influence the analyte (particularly for thermally labile compounds).

Mass transfer (**C**) relates to the molecule’s affinity for the stationary phase, which effects the retention factor (**k**), due to traverse diffusion of compounds, in and out of the stationary phase and the mobile phase. Higher flow rates will increase mass transfer which can lead to band broadening (see Figure 3.25a). Reducing the flow rate and increasing the temperature will reduce the mass transfer in both GC and LC analysis. Narrow bore columns (<i.d.) provide greater efficiency in GC analysis, however, peak capacity is reduced in comparison to wide bore columns. Reducing the particle size in LC analysis will reduce **C** yet will increase pressure in the system.

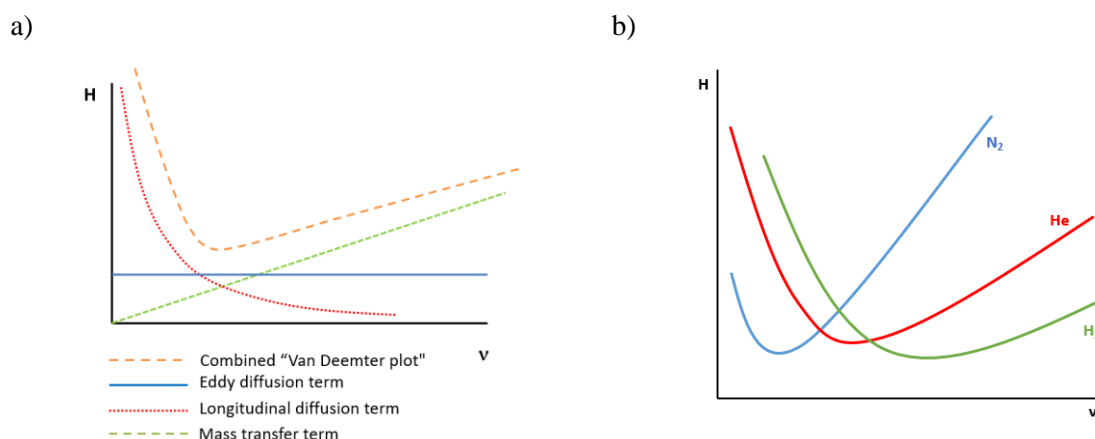


Figure 3.25: Combined Van Deemter Plots: a) Column Contributions b) Carrier Gas for GC where H = plate height and v = linear velocity of mobile phase (cm/sec)

3.3.4.3 Chromatogram

The output obtained from GC or LC analysis is known as a chromatogram. Each peak represents either one resolved compound, or two or more co-eluting compounds. As analytes travel through the instrument, they are separated and elute to the detector. Compounds which do not interact with the stationary phase will be eluted earlier than those which diffuse into the stationary phase.

As each compound elutes from the column, the detector computes this into a signal, which appears as a peak on the chromatogram (see Figure 3.26). The time taken for the signal to reach the detector is known as the retention time of the compound (RT, displayed on the x-axis). When coupled to a mass spectrometer, the total ion chromatogram (TIC) is formed by the sum of the intensities for all mass spectral peaks belonging to the same scan (see 3.4 Mass Spectrometry Techniques). Without a mass spectral detector, retention times are often used for identification purposes, provided analyte standards are ran on the same column, with the same chromatographic method.

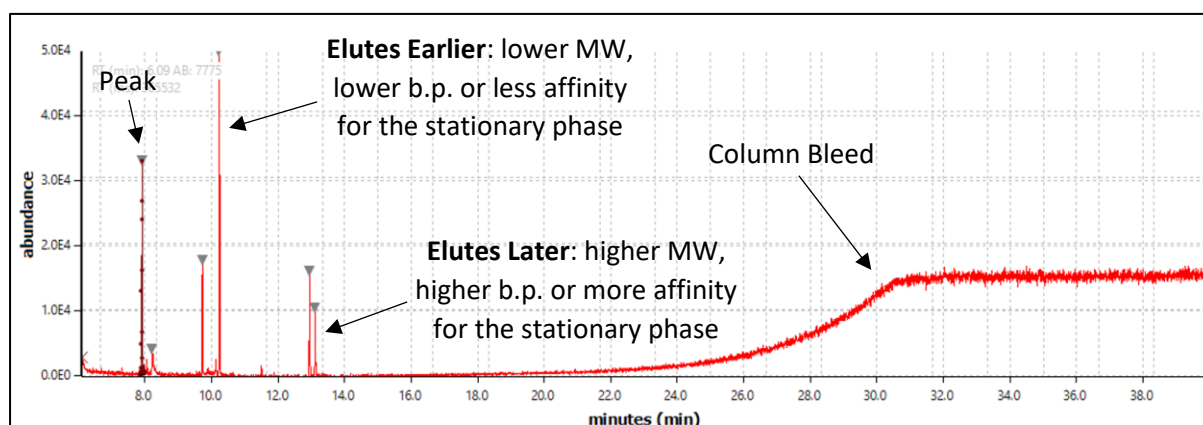


Figure 3.26: Annotated Gas Chromatography Chromatogram Example. The chromatograms produced using LC are similar, as analytes will elute in order of affinity for the stationary phase, producing peaks. Column bleed is not as prevalent in LC.

An increase in baseline towards the end of the chromatographic run (in gas chromatography), is known as column bleed. This is caused by the breakdown of the stationary phase when the column is heated to temperatures close to the upper limit of the column. Column bleed is not detrimental to the instrument, and should not impose any issues, providing analytes do not elute within this region.

3.4 Mass Spectrometry Techniques

Mass spectral detectors are predominant in pharmaceutical analysis due to their ability to elucidate analyte compounds from large mixes and matrices. The powerful detectors are therefore useful when analysing complex matrices, where many compounds are present, and may co-elute, or when undertaking non-targeted analysis, as compounds are not known prior to identification.

Mass spectrometers contain three main components: an ion source which produces the ions, a mass analyser which separates the ions based on their mass to charge ratio (m/z), and a detector, all stationed within a high vacuum system controlled by a turbomolecular pump.

Ion sources include electrospray ionisation (ESI), electron impact (EI), chemical ionisation (CI) and matrix assisted laser desorption ionisation (MALDI). Various mass analysers are available including single and triple quadrupoles and high-resolution mass analysers such as ion traps (orbitrap) and time of flight (TOF). Detection is commonly an electron multiplier; however, microchannel plates and photomultipliers can also be used. The choice of ion source, mass analyser and detector, is usually dependant on the analysis technique (ESI usually chosen for LC, whilst EI for GC), the cost of the instrument (single quadrupoles are far cheaper than TOF, however less sensitive) and the analysis being undertaken (resolution increases with instrument cost).

Numerous analysers were used in connection with the different chromatographic instruments for this study. One dimensional GC is coupled with a single quadrupole mass spectrometer, with an electron impact ionisation source, two-dimensional GC required a more powerful mass spectrometer, and thus, is coupled to a TOF, which also contains an electron impact source, and the LC tandem MS required a high-resolution mass analyser, and thus was coupled to an orbitrap, with an electrospray source. These ion sources and mass analysers are described below in more detail.

3.4.1 Types of Ionisation

3.4.1.1 Electron Impact (EI)

Electron impact ionisation was the original ionisation method and is still widely used in gas chromatography applications today. The principle of the method is simple; the sample is bombarded with electrons generated from a tungsten (or less commonly rhenium) filament. The high energy electron beam (usually set to 70 eV) breaks the intermolecular bonds of the analyte compounds (which have less energy, between 4-7 eV) causing extensive fragmentation (see Figure 3.27). Applications are limited, in terms of analyte compound, as the ionisation will only occur when the molecule is in the gas

phase. Therefore, analytes which are involatile or thermally unstable would not be suited to this ionisation technique. The extensive fragmentation produced is known as a hard ionisation technique. The complex fragmentation pattern produced provides a unique fingerprint-like mass spectra which is used for compound identification.

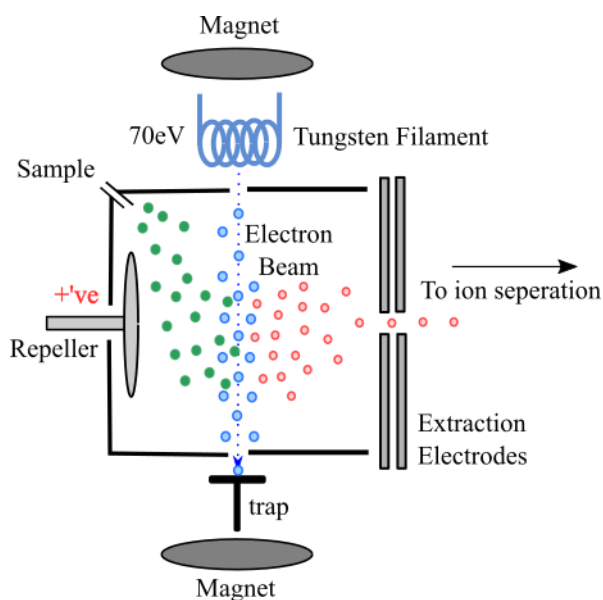


Figure 3.27: Schematic of electron impact (EI) ionisation. Adapted from (Electron Impact - an Overview | ScienceDirect Topics, n.d.) . Green balls represent the sample, blue balls represent electrons, and the red balls represent generated ions. The sample passes through the electron beam, where ions are generated.

The molecule is bombarded with electrons, which first forms the molecular ion. The molecular ion, generally $[M+H]^+$, which bears a positive charge, due to the loss of one electron. The remaining unpaired electron (represented by a dot) can be removed by breaking any single bond in the molecule, producing a cation and/or a radical (see Figure 3.28). Produced cations can lose a number of neutral fragments, such as water (H_2O) or carbon dioxide (CO_2). The order of the loss (radical then neutral) can occur in a different order (neutral then radical); however, after the loss of one radical, no further radicals can be lost. Some common fragment losses in EI can be found in Appendix A.

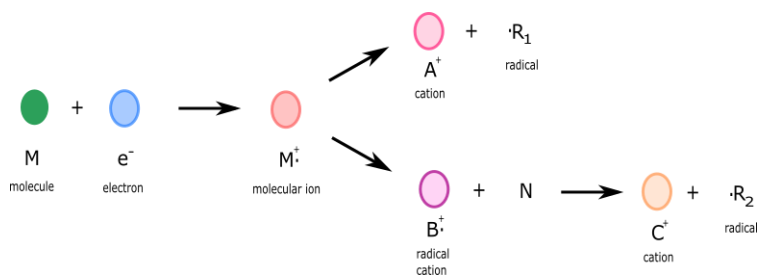


Figure 3.28: Electron Impact Ionisation - production of molecular ions, cations, and radicals.

The produced mass spectrum illustrates the fragmentation pattern for the analyte under investigation. To understand further, ketoprofen will be used as an example (see Figure 3.29). The molecular ion is generally the ion with the highest m/z ratio (m/z 254 for ketoprofen, the molecular mass); however, is not always the most abundant ion on the MS when PhCs are analysed. The ion which is in greatest abundance is known as the base peak, in the case of ketoprofen, m/z 105. The structure of the fragments which produce other abundant ions in the mass spectrum can be elucidated from the m/z ratios. For example, m/z 209 is formed from the removal of a carboxylic acid group from the ketoprofen molecule (see Figure 3.29b). Numerous fragmentation patterns or rearrangements are observed in electron impact fragmentation. The alpha-homolytic cleavage is the most common fragmentation observed in fragmentation of PhC molecules. Ring fragmentation is often observed in PhCs which bear nitrogen containing rings whilst McLafferty rearrangements are relatively uncommon in PhC molecules, though are more common with fatty acid esters.

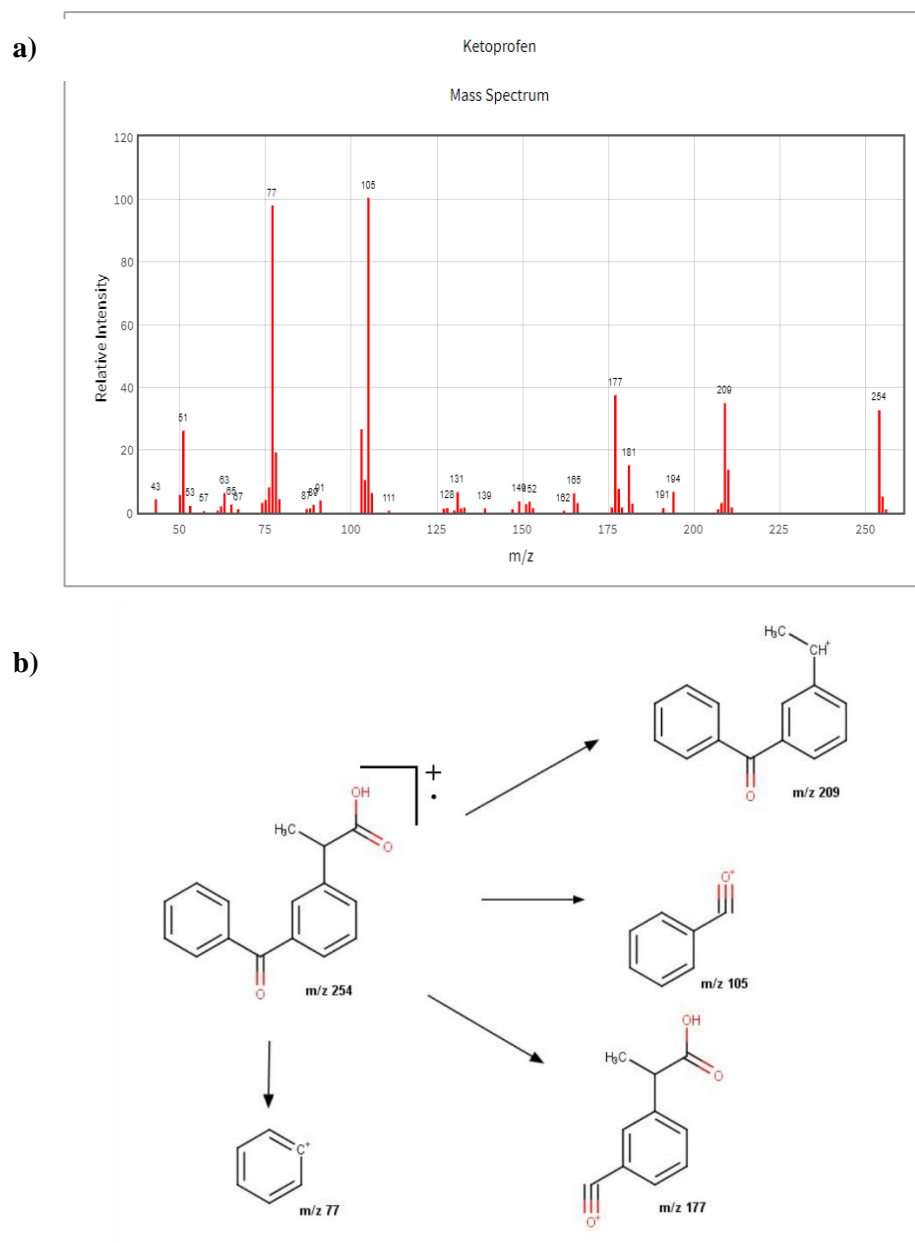


Figure 3.29: Ketoprofen a) NIST Library EI Mass Spectra b) Fragmentation of ketoprofen to produce the most abundant m/z ions depicted in the EI mass spectra

When the mass spectrum of the analyte is obtained, it can be compared to a library for identification. The most common library used is the National Institute of Science and technology (NIST) mass spectral library, which contains the EI mass spectra of over 300,000 compounds (National Institute of Standards and Technology, 2009).

3.4.1.2 Electrospray Ionisation (ESI)

Electrospray ionisation is the most commonly used ionisation technique in liquid chromatography mass spectrometry methods. Known as a soft ionisation technique, the compound does not undergo as intense fragmentation and produces less fragment ions than electron impact ionisation. The sample elutes from the LC in and is sprayed into the MS through a steel (or quartz) capillary needle held at a high potential

(+4.5 kV), creating an aerosol. The high potential of the needle causes electrons to remain in the needle, separating them from the positive ions. The positive ions are repelled by the capillary at a force which overcomes the surface tension of the liquid, creating a Taylor cone at the tip of the needle, which breaks up creating charged droplets. The highly charged droplets have an excess of positive ions which cause Coulombic repulsion, breaking down the charged droplets by explosion. Additionally, evaporation of the solvent reduces the size of the droplets, increasing the positive charge, which causes further break down. This breakdown cycle repeats, with droplets reducing in size, until single positively charged gas phase ions are produced (see Figure 3.30). These ions are then separated in the mass analyser.

The process described above is for positive ion mode, however, ESI can also be operated in negative ion mode, where the process remains primarily the same, with the capillary needle set to a negative voltage (-4.5 kV); which retains positive ions and allows negative ions to reach the mass analyser.

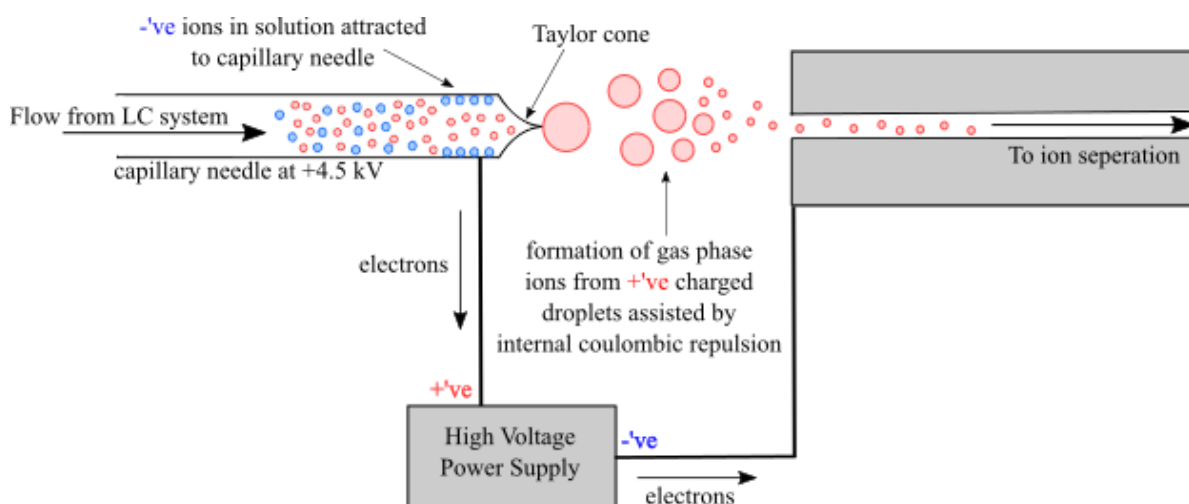


Figure 3.30: Schematic of an electrospray ionisation source; eluent enters the MS system through a capillary needle, where negative ions are trapped, and positive ions in solution create a Taylor cone at the tip of the needle, due to reduction in surface tension. The droplets reduce in size due to internal coulombic repulsion and evaporation until singular

Akin to the EI, a molecular ion is formed: $[M+H]^+$, or $[M-H]^-$ for positive and negative ion mode respectively. Due to the 'soft' ionisation technique used in ESI, little fragmentation occurs, and so the mass spectra contain fewer fragment ions in comparison to EI. The molecular ion is not always the most abundant ion, although this is quite common in ESI. Often additional ions relating to the molecular ion are present, due to the formation of adducts. Adducts are often formed due to components in the mobile phase. Sodium, potassium, and methanol can all bind to non-ionisable compounds in the sample, producing adducts with a higher m/z ratio than the molecular ion. This is particularly noticeable in the analysis of ketoprofen by LC-MS, where the base peak in both positive and negative ion mode are adduct formations ($+CH_3OH$ and $+HCOOH$, respectively) (Themes, 2016). A list of common adduct formations is found in Appendix A. The use of high-quality solvents is essential for ESI in order to overcome or reduce the formation of adducts.

ESI is often coupled to LC as it can tolerate a high flow of solvent (up to 200 μL), making it ideal for trace analysis or impurity profiling. A low flow rate for both the sample and the nebuliser gas increases the sensitivity of the method.

3.4.2 Types of Mass Analyser

3.4.2.1 Single Quadrupole

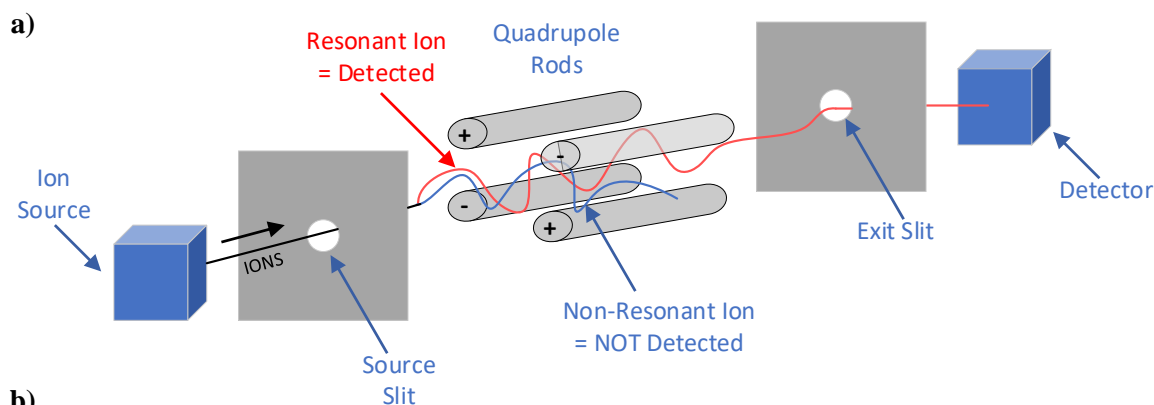
Single quadrupole mass spectrometers are common in analytical laboratories, and often are coupled to an LC or a GC instrument. Composed of four parallel metal rods, the analyser uses a combination of RF and DC voltages to operate the mass filter, allowing only one ion to pass through at one time (see Figure 3.31a).

Column eluate enters the mass spectrometer through the heated transfer line; where the compound is ionised and fragmented by the ion source (either EI or ESI, see previous), before entering the mass analyser. Separation occurs based on the mass to charge ratio (m/z) of the ions. Ions are accelerated through a magnetic field (produced by the quadrupole rods), deflecting ions based on their mass; deflection increases with lower masses. Upon reaching the detector, a mass spectrum is produced illustrating the relative abundances of the m/z ions. This unique fragmentation pattern is compared to that of the NIST library, and an identification is produced.

Single quad mass spectrometers are able to operate in full scan mode (scan) or single ion monitoring (SIM) mode, which is selected by the operator prior to analysis. Scan mode can be used for qualitative and quantitative analysis as a range of ions are selected dependant on the analytes (generally m/z 50-500). SIM mode is used only quantitatively, as the detector only measures a specified mass. Increased sensitivity attributed to this method provides lower limits of detection (LoDs) for analyte compounds. Scan mode can be used to elucidate a unique ion for a specific compound, before analysing using SIM mode to increase the sensitivity for that compound.

Single quadrupole MS have only one mass filtering quadrupole, as per the name, whereas triple quadrupole mass spectrometers have two mass filtering quadrupoles (Q1 and Q3) separated by a collision cell (Q2) (see Figure 3.31b), which increases the sensitivity of the instrument (described further in 3.4.2.2 Tandem MS (MS/MS)). Although triple quadrupole mass spectrometers are becoming more prominent in laboratories, a single quadrupole was fitted to the GC in the research laboratory used in this thesis. For the work undertaken at GC-MS level, a single quadrupole mass analyser was sufficient.

Single Quadrupole



Triple Quadrupole

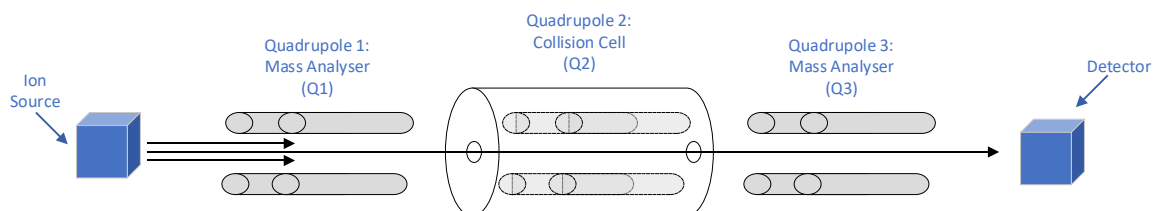


Figure 3.31: Schematic of Quadrupole Mass Analysers a) Single Quadrupole (adapted from (Argoti, 2008)) b) Triple Quadrupole running in SIM mode

3.4.2.2 Tandem MS (MS/MS)

ESI conditions produce little fragmentation, which can make identification more difficult. To increase the fragmentation, a triple quadrupole detector can be used in conjunction with the ESI. This process is known as tandem MS (MS/MS or MS²), and uses collision induced dissociation to produce a more fragmented mass spectrum. Tandem MS increases the specificity of the method, however, generally requires a high-resolution mass spectrometer such as a TOF or orbitrap. As described above, the triple quadrupole MS is divided into three quadrupoles, Q1 and Q3 are mass analysers and Q2 is the collision cell (see Figure 3.31b). For tandem MS, the analyte ion of interest, usually the molecular ion ($[M+H]^+$ or $[M-H]^-$ ion for positive and negative ionisation modes respectively) is selected as the precursor ion in Q1. The second quadrupole acts as a collision cell, where ions collide and fragment under argon gas. All fragmented ions then pass through the third quadrupole, where they are separated and sent to the detector (full scan), or a specific product ion can be selected (generally most abundant fragment ion); where all other ions will be discarded and only the selected ion reaches the detector (SIM). The energy of the collision cell can be controlled, with varying energies influencing the fragmentation pattern – which can cause issues with library comparisons. Library spectra must have undergone the same fragmentation, and thus the tandem MS conditions including collision energy, type of collision gas (less often nitrogen is used) and collision gas pressure must be the same. Although spectra produced by

MS/MS are similar to EI in terms of fragmentation, the spectra are not often comparable, and so NIST Library cannot be used for accurate identification.

Often analysts opt for a full scan in the first instance, to generate a mass spectra of the analyte using the molecular ion as the precursor ion. The most abundant fragment ion is then used as the product ion and the samples analysed further in a SIM analysis.

3.4.2.3 Time of Flight (TOF)

Time of Flight (TOF) is considered a more powerful mass analyser, with higher resolution, greater mass accuracy and increased sensitivity in comparison to quadrupole analysers. TOF instruments are compatible with various analysis methods, and are often coupled to chromatographic instruments, including the GCxGC in this study. TOF instruments are theoretically capable of detecting very large molecules (based on MW) with fairly high mass resolution for all analyses. Fast data acquisition rates (1000 full spectra per second) allow for a large volume of data to be gathered (TOF analysers have the ability to simultaneously detect all m/z ions in each measurement), increasing the speed and sensitivity of the analysis and the quality of the analyte identification (TOFWERK, 2020). TOF instruments are similar to orbitrap instruments (see below) in terms of resolution and accuracy, however, have lower introductory and operational costs.

The principle is simple, larger ions will take longer to travel along the flight tube thus, taking longer to reach the detector. Column eluate is bombarded with electrons (from an EI source), forming ions which vary in kinetic energy (proportional to the charge of the ion, m/z). These ions are introduced to the flight tube in pulses (by push pulse plate, see Figure 3.32), which then drift through the flight tube, focussed by both the ion focussing lenses and the reflectron before reaching the detector. Ions with greater kinetic energy penetrate further into the reflectron, and slower, heavier ions do not penetrate as deep. The time elapsed between introduction and detection is recorded, and so shorter times indicate lower masses and vice versa. Ion focussing prevents broad mass peaks, and thus increases resolution.

Due to the two-dimensional separation achieved with GCxGC, a large volume of data is produced. The high acquisition rates and full spectra scanning associated with TOF analysers are capable of acquiring and processing the volume of data produced from GCxGC analysis.

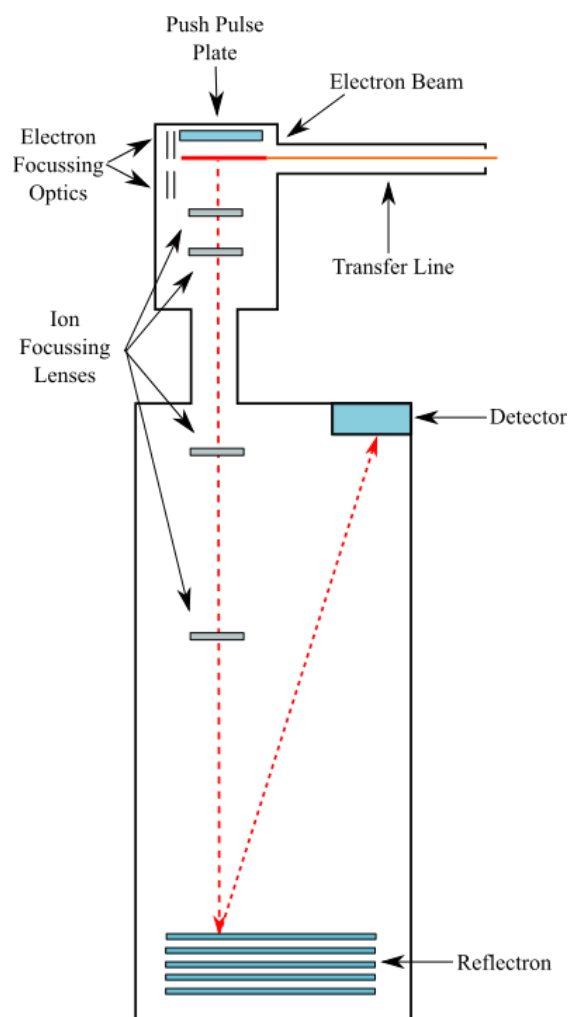


Figure 3.32: Basic Schematic of Time of Flight (TOF) Mass Spectral Detector, adapted from LECO (Joseph, n.d.). Eluate is bombarded with electrons, forming ions which are pushed into the flight tube in packets by the push pulse plate. Ions drift through the tube at varying rates dependant on the kinetic energy and molecular size. Larger ions take longer to reach the detector.

3.4.2.4 Orbitrap

Orbitraps are one of the newest mass analysers on the market, only commercially available since 2005. A powerful competitor to the TOF, the orbitrap can provide high resolution, however, is far more costly. The high-resolution mass spectrometer can produce a mass accuracy of up to six decimal places, with the ability to separate two peaks with minute mass differences (as little as 0.01 a.m.u.). Akin to many detectors, orbitraps are generally coupled to chromatography instruments, in particular LC, which is used in this study. Rapid scan speeds generate a large volume of data however increase the mass accuracy of the detection; thus, the method is termed 'high-resolution'. Generally, the instrument contains a quadrupole for ion selection, a collision cell for fragmentation, and an orbitrap for separation and thus is ideal for both targeted and non-targeted analysis of environmental samples.

The principle of the orbitrap is to 'trap' ions in an electric field and generate an image current. Ions are omitted from the ion source, captured, and focussed using a variety of lenses before travelling into the

bent flat pole, where uncharged and neutral species are filtered out. In full scan mode, ions pass through the quadrupole, and are collected in the C-trap in small “packets”. The ion packets are stabilised before being introduced to the orbitrap for detection. The orbitrap ‘traps’ ions in an electrostatic field, where the ions oscillate back and forwards, in an orbital motion around the central spindle (see Figure 3.33). The frequency of the rotation is converted to the m/z ratio by Fourier transform, with ions of different m/z ratios, having different oscillating frequencies.

The principle is similar for tandem MS (MS/MS) using an orbitrap, although only analytes of interest (target analytes) are selected in the first stage of the quadrupole. The selected ions are then fragmented in the collision cell (collision-induced fragmentation), producing fragment or product ions. The fragment ions are collected in the packets, and sent to the orbitrap, where again, different fragment ions will have different oscillating frequencies. The process repeats for all ions which are to be fragmented.

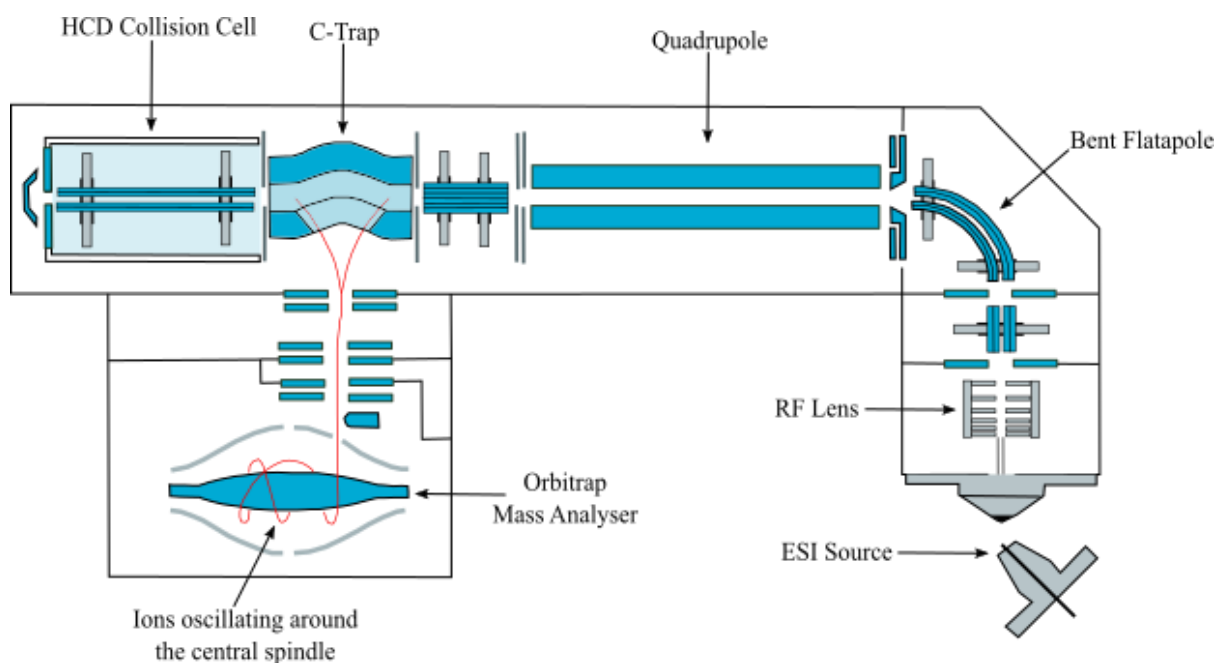


Figure 3.33: Schematic of a Q-Exactive Orbitrap Mass Spectrometer. Adapted from (Thermo Fisher Scientific, 2016).

Certain chromatography software’s (e.g., Xcalibur) allow the user to set a defined list of target compounds, known as an “inclusion list”. The inclusion list details parameters including expected mass to charge ratios (m/z), analyte chemical formula, potential adducts and a pre-set mass error range, which will be compared to features in experimental datasets.

The software monitors the data included in the inclusion list in each scan on the MS system, when a peak is detected which satisfies the criteria of one of the analytes on the inclusion list, an MS/MS spectrum is acquired for the associated precursor ion. Similarly, exclusion lists can also be defined, where a list of specific masses, corresponding to undesirable compounds, can be excluded/ignored. This tool helps to overcome problems of contamination whilst increasing selectivity of the method.

Chapter 4: Understanding and optimising conventional silylation for exhaustive derivatisation of pharmaceutical compounds

4.1 Introduction

4.1.1 Derivatisation of PhCs

Due to the hydrophilic nature of most pharmaceutical compounds (PhCs), derivatisation is required for compatibility with gas chromatography (GC) analysis. Derivatisation chemically transforms compounds, reducing the polarity, and increasing the volatility and thermal stability of the analytes (Pierce, 1968). Derivatisation of PhCs prior to analysis will enhance detection, improve peak shape, and support strengthen mass spectral identification due to unique fragmentation patterns associated with derivatised groups (Knapp, 1979; Lai & Fiehn, 2018).

PhCs tend to vary in size, structure, and polarity – complete derivatisation is dependent on the physicochemical properties of each PhC; and thus, derivatisation efficacy will differ between PhCs. Alkylation (esterification) (Jux et al., 2002; Marsik et al., 2017; Sacher et al., 2001; Ternes, 2001) and silylation (Caban & Stepnowski, 2018; Kumirska et al., 2019; Logarinho et al., 2016; Ternes, 2001) techniques have both been successfully applied to derivatise PhCs for analysis by GC. However, silylation seems to be the most widely used technique (Orata, 2012) based on the known success; the ability of silylation to derivatise a wide range of functional groups including alcohols, carboxylic acids, amines and amides (Blau & King, 1978); and the simplicity of the technique (no production of acidic by-products as seen in acylation (Knapp, 1979; Orata, 2012)).

4.1.2 Silylation

Silylation refers to the replacement of a labile hydrogen with a silyl group; generally, a trimethylsilyl group (TMS) unless otherwise stated. The mechanism is described as a nucleophilic substitution of the second order (S_N2), where a silicon atom is attacked instead of a carbon atom, and thus is often denoted as S_N2 -Si (Moldoveanu and David, 2014; Pierce, 1968). The reaction occurs when a nucleophile (labile hydrogen containing group on the PhC) attacks an electrophile (Si atom of the silylation reagent) (Caban & Stepnowski, 2018), forming the TMS derivative.

Ease of silylation decreases from OH>ArOH>COOH>NH>CONH; with ease decreasing from primary (1°) to tertiary (3°) alcohols and from primary to secondary (2°) for amines (Knapp, 1979; Moldoveanu and David, 2014; Orata, 2012; Pierce, 1968) in relation to the stability of the carbocation (see Chapter 3). The decrease in ease of silylation can be described by a number of molecular factors:

1. Strength of the electrophile (electrophilicity)
2. Strength of the nucleophile (nucleophilicity)
3. Electron withdrawing effects.
4. Steric Hindrance
5. Catalyst

An in-depth discussion of these factors can be found in Chapter 3 – Instrumental and Analytical Techniques under Derivatisation (pages 52-63).

It is proposed that the key to optimal silylation for PhCs lies within the theoretical background of the reaction. The fundamental principle behind all chemical reactions, including silylation is collision theory, thus this must also be considered when optimising the silylation reaction. Reactant molecules (in this case, the PhC and derivatisation reagent) must collide at the correct angle, with appropriate energy to overcome the repulsive forces of outer electrons (Lawson & Lower, 2013). Only successful collisions generate the desired TMS derivatives. The rate at which they collide is controlled by altering the parameters of the reaction including temperature and concentration. Increasing the temperature decreases the activation energy of the reactants, which increases the number of collisions and force at which the reactants collide – facilitating the reaction (Latham & Burgess, 1977). Increasing the reactant concentration increases the number of particles available for collision, thus increasing the reaction rate (Seoud et al., 2016). Addition of a catalyst also decreases the activation energy required for the reaction to occur, and so increases the likelihood of collisions. Thus, taking the aforementioned factors into consideration, practical parameters including derivatisation reagent choice, solvent choice, reaction time, reaction temperature and molar ratio are altered in order to optimise silylation for all PhCs in this study.

Many studies have varied derivatisation volume, reagent, reaction time and temperature to optimise silylation for a targeted set of PhCs, often compounds of the same therapeutic class (e.g., non-steroidal anti-inflammatory drugs (NSAIDs)) or with similar functional groups (e.g., acidic groups COOH). Optimised methods for similar compounds vary from study to study (see Table 4-1) - Caban *et al.* concluded 60 °C for 30 mins was sufficient for complete derivatisation of eight β -blockers and β -agonists with BSTFA + 1% TMCS (Caban et al., 2011), though Brunelli *et al.*, silylated six of the same compounds with MSTFA at 60 °C for 15 mins (Brunelli et al., n.d.). Sebök *et al.* optimised the derivatisation parameters for four NSAIDs to be 70 °C for 90 mins (Sebök et al., 2008), though Samaras

et al. found 20 mins at 70 °C (Samaras *et al.*, 2011), and Kumirska *et al.* found that 60 °C for 30 mins (Kumirska *et al.*, 2013) was optimal for a mixture containing the same compounds.

Therefore, the literature suggests that derivatisation optimisation is required prior to analysis in order to optimise analyte response. However, it is generally unknown which PhCs will be present in environmental samples, and so non-targeted analysis is undertaken in this thesis. This poses a challenge for derivatisation as the PhC analyte's physicochemical properties (including labile hydrogens) will vary greatly.

Therefore, there remains a real requirement for a derivatisation procedure which can derivatise a vast range of functional groups and PhCs, to allow for non-targeted analysis, which can be applied in a variety of environmental fields. This chapter aims to understand and optimise silylation parameters for derivatisation prior to non-targeted analysis of PhCs, by using a group of representative PhCs; whilst adhering to the 12 Principles of Green Chemistry (see Chapter 2).

Table 4-1: Optimal Derivatisation Temperatures and Times for the silylation of various PhCs found in literature. Optimal reagent indicated by an Asterix (*).

| Reference | Compounds | Conditions Tested | Optimal Temperature | Optimal Time |
|--|---|---|---------------------|--------------|
| Caban and Stepnowski (Caban & Stepnowski, 2018) | Paracetamol | Reagents: BSTFA + 1% TMCS* MSTFA Pyridine + 1% TMCS | 60 °C | 30 mins |
| Caban <i>et al.</i> (Caban <i>et al.</i> , 2011) | Acebutolol Atenolol Propranolol Metoprolol Nadolol Salbutamol Pindolol Terbutaline | Reagents: TMSDEA TMSI TMCS HMDS BSTFA + 1% TMCS* MSTFA Time (mins): 5, 15, 30, 45, 60 Temperature (°C): 30, 60, 90 | 60 °C | 30 mins |
| Kumirska <i>et al.</i> (Kumirska <i>et al.</i> , 2013) | Salicylic acid Ibuprofen Paracetamol Flurbiprofen Naproxen Diflunisal Ketoprofen Diclofenac Valproic acid Vigabatrin Primidone Terbutaline Salbutamol Propranolol Pindolol Nadolol | Reagents: TMSI BSTFA + 1% TMCS* MSTFA Volume of Pyridine (µL): 0, 25, 50 Time (mins): 30, 60 Temperature (°C): 60, 90, 120 | 60 °C | 30 mins |

| | | | | | |
|---|-------------------------------|--|------------|---------|--|
| Migowska <i>et al.</i> (Migowska et al., 2012) | Estrone | Reagents: BSTFA + 1% TMCS* MSTFA | 60 °C | 30 mins | |
| | Diethylstilbestrol | | | | |
| | 17 α -Ethinylestradiol | | | | |
| | 17 β -Estradiol | | | | |
| | Estriol | | | | |
| | Amitriptyline | | | | |
| | Imipramine | | | | |
| | Clomipramine | | | | |
| | Salicylic acid | | | | |
| | Ibuprofen | | | | |
| | Paracetamol | | | | |
| | Flurbiprofen | | | | |
| | Naproxen | | | | |
| | Diflunisal | | | | |
| Samaras <i>et al.</i> (Samaras et al., 2011) | Ketoprofen | Time (mins): 30, 60, 120 | 70 °C | 20 mins | |
| | Diclofenac | Temperature (°C): 60, 90 | | | |
| | Diethylstilbestrol | | | | |
| | Estrone | | | | |
| | 17 β -Estradiol | | | | |
| | 17 α -Ethinylestradiol | | | | |
| | Estriol | | | | |
| | Ibuprofen | Reagents: BSTFA + 1% TMCS* BSTFA | | | |
| | Naproxen | | | | |
| | Diclofenac | | | | |
| | Ketoprofen | | | | |
| | Bisphenol | Volume of Reagent (μL): 50, 100 | | | |
| | Triclosan | Volume of Pyridine (μL): 10, 25, 50 | | | |
| | Meclofenamic acid | Time (mins): 0, 20, 30 | | | |
| Sebök <i>et al.</i> (Sebök et al., 2008) | Ibuprofen | Reagents: HDMS + TFA* BSTFA MSTFA | 70 °C | 90 mins | |
| | Ketoprofen | | | | |
| | Naproxen | | | | |
| | Diclofenac | | | | |
| | | | | | Time (mins): 30, 60, 90, 120 |
| | | | | | Temperature (°C): 60, 70, 80 |
| Lacina <i>et al.</i> (Lacina et al., 2013) | Salicylic acid | Reagent: MSTFA* | 70 °C | 90 mins | |
| | Acetylsalicylic acid | | | | |
| | Clofibric acid | | | | |
| | Ibuprofen | | | | |
| | Acetaminophen | | | | Time (mins): 30, 60, 90, 120 |
| | Caffeine | | | | Temperature (°C): 30, 50, 70, 90 |
| | Naproxen | | | | |
| | Mefenamic acid | | | | |
| | Ketoprofen | | | | |
| | Diclofenac | | | | |
| Yilmaz and Arslan (B. Yilmaz & Arslan, 2009) | Metoprolol | Reagent: MSTFA | Room temp. | 10 mins | |
| | Atenolol | | | | |
| | | | | | Time (mins): 5, 10, 20 |

| | | Temperature (°C): Room temp, 50, 75 | | |
|--|-------------|---|-------|---------|
| Brunelli <i>et al.</i> (Brunelli et al., n.d.) | Terbutaline | Reagent: MSTFA* | 60 °C | 15 mins |
| | Salbutamol | | | |
| | Clenbuterol | No optimisation | | |
| | Alprenolol | | | |
| | Metoprolol | | | |
| | Pindolol | | | |
| | Atenolol | | | |
| Huggett <i>et al.</i> (Huggett et al., 2003) | Acebutolol | Reagent: MSTFA* | 60 °C | 15 mins |
| | Metoprolol | | | |
| | Nadolol | No optimisation | | |
| | Propranolol | | | |

4.2 Methods

4.2.1 Reagents

Pharmaceutical compounds paracetamol (CAS Number: 103-90-2), atenolol (29122-68-7), carbamazepine (298-46-4), diclofenac sodium (15307-79-6), ibuprofen (15687-27-1), warfarin (81-81-2), salicylic acid (69-72-7), clofibrac acid (882-09-7), metronidazole (443-48-1), triclosan (3380-34-5), ketoprofen (22071-15-4), sotalol (3930-20-9), dapsone (800-08-0), fluvastatin (93957-54-1); and internal standard phenanthrene (85-01-8) were purchased from Sigma-Aldrich. All pharmaceutical standards were of high purity grade (>90%). Ethyl acetate (141-78-6), pyridine (110-86-1), and methanol (67-56-1) were purchased from Sigma-Aldrich or Fisher Scientific. All solvents were of reagent quality or greater. N-trimethylsilyl-N-methyltrifluoroacetamide (MSTFA; 24589-78-4) and bis(trimethylsilyl)-trifluoroacetamide + 1% trimethylchlorosilane (BSTFA + 1% TMCS; 25561-30-2) was purchased from Sigma-Aldrich or Crawford Scientific and were of derivatisation grade or greater. Derivatisation agents were stored at 4 °C and -18 °C respectively, as per safety data sheets (SDS).

4.2.2 Pharmaceutical Compound Selection

Fourteen representative PhCs were chosen with respect to their LogP, molecular weight (MW), number and type of labile hydrogens (see Appendix). The compounds were chosen to cover a broad spectrum of physicochemical characteristics. LogP ranged from -0.459 to 4.982, covering both polar and non-polar PhCs. MW ranged from 151.06 to 411.18 g/mol; as GC applications are limited by the volatility of the compound, with MW >450 a.m.u often causing issues including poor or non-existent peaks (Kyle, 2017). The number of labile hydrogens per compound ranged from 1 to 4, with a functional group from each stage of the ease of silylation (OH>ArOH>COOH>NH>CONH) present. A list of selected physicochemical properties for selected compounds can be found in Table 4-2.

Table 4-2: Pharmaceutical compounds for spiked solutions: information on LogP, MW, and labile hydrogens

| Compound | LogP | MW (g/mol) | No of labile Hydrogens | Functional Groups |
|----------------|--------|------------|------------------------|-----------------------------------|
| Metronidazole | -0.459 | 171.1 | 1 | OH |
| Sotalol | -0.395 | 272.1 | 3 | OH, NH, SONH |
| Atenolol | 0.425 | 266.2 | 4 | OH, NH, NH ₂ |
| Paracetamol | 0.907 | 151.1 | 2 | ArOH, CONH |
| Dapsone | 1.27 | 248.1 | 4 | NH ₂ , NH ₂ |
| Salicylic Acid | 1.977 | 138.0 | 1 | COOH |
| Warfarin | 2.744 | 308.1 | 1 | COOH |
| Carbamazepine | 2.766 | 236.1 | 2 | CONH ₂ |
| Clofibric Acid | 2.899 | 214.0 | 1 | COOH |
| Ketoprofen | 3.613 | 254.1 | 1 | COOH |
| Fluvastatin | 3.826 | 411.2 | 3 | OH, OH, COOH |
| Ibuprofen | 3.843 | 206.1 | 1 | COOH |
| Diclofenac | 4.259 | 295.0 | 2 | COOH, NH |
| Triclosan | 4.982 | 288.0 | 1 | OH |

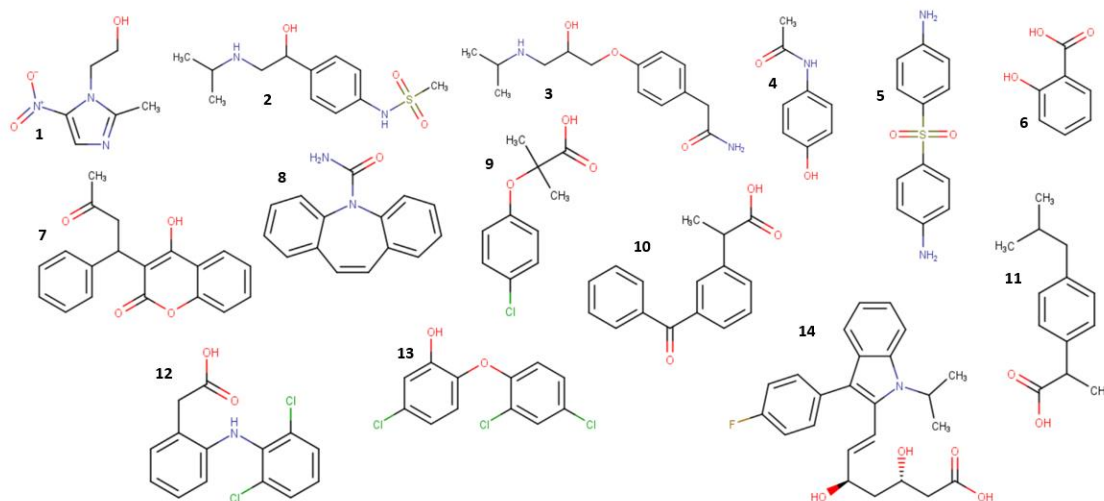


Figure 4.1: Chemical structure of the chosen compounds. 1: metronidazole, 2: sotalol, 3: atenolol, 4: paracetamol, 5: dapsone, 6: salicylic acid, 7: warfarin, 8: carbamazepine, 9: clofibric acid, 10: ketoprofen, 11: ibuprofen, 12: diclofenac, 13: triclosan, 14: fluvastatin

4.2.3 Derivatisation

4.2.3.1 Preparation of Solutions

Individual stock solutions of each pharmaceutical compound and a stock mixture of the fourteen PhCs, were prepared in methanol, all at 0.5 mg/mL. All stock solutions were stored in airtight containers at -20°C (Shanmugam et al., 2010) and renewed every three months. All individual working solutions, mixtures and dilutions were prepared on the day of analysis and stored in an airtight container at -20°C for inter-day replicates.

As this research is intended to be applied to non-targeted analysis in future applications phenanthrene was used as an internal standard following methods of Veenaas *et al.*, 2018, Shareef *et al.*, 2006 and Kumirska *et al.*, 2013. An individual phenanthrene stock solution (0.5 mg/mL) and working solution (0.05 mg/mL) were prepared in ethyl acetate and stored at -20 °C.

4.2.3.2 Solvent Comparison

Methanol has a labile hydrogen (OH) and thus cannot be used as the solvent for derivatisation. For derivatisation, a polar aprotic solvent is required, and thus, three solvents were chosen for comparison – ethyl acetate (EA), dichloromethane (DCM) and acetonitrile (MeCN).

To compare each solvent, 1.0 mL of the PhC mix stock solution in methanol (0.5 mg/mL) was evaporated and then reconstituted in 1.0 mL of each solvent. To this solution, 100 µL of MSTFA was added; and the sample heated to 60 °C for 30 mins. Analysis was conducted on the GC-MS (100:1 split). A scouting method was used for this method; thus, a longer runtime is observed.

4.2.3.3 Derivatisation Procedure

A 1.5 mL aliquot of the PhC Mix in MeOH (0.5 mg/mL) was evaporated to dryness and reconstituted in 0.8 mL ethyl acetate, concentrating the sample. Derivatisation was applied by adding 200 µL of MSTFA and heating to 60 °C for 30 mins (Butts, 1972; Orata, 2012). The solution was analysed in both derivatised and non-derivatised forms for comparison. For non-derivatised samples, 200 µL of ethyl acetate was added instead of MSTFA to ensure PhC concentrations remained the same (0.75 mg/mL).

4.2.4 Optimisation of Derivatisation

4.2.4.1 Preparation of Solutions

Individual stock solutions of each pharmaceutical compound and a stock mixture of five PhCs (atenolol, carbamazepine, diclofenac, paracetamol, and warfarin), were prepared in ethyl acetate or an ethyl acetate: acetonitrile (50% v/v) mix at 1 mg/mL and 0.5 mg/mL respectively. Individual working solutions and mixtures were prepared in ethyl acetate or acetonitrile, to relevant concentrations (~0.5 or 0.05 mg/mL) by sequential dilution of stock solutions. As before, all solutions were stored at -20 °C, stock solutions were renewed every three months and phenanthrene was used as the internal standard.

4.2.4.2 Derivatisation Procedure

N-trimethylsilyl-N-methyltrifluoroacetamide (MSTFA) was used to derivatise all pharmaceutical standards and mixtures unless stated otherwise in Table 4-3. Varying volumes (µL) of MSTFA were added to solutions whilst in a 2 mL GC vial, 200 µL glass insert, or 300 µL sonication vial (see Appendix B). Vials were either allowed to stand at room temperature or heated in a conventional oven for varying periods of time. Varying volumes of pyridine were added to the vials, to act as a catalyst in some reactions. All volumes and derivatisation methods can be found in Table 4-3. Derivatisation was always undertaken immediately before GC analysis to prevent degradation of derivatives.

Table 4-3: Sample preparation and derivatisation procedure for all experimental work conducted in Chapter 4. Details include PhCs analysed, calculated millimolar concentrations for PhCs, derivatisation reagent volume and corresponding calculated molar ratio, and derivatisation protocol. Millimolar concentrations were calculated using JChem for excel.

| Experiment | Compounds | No of mmoles (PhC*active sites) | Derivatisation Agent and Volume (µL) | Mmol Ratio (Der. Agent: PhC Active Sites) | Derivatisation Method | | | | |
|---|---------------|---------------------------------|--------------------------------------|---|--|--------|--------------|---|-------|
| Comparative study of silylation reagents: BSTFA + 1% TMCS vs MSTFA | Paracetamol | 0.0002 | BSTFA + 1% TMCS* | | Various volumes of BSTFA +1% TMCS and MSTFA (1, 5, 10, 20, 50, 100, 150, 200 µL) were added to 300 µL or 1 mL glass vial containing 40 µL of paracetamol individual working solution in ethyl acetate. 20 µL of phenanthrene stock solution in ethyl acetate was added as an internal standard. Vials were heated to 60 °C for 3 hours before analysis by GC-MS. Extended time to ensure all derivatisation had taken place for low volumes of derivatisation agent. | | | | |
| | | | | 1 | | 7:1 | | | |
| | | | | 5 | | 37:1 | | | |
| | | | | 10 | | 73:1 | | | |
| | | | | 20 | | 147:1 | | | |
| | | | | 50 | | 367:1 | | | |
| | | | | 100 | | 734:1 | | | |
| | | | MSTFA | 1 | 11:1 | | | | |
| | | | | 5 | 53:1 | | | | |
| | | | | 10 | 105:1 | | | | |
| | | | | 20 | 211:1 | | | | |
| | | | | 50 | 525:1 | | | | |
| | | | | 100 | 1050:1 | | | | |
| | | | | 150 | 1575:1 | | | | |
| | | | | 200 | 2101:1 | | | | |
| | | | | Molar Ratio and Reaction Time | Carbamazepine | 0.0002 | MSTFA | 1 | 32:1 |
| | | | | | | | | 5 | 158:1 |
| 7 | 222:1 | | | | | | | | |
| 10 | 317:1 | | | | | | | | |
| 20 | 633:1 | | | | | | | | |
| 50 | 1583:1 | | | | | | | | |
| 100 | 3165:1 | | | | | | | | |
| 120 | 3799:1 | | | | | | | | |
| Addition of a Catalyst | Carbamazepine | 0.0001 | MSTFA | 7 | 219:1 | | | | |
| MSTFA was added to a 300 µL sonication vial containing 65 µL EA, 40 µL of an individual carbamazepine working solution, and 25 µL pyridine. 20 µL of phenanthrene working solution was added. Samples | | | | | | | | | |

| Experiment | Compounds | No of mmoles (PhC*active sites) | Derivatisation Agent and Volume (μL) | Mmol Ratio (Der. Agent: PhC Active Sites) | Derivatisation Method |
|--|---------------|---------------------------------|---|---|--|
| Competing Reactions | Paracetamol | 0.0003 | MSTFA | | were left at room temperature for 5 mins before analysis. |
| | Warfarin | 0.0001 | 7 | 38:1 | Various volumes of MSTFA (7, 10, 20, 50 μL) were added to a 300 μL vial containing 100 μL of pharmaceutical mixture in MeCN:EA (1:1). 20 μL of phenanthrene working solution was added. Vials were left at room temperature and injected every 5 minutes for 90 minutes. |
| | Carbamazepine | 0.0002 | 10 | 55:1 | |
| | Atenolol | 0.0004 | 20 | 109:1 | |
| | Diclofenac | 0.0001 | 50 | 273:1 | |
| | | | | | |
| Optimisation of Silylation for PhCs by Design of Experiments | Carbamazepine | 0.0002 | MSTFA 7 | 222:1 | MSTFA was added to a 300 μL sonication vial containing 65 μL EA, 40 μL of the individual carbamazepine working solution and 25 μL of pyridine. 20 μL of phenanthrene working solution was added. Samples were added to a conventional GC oven set at various temperatures for various time periods before analysis. |

4.2.5 Response Measurements for TMS derivatives

4.2.5.1 Peak Areas

The efficiency of derivatisation was measured by the peak area (PA) of the analyte peak. Silylation is an S_N2 reaction, where the parent analyte is converted to its more thermally stable TMS derivative (Pierce, 1968). The reaction takes place until there is no more parent compound left to react, and the derivative has fully formed (i.e., no further increase in PA). Therefore, derivatisation was considered to be complete when the PA of the derivatised analyte peak remained constant (Caban et al., 2011; Lacina et al., 2013). All experiments followed this method, with the exception of the ‘Derivatisation’ and ‘Optimisation of Silylation method for Pharmaceuticals by Design of Experiments’ where response factors (Rf) were used as responses (see Section 4.2.5.2 Response Factor (Rf)).

Accounting for Dilution Factor

The derivatisation reagent was varied in some experiments, increasing the total volume of the sample. The concentration of the analyte in the resulting sample is therefore inversely proportional to the volume of derivatisation reagent added. In these instances, a dilution factor is applied. The dilution factor (DF) calculation is shown in equation (4-1). A worked example of the calculation can be found in Appendix B.

$$\text{Dilution Factor} = \frac{\text{Total volume of sample } (\mu\text{L})}{\text{Total volume of greatest dilution } (\mu\text{L})} \quad (4-1)$$

Peak areas were adjusted to account for the dilution, by multiplying the analyte peak areas by the calculated DF. This method was used for all experiments which included dilution. To ensure minimal variability in the detector, the peak area of the internal standard peak (phenanthrene) was monitored throughout the analyses (DF adjusted).

Minimising variance for data comparison

Peak areas of compounds are generally proportional to the concentration of the peak; with a larger peak area attributed to a higher concentration (Shimadzu, 2020). However, detector responses can differ between runs, and therefore comparison of peak areas can become challenging. To overcome this, particularly for the comparative study of silylation reagents: BSTFA + 1% TMCS vs MSTFA study, the peak areas of the responses were log transformed (\log_{10}) to minimise the variation of the data. This was performed using the “=LOG10” function on Microsoft Excel.

4.2.5.2 Response Factor (Rf)

Response factors (Rfs) were used in the ‘4.3.1 4.3.1 Derivatisation’ and the ‘4.3.2.5 Optimisation of Silylation method for Pharmaceuticals by Design of Experiment’ sections. In these experiments, there was no attributed dilution factor and thus Rfs could be used. Rfs were calculated by dividing the peak area of the analyte peak against the peak area of the internal standard (phenanthrene) (4-2).

$$Rf = \frac{(\text{Peak Area}_{\text{ANALYTE}})}{(\text{Peak Area}_{\text{INTERNAL STANDARD}})} \quad (4-2)$$

4.2.6 GC-MS Analysis

Analysis was conducted using an Agilent 7890A gas chromatograph coupled to an Agilent 5975C quadrupole mass spectrometer. Aliquots (1 μL) of derivatised sample were injected in split mode (100:1) onto an Agilent DB-5 (5% phenyl and 95% methylpolysiloxane) capillary column (30 m x 0.25 mm x 0.25 μm). An isocratic method was used (275 $^{\circ}\text{C}$ for 2.5 mins, or 275 $^{\circ}\text{C}$ for 3 mins), with a helium carrier gas flow rate of 2 mL/min. Inlet and transfer line temperatures were set to 270 $^{\circ}\text{C}$. Mass spectra were obtained in electron ionisation mode (70 eV), in full scan mode (50-550 amu). MS source and quad temperatures were 230 $^{\circ}\text{C}$ and 150 $^{\circ}\text{C}$, respectively. A quick method (of less than 5 mins) was applied to ensure silylation could be observed at various timepoints throughout the $\text{S}_{\text{N}}2$ reaction.

4.2.7 Software

Structures and reaction mechanisms were drawn using MarvinSketch 18.19.0 or ChemDraw 19.1.1.21 software. Chromatograms and mass spectrums were translated from Chemstation E.02.01.1177 to OpenChrom Community Edition 1.2.0 software for data analysis and annotation. Minitab 20.4.0.0 software was used for experimental design. RStudio 1.1.442 software was used to produce plots. Inkscape 0.92.3 will be used to produce all schematics and diagrams. JChem for Excel 18.20.0.353 was used to aid in molar ratio calculations.

4.2.8 Statistics

All statistical calculations were undertaken in Minitab (v20.4.0.0). Analysis of variance (ANOVA), 2-way t-tests and design of experiments (DOE) were conducted using the ‘ANOVA’, ‘Basic Statistics’ and ‘DOE’ functions in the software.

4.2.8.1 Analysis of Variance (ANOVA)

One-way ANOVA has 6 assumptions which must be met before analysis can be undertaken (Lund Research Ltd., 2018). Assumptions are as follows:

1. Is the dependent variable measured on a continuous level?
2. Does the independent variable consist of two or more categorical, independent groups?
3. Is there independence of observations (no relationship between observations in each group, or between each group)?
4. Are there any significant outliers?
5. Is the dependent variable approximately normally distributed for each group of the independent variable?
6. Is there homogeneity of variances?

All assumptions must be satisfied prior to ANOVA analysis. Outliers can pose a problem in the analysis and so must be removed prior to ANOVA (assumption 4). Assumptions 1-3 relate to the study design and variable choice, whereas assumptions 4-6 relate to the nature of the data. Assumptions 4-6 can be tested using the Minitab software (outlier test, normality test and test for equal variances respectively). The outcomes of the assumptions and ANOVA tests used in this study are located in Appendix B.

4.2.8.2 Two-sample t-tests

To compare means of two samples, 2-sample t-tests were applied. The tests calculate t-values from two independent groups, incorporating sample size and variability into the data. There are four assumptions which have to be met prior to conducting a 2-sample t-test (Minitab Inc., 2021a). These are as follows:

1. The data must be continuous.
2. The sample data must not be severely skewed.

3. The sample data should be selected randomly.
4. Each observation should be independent from all other observations.

The t-value calculation is shown in equation (4-3). The default null hypothesis is that the two means are equal ($H_0: \mu_1 - \mu_2 = \delta_0$). A p-value of <0.05 suggests that there is a statistically significant difference between the two means.

$$t - \text{value} = \frac{(\bar{X}_1 - \bar{X}_2)}{s} \quad (4-3)$$

where ' \bar{X} ' is the mean of the specified sample set and 's' is the sample standard deviation (as calculated for the test statistic). Unequal variance was assumed and so the sample standard deviation was calculated as below:

$$s = \sqrt{\frac{s_1^2}{n_1} + \frac{s_2^2}{n_2}} \quad (4-4)$$

where 's' is the sample standard deviation for the denoted sample, and 'n' is the sample size (Minitab Inc., 2021b).

4.2.8.3 Design of Experiments

To optimise the silylation method, design of experiments (DOE) approach was used. Parameters (temperature and time) were optimised using a fractional factorial design approach. Low and high levels were set to 30 °C and 70 °C for temperature, respectively and 30 mins and 60 mins for time. This allows for simultaneous optimisation of analytical conditions with relatively few experiments, reducing both analysis time and solvent waste. Response surface methodology (RSM) was used to mathematically fit the response values. Minitab 20.4.0.0 software was used to produce and evaluate the data obtained from the optimisation procedures.

4.3 Results and Discussion

4.3.1 Derivatisation

Most PhCs are considered to be polar in nature, as they contain polar functional groups such as OH, COOH and NH groups. PhCs therefore should be converted to their more volatile derivatives prior to GC analysis. Derivatives increase volatility and thermal stability, reduce polarity, and also generate characteristic mass spectral fragments, which can aid in identification (i.e., trimethylsilyl (TMS) derivatives produce distinctive ions at m/z 73) (Lai & Fiehn, 2018). To ensure all PhCs are detected and identified, 14 representative PhCs were used to optimise a derivatisation method.

4.3.1.1 Solvent Comparison

To determine the optimal solvent for reconstitution and derivatisation, three solvents were compared. Eleven out of 14 PhCs (sotalol, warfarin and dapsone which were $<LOD$) were identified on the

chromatograms in their fully derivatised form (see Appendix B) in both EA and DCM samples. Dapsone has two secondary (2°) amine groups and is only visible in its tetra-TMS form. Therefore, it seems like this compound may not have fully derivatised (as amines take longer to derivatise). Warfarin and sotalol have been identified in other experiments (see 4.3.1.2 Choice of Pharmaceuticals) and thus concentrations in this study may be too low for detection, or like dapsone, the compounds may have not fully derivatised. Diclofenac mono-TMS was not identified in the MeCN sample, suggesting complete silylation was not achieved in this solvent. For the identified peaks, in general, DCM had lower Rfs than MeCN and EA (see Figure 4.2), suggesting lower silylation efficacy in this solvent.

With a LogP of 0.73, ethyl acetate is slightly less polar than acetonitrile (LogP 0.34) and more polar than dichloromethane (LogP 1.25). All solvents have a boiling point of <100 °C (DCM- 40 °C, EA – 77 °C and MeCN – 82 °C), which result in low retention in GC analysis. This is particularly desirable for non-targeted methods, as the solvent will not interfere with early eluting unknown compounds.

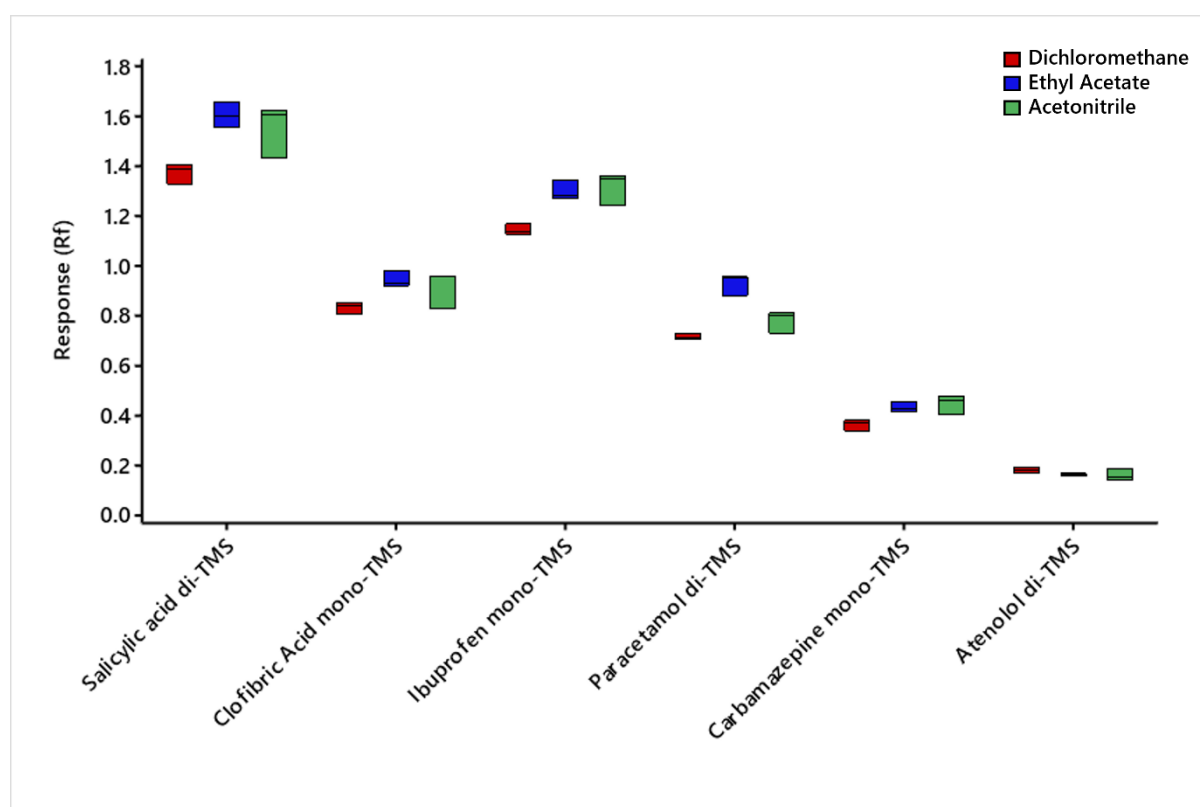


Figure 4.2: Comparison of response factors ($n=3$) for each identified PhC (0.5 mg/mL) in three reconstitution solvents: ethyl acetate, dichloromethane, and acetonitrile. Generally, Rfs were lower for dichloromethane, whilst ethyl acetate and acetonitrile were similar.

In terms of green chemistry, a solvent risk rating has been developed. Taking many solvent selection guidelines (SSGs) into consideration, an algorithm was created which considered many physicochemical properties (including LogP, $BOD_{1/2}$, and fish LC_{50}), to determine the risk rating of

over 150 traditional solvents used in analytical chemistry (Gałuszka et al., 2013; Kokosa, 2019; E. Yilmaz & Soylak, 2020). The ideal solvent risk rating is 1.000 (water), suggesting that the closer to 1 the value, the more environmentally friendly the solvent. Ethyl acetate was given a solvent risk ranking of 0.8868, acetonitrile 0.8677 and dichloromethane 0.7150 (Kokosa, 2019; E. Yilmaz & Soylak, 2020). This suggests that ethyl acetate is the most environmentally friendly solvent tested, and dichloromethane the least friendly. Ethyl acetate is considered one of the least environmentally harmful organic solvents as it can easily be broken down in both water and air (Ihme, 2020). DCM is considered a highly hazardous and undesirable solvent (Byrne et al., 2016; E. Yilmaz & Soylak, 2020), whilst acetonitrile has been classed as a problematic solvent (Alder et al., 2016; Henderson et al., 2011). Therefore, ethyl acetate was chosen as the reconstitution solvent in line with the green chemistry objective, 'Safer Solvents and Auxiliaries' (Anastas & Warner, 1998) as it is more environmentally friendly and less toxic than DCM (Alder et al., 2016; Byrne et al., 2016; Henderson et al., 2011).

4.3.1.2 Choice of Pharmaceuticals

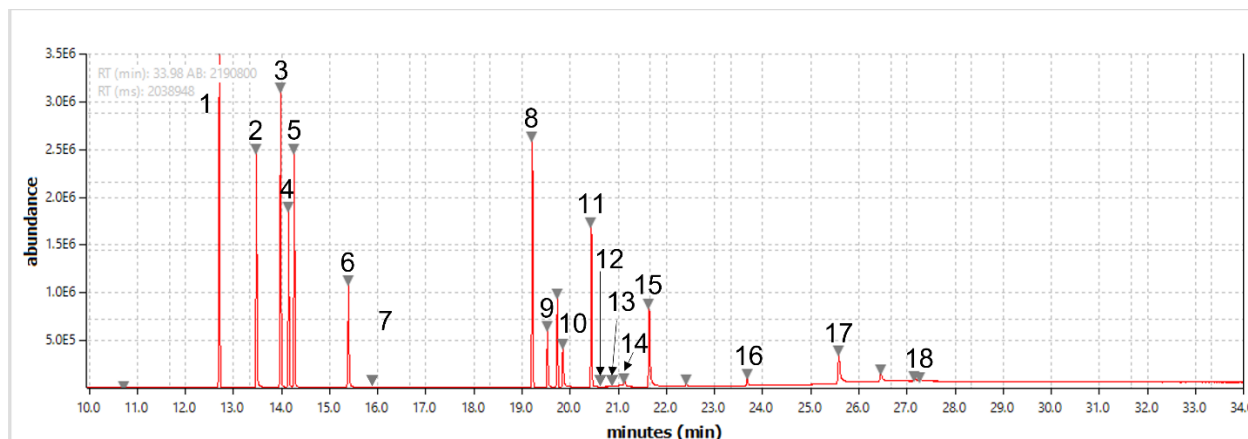
Initially, a scouting method with a split of 100:1 was utilised to determine the number of PhCs which could be identified on the GC. A high concentration (0.94 mg/mL) of the PhC mix in ethyl acetate was chosen to evaluate the improvements silylation has on PhC detection and identification. To ensure the PhCs were well above the LOD for the preliminary studies, and thus a high split ratio was used.

Only 47% of PhCs were identified in their non-derivatised form: ibuprofen, metronidazole, triclosan, diclofenac, carbamazepine, sotalol and dapson. Whereas all PhCs with the exception of fluvastatin were identified in their derivatised form. Fluvastatin has a high MW (411.18 g/mol) which is already in the upper end of the GC limitations (high MW = low volatility). With three potential silylation points (OH, OH, COOH), the addition of 3 TMS groups would add >200 a.m.u. to the already large molecule (MW= 627.18 g/mol). In this instance, silylation will not increase the volatility of the compound, instead hindering its analysis.

Full derivatisation for all compounds was not achieved in the derivatised sample. Diclofenac, carbamazepine and dapson were all present in their non-derivatised form (Figure 4.3), and paracetamol mono-TMS was present, suggesting full silylation had not occurred for this compound either. This may be due to the molar ratio and the 30-minute derivatisation period. Orata suggests that some hindered compounds may require heating of up to 16 hours (Orata, 2012), and thus may not be fully silylated in the 30-minute period. The molar ratio is low (13:1, MSTFA: PhC*active sites), suggesting a second order reaction rate, where full silylation of all PhCs would be possible if the derivatisation time was increased significantly.

The chromatograms for the derivatised sample, were far superior in terms of resolution, peak shape, and baseline. The DB-5 column used for the analysis is a non-polar column. The polarity of the PhCs is reduced through derivatisation, increasing the compounds affinity for the non-polar stationary phase.

Compounds are retained longer, selectivity and resolution are increased and thus, the chromatography improves. The improved chromatography coupled with the increased number of PhCs visible on the chromatogram highlights the requirement for derivatisation in the method.



| Peak Number | Retention Time (mins) | Compound |
|-------------|-----------------------|-------------------------|
| 1 | 12.704 | Salicylic Acid di-TMS |
| 2 | 13.472 | Clofibric Acid mono-TMS |
| 3 | 13.974 | Ibuprofen mono-TMS |
| 4 | 14.142 | Paracetamol di-TMS |
| 5 | 14.257 | Metronidazole mono-TMS |
| 6 | 15.383 | Paracetamol mono-TMS |
| 7 | 15.782 | Phenanthrene |
| 8 | 19.213 | Triclosan mono-TMS |
| 9 | 19.524 | Diclofenac |
| 10 | 19.848 | Ketoprofen mono-TMS |
| 11 | 20.437 | Carbamazepine mono-TMS |
| 12 | 20.598 | Sotalol mono-TMS |
| 13 | 20.668 | Diclofenac mono-TMS |
| 14 | 21.130 | Carbamazepine |
| 15 | 21.638 | Atenolol di-TMS |
| 16 | 23.677 | Warfarin mono-TMS |
| 17 | 25.583 | Dapsone |
| 18 | 27.148 | Dapsone tetra-TMS |

Figure 4.3: Derivatised PhC Mix in EA (0.5 mg/mL) and Derivatised Sotalol in EA (0.5 mg/mL) chromatogram and corresponding identified peaks. Phenanthrene (0.05 mg/mL) used as the internal standard (RT – 15.782). Scouting method used to determine GC method and to ensure all PhCs were detected on the chromatogram in their derivatised form. Fluvastatin is the only compound not detected.

4.3.2 Optimisation of Derivatisation

PhCs have a broad range of chemical properties and structures, which introduces a challenge when derivatising. A derivatisation method which is applicable to a range of PhCs will simplify the determination of these analytes in various samples and matrices (Caban et al., 2011).

4.3.2.1 Comparative study of silylation reagents: BSTFA + 1% TMCS vs MSTFA

The literature suggests that the strength of the electrophile (in this instance, the derivatisation reagent) can have an impact on the silylation reaction. In this reaction, electrophile strength is directly related to

the strength of the derivatisation reagent – a strong silylation reagent is required to derivatise all labile hydrogens to TMS derivatives. Both BSTFA and MSTFA are considered to be strong silylation reagents with similar silylation potential (Moldoveanu and David, 2014) and therefore were studied in more detail to determine which silylation reagent to use for duration of the study.

Paracetamol was chosen for this experiment as it contains two groups which undergo silylation: a phenol group (ArOH – easily silylated) and an amide group (CONH – difficult to silylate). Paracetamol is known to silylate quickly and easily, with both mono- and di-TMS derivatives of paracetamol visible on the chromatograms; their presence indicating the progression of the silylation reaction (Figure 4.4). This is captured by the formation and subsequent reduction of the mono-TMS peak, and the formation and plateau of the di-TMS peak (see Figure 4.5).

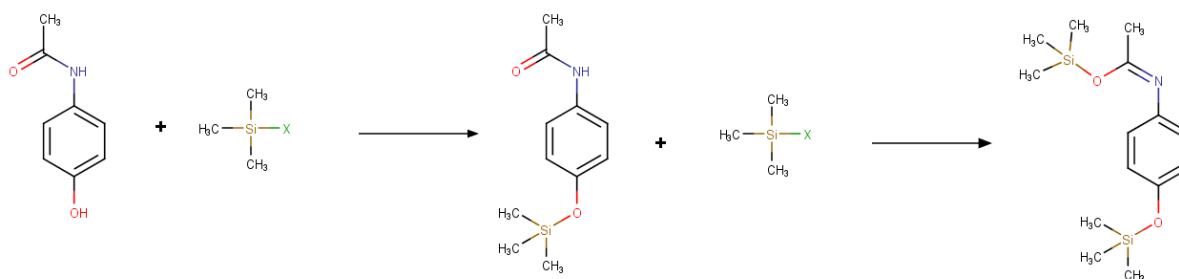


Figure 4.4: Silylation of Paracetamol by X-TMS. The phenol group undergoes silylation first, producing paracetamol mono-TMS. This molecule reacts with another X-TMS group, where the amide group is silylated on the oxygen atom, forming paracetamol di-TMS. Mono- and di-TMS mass spectra and fragmentation patterns are located in the Appendix.

Molar Ratio

In order to compare the two derivatisation reagents, the reagent volume must first be converted to molar ratio. The volume of the derivatisation reagent is proportionate to the concentration of the PhCs and the number of active sites it contains. Thus, the volume of reagent used in this experiment may bear different results if a greater concentration of paracetamol is used, or if another PhC with more active sites (for example, atenolol – 4 active sites) is studied. Whereas the molar ratio between the number of active sites of the PhC and the derivatisation reagent, produces a more accurate description of the silylation potential of each reagent.

Molar ratio is dependent on the MW and the density of the derivatisation reagent. MSTFA has a lower MW (199.25 g/mol compared to 257.4 g/mol for BSTFA) but higher density to BSTFA (1.075 g/mL compared to 0.96 g/mL for BSTFA). Thus, a greater number of moles are available, and an increased molar ratio is obtained with MSTFA in comparison to equivalent volumes of BSTFA. Although BSTFA contains two TMS groups, it is widely accepted that the PhC (nucleophile) will attack the oxygen atom on the BSTFA molecule, as the nitrogen atom possesses no vacant orbitals (Caban & Stepnowski, 2018;

Stalling et al., 1968). Therefore, BSTFA only contains one potential silylation site, similar to that of MSTFA.

The response of both the paracetamol mono-TMS and di-TMS derivatives were plotted against molar ratio (see Figure 4.5). The silylation reaction is observed, with paracetamol converting first to the mono-TMS derivative, and then to the di-TMS derivative. Full silylation is considered to be achieved when a plateau in response is reached by the paracetamol di-TMS derivative. At this point, no further silylation can be achieved, and the reaction has reached its endpoint. In this study, the plateau is defined as the point where no statistically significant difference is observed between responses of paracetamol di-TMS at increasing molar ratios.

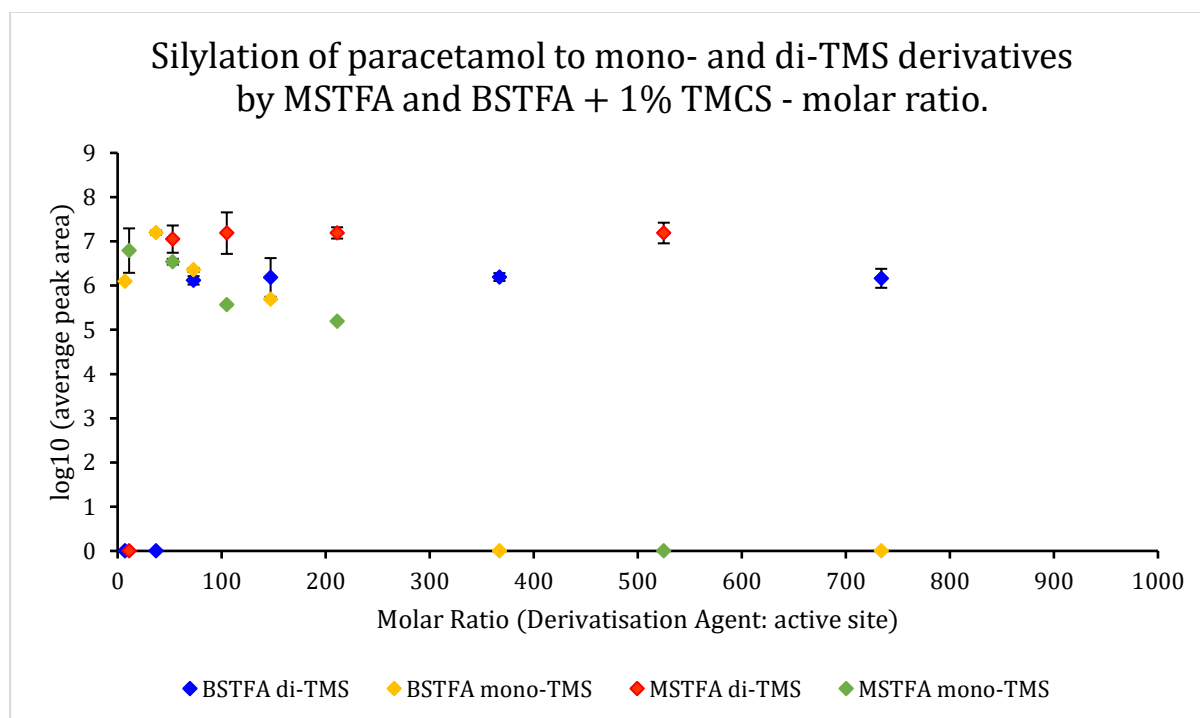


Figure 4.5: Silylation of paracetamol to its mono- and di-TMS derivatives. Average log-transformed PAs of mono- and di-TMS derivatives by molar ratio of BSTFA + 1% TMCS and ratio of MSTFA: PhC active sites (0-1000:1).

ANOVA analysis ($n=3$, p -value = 0.05) determined that a plateau was reached a molar ratio of 105:1 (10 μ L) for MSTFA and 734:1 (100 μ L) for BSTFA + 1% TMCS (see Table 4-4). This suggests that the full silylation of paracetamol is achieved with a far lower molar ratio (and volume) of MSTFA. It should be noted that the rate of reaction cannot be determined as the plateau response is defined by peak area and not analyte concentration, and time is constant throughout the study (it is not a kinetic curve).

Table 4-4: Determination of a statistically significant plateau for full paracetamol silylation: BSTFA + 1% TMCS and MSTFA (ANOVA analysis). All data satisfied all ANOVA criteria (see Appendix)

| ANOVA analysis of paracetamol di-TMS responses (p = 0.05) | | | |
|---|---|----------------------------|--|
| Reagent | Initial Molar Ratio of possible Plateau | End Molar Ratio of Plateau | Statistically significant difference (p-value) |
| BSTFA + 1% TMCS | 7 | 1468 | 0.000 |
| | 37 | | 0.000 |
| | 73 | | 0.000 |
| | 147 | | 0.006 |
| | 367 | | 0.007 |
| | 734 | | 0.821 |
| | 1101 | | 0.930 |
| MSTFA | 11 | 2100 | 0.000 |
| | 53 | | 0.000 |
| | 105 | | 0.058 |
| | 211 | | 0.050 |
| | 525 | | 0.120 |
| | 1050 | | 0.443 |
| | 1575 | | 0.383 |

Comparable repeatability was observed for both derivatisation reagents: all RSDs <10% for both di-TMS derivatives, and below 20% for mono-TMS derivatives. The mono-TMS derivative is rapidly converted to the di-TMS derivative, and thus this may explain the larger RSDs for these peaks.

To compare silylation efficacy, a PA plateau value ($PA_{\text{PlatMSTFA}} = 7.18$) was established by taking the average PAs ($\log_{10}(PA \cdot DF)$, $n=3$) for volumes of MSTFA between 10 μL and 200 μL (105:1-1575:1). When repeated for the BSTFA + 1% TMCS volumes between 100-200 μL (734:1 – 1101:1), the $PA_{\text{PlatBSTFA+1\%TMCS}} = 6.17$ ($n=3$). A 2-sample T-test determined that there was a statistically significant difference between the PA_{Plat} values, indicating that MSTFA obtained a greater response when silylation was considered complete.

Atom Economy

The efficiency of the derivatisation reaction is often measured only by the response of the derivatised peak; few taking the parent compound into consideration (Caban & Stepnowski, 2018; Moldoveanu and David, 2014; Pierce, 1968). There is little information attributed to the extent of the use of the derivatisation reagent, or to the extent of the formation of by-products or waste (Royal Society of Chemistry, 2019). The second principle of Green Chemistry highlights the requirement for atom economy (Anastas & Warner, 1998): “*methods should be designed to maximise incorporation of all materials used in the process into the final product*” (American Chemical Society, 2022). Thus, reducing atom wastage. Generally, substitution reactions, such as silylation, are considered to be less economical than addition or rearrangement reactions, however are more economical than elimination reactions (Cann, 2021).

Atom economy is calculated as follows:

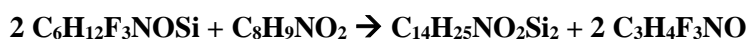
$$\% \text{ Atom Economy} = \left(\frac{\text{MW of desired product}}{\text{MW of all reactants}} \right) * 100 \quad (4-5)$$

In our reaction, paracetamol is converted to its di-TMS derivative.



The calculation of atom economy for both reagents is shown below:

MSTFA:



$$\% \text{ Atom Economy} = \left(\frac{295.53 \text{ g/mol}}{(2 * 199.25 \text{ g/mol}) + 151.16 \text{ g/mol}} \right) * 100 \quad (4-6)$$

$$\% \text{ Atom Economy} = 54\%$$

BSTFA:



$$\% \text{ Atom Economy} = \left(\frac{295.53 \text{ g/mol}}{(2 * 257.40 \text{ g/mol}) + 151.16 \text{ g/mol}} \right) * 100 \quad (4-7)$$

$$\% \text{ Atom Economy} = 44\%$$

An annotated reaction which highlights atoms which are wasted can be found in Appendix B. MSTFA has a greater atom economy, with 54% of reactants used to form the derivative, than BSTFA (only 44% of reactants are used). It should also be noted that the atom economy was calculated for BSTFA alone. The reagent which was used in the study included 1% TMCS (MW = 108.64 g/mol), which acts as a catalyst. Therefore, these additional atoms would also contribute to the calculation and result in a reduced atom economy for BSTFA. Therefore, the use of MSTFA would provide a more environmentally friendly reaction.

Thus, taking into consideration the previously mentioned experimentally acquired benefits of MSTFA, coupled with the addition of the increased atom economy, MSTFA can be said to be the optimal derivatisation reagent (of those studied) for derivatisation of paracetamol.

Other studies which compared MSTFA and BSTFA + 1% TMCS also concluded that MSTFA provided comparable results to BSTFA + 1% TMCS for silylation of paracetamol (Caban & Stepnowski, 2018), NSAIDs (Kurkiewicz et al., 2010; Migowska et al., 2012), steroids (Budzinski et al., 2006), β -blockers and β -agonists (Caban et al., 2011) and a mixture of PhCs (Kumirska et al., 2013) with Caban *et al.* concluding that MSTFA is a stronger silylation reagent for β -blockers and β -agonists, than BSTFA + 1% TMCS (Caban et al., 2011). However, each of these studies based their results on the volume of derivatisation reagent used; therefore, to compare, molar ratios were calculated for each of these studies (see Table 4-5). Calculated molar ratios were far larger than those used in this study (>100 fold).

Regardless, the conclusions drawn in each study remain the same: MSTFA provides comparable results to BSTFA + 1% TMCS, however akin to this study, MSTFA provides the comparable silylation consistently with a greater calculated molar ratio per μL of reagent used. This coupled with the lower volume of MSTFA required for the plateau (105:1 = 10 μL), and increased atom efficiency; MSTFA can be said to be the optimal choice between the two reagents for the silylation of paracetamol. Thus, MSTFA was determined suitable for the study and used in all further experiments.

Table 4-5: Calculated molar ratios for MSTFA and BSTFA + 1% TMCS of four independent studies which compared silylation efficiencies of MSTFA and BSTFA + 1% TMCS on silylation of various of PhCs. Each study did not vary the volume of reagent used.

| Paper | PhCs | Reagent and Volume used (μL) | Calculated molar ratios |
|----------------------------|----------------------|---|----------------------------|
| (Caban & Stepnowski, 2018) | paracetamol | MSTFA 100 μL | MSTFA 81502:1 |
| | | BSTFA + 1% TMCS 100 μL | BSTFA + 1% TMCS 56965:1 |
| (Migowska et al., 2012) | paracetamol | MSTFA | MSTFA |
| | acetylsalicylic acid | 50 μL | 15109:1 |
| | ibuprofen | BSTFA + 1% TMCS | BSTFA + 1% TMCS |
| | aminopyrine | 50 μL | 5280:1 |
| | flurbiprofen | | |
| | naproxen | | |
| | diflunisal | | |
| | ketoprofen | | |
| | diclofenac | | |
| | indomethacin | | |
| | diethylstilbestrol | | |
| | estrone | | |
| | estradiol | | |
| | ethinylestradiol | | |
| (Caban et al., 2011) | acebutolol | MSTFA | MSTFA |
| | atenolol | 50 μL | 5468:1 |
| | propranolol | BSTFA + 1% TMCS | BSTFA + 1% TMCS |
| | metoprolol | 50 μL | 1911:1 |
| | nadolol | | |
| | salbutamol | | |
| | pindolol | | |
| (Kumirska et al., 2013) | NSAIDS | NSAIDS | NSAIDS |
| | salicylic acid | MSTFA | MSTFA |
| | ibuprofen | 50 μL | 22579:1 |
| | paracetamol | BSTFA + 1% TMCS | BSTFA + 1% TMCS |
| | flurbiprofen | 50 μL | 7891:1 |
| | naproxen | | |
| | diflunisal | | |
| | ketoprofen | | |
| | diclofenac | | |
| | ANTIPILEPTICS | ANTIPILEPTICS | ANTIPILEPTICS |
| | valproic acid | MSTFA | MSTFA |
| | vigabatrin | 50 μL | 34277:1 |
| | primidone | BSTFA + 1% TMCS 50 μL | BSTFA + 1% TMCS 11979:1 |
| B-AGONISTS | B-AGONISTS | B-AGONISTS | |
| terbutaline | MSTFA | MSTFA | |
| salbutamol | 50 μL | 55182:1 | |

| Paper | PhCs | Reagent and Volume used (μL) | Calculated molar ratios |
|-------|--|---|---|
| | | BSTFA + 1% TMCS 50 μL | BSTFA + 1% TMCS 19284:1 |
| | B-BLOCKERS propranolol pindolol nadolol | B-BLOCKERS MSTFA 50 μL BSTFA + 1% TMCS 50 μL | B-BLOCKERS MSTFA 41193:1 BSTFA + 1% TMCS 14396:1 |
| | ESTROGENIC COMPOUNDS estrone diethylstilbestrol ethinylestradiol estradiol estriol | ESTROGENIC COMPOUNDS MSTFA 50 μL BSTFA + 1% TMCS 50 μL | ESTROGENIC COMPOUNDS MSTFA 37812:1 BSTFA + 1% TMCS 13214:1 |
| | ANTIDEPRESSANTS amitriptyline imipramine clomipramine | ANTIDEPRESSANTS MSTFA 50 μL BSTFA + 1% TMCS 50 μL | ANTIDEPRESSANTS No active sites – no molar ratio |

4.3.2.2 Molar Ratio and Reaction Time

In order to determine the optimal parameters for the silylation reaction, the relationship between molar ratio and reaction time was investigated. Literature suggests that increasing the reaction time will improve the yield of a silylation derivative (Sigma Aldrich, 1997). A plateau in response is expected, where the analyte has reached full silylation, and no derivatisable parent compound remains. Increasing the volume of reactant is expected to reduce the reaction time, as the rate of reaction increases (see equation (3-2)). MSTFA was added to the reaction in various volumes, though always in great excess (>100:1). Therefore, a change in concentration of MSTFA in the bimolecular reaction would have a negligible effect on the reaction ($k \rightarrow k'[\text{MSTFA}]^0$) and a pseudo-first order reaction rate was expected.

In order to capture the kinetic curve of the silylation reaction, carbamazepine was chosen instead of paracetamol for this study as it contains a difficult to silylate group (CONH_2 amide), and full silylation had not been achieved in previous studies (see 4.3.1.2 Choice of Pharmaceuticals). The reaction rate of the paracetamol silylation occurred rapidly (<5 mins, particularly with greater volumes of MSTFA) whereas silylation of carbamazepine (an amide) is known to take longer and thus the slower reaction allowed for the kinetic curve to be obtained.

Average carbamazepine and carbamazepine mono-TMS responses ($n=3$) were recorded to determine the yield of the reaction. Carbamazepine is only silylated to the mono-TMS derivative: the addition of the bulky TMS group to the nitrogen atom; prevents a second TMS group accessing the remaining labile hydrogen because of steric hindrance (Blau & King, 1978) (see Figure 4.6).

Carbamazepine is the only analyte, and thus the only potential point of silylation. All parameters which have been shown to catalyse the silylation reaction, i.e., the addition of pyridine or application of heat (Pierce, 1968), were not applied to ensure that the molar ratio was the only parameter driving the reaction. Initially MSTFA volumes of 1-10 μL were investigated, however upon data analysis, a further study with greater volumes of MSTFA was undertaken (10 μL -120 μL). However, the second study was undertaken >6 months later than the original, with newly prepared solutions, which may explain the variance in obtained response. To account for this, data from each study was plotted on separate charts, and no comparisons were drawn between the two studies.

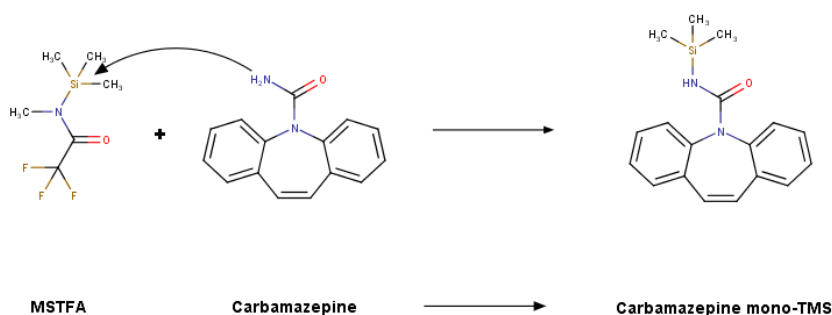


Figure 4.6: Silylation of carbamazepine-to-carbamazepine mono-TMS. The addition of the TMS group causes steric hindrance which prevents a second reaction on the remaining labile hydrogen. Thus, no carbamazepine di-TMS can be formed.

Akin to a pseudo-first order reaction, increasing the volume of MSTFA (from 1-10 μL) increased the overall rate of reaction (Figure 4.7a). Responses (PA*DF) for carbamazepine mono-TMS increased and carbamazepine responses decreased over time with increasing molar ratio (1-10 μL). The MSTFA reaction at 1 μL was not shown on Figure 4.7a, as no carbamazepine mono-TMS peak was formed within the 35 min period. The molar ratio for this reaction was <100:1 (32:1); which suggests the reaction is occurring, though at a much slower rate (Lua et al., 2013); more respective of a second order reaction. Thus, the data suggests that an increased MSTFA excess produces a higher yield of derivative at a faster rate. Specific reaction rates could not be calculated as response was measured in peak area and not analyte concentration. Although a rate cannot be calculated, the curve is reflective of a pseudo-first order reaction ($[A]$ vs time).

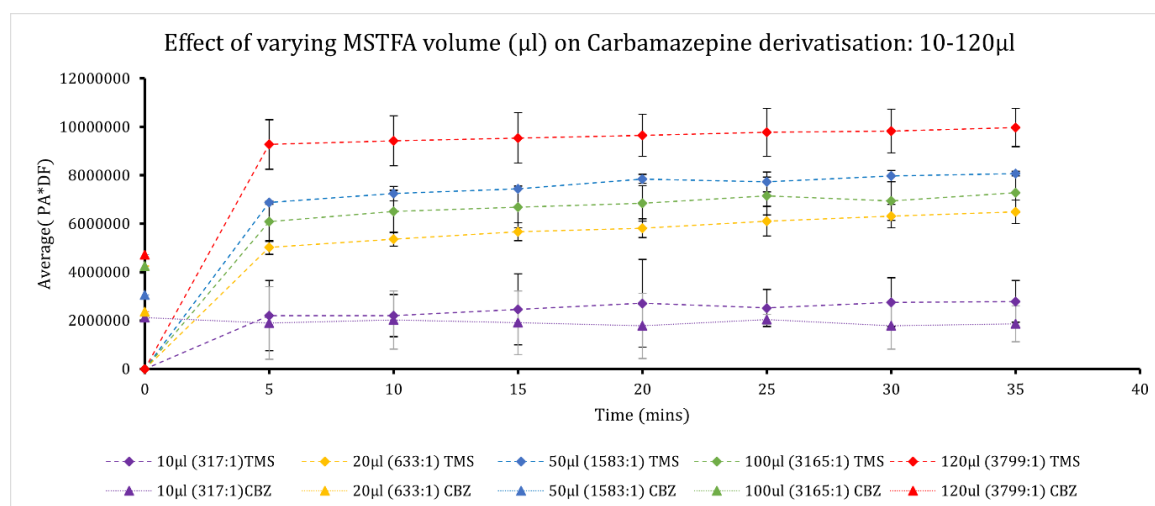
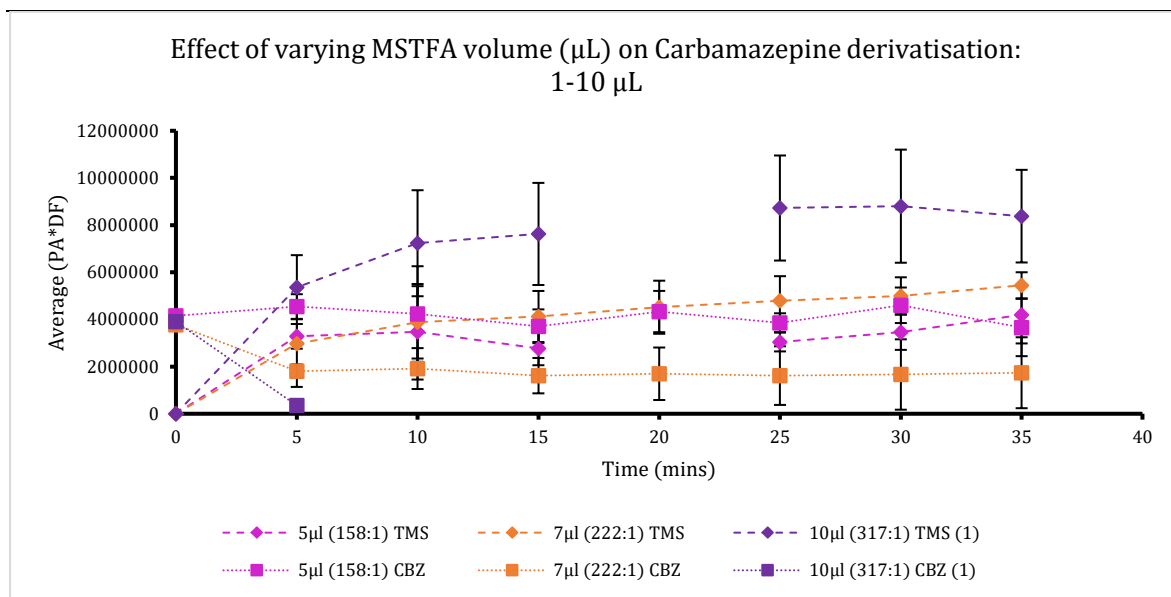


Figure 4.7: Silylation of carbamazepine: Effect of varying Molar ratio (MSTFA: PhC active sites) on silylation of carbamazepine-to-carbamazepine mono-TMS. a) 1-10 μL (32:1 – 317:1) Results for 32:1 are not shown, as carbamazepine mono-TMS was not produced. b) 10-120 μL (317:1-3799:1). Results are shown in separate plots as preparation and analysis was conducted months apart – which may explain variance in response.

It was expected that when all the parent PhC had silylated, no further derivatised product would be produced (full derivatisation) and a plateau in response will be observed. To determine when the reaction would reach the expected plateau (full derivatisation), the volume of MSTFA was increased further ($>10 \mu\text{L}$) (see Figure 4.7b). As with paracetamol in Section 4.3.2.1 Comparative study of silylation reagents: BSTFA + 1% TMCS vs MSTFA, the plateau is defined as the point where no statistically significant difference is observed between responses of carbamazepine mono-TMS at the increasing molar ratios.

ANOVA analysis ($n=3$, $p\text{-value} = 0.05$) concluded that a plateau was reached from 5-35 mins for 10, 100 and 120 μL MSTFA, 10-35 mins for 20 μL MSTFA and 15-35 mins for 50 μL MSTFA. However,

it must be noted that although 10 μL MSTFA reached a plateau after 5 mins, a carbamazepine peak was still present (Figure 4.7b), suggesting full silylation had not occurred. Full silylation was not achieved within 5 mins for 20 μL or 50 μL but was observed for 100 μL and 120 μL suggesting that, as theorised, increasing the volume of MSTFA, increases the rate of reaction.

When the plateau is reached, the observed response is expected to be the same regardless of MSTFA volume, as the reaction has reached full silylation. However, in this study, this is not the case. Figure 4.8 illustrates the plateau responses for the various MSTFA volumes (at equivalent molar ratios). The carbamazepine mono-TMS responses differ significantly ($p\text{-value} < 0.001$) at different molar ratios.

Therefore, it is proposed that the plateau is reached when the reaction has reached dynamic equilibrium. Dynamic equilibrium is defined as the state of equilibrium where the rate of the forward and reverse reactions are equal, for a reversible reaction in a closed system (Lee, 2020; Smith, 2019). Silylation is considered a reversible reaction (Kashutina et al., 1975), thus as the response of the TMS derivative remains constant at the plateau, the response of the reactants can be assumed to remain constant (though not measured), and so the dynamic equilibrium can be said to have been reached.

Le Chatelier's principle states that a change in reaction conditions (including concentration, temperature, or pressure) will cause a predictable shift in equilibrium position, to counteract the change and re-establish the equilibrium (Smith, 2017). Increasing the volume of MSTFA, increases the molar concentration (and molar ratio) of the reactant, thus, to counteract, the equilibrium shifts towards the right to form more product (PhC TMS derivative) (see (4-8)). This is observed in this study, as an increased response for the TMS derivative is observed, when MSTFA volume is increased (see Figure 4.7).

The equilibrium constant (K) remains constant for all volumes of MSTFA as K is independent of reactant and product concentrations (Clark, 2015; Helmenstine, 2019). The shift in equilibrium caused by the increase in MSTFA occurs, until a new balance is reached, and K returns to the same value as before (4-9).



$$K = \frac{([\text{PhC Derivative}][\text{MSTFA Derivative}])}{([\text{PhC}][\text{MSTFA}]^2)^*} \quad (4-9)$$

**When in a pseudo-first order reaction, [PhC] would be the only reactant, though the basis of the equilibrium would remain the same.*

Therefore, overall, increasing the volume of MSTFA increases the rate of the silylation reaction as expected. However, the response of the carbamazepine mono-TMS peak increases with increasing MSTFA volume, suggesting the reaction is an equilibrium, which shifts with increasing volume. Thus, increasing the volume of MSTFA, will increase the production of carbamazepine mono-TMS.

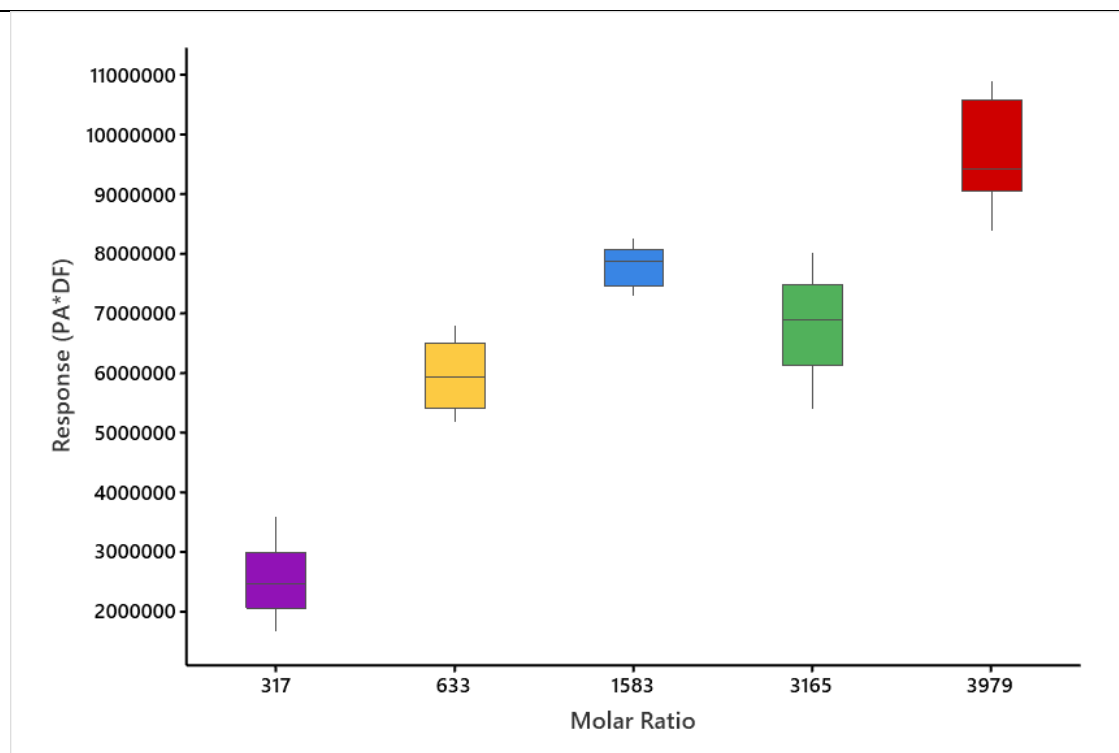


Figure 4.8: Boxplot of Molar Ratio vs Plateau Response (PA*DF) for 10-120 μL (317-3979) MSTFA. – a difference in response is observed at the statistically significant plateau ($P = 0.05$) for the different molar ratios suggesting the silylation reaction has reached an equilibrium. Plateau responses were calculated from 5-35 mins for all molar ratios, except from 633 (20 μL – 10-35 mins) and 1583 (50 μL – 15-35 mins).

4.3.2.3 Addition of a Catalyst

Catalysts are often added to derivatisation reactions in the form of pyridine or TMCS to facilitate the $\text{S}_{\text{N}}2$ reaction and reduce sample preparation time (Knapp, 1979; Pierce, 1968). To observe the effects of a catalyst on derivatisation of a PhC, pyridine was added to a carbamazepine sample with MSTFA, and results recorded. Carbamazepine remained the analyte of choice as it contains an amide group - considered to be the most difficult to silylate. Pyridine was chosen as it is a common laboratory chemical and in previous studies it was observed that the addition of TMCS had little effect on the silylation of paracetamol (see 4.3.2.1 Comparative study of silylation reagents: BSTFA + 1% TMCS vs MSTFA).

To ensure that the addition of pyridine (25 μL) was the only factor affecting the rate of silylation; samples were allowed to stand at room temperature (24.8-25.8 $^{\circ}\text{C}$, no heat applied) for 5 mins before analysis on the GC-MS. Very little MSTFA was added (7 μL – 219:1) to reduce the molar ratio as low as possible. In the previous experiments, addition of 10 μL had shown to fully silylate carbamazepine, whilst 7 μL showed partial silylation, but also had underderivatised parent compound. It was theorised that this volume (7 μL) would show the full catalytic effects of the pyridine addition. For comparison, pyridine was substituted with ethyl acetate to give a sample with no catalyst added.

The average PA ($n=6$) of carbamazepine mono-TMS showed a statistically significant increase (p -value < 0.001) when pyridine was added to the sample (see Appendix B). The addition of pyridine converted

the carbamazepine to its mono-TMS derivative, with no detectable carbamazepine parent peak present. Carbamazepine peaks were detected in all samples where pyridine was substituted for ethyl acetate. The addition of pyridine increased reproducibility of the method, with RSDs decreasing from 15% to 10%. Therefore, as no other factors were applied to this method, it can be concluded that the addition of pyridine has a statistically significant effect on the silylation of carbamazepine.

4.3.2.4 Competing Reactions

The parameters tested up to this point in the study are those which are generally taken into consideration when optimising a new silylation method. However, we propose that the derivatisation efficacy may be hindered by the possibility of competing reactions, particularly when more than one analyte is silylated. Competing reactions, or parallel reactions, are defined as two or more independent reactions which occur concurrently, share at least one common reactant, and produce different or partially different products (Rakitzis & Papandreou, 1999; Tuckerman, 2015). In this case, the PhCs all compete for the shared MSTFA, producing different PhC derivatives.

Competing reactions are of interest in the scientific community in a variety of areas, including for S_N2 reactions in which an electrophile reacts with two different nucleophiles (Rakitzis & Papandreou, 1999). In this case, all PhCs (nucleophiles) will compete for the same common reactant (MSTFA, electrophile), with each reaction leading to a different TMS derivative (see Figure 4.9). Due to the competing reactions, it is hypothesised to have a negative effect on reaction rate, as all compounds are competing for the same reagent, MSTFA.

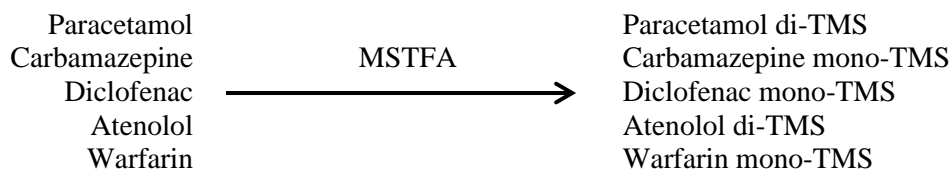


Figure 4.9: Example of competing reactions - all PhCs compete to react with MSTFA, to form different TMS derivatives

As discussed previously, silylation reactions are said to be pseudo-first order reactions (see 4.3.2.2 Molar Ratio and Reaction Time), which suggests that the reaction rates will follow a competitive first order parallel reaction mechanism, provided MSTFA is in a large excess (>100:1).

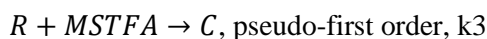
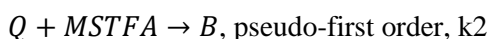
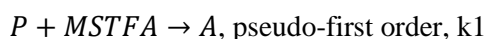


Figure 4.10: Example of competitive first order parallel reaction rates, where P, Q and R are PhCs and A, B and C are their respective TMS derivatives.

The products A, B and C (TMS derivatives of P, Q and R) are formed in the ratio of the corresponding rate constants k_1 , k_2 , and k_3 , respectively. The concentration of MSTFA will decrease with a rate

constant which is the sum of k_1 , k_2 and k_3 (Seoud et al., 2016). Thus, the rate of TMS formation should be consistent with the rate of common reagent disappearance, MSTFA.

Generally, parallel reactions have one main reaction, accompanied by smaller, side reactions. Based on the ease of silylation, the main reaction is likely to be the silylation of an unhindered OH group (easiest to silylate), with the remaining functional groups as the side reactions. An example of the expected product formation and MSTFA decline is shown in Figure 4.11.

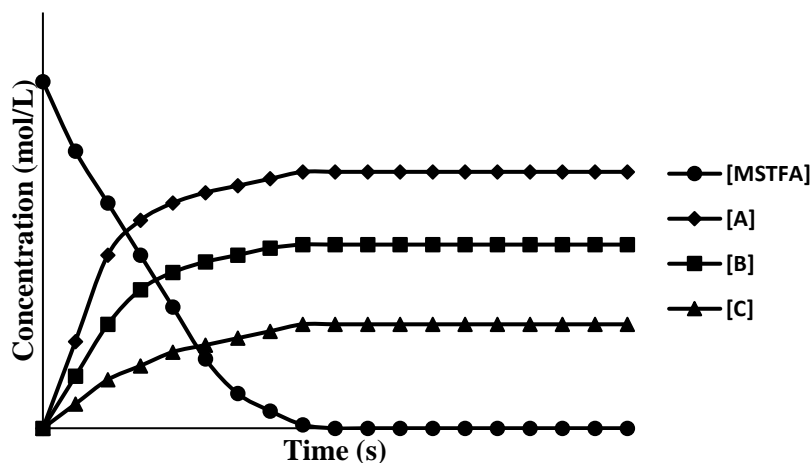


Figure 4.11: Parallel reaction: plot of $[MSTFA]$, $[A]$, $[B]$ and $[C]$ over time (s). Reaction $P + MSTFA \rightarrow [A]$ is seen as the main reaction whilst $Q + MSTFA \rightarrow [B]$ and $R + MSTFA \rightarrow [C]$ as side reactions.

To determine whether competing reactions influence the efficacy of the silylation reaction, a PhC mixture was silylated with various volumes of MSTFA. Analyte PhCs were chosen based on the number and type of labile hydrogens (paracetamol – ArOH, CONH, carbamazepine – CONH₂, diclofenac – COOH, NH, atenolol – OH, NH, CONH₂, and warfarin – COOH) to ensure all functional groups (both easy and difficult to silylate), and a range in the number of active sites were included.

Four out of five PhCs were detected in the PhC mixture in their derivatised form. Akin to carbamazepine, diclofenac converts only to the mono-TMS derivative (silylation of a carboxylic acid group) with no further silylation to the di-TMS derivative (secondary amine) due to steric hindrance caused by the addition of the initial TMS group. Paracetamol and atenolol both silylate to their di-TMS derivatives. This is complete derivatisation for paracetamol (ArOH, then CONH), and partial derivatisation for atenolol (OH and NH silylated, NH₂ not silylated). This is consistent with other studies whom also fail to reach the tri-TMS or tetra-TMS derivatives of atenolol with silylation, reaching only the mono-O-TMS (Caban et al., 2011) or di-N,O-TMS derivatives (Brunetto et al., 2015; B. Yilmaz & Arslan, 2009, 2010). All pharmaceuticals reached a statistically significant plateau (p-value = 0.05, between 5 and 45 mins) within the first 5 mins for all volumes of MSTFA suggesting that competition for MSTFA was not an issue for these compounds. A peak for warfarin mono-TMS derivative is present

in some chromatograms however generally has a S/N below 3 (<LOD). When analysed individually, warfarin is easily detected as its mono-TMS derivative (see Appendix B). Therefore, this suggests that competition for the derivatisation reagent can have an effect on the silylation of warfarin.

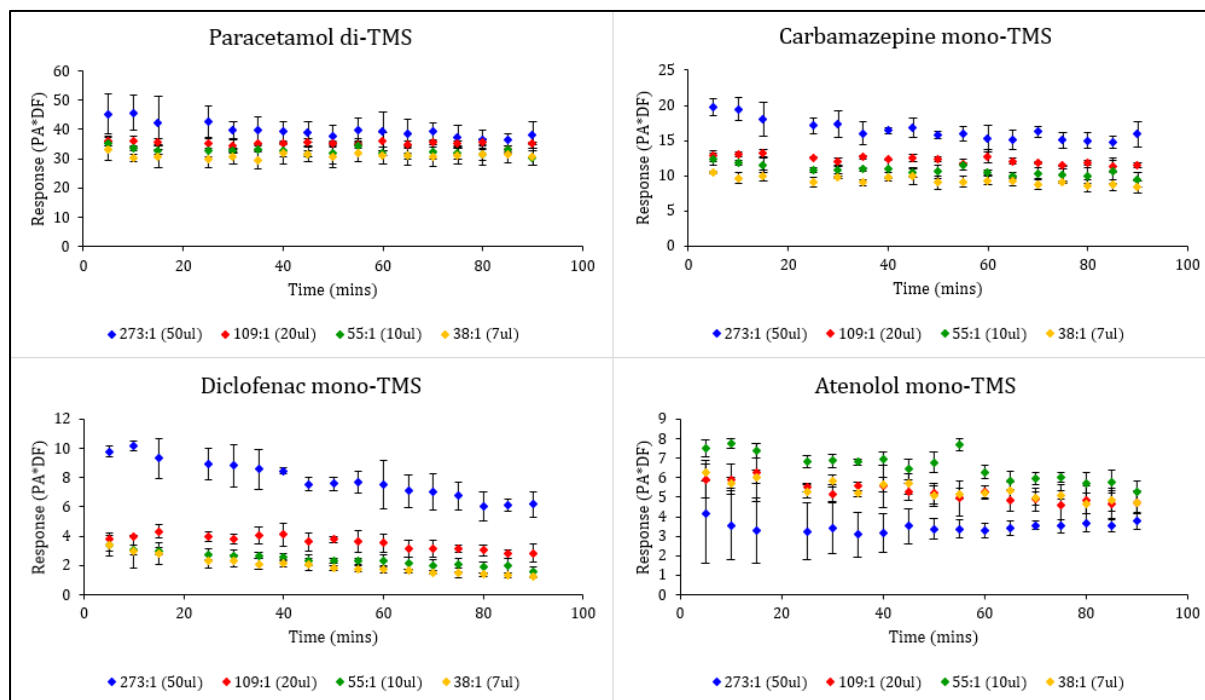


Figure 4.12: Effect of varying molar ratio (MSTFA: PhC*active sites) on a pharmaceutical mixture a) kinetics over time i) paracetamol di-TMS ii) carbamazepine mono-TMS iii) diclofenac mono-TMS iv) atenolol di-TMS. PAs were normalised by dividing by the dilution factor.

A slightly negative trend can be seen for diclofenac mono-TMS and carbamazepine mono-TMS, with an increase in reaction time (see Figure 4.12). This phenomenon was observed by Caban *et al.*, with responses of multiple TMS derivatives decreasing after 30 minutes when silylated with BSTFA + 1% TMCS at 60 °C (Caban *et al.*, 2011). In the study, the decline in some PhCs derivatives (nadolol mono-TMS and atenolol mono-TMS) may be attributed to the formation of a di-, tri- or tetra-TMS derivative. However, the phenomenon was also observed for salbutamol tri-O-TMS and terbutaline tri-O-TMS, which, to the authors knowledge do not convert further to their tetra-TMS derivatives (Jacobsson *et al.*, 1980; Lindberg & Jönsson, 1982). Caban indicated that reaction times longer than 45 mins had a reduction in the effectiveness of the PhC silylation in a mixture, which is indicated by both compounds in this study (see Figure 4.12). This phenomenon was also recorded by Djatmika & Ding, 2016 when optimising silylation of four parabens and. Giandomenico *et al.*, 2011 for NSAIDs; with an increased reaction time having a negative effect on responses when in a mixture. The stability of TMS derivatives is thought to decrease with time, as secondary reactions including hydrolysis occur (Kataoka, 2014). This may explain the small decrease in response over time.

Increasing the volume of MSTFA, and subsequently the total molar ratio (MSTFA: no of active sites on all PhC analytes), had an increasing effect on the response for diclofenac mono-TMS - with a statistically significant difference (p-value < 0.001) between the response for 20 μ L and 50 μ L MSTFA (see Figure 4.13). An increase in response was also observed with carbamazepine mono-TMS (p-value < 0.001), and paracetamol di-TMS (p-value < 0.001) with increasing MSTFA volume (7-50 μ L). Although, atenolol di-TMS shows a decrease in response as MSTFA volume is increased beyond 10 μ L. A statistically significant difference is observed between each MSTFA volume (p-value < 0.05), suggesting increasing MSTFA volume >10 μ L has a negative effect on the formation of atenolol di-TMS. However, atenolol di-TMS is a relatively small peak which slightly shoulders the carbamazepine mono-TMS peak; therefore, this may cause issues with integration which may explain the decreasing PA, particularly as the PA of the carbamazepine mono-TMS peak is increasing. Therefore, it is recommended that in future analysis, the resolution between the carbamazepine and atenolol TMS peaks is increased to prevent shouldering.

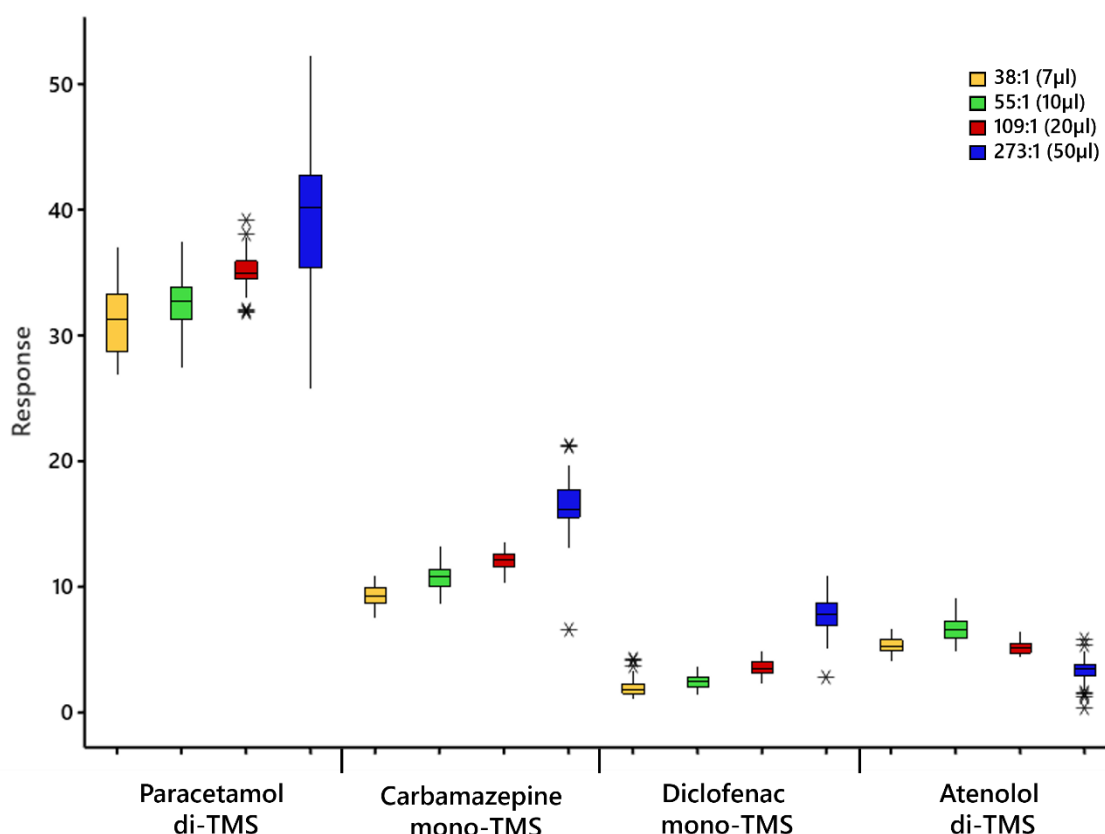


Figure 4.13: Boxplots highlighting the average PA*DF for each derivatised compound over a 90-minute time period with varying molar ratios. Paracetamol di-TMS, carbamazepine mono-TMS, diclofenac mono-TMS and atenolol di-TMS.

Therefore overall, increasing the volume of MSTFA (in turn, increasing the molar ratio), has a positive influence on the silylation of 75% of compounds. This again suggests that increasing the volume of

MSTFA, will shift the equilibrium to the side of the reactants, increasing the response of the derivatives. Therefore, 50 μ L of MSTFA will be used for the optimised method.

Most studies do not vary the volume of derivatisation agent used for silylation of multiple PhCs, instead opting to vary the type of reagent or other silylation conditions (time, temperature, solvent etc.) to optimise their method. Therefore, comparison of results of this study to others is limited, though increasing the volume of reagent (thus, increasing the molar ratio) has been shown to increase the response of acidic pharmaceuticals in a mixture (including diclofenac) in two different studies (Gumbi et al., 2017; Samaras et al., 2011).

Overall, a higher molar ratio increased the response of carbamazepine mono-TMS when studied individually (see 4.3.2.2 Molar Ratio and Reaction Time) and 75% of compounds when studied in a mixture (see 4.3.2.4 Competing Reactions). The addition of a catalyst increased the response of analytes, which in turn, reduced the reaction time of the sample (see 4.3.2.3 Addition of a Catalyst). Reaction time is also thought to be reduced by the application of heat (Pierce, 1968). Thus, to optimise all experimental parameters, and establish a suitable silylation method, a design of experiments approach was used.

4.3.2.5 Optimisation of Silylation method for Pharmaceuticals by Design of Experiments

To optimise the silylation parameters (reaction time and temperature), a design of experiments (DOE) approach was undertaken. Firstly, a DOE factorial design was applied to determine significant parameters which affect derivatisation – time, temperature and addition of pyridine were used as parameters in this stage.

Carbamazepine was again selected as the analyte pharmaceutical, as the amide group is the hardest to silylate; and thus, in theory, if this group silylates then the experiment parameters will be sufficient for other, easier to silylate groups (such as OH or COOHs). As before, the Rf of the carbamazepine and carbamazepine mono-TMS peaks were used as an indicator of the completeness of the silylation reaction - a large carbamazepine mono-TMS response, and a low carbamazepine response indicates the reaction is near completion/reached equilibrium.

4.3.2.5.1 DOE Factorial design

The only statistically significant factor effecting both the carbamazepine (CBZ) and carbamazepine mono-TMS (CBZ-TMS) response was determined to be the addition of pyridine (Figure 4.14a+b). This is expected as pyridine has been shown to catalyse the reaction (see 4.3.2.3 Addition of a Catalyst). The reaction time also had a significant effect on the carbamazepine response. Reaction temperature did not meet the requirements to be a significant parameter.

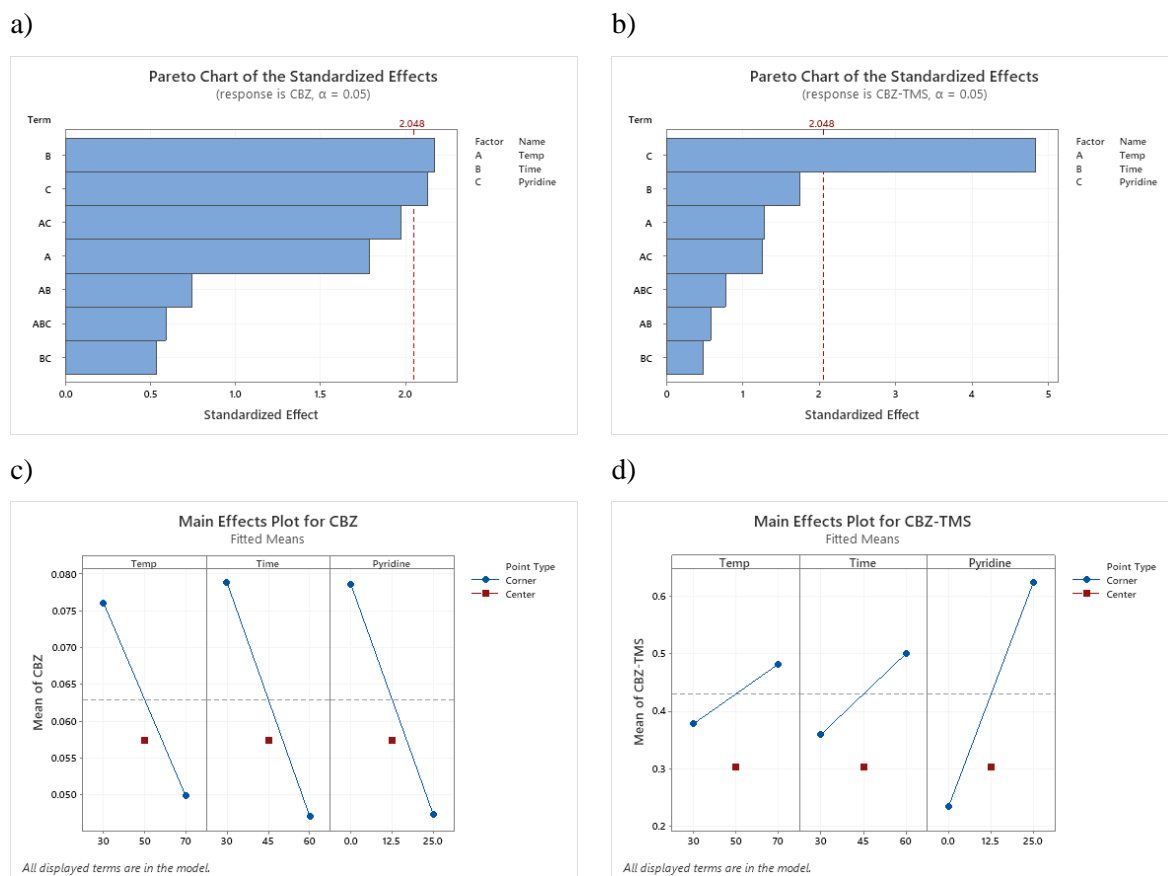


Figure 4.14: Design of Experiment, Initial Factorial Design Results. Pareto Charts a) carbamazepine and b) carbamazepine mono-TMS. Addition of pyridine (μL) and silylation time (mins) are considered significant parameters in this reaction. Associated Main Effects Plots c) carbamazepine d) carbamazepine mono-TMS. Increasing all parameters was shown to increase carbamazepine mono-TMS response and decrease carbamazepine response.

Increasing oven temperature increased the carbamazepine mono-TMS response and decreased the carbamazepine response (Figure 4.14c+d) – this is expected as heat is known to catalyse silylation of hindered groups (Orata, 2012), and thought to lower the activation energy required for collisions. A similar response was observed when reaction time was increased from 30 to 60 mins. Nitrogenous groups (amines and amides) tend to take longer to silylate than hydroxyl (OH) groups. Thus, an increased time allows for more reactions to take place, facilitating the mono-TMS response. As expected, increasing the volume of pyridine, also increased the mono-TMS response – pyridine acts as an acid scavenger, which catalyses the reaction (Shareef et al., 2006). The addition of pyridine gave rise to the largest increase which explains statistical significance of this parameter in the screening design.

The results are comparable to many silylation procedures in other studies which have similar temperatures, however generally have shorter heating times (20-30 mins) (Giordano et al., 2016; Lajeunesse & Gagnon, 2007). Therefore, a DOE response optimisation study was applied to optimise the parameters further. The addition of pyridine has shown to aid in silylation (see section 4.3.2.3

Addition of a Catalyst) and may be suppressing the influence of the other factors on the response, thus was removed from the response optimisation.

4.3.2.5.2 DOE Response Optimisation

To determine the specific temperature and reaction time required for optimal silylation, response optimisation was applied. The factorial design indicated that higher temperatures increase response, and thus the temperature range was increased to 50-80 °C. To ensure that only the time and temperature parameters were optimised, a small amount of MSTFA was added (7 μ L, 222:1), as it has been previously determined that increasing MSTFA will increase the carbamazepine mono-TMS response (see Section 4.3.2.2 Molar Ratio and Reaction Time).

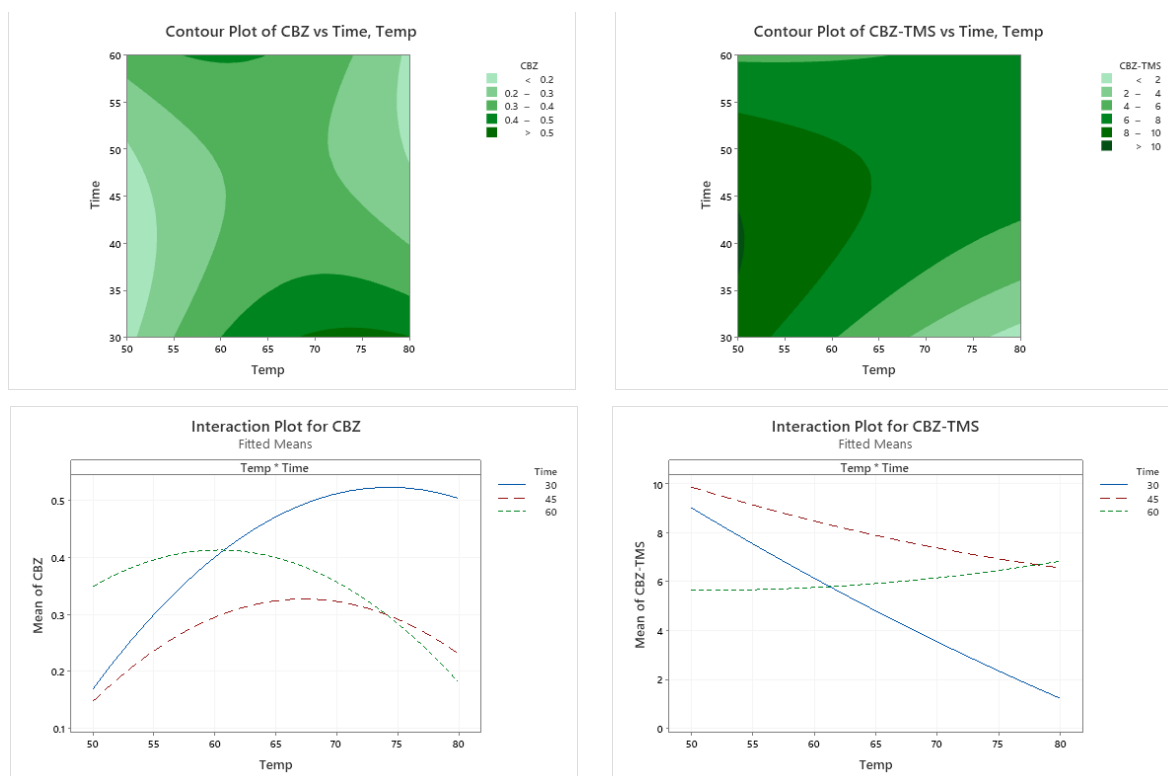


Figure 4.15: Response optimisation of conventional parameters for the carbamazepine silylation reaction. Contour plots of a) CBZ and b) CBZ-TMS. Interaction plots of c) CB and d) CBZ-TMS. Response optimisation of both time and temperature.

The response optimisation chart (see Appendix B) concluded that a temperature of 50 °C and a reaction time of 40 mins was optimal for silylation of carbamazepine. Further increasing the time or temperature reduced the desired response (Figure 4.15a+b). Interaction plots suggest that it is a combination of temperature and time which provide the optimal conditions (Figure 4.15c+d); where increasing temperature reduces the mono-TMS response for 30- and 45-minute reaction periods. However, increasing the temperature showed little change in the mono-TMS response for 60-min reaction periods. An interaction between 60 °C for 30 mins and 60 °C for 60 mins is observed on both interaction plots (Figure 4.15c+d). The responses for both analytes are similar at these parameters. This would suggest that increasing the reaction time from 30-60 mins, would not be beneficial, as concluded by Kumirska

et al. and Migowska *et al.* (Kumirska *et al.*, 2013; Migowska *et al.*, 2012). Regardless, the mono-TMS responses for both 30 and 60 mins were lower than that of 45 mins. Overall, a reaction time of 45 mins maximised the mono-TMS response and minimised the carbamazepine response, as desired.

The optimised parameters of 50 °C for 40 mins, do not differ greatly from those found in literature (see Table 4-1). Although the temperature is lower than the 60°C used in many studies (Caban & Stepnowski, 2018; Kumirska *et al.*, 2019; Migowska *et al.*, 2012), the reaction time lies within the range of 10-90 mins found in literature. Therefore, these conditions were deemed sufficient for complete silylation of carbamazepine.

Overall, it seems that silylation must be optimised for each individual study – conditions are dependent on the number and type of PhC being analysed. However, this poses a challenge when non-targeted analysis is applied, as the type and number of analytes is unknown. It is recommended that a strong silylation reagent (MSTFA) should be initially tested at three volumes (50 µL, 100 µL and 150 µL) when silylating a sample in which the PhC load is unknown. Samples should be heated to 50°C for 40 mins and analysed using the desired GC-MS method at three different time periods. Three response peaks should be chosen and responses of the three reagent volumes compared. If responses plateau and are similar between the volumes, then the lowest volume of derivatisation reagent should be chosen.

4.3.2.5.3 Application of optimised method to a mixture

To ensure the optimised derivatisation method was applicable to a wider range of PhCs, the method was applied to previously analysed PhCs which vary in number and type of functional group (atenolol, diclofenac, paracetamol, warfarin, and carbamazepine). Each PhC was analysed individually and as part of a PhC mixture (0.1 mg/mL). A 50 µL aliquot of MSTFA was added to each vial based on previous results (see 4.3.2.4 Competing Reactions). Increasing the MSTFA volume further (>50 µL) may have further influenced silylation rate and TMS response, however, would have required further study and would reduce the atom economy of the reaction.

Complete derivatisation was achieved for each individual compound. A decrease in average Rf for 80% of compounds was observed when analysed in a mixture – only responses for diclofenac increased (Table 4-6 and Figure 4.16). This is consistent with the equilibrium theory discussed in the previous section (see 4.3.2.4 Competing Reactions). Thus, it suggests that increasing the volume of MSTFA may increase the response of the PhC mixture. All RSDs are below 10, which is deemed acceptable. Therefore, this method was considered acceptable for derivatisation of various PhCs, and thus can be used to derivatise pharmaceutical compounds in non-targeted analysis.

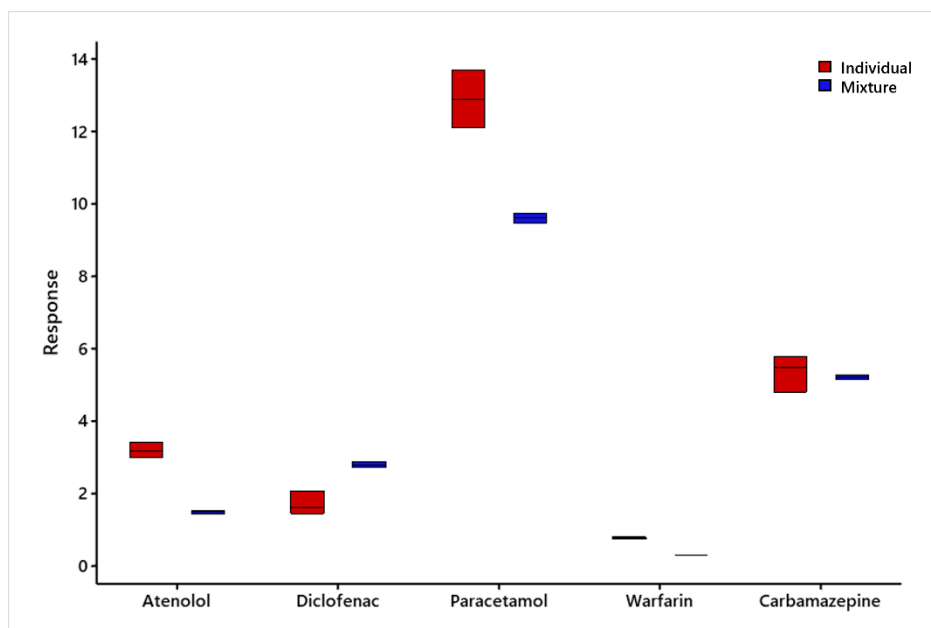


Figure 4.16: Average Rf responses ($n=3$) for five PhCs silylated both individually and in a mixture using optimised method (40°C for 50 mins).

Table 4-6: Average Rf responses ($n=3$) for five PhCs when silylated using the optimised DOE derivatisation method (50°C for 40mins). Comparison of individual PhCs vs PhCs in a mixture. %RSD highlighted in brackets.

| Compound | Average Rf: Individual | Average Rf: PhC Mix | Statistically significant Increase/Decrease when in a Mix |
|------------------------|------------------------|---------------------|---|
| Atenolol di-TMS | 3.19 (6.32) | 1.48 (4.26) | Decrease |
| Diclofenac mono-TMS | 1.52 (7.35) | 2.79 (3.83) | Increase |
| Paracetamol di-TMS | 12.87 (6.18) | 9.60 (2.10) | Decrease |
| Warfarin mono-TMS | 0.76 (6.14) | 0.31 (0.98) | Decrease |
| Carbamazepine mono-TMS | 5.35 (9.24) | 5.20 (1.79) | No stat. sig. diff. |

4.4 Conclusions

In this chapter, several aspects of silylation for the derivatisation and analysis of five PhCs (atenolol, paracetamol, carbamazepine, diclofenac, and warfarin) using GC-MS were evaluated. Of the silylation reagents tested (MSTFA and BSTFA + 1% TMCS), MSTFA was found to be the most effective for derivatisation of the target compounds. An increase in molar ratio was identified with a lower volume of reagent. The addition of pyridine as a catalyst increased the derivative response. Increasing the volume of MSTFA, in turn increasing the molar ratio, increased the desired response: responses of derivatised PhC peaks increased, whilst parent PhC compound responses decreased. Competing reactions of PhCs for MSTFA were shown to reduce the response of warfarin mono-TMS. Optimal PhC responses were obtained with $50\ \mu\text{L}$ of MSTFA, heated to 50°C for 40 mins. This method is comparable

to those found in literature for similar studies. The optimised method proved suitable for a number of pharmaceutical compounds, when analysed both individually and in a mixture; although responses of the majority of derivatised compounds decreased when analysed in a PhC mixture, thought to be due to competing reactions. Therefore, increasing the volume of MSTFA may increase the PhC derivative response when in a mixture. The optimised method would be suitable for application in non-targeted analysis; though it is recommended to use three different MSTFA volumes initially, and monitor response of three compounds, before choosing a reagent volume.

Chapter 5: Investigation into the use of ultrasonication for the extraction and derivatisation of pharmaceutical compounds from biosolid samples

5.1 Introduction

5.1.1 Sonochemistry and Green Chemistry

When ultrasound is applied to chemical applications, it is termed ‘sonochemistry’ or more generally ‘sonication’. Ultrasound (US) increases number and speed of collisions between molecules (Doktycz & Suslick, 1990; Prozorov et al., 2004; Wang et al., 2021) facilitating and accelerating many sample preparations steps including extraction (UAE) and derivatisation (UAD), which in turn decreases analysis time (Chatel, 2018). Decreased solvent consumption and thus cost per sample, make this technique more affordable (Díaz & Peña-Alvarez, 2017); whilst accuracy and precision of some analytical techniques are also increased (Yebra, 2012). The energy savings attributed to the reduced sample preparation time (Chatel, 2018), align with Green Chemistry principle 6 – design for energy efficiency (American Chemical Society, 2020; Anastas & Warner, 1998) and the reduction in waste with principle 1 – prevention (Al-Khazrajy & Boxall, 2017; Cravotto & Cintas, 2006; Díaz & Peña-Alvarez, 2017).

The derivatisation method developed in Chapter 4 requires heating to 50 °C for 40 mins, which is energy and time intensive. Applying ultrasound has shown to facilitate the silylation of oxygenated compounds (carboxylic acids, sugars and phenols) (Pietrogrande et al., 2017), triterpenic compounds (oleanolic acid, ursolic acid, uvaol and erythrodiol) (Sánchez Ávila et al., 2007) and estrogenic compounds (E1, E2, EE2 and E3) (Vallejo et al., 2010), reducing derivatisation time by >85% in each study. This suggests that the application of ultrasound should be sufficient for aiding in derivatisation of a range of PhCs. Therefore, this study investigated the use of ultrasound application to reduce time and energy expenditure in the derivatisation of PhCs.

In most studies, a sonication probe (direct sonication) or sonication bath (indirect sonication) are used to implement the ultrasound (Gago-Ferrero et al., 2015; Martín et al., 2010; Pietrogrande et al., 2017; Sánchez Ávila et al., 2007; Vallejo et al., 2010). Each has limitations, with increased possibility of cross-contamination when using a probe (Vallejo et al., 2010), and lack of uniformity in the ultrasound

transmission when using a bath (Delgado-Povedano & Luque de Castro, 2013). Here, we investigate the use of a novel technique, applying intense indirect sonication via a sonotrode device. Sonotrodes apply uniformly intense US (Tiwari, 2015), whilst eliminating the possibility of sample loss or contamination, as sample is not in direct contact with the probe.

5.1.2 Optimised UAE methods for PhCs

Many studies have optimised UAE methods for extraction of PhCs and PCPs; however, optimisation is generally limited to a handful (<10) of targeted compounds (Albero et al., 2019; Al-Khazrajy & Boxall, 2017). The optimised methods of Gago-Ferreiro *et al.* and Martín *et al.* are of interest to this study, due to the large number of targeted compounds and the similar sample matrix. Gago-Ferreiro *et al.* (Gago-Ferreiro et al., 2015) extracted 148 illicit drugs and PhCs from sewage sludge and Martín *et al.* (Martín et al., 2010) extracted 16 PhCs from the same matrix. The methods (described below) were used to inform the UAE method development process for this study.

5.1.2.1 Gago-Ferreiro et al. Method (Gago-Ferreiro et al., 2015)

Aliquots of 0.1g of freeze-dried sludge were spiked with PhC surrogates (148 PhCs) and kept in contact overnight. Samples were extracted with 2 mL of methanol: MilliQ water (pH 2.5, formic acid 0.5% and 0.1% EDTA). After the addition of the solvent, samples were vortexed for 1 min, followed by ultrasonication extraction for 15 min at 50 °C. Post-extraction, samples were centrifuged for 10 min at 4000 rpm. This process was repeated for 3 cycles, and the supernatants combined. The sample was evaporated to dryness under a gentle stream of nitrogen gas, at 40°C; and reconstituted in 0.5 mL methanol: water (0.05% formic acid, 25:75 (v/v)). Samples were filtered through 0.2 µm RC syringe filters and transferred to a glass vial for HPLC-MS/MS analysis in selected reaction monitoring (SRM) mode. Recoveries of analyte PhCs ranged from 16 to 110%; with the majority of compounds (77%) falling between 50-110%. Low recoveries (<30%) were attributed to high LogP values (>4), for example gemfibrozil. Low recoveries were not considered to impede reliable determination, as sensitivity and reproducibility were satisfactory. All RSDs were <20% for the method suggesting good reproducibility and precision. Ion suppression and enhancement caused by matrix effects were calculated to be -92 to -3%, and 11-90% respectively.

5.1.2.2 Martín et al. Method (Martín et al., 2010)

Aliquots of sample (1.0 g primary/secondary sludge, 1.5 g of digested sludge and 2.0 g of compost) were sequentially extracted with 5 mL methanol, 2 mL methanol and 2 mL acetone. After addition of the solvent, the sample was shaken vigorously for 30 s before sonication was applied for 15 mins. Samples were centrifuged at 4000 rpm for 20 mins. This process was repeated for each extraction step, and the supernatants combined. Extracts were evaporated to 200 µL under a gentle stream of nitrogen; subsequently diluted to 250 mL with acidified deionised water. The sample was subjected to a sample

clean up step (SPE, 60 mg Oasis HLB) before evaporating eluate and reconstituting in 150 μ L of methanol for LC-DAD analysis coupled with a fluorescent detector. Recoveries ranged from <15% (paracetamol) to 115%, with RSDs ranging from 0.1% to 23%. Matrix effects were not studied, though spiked chromatograms (see Figure 5.1) suggests that matrix interference is likely to be present.

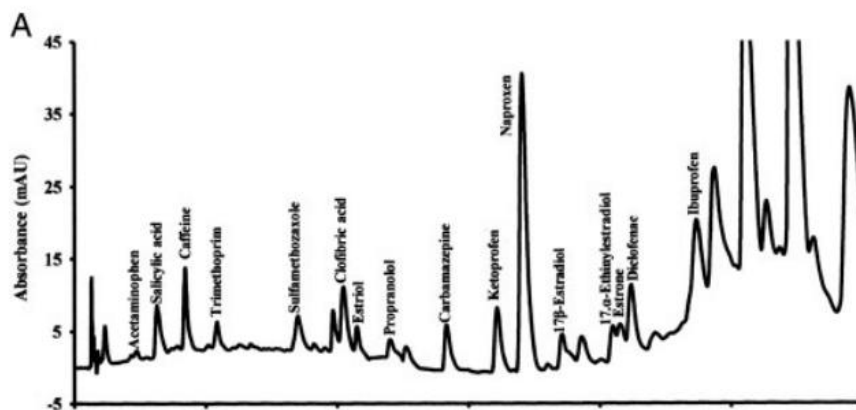


Figure 5.1: Martín et al. (Martín et al., 2010), HPLC-DAD chromatogram of a spiked compost sample. PhCs spiked at a concentration level of 300 μ g/kg. Although matrix effects were not discussed, it seems that matrix effects are likely to contribute.

Both methods utilise LC as the analysis method, with samples extracted, treated (with EDTA) and filtered prior to analysis. Regardless, issues with signal suppression and enhancement were observed, due to the complex sample matrix and electrospray ionisation technique (Panuwet et al., 2016). GC methods tend to use electron impact ionisation, and although still present, matrix effects are not as problematic. This study investigates the use of GC as the analysis method for derivatised biosolid extracts.

With the concept of Green Chemistry more widely acknowledged and implemented, a sample preparation method for analysis of PhCs in biosolids and sludge, which meets the sustainable requirements is desirable. The benefits of sonochemistry on extraction and derivatisation have been widely detailed in literature (Chatel, 2018; Seidi & Yamini, 2012). Indirect and direct ultrasound have been shown to reduce reaction times for several derivatisation and extraction methods through sonication baths and probes; however, only one study has utilised indirect sonication through sonotrodes for successful UAE and UAD (Sampsonidis, 2019). Therefore, this research will investigate and optimise the sonication parameters (time, amplitude, pulse and solvent) required for the derivatisation and extraction of pharmaceutical compounds from biosolid samples using a sonotrode device.

5.2 Methods

5.2.1 Reagents

Pharmaceutical compounds paracetamol (CAS Number: 103-90-2), atenolol (29122-68-7), carbamazepine (298-46-4), diclofenac sodium (15307-79-6), ibuprofen (15687-27-1), warfarin (81-81-2), salicylic acid (69-72-7), clofibrac acid (882-09-7), metronidazole (443-48-1), triclosan (3380-34-5), ketoprofen (22071-15-4), sotalol (3930-20-9), dapsone (800-08-0), fluvastatin (93957-54-1); and internal standard phenanthrene (85-01-8) were purchased from Sigma-Aldrich. All pharmaceutical standards were of high purity grade (>90%). Ethyl acetate (141-78-6), pyridine (110-86-1), and methanol (67-56-1) were purchased from Sigma-Aldrich or Fisher Scientific. All solvents were of reagent quality or greater. N-trimethylsilyl-N-methyltrifluoroacetamide (MSTFA; 24589-78-4) was purchased from Sigma-Aldrich or Crawford Scientific and was of derivatisation grade or greater. MSTFA was stored at 4 °C, as per safety data sheets (SDS).

5.2.2 Stock Solution Preparation

Individual stock solutions of each pharmaceutical compound and a stock mixture of the fourteen PhCs (detailed in Chapter 4), were prepared in methanol, at a concentration of 0.5 mg/mL. Stock solutions were stored in airtight containers at -20°C. Working solutions were prepared in MeOH on the day of analysis and stored in an airtight container at -18°C for inter-day replicates.

As this research is intended to be applied to non-targeted analysis in future applications phenanthrene was used as an internal standard following methods of Veenaas et al., 2018, Shareef et al., 2006 and Kumirska et al., 2013. An individual phenanthrene stock solution (0.5 mg/mL) and working solution (0.05 mg/mL) were prepared in ethyl acetate and stored at -18°C.

5.2.3 Biosolid Sample Collection and Preparation

5.2.3.1 Sample Collection

Treated AngloScottish biosolid samples were collected in December 2017 from James McCaig Farms located in Wester Jawcraig, Scotland. Samples were freeze-dried and stored in the dark at room temperature until analysis. Biosolid samples were spherical in nature, light brown in colour, and varied from around 0.2- 0.8 cm in size. For extraction, all biosolid samples were ground with a mortar and pestle. When ground, the pellets produced a flake-like powder (see Appendix C).

5.2.3.2 Optimised Extraction Procedure

The optimised extraction method followed an adapted version of the extraction method developed by Gago-Ferrero *et al.* (Gago-Ferrero et al., 2015). A mass of biosolid (1 g) was accurately measured into a 10 mL glass vial. Aliquots (2 mL) of acidified methanol: water (50:50, pH 2.5, 0.1 % formic acid)

were added, the vial sealed, and the subsequent suspension vortexed for 1 minute. The vial was then added to the sonotrode device and ultrasound applied (40 % pulse, 80 % amplitude) for 5 minutes. The vial was centrifuged at 5000 rpm for 10 mins, carefully decapped, and the supernatant collected in a separate 10 mL vial. This process was repeated twice more (three cycles) combining the supernatants each time. The resulting solution was then evaporated to dryness at a gentle heat (40 °C) on a hotplate overnight. After all solution had evaporated and vial had cooled to room temperature, an aliquot of ethyl acetate (100 µL) was added and centrifuged for 5 mins at 5000 rpm. This vial and contents after each step are shown in Appendix C. The ethyl acetate solution was transferred to a 300 µL sonication vial for derivatisation, prior to GC-MS analysis.

5.2.3.3 Optimised Derivatisation Procedure

Akin to Chapter 4, N-trimethylsilyl-N-methyltrifluoroacetamide (MSTFA) was used as the derivatisation agent. To the 100 µL ethyl acetate sample (from the extraction step), 25 µL of pyridine, 25 µL of the phenanthrene working solution (0.05 mg/mL) and 100 µL of MSTFA were added. Vials were capped and sonicated at optimised parameters of 40% pulse, 60% amplitude for 30s. Derivatisation was undertaken immediately before GC analysis to prevent degradation of derivatives.

5.2.4 Sonotrode Device

Extraction and derivatisation were optimised through application of ultrasound. The sonotrode (S26d2), VialTweeter (S26d11x10), VialPress, and digital ultrasonic generator and transducer (UP200St) were all purchased from Hielscher Ultrasonics GmbH, Germany. All samples were attached via the VialPress (see Figure 5.2), with plastic adapters made to suit each type of vial. The adapters prevent the glass vials from deterioration or breakage and allow the sonication to continue to be uniform for each sample. Analysis was conducted in a soundproof sonication box to protect hearing, and for the unlikely chance of vial explosion.

Robust 10 mL glass crimp seal headspace vials were used for extraction. For derivatisation, 300 µL glass crimp seal vials were used. Initial trial and error tests were conducted to determine the system's operating range for both analyses.

As with both analyses, an air gap must be left between the sample and the crimp seal cap, to allow for expansion during sonication. The sealed vial is positioned between the probe and corresponding VialPress (see Figure 5.2) and the sonication parameters (pulse, amplitude, and time) are controlled remotely (UP200St). The full set-up is illustrated in the Appendix. As the sonotrode is not submerged in the sample (unlike a probe), there is no chance of cross contamination, nor is there requirement to control variables associated with an ultrasonic bath (water volume in bath, water temperature etc.) (Seidi & Yamini, 2012). However, due to the indirect sonication, the vial temperature will increase and cannot be controlled. This is a known limitation to the analysis.

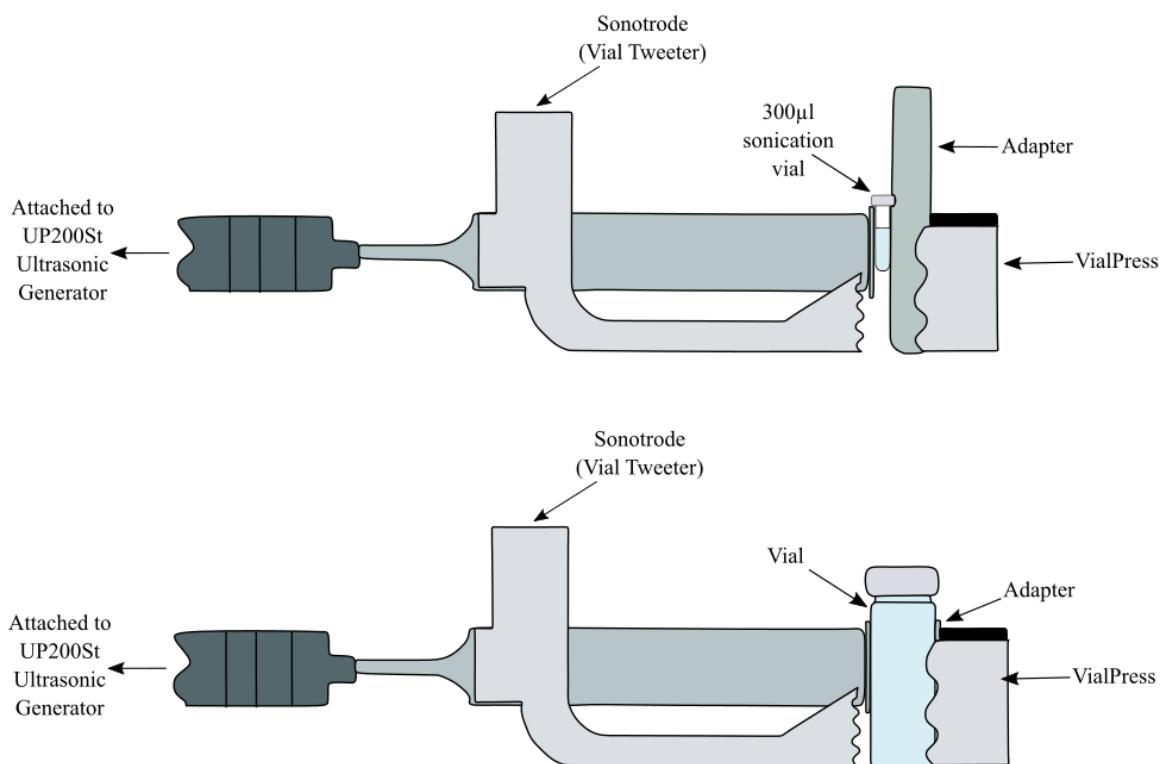


Figure 5.2: UP200St Ultrasonic Probe VialTweeter and VialPress attachments: Vial positioned in the VialPress. a) sonication set-up, 300 µL glass crimp seal vial with large plastic adapter b) extraction set-up, 10 mL glass crimp seal vial, with fine plastic adapter

5.2.5 GC-MS Analysis

All analysis was conducted using an Agilent 7890A gas chromatograph coupled to an Agilent 5975c quadrupole mass spectrometer. Aliquots (1 µL) of sample were injected onto an Agilent DB-5 (5% phenyl and 95% methylpolysiloxane) capillary column (30 m x 0.25 mm x 0.25 µm). Three different GC-MS methods were used throughout the study. Parameters of each are defined below:

5.2.5.1 Method 1 –Assessing PhC Detection on GC-MS

A scouting method was applied to assess which PhCs will be detected using the GC-MS and whether an isocratic method or temperature programme would be required for the analysis. The method was operated in split mode (100:1) due to the high PhC concentration in the initial runs (0.5 mg/mL). The initial oven temperature was 40 °C, increasing by 10 °C/min to 300 °C, with a hold time of 10 mins. Total run time was 36 mins. Inlet and transfer line temperatures were set to 270 °C. Mass spectra were obtained in electron ionisation mode (70 eV), in full scan mode (45-550 amu). MS source and quad temperatures were 230 °C and 150 °C, respectively.

5.2.5.2 Method 2 – Biosolid Samples Method

For recovery and non-targeted analysis of the biosolid samples, the following method was used. The method was operated splitless mode to obtain as much information about the samples as possible, including PhCs present at low concentrations. The initial oven temperature was 100 °C, increasing by 10 °C/min to 300 °C, with a 10 min hold time, a total run time of 30 mins. Inlet and transfer line temperatures were set to 270 °C. Mass spectra were obtained in electron ionisation mode (70 eV), in full scan mode (45-650 amu). MS source and quad temperatures were 230 °C and 150 °C, respectively.

5.2.5.3 Method 3 – Derivatisation Optimisation Method

To optimise derivatisation, the short method used in Chapter 4 was applied. The method was operated in split mode (100:1) to overcome high concentrations. An isocratic method was used: oven temperature was 275 °C with a total run time of 3 minutes. Inlet and transfer line temperatures were set to 270 °C. Mass spectra were obtained in electron ionisation mode (70 eV), in full scan mode (50-550 amu). MS source and quad temperatures were 230 °C and 150 °C, respectively.

5.2.5.4 Response Measurements for TMS derivatives

The efficiency of derivatisation was measured by calculating the response factor (Rf): dividing the peak area of the analyte peak against the peak area of the internal standard (phenanthrene) (5-1). Derivatisation was considered to be complete when the Rf of the analyte peak remained constant (Caban et al., 2011; Lacina et al., 2013). All experiments followed this method, with Rfs used as responses in the design of experiments (DOE).

$$Rf = \frac{(Peak\ Area_{ANALYTE})}{(Peak\ Area_{INTERNAL\ STANDARD})} \quad (5-1)$$

5.2.6 Software

Chromatograms and mass spectrums were translated from MSD Chemstation E.02.01.1177 to OpenChrom Community Edition 1.2.0 software for data analysis and annotation. Minitab 20.4.0.0 software was used for experimental design and analysis. Inkscape 0.92.3 was used to produce all schematics and diagrams. MarvinSketch 18.19.0 was used to produce all chemical structures.

5.2.7 Ultrasonic Assisted Extraction (UAE) Method Development

To optimise the UAE method, various individual parameters had to be optimised. The UAE method was based on the method of Gago-Ferrero, Borova, et al., 2015, though had to be adapted for use with a sonotrode and GC-MS analysis. The optimisation of the extraction parameters is illustrated in Figure 5.3, and detailed below.

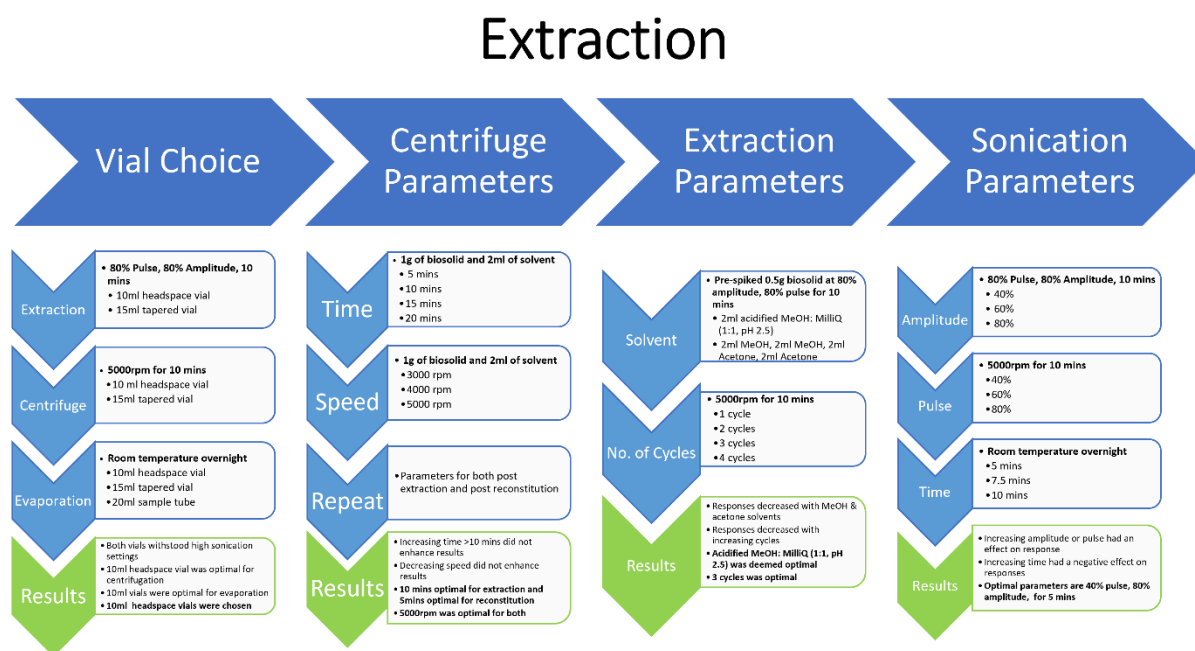


Figure 5.3: Optimisation of the Ultrasonic Assisted Extraction method. A flow chart highlighting the parameters which were optimised for efficient PhC extraction from biosolid samples using a UAE sonotrode device.

5.2.7.1 Vial Choice

The choice of vessel for the sonication process and subsequent centrifugation and evaporation is essential for routine sample preparation. Vials must be able to hold the required volume of solvent including the specified amount of biosolid; and withstand the sonication and centrifugation parameters. A large sample surface area was desirable to increase the speed of evaporation, which would aid in reducing sample preparation time.

Two vials were tested: 10 mL glass crimp seal headspace vials and 15 mL tapered glass centrifuge tubes. Various times, amplitudes and pulses were investigated in a ‘trial and error’ manner to establish the operating range of the sonication parameters.

A Hettich EBA 20 zentrifugen centrifuge and a Thermo Scientific Multifuge X1R centrifuge, with the addition of vial adapters (made in-house) were used to centrifuge the glass vials. After vial choice was made, centrifuge parameters were investigated further (see 5.2.7.2 Centrifuge Parameters) to determine optimal parameters for both post-sonication and post-reconstitution.

To determine the best vials for sample evaporation and reconstitution, three vials were tested: 10 mL glass headspace vials, 15 mL glass centrifuge tubes and 20 mL glass sample tubes. To each, 6 mL of the extraction solvent (50:50 MeOH: Water @ pH 2.5) was added and allowed to evaporate in the fume hood overnight. This represents the total volume of extraction solvent that was used in the optimised method.

5.2.7.2 Centrifuge Parameters

Various centrifuge settings were trialled for both post-sonication and post-reconstitution, to determine the optimal settings. The centrifuge process should provide a clear supernatant and compact the biosolid to an extent which it is not easily disturbed when removing the supernatant. Post-reconstitution centrifugation should ensure that any residual biosolid particles remain in the vial once the solvent is removed. Varied parameters included revolutions per minute (3000, 4000, 5000 rpm (equivalent to 1107, 1968 and 3075 relative centrifugal force respectively)) and centrifuge time (5, 10, 15, 20 mins). Trial and error with visual comparison was used to determine suitable parameters.

5.2.7.3 Extraction solvents and number of cycles

To determine which extractant solvents to use (following either (Gago-Ferrero et al., 2015) or (Martín et al., 2010)), and simultaneously determine the number of cycles required; ~0.5 g of the ground biosolid sample was spiked with 1 mL of PhC mixture in methanol (0.5 mg/mL) and allowed to evaporate overnight. As sonication parameters had not yet been optimised, extractions were undertaken at the greatest parameters achievable without vial breakage (80% amplitude, 80% pulse and 10 mins).

Sequential extraction was implemented for the two methods. Each biosolid sample was extracted and centrifuged before the supernatant was collected. In this study, the supernatant collected from each extraction step were not combined, but instead kept separate to determine the extraction efficiency of each extraction cycle. A total of 4 extraction cycles were undertaken. The samples were then evaporated to dryness at a gentle heat (40 °C); and reconstituted in 1 mL of ethyl acetate. Two samples of each were analysed, one in the non-derivatised and one in the derivatised form. Derivatised samples were heated to 50 °C for 40 mins (optimised method from Chapter 4) prior to GC-MS analysis.

5.2.7.4 Sonication Parameters

As a sonotrode application has not been performed previously, a DOE approach was employed with regards to better understand the role of sonication on derivatisation efficiency; and further to model it so optimised conditions can be determined. Sonication parameters tested included amplitude (%), pulse (%) and time (mins).

Initially, investigation into the sonication parameters determined the upper and lower limits of the parameters for the DOE. The parameters (80% amplitude, 80% pulse, 10 mins) were based on previous trial and error experimental runs, with the ability of the vial to withstand the sonication and the PhCs responses closely monitored.

After the initial investigations, a 2-level fractional factorial design was prepared with 3 factors: time (secs), pulse (%) and amplitude (%). All factors were set as numeric factors. The $\frac{1}{2}$ fraction factorial (III) design ($2^{(3-1)}$, 1 block and 1 centre point) produced 5 chromatographic runs which encompass a

high, mid, and low setting for each of the parameters. Runs are automatically randomised by the Minitab software. Optimal parameters were determined by fitting a response surface regression model (RSM) to the data. DOE run parameters are detailed in Table 5-1.

Sample preparation included spiking 0.1 g of ground biosolid sample with 1.0 mL of 1000 µg/L PhC mixture. The large concentration was used to ensure PhCs would be detected easily. Samples were extracted, evaporated, reconstituted and derivatised, as detailed above. Rfs for ibuprofen mono-TMS, triclosan mono-TMS and carbamazepine mono-TMS were used as the response. These PhCs were chosen as they were distributed at the start, mid and near end of the chromatogram.

Table 5-1: DOE Fractional Factorial Design: Sonication Parameters (Pulse, Amplitude and Time) for optimisation of extraction. Each run represents a unique combination of factor levels.

| Run Order | Pulse (%) | Amplitude (%) | Time (mins) |
|-----------|-----------|---------------|-------------|
| 1 | 80 | 40 | 5 |
| 2 | 60 | 60 | 7.5 |
| 3 | 80 | 80 | 10 |
| 4 | 40 | 40 | 10 |
| 5 | 40 | 80 | 5 |

5.2.7.6 Mass of Biosolid and Recovery

To determine the recovery of the method, 6 biosolid samples were spiked with 1 mL of 250 µg/L PhC mix prior to extraction (SBE) and 6 spiked after extraction (SAE). The samples were prepared and extracted with the optimised sonication parameters; and ran in duplicate on the splitless GC method.

The amount of biosolid (or sludge sample) extracted in literature ranges from 0.04 g to 10 g (Albero et al., 2019; Al-Khazrajy & Boxall, 2017; Bossio et al., 2008; Ding et al., 2011; Gago-Ferrero et al., 2015; Golet et al., 2002; Samaras et al., 2013). To determine the optimal mass of biosolid to be extracted, three masses were investigated – 0.1, 0.5 and 1.0 g. Above 1.0 g, it was found that the volume of extraction solvent (2 mL) was completely absorbed, and no supernatant was able to be collected.

5.2.8 Ultrasonic Assisted Derivatisation (UAD)

Ultrasonic assisted derivatisation has been shown to facilitate silylation, reducing derivatisation time to as little as 1 minute (Vallejo et al., 2010). However, to the author's knowledge, no study uses ultrasound to silylate a range of PhCs, nor uses a sonotrode device to implement the ultrasound. As using the sonotrode for derivatisation is a novel technique, sonication parameters must be optimised. To determine the optimal parameters for the derivatisation of PhCs, design of experiment was applied. The optimisation of the derivatisation using sonication parameters is illustrated in Figure 5.4, and detailed below.

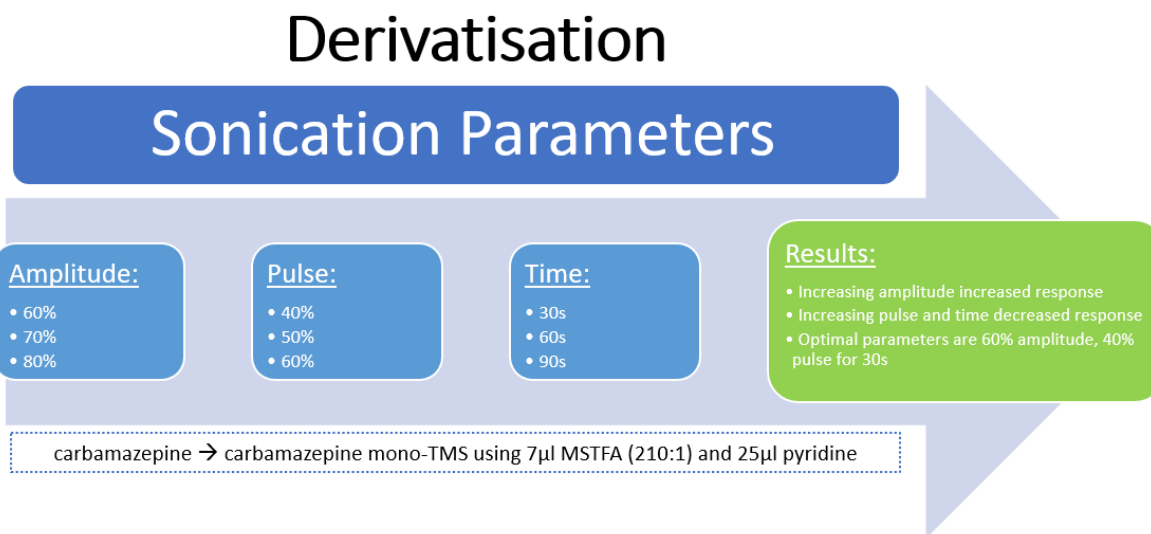


Figure 5.4: Flow chart for optimisation of UAD silylation using the sonicator. Parameter's amplitude, pulse and time optimised using design of experiment (DOE).

Carbamazepine was once again used as the analyte of choice. Carbamazepine mono-silylates on the CONH₂ amide to form carbamazepine mono-TMS. No further silylation is possible due to steric hindrance (Blau & King, 1978). As amides are notoriously difficult to silylate, it is expected that all other, easier to silylate groups will have reached full silylation, prior to carbamazepine.

To ensure that the sonication parameters were the driving factor behind the derivatisation reaction, the volume of MSTFA was kept to a minimum (7 µL MSTFA = molar ratio of 210:1, MSTFA: carbamazepine).

Sample preparation was as follows: MSTFA was added to a 300 µL sonication vial containing 65 µL ethyl acetate, 40 µL of the individual carbamazepine working solution (0.049 mg/mL) and 20 µL of phenanthrene working solution (0.05 mg/mL). If specified, 25 µL of pyridine was added, substituted with 25 µL of ethyl acetate if no pyridine was to be included. Samples were capped and positioned in the sonotrode device using the plastic adapter (see Figure 5.2). Sonication parameters amplitude (%), pulse (%) and time (min) were varied in accordance with the experimental design. Immediately after sonication, samples were analysed by GC-MS (see 5.2.5.3 Method 3 – Derivatisation Optimisation Method). Rfs for all carbamazepine and carbamazepine mono-TMS peaks were calculated.

5.2.8.1 Definitive Screening Design

Initially, a definitive screening design (DSD) was applied to determine significant parameters. The design was prepared with four factors: sonication time (mins), amplitude of the sonication wave (%), sonication pulse (%) and the addition of pyridine. The first three factors were set as numeric, and the addition of pyridine set as categorical. When included (Yes), a 25 µL aliquot of pyridine was added to the sample. In total, 14 runs were performed, with GC-MS analysis conducted immediately after

derivatisation. All runs were created in Minitab and were randomised. The screening design is detailed in Table 5-2.

Table 5-2: Definitive Screening Design for Ultrasonic Assisted Derivatisation. Each run represents a unique combination of factor levels.

| Run Order | Time (s) | Amplitude (%) | Pulse (%) | Pyridine (μL) |
|-----------|----------|---------------|-----------|----------------------------|
| 1 | 60 | 70 | 50 | No |
| 2 | 90 | 80 | 40 | No |
| 3 | 60 | 80 | 60 | Yes |
| 4 | 30 | 80 | 40 | Yes |
| 5 | 30 | 60 | 60 | Yes |
| 6 | 90 | 80 | 50 | Yes |
| 7 | 30 | 80 | 60 | No |
| 8 | 30 | 60 | 50 | No |
| 9 | 90 | 60 | 60 | No |
| 10 | 90 | 60 | 40 | Yes |
| 11 | 60 | 60 | 40 | No |
| 12 | 30 | 70 | 40 | Yes |
| 13 | 60 | 70 | 50 | Yes |
| 14 | 90 | 70 | 60 | No |

Rfs were calculated for both carbamazepine and carbamazepine mono-TMS and used as responses for DOE model fitting. The design was analysed using Minitab's DOE functionality. Results from the screening study provided an initial understanding of the significant factors affecting the reaction, indicating experimental conditions for the creation of a more detailed modelling study for response optimisation.

5.2.8.2 Response Optimisation

A 2-level full factorial face centred ($\alpha=1$) central composite design (CCD) with 6 centre and 6 axial points, was applied to optimise the sonication parameters. Parameters and settings included amplitude (40%, 50%, 60%), pulse (40%, 50%, 60%) and time (30 s, 45 s, 60 s). All factors were set as numeric. A face-centred design was chosen due to practicality issues: the pulse parameter can only be set in increments of 10% - other RSMs use out-of-plane axial points which are not possible to process (i.e., a pulse setting of 68%) (Wagner et al., 2014). In total, 20 runs were performed. The CCD design is described in Table 5-3. The response optimisation process was conducted on Minitab using the integrated response optimisation functionality.

As before in Chapter 4, Rfs of carbamazepine and carbamazepine mono-TMS were used as the response. The response optimiser was set to maximise the carbamazepine mono-TMS response and

minimise the carbamazepine response. Once optimised, additional ultrasonic assisted derivatisation runs were performed at optimised parameters to test for repeatability.

Table 5-3: Face-centred (a=1) central composite design (CCD) parameters for response optimisation of the silylation of carbamazepine.

| Run Order | Time (s) | Amplitude (%) | Pulse (%) |
|------------------|-----------------|----------------------|------------------|
| 1 | 45 | 50 | 50 |
| 2 | 45 | 50 | 50 |
| 3 | 30 | 40 | 40 |
| 4 | 60 | 50 | 50 |
| 5 | 45 | 50 | 50 |
| 6 | 30 | 40 | 60 |
| 7 | 45 | 50 | 60 |
| 8 | 60 | 40 | 60 |
| 9 | 30 | 60 | 60 |
| 10 | 45 | 40 | 50 |
| 11 | 60 | 40 | 40 |
| 12 | 60 | 60 | 40 |
| 13 | 45 | 50 | 50 |
| 14 | 30 | 60 | 40 |
| 15 | 60 | 60 | 60 |
| 16 | 45 | 50 | 50 |
| 17 | 45 | 50 | 50 |
| 18 | 30 | 50 | 50 |
| 19 | 45 | 50 | 40 |
| 20 | 45 | 60 | 50 |

5.2.9 Application to Biosolid Samples

The optimised extraction and derivatisation methods were applied to three non-spiked biosolid samples in order to determine the PhC load of the biosolid samples. Aliquots of 1.0 g of ground biosolid were extracted using the sonotrode and evaporated to dryness overnight at 40 °C. Samples were reconstituted in 100 µL of ethyl acetate. Phenanthrene and pyridine (25 µL each) and 100 µL of MSTFA was added to the sample to derivatise. Ultrasound was applied via the sonotrode with optimised parameters, and samples were analysed immediately in duplicate on GC-MS. This is illustrated in Figure 5.5.



Figure 5.5: Flow chart of the optimised extraction and derivatisation method applied to biosolid samples. More details of volumes and sonication and centrifugation parameters can be found in section 5.2.3 Biosolid Sample Collection and Preparation.

5.3. Results and Discussion

5.3.1 Ultrasonic Assisted Extraction (UAE) Method Development

5.3.1.1 Vial Choice

Sonication

Trial and error investigations established that both vial types (10 mL glass headspace vials and 15 mL glass centrifuge tubes) withstood 10 mins at 80% amplitude and 80% pulse with no breakages; however, vials were very warm to touch after 10 mins, and any further time may have caused fractures or other irreparable damage to the vials. Increasing amplitude or pulse beyond 80% may have also caused vial breakage and thus this remained the highest parameters.

Centrifugation

Post-extraction centrifugation was best in the 10 mL glass headspace vial. The 20 mL sample tubes were too fragile to centrifuge. The tapered 15 mL centrifuge vials compacted the biosolid pellet at a slant, which was easily disturbed when trying to remove the supernatant. The 10 mL headspace vials compacted the biosolid into a thin layer, with the supernatant easily accessible. Therefore, the 10 mL headspace vials were chosen for the extraction process.

Evaporation

Evaporation of the supernatants contributes to the majority of the sample preparation time and thus reducing this time would be desirable. The 10 mL headspace vials proved to be the quickest for evaporation (~26 h); followed by the 20 mL sample tube (~35 h) and finally the 15 mL centrifuge tube (>48 h). This is expected to be due to the increased surface area of the sample in the 10 mL vials (23mm diameter) in comparison to the 15 mL centrifuge tubes (17 mm diameter).

In addition, acceleration of the evaporation was achieved by the addition of gentle heat (40 °C). Application of 40 °C reduced the evaporation time from 26 h to 12 h for full evaporation in a 10 mL headspace vial. It is to be noted that a 40-45 °C heat setting has been used in previous studies to evaporate extraction solvents (Antonić & Heath, 2007; Gago-Ferrero et al., 2015; Löffler & Ternes, 2003; López Zavala & Reynoso-Cuevas, 2015); and thus, 40 °C was used in all samples to increase evaporation speed.

Due to the ability to withstand vigorous sonication, high speed centrifugation and quick evaporation, the 10 mL glass headspace vials were used for the duration of the project.

5.3.1.2 Centrifuge parameters

Optimised parameters were determined to be 5000 rpm for 10 mins after each extraction step and 5000 rpm for 5 mins after reconstitution. Increasing centrifuge time did not positively correlate with less suspended biosolid particles. It was observed that increasing time >10 mins, increased sample preparation time, without improving results. Decreasing speed (rpm), had a negative effect on the compaction of the biosolid sample, which allowed for suspended particles to be visible within the supernatant. The centrifuge limit was 5000 rpm and so further increasing rpm could not be trialled.

A centrifuge time of 10 mins was also used by Gago-Ferro *et al.* however, a reduced speed (4000 rpm) was applied (Gago-Ferrero *et al.*, 2015). The lower speed may be attributed to the smaller amount of sample (0.1 g) for Gago-Ferro, in comparison to this study. Martín *et al.* also applied a speed of 4000 rpm, though centrifuged for 20 mins after each extraction step for a 2.0 g sample (Martín *et al.*, 2010). However, Al-Khazrajy and Boxall only centrifuged for 10 mins at 4500 rpm for 5.0 g of sediment sample (Al-Khazrajy & Boxall, 2017). Therefore, it seems centrifuge time and speed are dependent on the type and amount of sample weighed. The overall sample preparation time must be taken into consideration, and a decision made on whether the excess time is justifiable. The optimised parameters in this study are deemed acceptable as the parameters are similar to those used in two literature studies.

5.3.1.3 Choice of extraction solvents and number of cycles

To determine the optimal number of extraction cycles, spiked biosolid samples were extracted and centrifuged, with supernatants kept separate for each extraction step. A high PhC concentration was used to ensure the PhCs were detected in all extracts, and to ensure the method was sufficient at extracting concentrations far larger than those expected in the collected biosolid samples.

As expected, derivatised PhCs were observed in extracts 1 through 3, with decreasing response factors (see Table 5-4 and Figure 5.6). Overall, the Rf of each PhC decreased by around 80%, suggesting near full extraction for all PhCs. It must be noted that the sample analysed is quite concentrated (PhCs spiked at 1 mg/g) which is x10,000 greater than concentrations expected in environmental samples (Albero *et al.*, 2014; Ding *et al.*, 2011; Ternes *et al.*, 2005). Therefore, it can be expected that at an environmentally relevant concentration, for example a non-spiked sample, there is unlikely to be any PhC left to extract after the third extract. An extra extraction cycle (4th extract) would increase sample preparation, extraction time and solvent consumption with little benefit. With the possibility of no further PhC extraction at lower, environmentally relevant concentrations, a fourth extraction step cannot be justified. It was decided that 3 cycles would be sufficient for this method, consistent with Gago-Ferrero (Gago-

Ferrero et al., 2015), Martin (Martín et al., 2010) and Al-Khazrajy and Boxall (Al-Khazrajy & Boxall, 2017).

Table 5-4: Response factors for PhC peaks after each extraction stage (1-3). Response factors (Rf) declined rapidly with each extraction step. Overall percentage decrease for all PhCs was >79% which suggests that the PhC has nearly been fully extracted.

| Compound | Rf | Rf | Rf | Overall % Decrease |
|-------------------------|-----------|-----------|-----------|-----------------------|
| | Extract 1 | Extract 2 | Extract 3 | |
| Salicylic Acid di-TMS | 1.5814 | 1.1209 | 0.2318 | 85 |
| Clofibric acid mono-TMS | 4.3884 | 2.5523 | 0.6589 | 85 |
| Ibuprofen mono-TMS | 6.4579 | 3.4988 | 1.3812 | 79 |
| Paracetamol di-TMS | 6.7352 | 3.5907 | 1.2822 | 81 |
| Triclosan mono-TMS | 8.8672 | 4.5596 | 1.8303 | 79 |
| Carbamazepine mono-TMS | 7.3945 | 3.6781 | 1.2077 | 84 |
| Diclofenac mono-TMS | 3.3992 | 1.8306 | 0.6189 | 82 |
| Warfarin mono-TMS | 0.2598 | 0.0000 | 0.0000 | 100 |

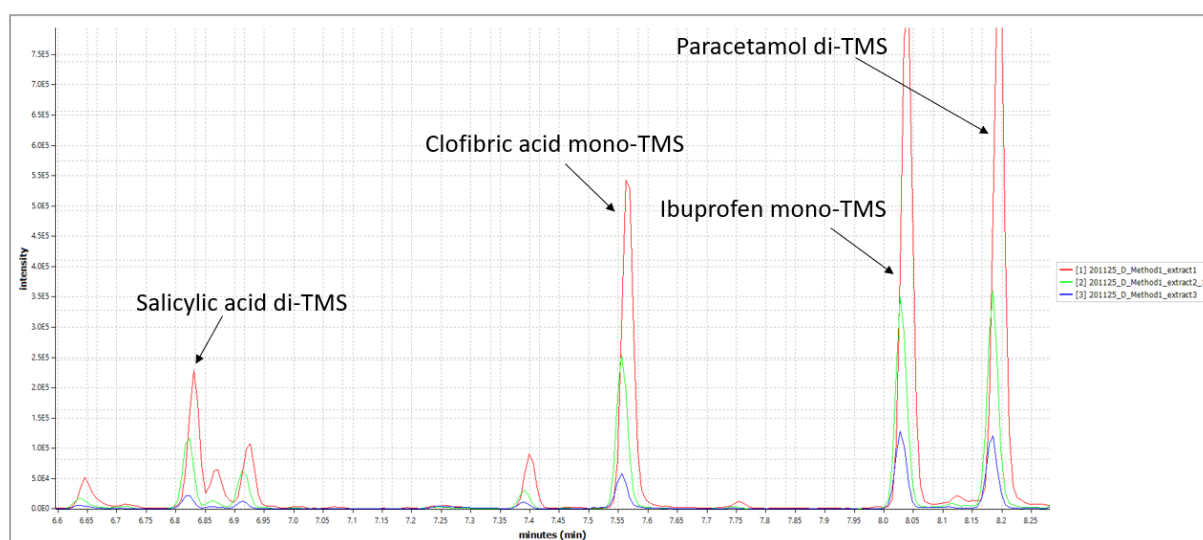


Figure 5.6: Comparison of 1st to 3rd extracts to determine number of cycles. Chromatogram shown from 6.6 to 8.3 mins to highlight the derivatised PhC peaks in this region (salicylic acid di-TMS, clofibric acid mono-TMS, ibuprofen mono-TMS, and paracetamol di-TMS). Peak areas for 4th extract were determined to be too small to justify another extraction step. Red = 1st extract, Green = 2nd extract, Blue = 3rd extract.

5.3.1.4 Sonication parameters

Sonication parameters (amplitude, pulse and time) were optimised using DOE, where the Rfs of PhCs were used as the response. Although the samples were spiked with the full range of PhCs, co-elution of fatty acids peaks caused issues with detection. In total, only three responses were analysed: ibuprofen mono-TMS (COOH), triclosan mono-TMS (OH) and carbamazepine mono-TMS (CONH₂). These responses ranged the full chromatogram and incorporated more than one derivatisable functional group and thus are sufficient for optimising the sonication parameters.

Interaction plots (see Figure 5.7) suggest slight interaction between pulse and amplitude for ibuprofen mono-TMS. All lines are near parallel which suggests the interaction is low for ibuprofen mono-TMS. No other interactions are observed for the other parameters, suggesting that ibuprofen mono-TMS is somewhat unaffected by alteration of the sonication parameters. Contrarily, all lines representing triclosan and carbamazepine show an increase or decrease in response, suggesting the silylation yield is influenced by the sonication parameters. Interaction between time and both pulse and amplitude are observed for triclosan mono-TMS and carbamazepine mono-TMS. As the lines are more perpendicular than parallel, it suggests that the amplitude and time has a greater interaction effect than the interaction of pulse and time.

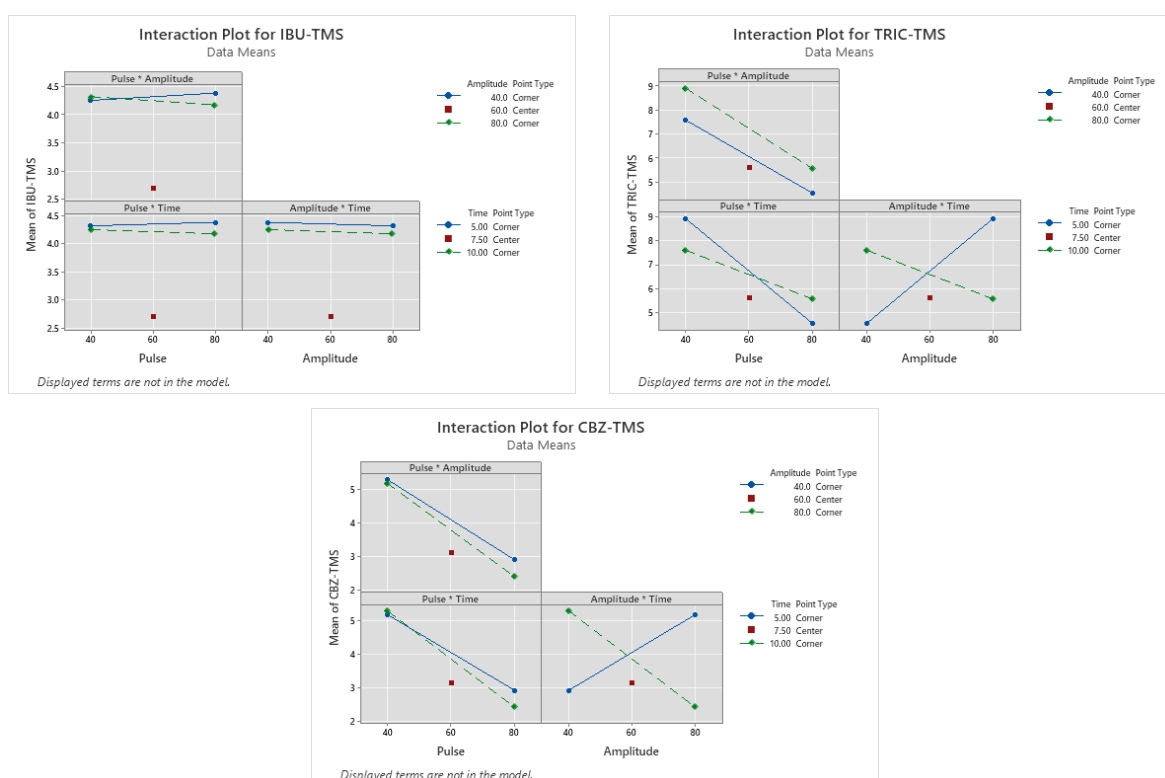


Figure 5.7: DOE response interaction plots for responses a) ibuprofen mono-TMS b) triclosan mono-TMS and c) carbamazepine mono-TMS. Parameters analysed: pulse (40, 60, 80%), amplitude (40, 60, 80%) and time (5.0, 7.5, 10.0 mins). The slope of each line indicates the effect of the parameter on the response. A larger gradient suggests a greater response. Parallel lines suggest no interaction.

Response optimisation was applied to determine the optimal responses based on the fractional factorial design. Minitab computes a response optimisation plot based on the responses of the three derivatised PhCs (see Figure 5.8). Optimal sonication parameters were determined to be 40% pulse, 80% amplitude for a 5-minute time-period. The overall composite desirability is determined to be 0.9743. As this value is close to 1.000 it suggests that the optimised settings achieve favourable results for all responses as a whole (Minitab Inc., 2017). Therefore, these optimised parameters were used throughout the experiment.

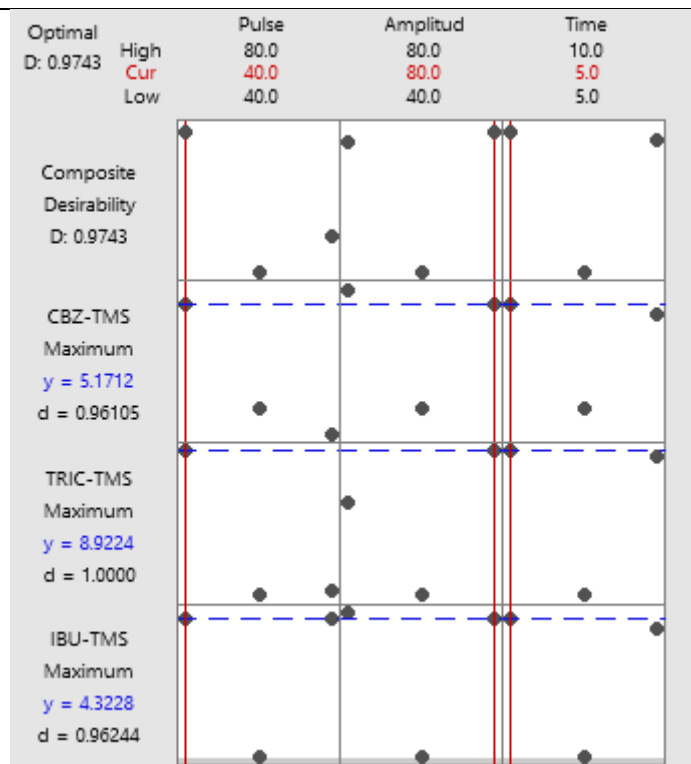


Figure 5.8: DOE response optimisation for UAE. Response of ibuprofen mono-TMS, Triclosan mono-TMS and carbamazepine mono-TMS. Optimal parameters determined to be 40% pulse, 80% amplitude for a 5-minute time-period. Composite desirability = 0.9743 suggesting the responses for all compounds have been maximised.

5.3.1.5 Mass of biosolid and Recovery

To determine the optimal mass of biosolid to be extracted, and simultaneously determine relative recoveries of the extraction method, biosolid samples were spiked with the PhC standard mix. Samples were extracted with the optimised extraction method and analysed on GC-MS. Five PhCs were identified in all spiked biosolid samples (unhindered and $S/N > 3$) for the three biosolid masses tested (0.1 g, 0.5 g and 1.0 g): salicylic acid mono-TMS, ibuprofen mono-TMS, paracetamol di-TMS, triclosan mono-TMS and carbamazepine mono-TMS.

Ibuprofen mono-TMS was not identified in the 0.1 g SAE samples and so recovery could not be calculated for this peak. Response factors (Rfs) for each compound were calculated as the comparative response. Average Rfs ($n=6$) for the SBE and SAE were used to calculate relative recoveries for the five PhCs. Recoveries and associated RSDs are recorded in Table 5-5.

Table 5-5: Relative Extraction Recoveries for 5 PhCs extracted from 0.1 g, 0.5 g and 1 g ground biosolid samples. Recoveries calculated by spiking before and after extraction, and comparing. Average recoveries (n=6) detailed. RSD ranges calculated from SBE and SAE samples to give RSD range.

| Compounds | RT (mins) | Relative Recovery | | | | | |
|-------------------------|-----------|-------------------|------|-----|---------------|-------|--------------|
| | | Recovery (%) | | | RSD Range (%) | | |
| | | 0.1g | 0.5g | 1g | 0.1g | 0.5g | 1g |
| Salicylic Acid mono-TMS | 6.8 | 128 | 87 | 92 | 13-22 | 26-39 | 19-22 |
| Ibuprofen mono-TMS | 8.07 | ND | 126 | 163 | ND | 25-46 | 5-26 |
| Paracetamol di-TMS | 8.1 | 112 | 95 | 106 | 26-32 | 22-29 | 12-14 |
| Triclosan mono-TMS | 13.2 | 62 | 103 | 65 | 23-36 | 31-34 | 28-29 |
| Carbamazepine mono-TMS | 14.4 | 82 | 107 | 109 | 19-33 | 11-16 | 6-7 |

*ND = not detected. Ibuprofen mono-TMS was not detected in any SAE samples for the 0.1g samples, and so recovery and %RSD could not be calculated.

The relative recovery ranges widely for the three masses of biosolid measured. The lowest recovered compound was triclosan mono-TMS for 0.1 g and 1.0 g, and salicylic acid di-TMS for 0.5 g of sample. However, all relative recoveries were >60% suggesting this method is suitable for these compounds.

Due to the increased recoveries and lower RSDs established with 1.0 g of biosolids, this mass was used in all sample preparation in the optimised method. Absolute recovery was determined by comparing the Rfs of the SBE samples to that of a PhC Standard Mix. Absolute recovery ranged from 8-64%; with only one compound (paracetamol) over 50% (see Table 5-6) which is lower than those obtained by Gago-Fererro et al. (Gago-Ferrero et al., 2015) (50-120% for 70% of analytes).

However, it would seem that the reduction in recovery is mostly attributable to derivatisation, than to signal suppression. From Chapter 4, it is understood that an increased excess in molar ratio produces a higher yield of derivative. As mentioned in Chapter 4, the molar ratio (excess) cannot be calculated for a non-targeted sample, as the sample content is unknown. Biosolids, by nature have a complex matrix, which contains many derivatisable compounds such as fatty acids. The additional derivatisable compounds in the matrix, increase the number of active sites, and therefore the molar ratio is far lower than anticipated, cumulating in a response reduction for PhC derivatives. The PhC standard on the other hand, does not have any interfering components and so the molar ratio is far higher, and a larger PhC TMS response is obtained. Thus, when compared, the absolute recovery will seem lower than it perhaps is.

This also attributes to the high RSDs obtained for both relative recovery and absolute recovery (5-29%). In Chapter 4, derivatisation was applied to PhC standards, and all resultant RSDs were <10%. In this chapter, the same derivatisation method (50 °C for 40 mins) was applied to the extracted biosolid samples, and the RSDs increased. Therefore, it is likely that competing reactions (from matrix

components) and the randomness of the successful collisions introduce variance to the derivatisation and overall derivatised responses.

Table 5-6: Absolutely recovery values for GC-MS method. Recovery calculated by dividing the SBE samples, by the PhC mix Standard and multiplying by 100. Lower recoveries suggest interference from matrix components.

| Compound | Absolute Recovery (n=3) | | | | | | |
|------------------------|-------------------------|---------|--|----------------------------|-----------------------|---|----|
| | PhC Standard | | Average % Decrease (PAR) Biosolid 1 | Recovery (%) Biosolid 1 | RSD (%) Biosolid 1 | Average % Decrease (S/N) Biosolid 1 | |
| | Average PAR | RSD (%) | | | | | |
| Salicylic acid di-TMS | 0.377 | 3 | 48.9 | 61 | 39 | 13 | 72 |
| Ibuprofen mono-TMS | 0.339 | 3 | 68.2 | 92 | 8 | * | 89 |
| Paracetamol mono-TMS | 0.273 | 1 | 59.7 | 36 | 64 | 26 | 79 |
| Triclosan mono-TMS | 0.208 | 2 | 62.3 | 52 | 48 | 23 | 49 |
| Carbamazepine mono-TMS | 0.129 | 2 | 32.1 | 79 | 21 | 19 | 36 |

*No RSD could be calculated, as only identified >LOD in one replicate

5.3.2 Ultrasonic Assisted Derivatisation (UAD)

5.3.2.1 Definitive Screening Design (DSD)

In Chapter 4, the time and temperature required for silylation of carbamazepine were determined to be 50 °C for 40 mins. However, it has been shown that the application of ultrasound can reduce derivatisation time significantly (Vallejo et al., 2010), with comparable responses of derivatised products. Reducing derivatisation time, with reduce overall sample preparation time, reducing costs, energy consumption and total analysis time. Therefore, to determine whether the sonotrode device can be used to silylate PhCs and significantly reduce sample preparation time, a DOE approach was undertaken. Carbamazepine was used as the analyte in this study, due to the silylation occurring at the amide group (difficult to silylate), and to allow for comparison of the optimised oven method (Chapter 4). A DSD was applied to determine statistically significant parameters affecting the silylation of carbamazepine. Both carbamazepine and carbamazepine mono-TMS were used as responses. A large carbamazepine response will indicate incomplete derivatisation.

Pareto charts for both carbamazepine and carbamazepine mono-TMS were produced to determine statistically significant parameters (see Figure 5.9). The only statistically significant parameter (p-value threshold = 0.05) for carbamazepine mono-TMS response was the addition of pyridine. Carbamazepine shared this significant parameter, however it was also found that the amplitude of the sonication wave was statistically significant. Ideally, this peak will reduce as the reaction occurs, and thus it would suggest that amplitude (%) may play a role in this.

Pyridine had been shown to catalyse the silylation of carbamazepine when optimising the conventional oven method in Chapter 4. To ensure this was also true of the sonication method, it was included in the initial design. However, the large catalytic effect of the pyridine addition may be suppressing the other factors in the design. Therefore, it was concluded that pyridine should be added to the samples at a consistent volume (25 μL – as with Chapter 4) for the remainder of the DOE. All remaining parameters (amplitude, pulse, and time) were further optimised by fitting a response surface regression model to the data.

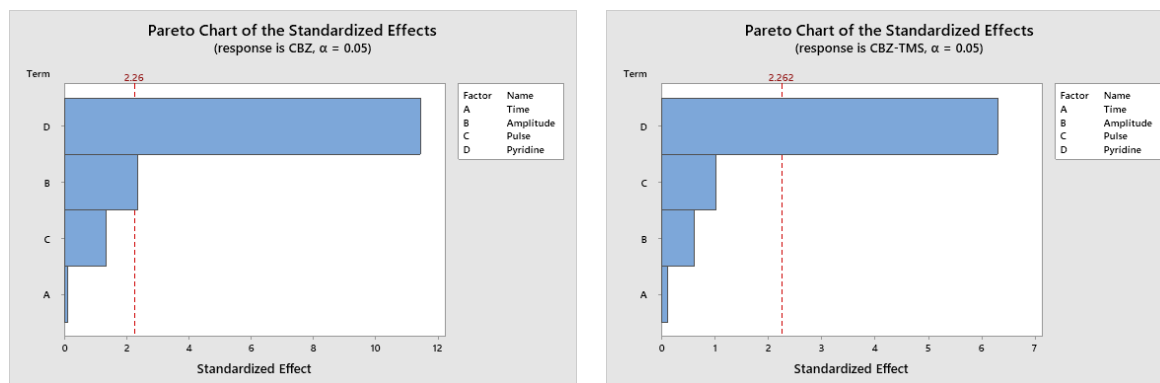


Figure 5.9: Pareto Charts for the standardised effects of the Definitive Screening Design of sonication parameters for the silylation of carbamazepine-to-carbamazepine mono-TMS. a) carbamazepine b) carbamazepine mono-TMS. The red line indicates the statistical significance threshold (p -value = 0.05). Statistically significant factors include the addition of pyridine (both) and the amplitude of the sonication wave (carbamazepine only).

5.3.2.2 Response Optimisation

The optimisation of the sonication parameters (amplitude, pulse, and time) was performed by fitting a response surface regression model (RSM) to the data. Contour plots were established to illustrate the effect of each factor on the carbamazepine mono-TMS response (see Figure 5.10). Operating the sonotrode at a low pulse and a higher amplitude increased the carbamazepine mono-TMS response. Generally, increasing time, decreased the carbamazepine mono-TMS response, indicating that a lower time setting would be beneficial.

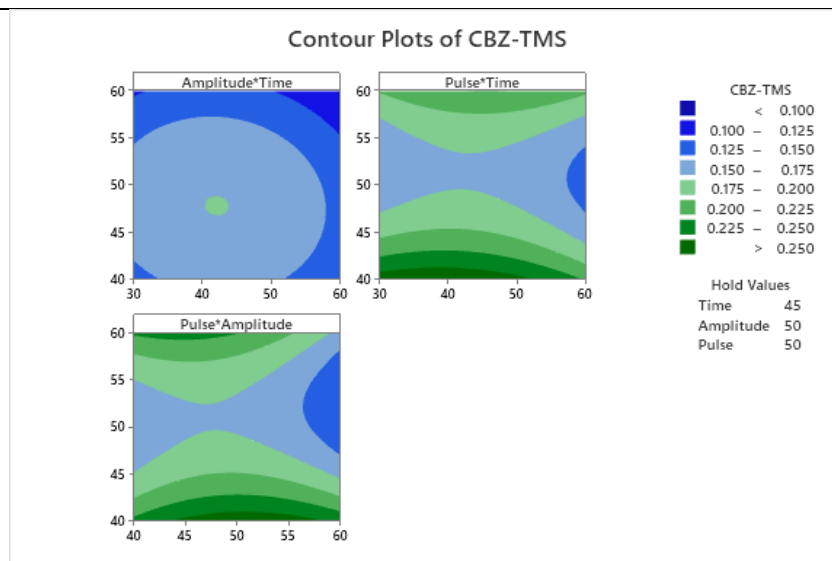


Figure 5.10: Contour plot for Carbamazepine mono-TMS for the face-centred ($\alpha=1$) central composite design. All parameters (pulse, amplitude, and time) are shown. Dark green areas show greatest R_f , which is optimal.

To determine the optimal sonication parameters for silylation, a response optimisation plot was obtained. The response optimisation function on Minitab (which identifies the combination of variable settings that jointly optimise a single response or set of responses (Minitab Inc, 2022)) was used to optimise the response of both the carbamazepine and carbamazepine mono-TMS responses. Programmed to maximise the carbamazepine mono-TMS response, and minimise the carbamazepine response, the optimised parameters were determined to be 60% amplitude, 40% pulse for a 30s time-period. A composite desirability score of 0.8173, indicates that the settings produce favourable results for responses as a whole. The optimisation plot and composite desirability values for each response are shown in Figure 5.11.

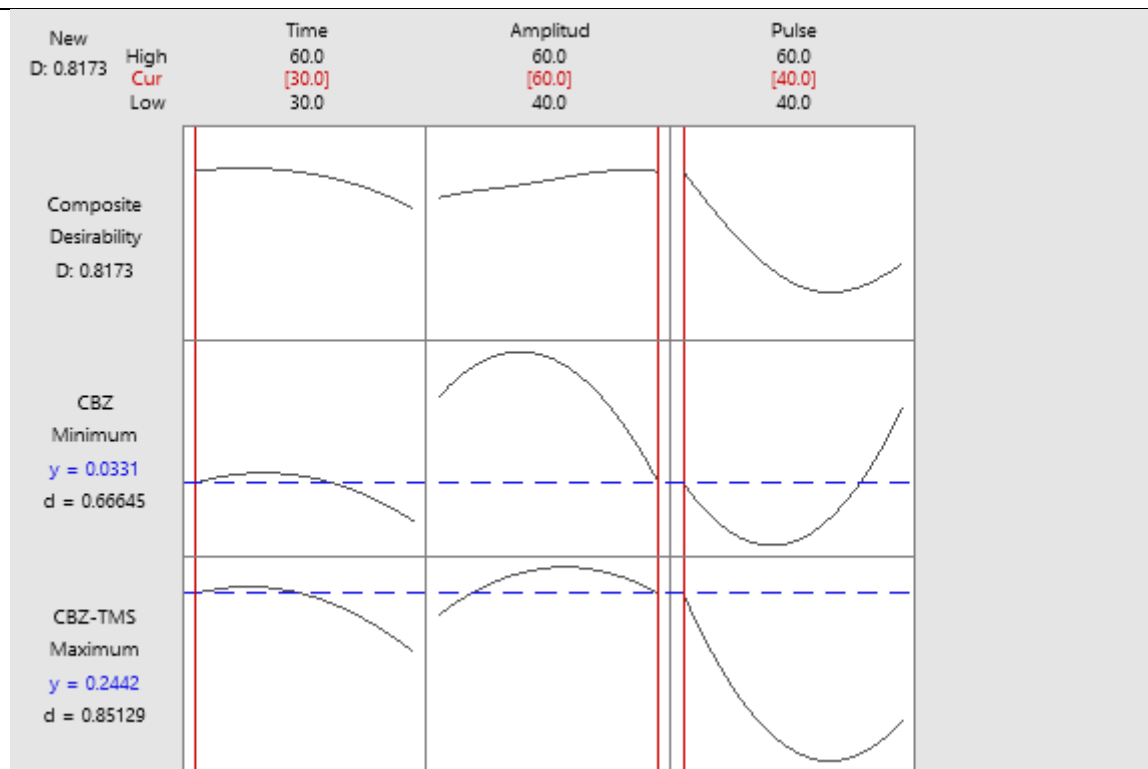


Figure 5.11: Response optimisation chart for the face-centred ($\alpha=1$) central composite design. Carbamazepine mono-TMS response maximised, and carbamazepine response minimised. Optimal parameters are 60% amplitude, 40% pulse for 30 seconds.

In Chapter 4, it was established that increasing the derivatisation time (> 40 mins), decreased the response of carbamazepine mono-TMS. This is replicated here, where a decrease in carbamazepine mono-TMS response is obtained with increasing sonication time. The carbamazepine mono-TMS response is also reduced with increasing the sonication pulse. A 40 % pulse indicates that sonication will be applied to the vial in short bursts which account for 40 % of the total derivatisation time. When sonication is applied, the vial and its contents will increase in temperature. Therefore, increasing the pulse to 60 % will prolong the increased temperature and reduce the response. This is similar to the results of Chapter 4, where increasing the oven temperature decreased the carbamazepine-TMS response. Applying heat is thought to facilitate silylation, particularly for hindered compounds. Though Orata suggests derivative breakdown can be observed with high temperatures (>60 °C) when applied for prolonged periods of time (>15 mins) (Orata, 2012). An increase in amplitude is beneficial for a large decrease in carbamazepine response, however, does have a slightly negative effect on the carbamazepine mono-TMS response, when reaching the maximum limit (60 %) – however this is a small compromise to make, and decreasing the value does not increase the composite desirability greatly.

Zhang *et al.* found that an increasing amplitude of an ultrasonic bath to 100% maximised the silylation of the majority of organic acids derivatised in the study (Zhang *et al.*, 2021). Sánchez-Ávila *et al.* found that 70% amplitude was optimal for silylation of triterpenes (Sánchez Ávila *et al.*, 2007), whereas Orozco-Solano and Luque de Castro found that 40% amplitude was optimal for silylation of sterols and fatty acids (Orozco-Solano *et al.*, 2010) when using a sonication probe. This would suggest that an increased amplitude is required when applying ultrasound with an ultrasonic bath. This may be due to the indirect sonication, where the uniformity of the sonication distribution is low, as waves must travel through a liquid to the sample vial (Hielscher Ultrasound Technology, 2022). The amplitude can be reduced when using a probe, as intensity is much greater, which increases efficiency. The optimised amplitude in this study (60%) is similar to those used with sonication probes, suggesting the sonotrode, though indirect sonication, is more comparable to the sonication probe, than the bath.

Comparison to the optimised oven method revealed no statistically significant difference (p -value = 0.262) between the carbamazepine mono-TMS responses for the two methods (see Appendix C). This suggests that the short 30 s sonication method is as sufficient for derivatising carbamazepine to carbamazepine mono-TMS as 40 mins in an oven, reducing the derivatisation time by 99%.

5.3.2.3 Repeatability

The repeatability of the optimised method was determined by analysing six carbamazepine samples and calculating the relative standard deviation. The RSD for carbamazepine was calculated to be 8%, and carbamazepine mono-TMS, 36%.

The silylation reaction is known to convert carbamazepine into carbamazepine mono-TMS, with a reduction in carbamazepine response suggesting the reaction is underway. The non-derivatised carbamazepine response is low (average 0.036, $n=6$) and has an acceptable %RSD. This suggests that carbamazepine is in the process of derivatising and can be assumed to be derivatising at the same rate in all samples. As detailed in Chapter 4, the reaction is thought to be at equilibrium, and it would be assumed that as the carbamazepine parent response were similar, that the response of the carbamazepine derivative peaks should be similar. However, this is not the case. The carbamazepine mono-TMS response replicates have an RSD of 36% indicating issues with stability.

The stability of the TMS derivatives depend on the analyte compound: amino acid derivatives are easily hydrolysed at room temperature, whereas sugar derivatives are stable under the same conditions (Thermo Fischer Scientific Inc., 2008). TMS derivatives of PhCs were deemed stable for 4 days based on (Lacina *et al.*, 2013), though Noctor *et al.* concluded that some TMS derivatives are unstable after 2.5 h (Noctor *et al.*, 2007). (Yu & Wu, 2012) managed to derivatise carbamazepine with N-methyl-N-(tert-butyldimethylsilyl)trifluoroacetamide (MTBSTFA) (70 °C for 60 mins) with an RSD <5% for all carbamazepine mono-TMS replicates. However, MTBSTFA derivatives are known to be less moisture

sensitive and up to 10,000x more stable than their TMS counterparts (Orata, 2012; Sobolevsky et al., 2003). It must be noted that these studies all used a conventional heating method for derivatisation.

The driving process behind sonication is cavitation (see Chapter 3). The collapse of the cavitation bubble drives the silylation reaction. Though, this process also produces free radicals which can induce a variety of chemical reactions, including secondary reactions (like hydrolysis) and degradation of target analytes (Tiwari, 2015). The sonication method produced an RSD of 36%, whereas the optimised oven method RSD was <10%. This suggests that the stability of the derivatives is the source of the variability, with sonication increasing the possibility of secondary or degradation reactions

As this method is qualitative, the repeatability and robustness of the method are crucial to the success of the study. Thus, in future research, it is recommended that the sonication method be optimised again, using RSD as the response variable, instead of yield.

5.3.3 Applicability to biosolid samples

5.3.3.1 Application to non-spiked biosolid samples

To determine the PhC load of the biosolid samples, non-spiked samples were extracted, derivatised and analysed using the optimised methods. In this study, qualitative data is collected to determine the PhC load of the samples, and quantification is not a primary focus.

Salicylic acid di-TMS (RT = 6.885 mins, average S/N = 30 (n=3)), ibuprofen mono-TMS (RT = 7.788 mins, average S/N = 34), paracetamol di-TMS (RT = 7.918 mins, average S/N = 28) and carbamazepine mono-TMS (RT = 14.083 mins, average S/N = 19) were detected in 100% of analysed non-spiked biosolid samples. Although peak height was low, all peaks were greater than a S/N ratio of 3, thus above the limit of detection (see Figure 5.12).

Paracetamol, ibuprofen and aspirin are three of the most commonly prescribed NSAIDs and analgesics in the UK (NursingNotes, 2017). Salicylic acid is a major metabolite of aspirin, and an independent medication used in treatment of dermatological conditions. All are also available over the counter, and thus high consumption and excretion is expected. Carbamazepine is a one of the top 10 anti-convulsant medication prescribed in the UK (NursingNotes, 2017) and was considered a candidate for the Water Framework Directive Watchlist (European Commission. Joint Research Centre., 2020) due to its persistence in the environment. The recalcitrant nature of the PhCs combined with the inefficient WWTP processes, contributes to their routinely detectable presence in sludge and biosolid samples.

Albero *et al.* (Albero et al., 2014) detected paracetamol, ibuprofen and salicylic acid in 100% (90% for salicylic acid) of analysed biosolid samples with concentrations ranging from 21 to 1111 ng/g. Gago-Ferrero *et al.* detected salicylic acid and carbamazepine in 100% of analysed biosolid samples, with concentrations ranging from 12-113 ng/g. Similarly, McClellan and Halden (McClellan & Halden,

2010) observed carbamazepine in 100% and ibuprofen in 80% of analysed biosolid samples, with mean concentrations of 163 and 246 $\mu\text{g/g}$ respectively. Whereas, Ding *et al.* (Ding *et al.*, 2011), detected carbamazepine in 80% of analysed biosolid samples with concentrations ranging from 5-22 ng/g . Therefore, it suggests that the detected PhCs are present in nearly all biosolid samples, though concentration is not homogenous. It must be noted that targeted analysis was used for all studies, and thus, PhCs which were not targeted are not necessarily absent from the biosolid samples in each study. This highlights the requirement of a non-targeted analysis, which would overcome this issue.

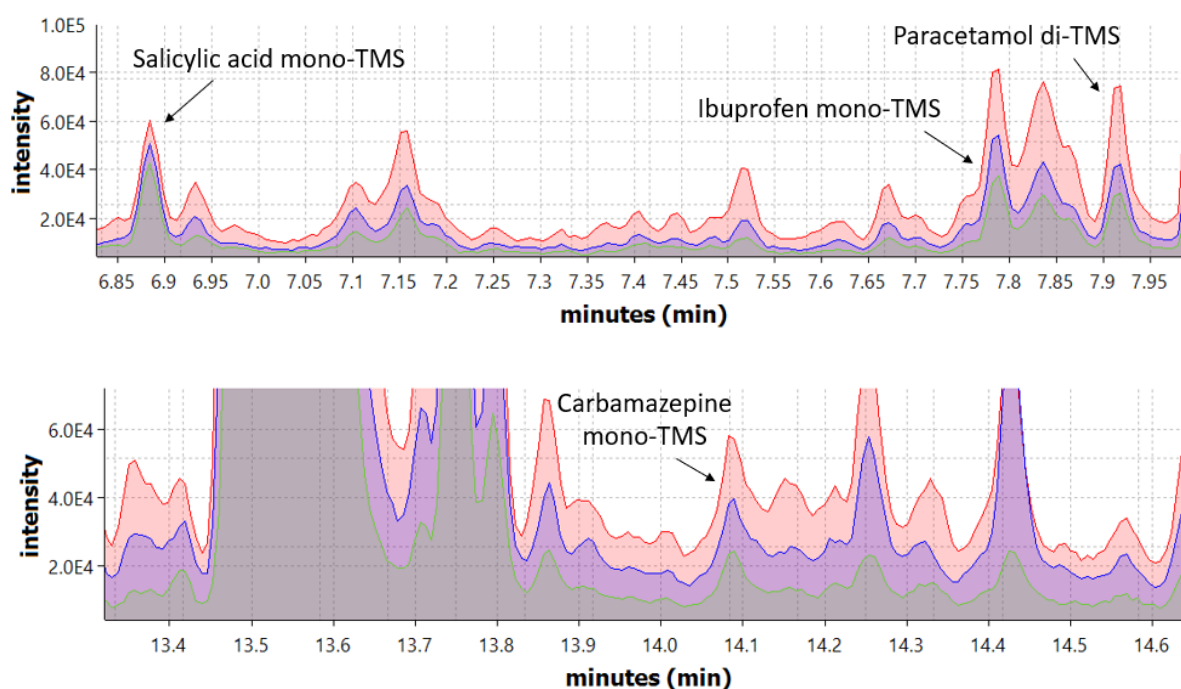


Figure 5.12: Total ion chromatogram (TIC) overlay of non-spiked biosolid samples extracted using the optimised method from 1.0g of ground biosolids. A) ibuprofen mono-TMS, salicylic acid di-TMS, and paracetamol di-TMS detected in all samples ($n=3$) B) carbamazepine mono-TMS peak identified in all samples

No other PhCs were easily detected in the non-spiked samples using the optimised method. However, this may be for one of two reasons. Firstly, the concentration of the PhC may be below the detection limit of the quadrupole MS. In this case PhCs are said to be <LOD, or not detected in the non-spiked biosolid samples, as their presence at concentrations below the LOD cannot be ruled out. Further investigation with the use of a high-resolution MS detector may elucidate more PhCs in the non-spiked samples, as detector sensitivity is increased. Secondly, large derivatised fatty acid peaks co-elute with analyte PhCs, for example metronidazole mono-TMS and ketoprofen mono-TMS co-elute with dodecanoic acid mono-TMS and sebacic acid mono-TMS, respectively. Thus, their presence or absence within the biosolid sample cannot be fully determined with this method.

To overcome both issues, it is recommended to use an advanced chromatographic technique, such as two-dimensional comprehensive gas chromatography (GCxGC). GCxGC separates samples on two orthogonal columns, providing better separation efficiency and an increased peak capacity (Lacina et al., 2013). The separation on the second dimension prevents co-elution, eliminating hidden peaks. Using a high-resolution mass spectrometer, such as a time of flight (TOF) detector, increases the sensitivity of the method, reducing the method detection limits. This is investigated further in Chapter 6.

5.3.3.2 Comparison to Gago-Fererro *et al.* and Green Chemistry

The optimised method was compared to Gago-Fererro *et al.* method (Gago-Fererro et al., 2015), as this was used as the basis for the study. Comparison of sample preparation time, solvent consumption, and the alignment of the method to the '12 Green Chemistry Principles' are evaluated. Comparison of the optimised derivatisation method to the method optimised in Chapter 4 is also discussed.

Extraction

The optimised extraction method was shown to sufficiently extract 4 PhCs from 1.000 g of biosolid sample. In both the optimised and original method, 2 mL aliquots of acidified methanol: water (50:50, pH 2.5, 0.1% formic acid) were used for 3 cycles. Therefore, the optimised method produced no reduction in solvent consumption at this stage. However, no EDTA was added to the samples, due to the incompatibility with GC analysis. Although EDTA has a low toxic impact, it has been shown to have poor degradation, with concerns over the metal chelating properties mobilising heavy metals in environmental settings (Xie, 2009). Including EDTA in the sample preparation, increases the overall number of compounds added to the reaction, which will result in an increase in waste products. Therefore, the omission of EDTA in the study aligns with Green Chemistry Principles 2 and 5 – atom economy and safer solvents and auxiliaries (Anastas & Warner, 1998).

In terms of sonication, the optimised method reduced the sonication time to 5 mins per cycle, a total of 15 mins per sample. In comparison, Gago-Fererro et al. sonicated for 15 mins at 50 °C per cycle, a total of 45 mins per sample. The optimised method reduces the sonication time by 67%, and overall sample preparation time by 40%. Additionally, the optimised method does not require heating, in comparison to the original method. Both factors will significantly reduce energy consumption.

Derivatisation

The optimised sonication method allows for derivatisation to be complete within 30 s: in comparison to 40 mins for the oven method (Chapter 4). This is a reduction of 98.8%, which will vastly reduce sample preparation time. The reduction in energy required is also substantial, as energy for 30 s sonication will be far less than that required to heat and maintain an oven at 50°C. Although, more than one sample can be heated in an oven simultaneously, in comparison, only one sample can be sonicated

at a time. However, it would require a sample set of >60 (taking the time of placing samples in and out of the sonotrode into consideration), to warrant using the oven method. Below this, the sonication method is more suitable. Further investigation into increasing the number of samples which can be sonicated simultaneously is ongoing.

Green Principle number 8 – ‘Reduce derivatives’ states that ‘unnecessary derivatisation should be minimised or avoided if possible’ (Anastas & Warner, 1998) to further reduce waste caused by derivatisation reagents. It should be noted that in order for PhCs to be detected on GC, derivatisation is required. Although the optimised method requires derivatisation prior to GC-MS analysis, the reduction in solvent consumption using GC would be favourable. Gago-Ferreiro *et al.* used a flow rate of 100 $\mu\text{L}/\text{min}$ for the LC-MS/MS analysis. With a run-time of 37 minutes, this amounts to 3.7 mL per sample. In comparison, the optimised method uses 100 μL of MSTFA to derivatise each sample for GC analysis – a reduction of 97.3% in solvent consumption. Although LC mobile phase components (MeOH, MeCN and water) will be cheaper per mL, in comparison to MSTFA; the upkeep of the LC-MS/MS in comparison to the GC-MS instrument will be considerably more (Bootman, 2021; Sparkman *et al.*, 2011). Therefore, derivatisation is considered necessary, as the use of GC will reduce solvent waste and consumption.

Therefore, per sample, the total sample preparation time for the optimised method is 50.5 mins in comparison to 80 mins for the original method (excluding sample evaporation in both methods) – a decrease of 37 %. In terms of solvent consumption (mobile phase vs derivatisation reagent), the optimised method has a reduction in solvent of 97 %.

5.4 Conclusions

In this chapter, a method for extracting and derivatising PhCs from biosolid samples using ultrasound was investigated. An adapted version of the extraction method used in Gago-Ferreiro *et al.* (Gago-Ferreiro *et al.*, 2015) was determined to be optimal for the extraction of 14 PhCs. Optimised method included three cycles of 2 mL acidified MeOH: MilliQ (1:1, pH 2.5), sonicated for 5 mins, and centrifuged for 10 min at 5000 rpm to extract PhCs from 1.0 g of biosolid. Extracted samples were evaporated to dryness, and reconstituted in ethyl acetate, derivatised via sonication and analysed by GC-MS. Optimised parameters were determined to be 40 % pulse, 80 % amplitude for 5 mins for extraction and 40 % pulse 60 % amplitude for 30 s for derivatisation. Relative recoveries ranged from 65-163 % and absolute recoveries from 8-64%. No statistically significant difference was observed between the responses of the optimised sonication method and optimised oven method from Chapter 4, though a 99 % reduction in derivatisation time was obtained.

The optimised sonication method decreased overall sample preparation time by 37 % and solvent reduction by 97 % in comparison to the Gago-Ferreiro *et al.* method aligning with Green Chemistry

principles 1 – ‘Prevent Waste’ and 6 – ‘Design for Energy Efficiency’. Competition for derivatisation reagent from matrix components and TMS stability issues resulted in high RSDs. Application to non-spiked biosolid samples identified four derivatised compounds, salicylic acid di-TMS, ibuprofen mono-TMS, paracetamol di-TMS and carbamazepine mono-TMS in 100 % of analysed samples.

In terms of non-targeted analysis, the novel method can be used to extract and derivatise non-spiked biosolid samples, although the large RSDs attributed to the UAD method and TMS stability have to be taken into consideration. In further work, the UAD method should be optimised again with a focus on repeatability, rather than derivatisation yield. The analysis by GC-MS is not sufficient for non-targeted analysis due to the issues with co-eluting peaks. The large fatty acid peaks are known to hide peaks attributing to derivatised pharmaceuticals (e.g., ketoprofen), though may hide more PhCs which are not targeted in this study. Therefore, to overcome this issue, the application of advanced chromatographic techniques such as two-dimensional gas chromatography is advised.

In the following Chapter, the semi-targeted characterisation of Biosolid samples is discussed. The method employs two-dimensional comprehensive gas chromatography (GCxGC), an advanced chromatographic technique with powerful separation abilities.

Chapter 6: Application of advanced chromatographic techniques in the non-targeted analysis of pharmaceutical compounds in biosolid samples

6.1 Introduction

6.1.1 Analysis Methods

As discussed in Chapter 2, analysis of emerging pharmaceuticals in complex environmental matrices is often undertaken by chromatographic methods coupled with mass spectrometers. Both gas and liquid chromatography (GC and LC, respectively) have been utilised, though due to the polar nature of PhCs, LC coupled to tandem MS, is often the preferred technique (Mohapatra et al., 2016). As described in Chapter 4, GC analysis requires an additional derivatisation step to reduce the polarity and increase the volatility of the PhCs for analysis, which can increase sample preparation time. Though, as concluded in Chapter 5, derivatisation can be undertaken in less than 1 minute; thus, the additional sample preparation time is negligible.

However, one-dimensional GC has shown to have issues with co-elution when analysing complex samples, such as biosolids (see Chapter 5). This would hinder non-targeted analysis, as some analytes may be hidden by larger peaks (either other analytes or interferences). The addition of a secondary, orthogonal column in two-dimensional comprehensive gas chromatography (GCxGC) analysis, increases resolution, preventing co-elution (Lacina et al., 2013). The increased separation efficiency and peak capacity achieved with GCxGC highlights the high potential and compatibility for non-targeted analysis of PhCs in complex matrices like biosolids.

GCxGC has previously been used for analysis of emerging contaminants in water (Marsik et al., 2017; Matamoros et al., 2010), wastewater (Kopperi et al., 2013; Lacina et al., 2013) and sludge matrices (Veenaas et al., 2018); though often targeted analysis is undertaken to identify and quantify the contaminants. Non-targeted analysis is more complex, though allows for a more in-depth characterisation of the sample – providing data on all detected compounds; some of which may have been missed if targeted analysis was applied. This is of particular relevance in environmental pollution as the detrimental environmental effects are considered to be the result of a few known PhCs; though these only represent a small proportion of known and unknown (or yet to be identified) parent PhCs, metabolites and transformation products (Gago-Ferrero et al., 2015). Applying non-targeted analysis to

environmental monitoring could detect and identify potentially toxic compounds which are not presently monitored – whilst reducing the likelihood of analyte misdetection (González-Gaya et al., 2021).

6.1.2 Data Processing Workflow

Non-targeted analysis requires advanced separation techniques and high-resolution detectors (such as GCxGC-TOFMS). These instruments generate a large volume of data (>30,000 peaks per sample) which requires thorough data processing before conclusions can be drawn. Data interpretation can be an arduous and time-consuming process, therefore, data processing workflows which can apply chemometric techniques, to elucidate similarities and variances within samples simultaneously are desired (Fisher et al., 2021; Freye et al., 2019; González-Gaya et al., 2021; Prebihalo, 2020). Many use a tile-based approach to facilitate non-targeted differential analysis of raw GCxGC data (Parsons et al., 2015; Watson et al., 2016). This approach eliminates time consuming peak finding and deconvolution stages (Parsons et al., 2015), providing rapid and robust comparison of raw data (LECO, 2020). Each GCxGC chromatogram is divided up into small tiles of a user specified size - the average width of a peak in the chromatogram (Figure 6.1). Raw data in each tile is compared, and variance between tiles in more than one sample is highlighted. Variation within the specified samples is identified and multivariate analysis (in particular, principal component analysis (PCA)) is used to illustrate the difference (LECO, 2020, 2021).

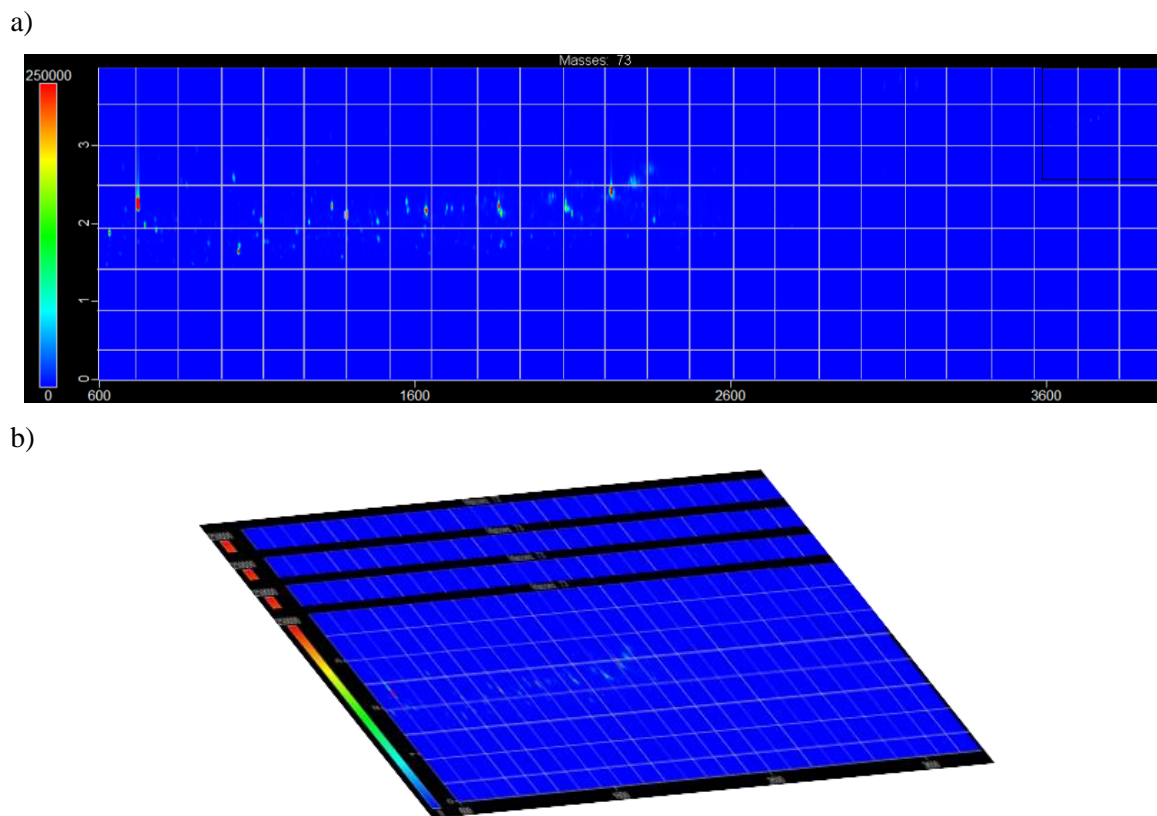


Figure 6.1: ChromaTOF Tile software: How it works a) Formation of Tiles on reference chromatogram, b) Tiles applied to all Chromatograms and compared. For the purpose of illustration, Tile sizes are much larger than appropriate for the chromatogram. Adapted from (LECO, 2020).

Variance in the compared chromatogram produces a hit known as a Feature. This is a variable which is measurable across all of the chromatograms, regardless of sample class. Features are defined as specific m/z ratios and RTs (found in a tile hit) which correspond to an analyte in the sample. The intensity of the feature is given by the feature area – similar to that of peak intensity on a one-dimensional chromatogram (LECO, 2020).

The multi-variate analysis is dependent on the given Fischer-ratio (F-ratio) threshold. F-ratios are a calculated numerical value, which are used to detect statistically significant differences between sample classes (LECO, 2020). F-ratios are calculated by dividing inter-class variation by intra-class variation (6-3). Inter-class variation (σ_{class}^2) is calculated following equation (6-1); where n_i is the number of measurements in the i th class; \bar{x}_i is the mean of the i th class; \bar{x} is the overall mean and k is the number of classes. Intra-class variation (σ_{error}^2) is calculated using equation (6-2); where \bar{x}_{ij} is the i th measurement of the j th class and N is the number of samples (Parsons et al., 2015).

$$\sigma_{class}^2 = \frac{\Sigma(\bar{x}_i - \bar{x})^2 n_i}{(k-1)} \quad (6-1)$$

$$\sigma_{error}^2 = \frac{\Sigma(\Sigma(\bar{x}_{ij} - \bar{x})^2) - (\Sigma(\bar{x}_i - \bar{x})^2 n_i)}{(N-k)} \quad (6-2)$$

$$Fischer\ Ratio = \frac{class\ to\ class\ variation}{within\ class\ variation} = \frac{\sigma_{class}^2}{\sigma_{error}^2} \quad (6-3)$$

F-ratios are calculated for each m/z in a tile and are used to indicate whether a feature differs significantly between samples or classes. Large F-ratios suggest sample variation is different between classes, but consistent within classes (Figure 6.2a+b), and small F-ratios suggest the feature is similar in all classes (inter-class), or different between samples of the same class (intra-class) (Figure 6.2c+d). Features with low F-ratios are likely to be filtered from the results list – but are maintained by lowering the F-ratio threshold.

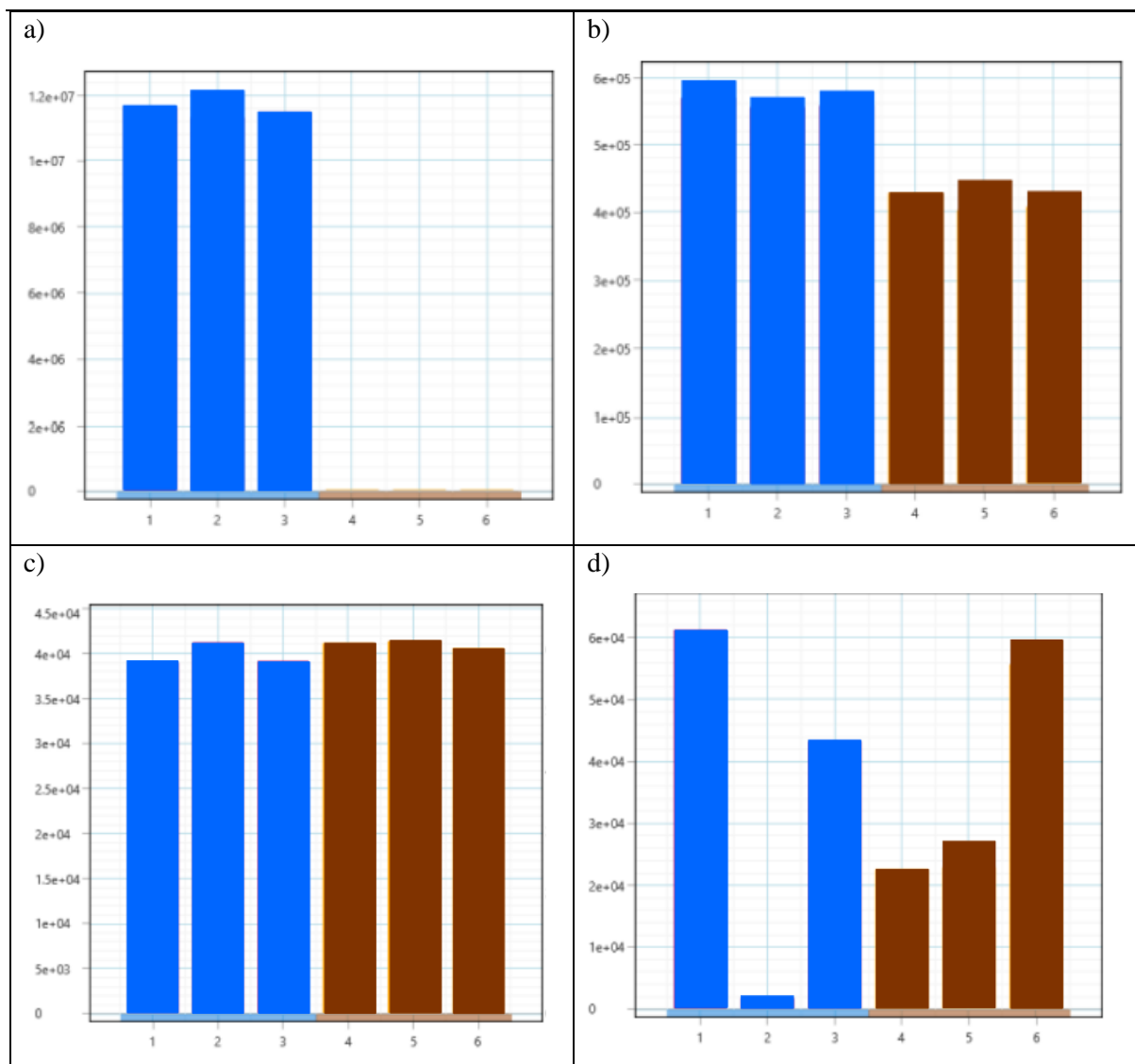


Figure 6.2: Feature intensity vs sample number at differing F-ratios. a) High F-ratio – large differences between classes b) small differences between classes c) Low F-ratio: small difference between class d) large difference between samples of same class. Adapted from (LECO, 2020).

The aim of this chapter was to validate the use of two-dimensional gas chromatography for non-targeted analysis of PhC load in biosolid samples. To investigate the ability and limitations of the GCxGC method, a comparison was drawn between the ‘gold standard’ LC-MS/MS method of Gago-Ferrero *et al.* (Gago-Ferrero *et al.*, 2015); and the novel method with one-dimensional GC-MS analysis (Chapter 5). Comparisons were drawn between identified compounds, sample preparation times and energy and solvent consumptions (in line with Green Chemistry principles). The tile-based non-targeted analysis workflow was applied to three biosolid samples to highlight inter- and intra- sample variance.

6.2 Methods

6.2.1 Reagents

Pharmaceutical compounds paracetamol (CAS Number: 103-90-2), atenolol (29122-68-7), carbamazepine (298-46-4), diclofenac sodium (15307-79-6), ibuprofen (15687-27-1), warfarin (81-81-2), salicylic acid (69-72-7), clofibrac acid (882-09-7), metronidazole (443-48-1), triclosan (3380-34-5), ketoprofen (22071-15-4), sotalol (3930-20-9), dapsone (800-08-0), fluvastatin (93957-54-1); and internal standard phenanthrene (85-01-8) were purchased from Sigma-Aldrich. Deuterated standards paracetamol D4 (64315-36-2), carbamazepine D10 (132183-78-9), atenolol D7 (1202864-50-3) and clofibrac acid D4 (1184991-14-7) (all 100 µg/mL in acetonitrile) were purchased from Qmx Laboratories Ltd. All pharmaceutical standards were of high purity grade (>90%). Ethyl acetate (141-78-6), pyridine (110-86-1), formic acid (64-18-6) and methanol (67-56-1) were purchased from Sigma-Aldrich or Fisher Scientific. All solvents were of reagent quality or greater. A MilliQ Ultrapure water system was used. N-trimethylsilyl-N-methyltrifluoroacetamide (MSTFA; 24589-78-4) was purchased from Sigma-Aldrich or Crawford Scientific and was of derivatisation grade or greater. MSTFA was stored at 4 °C, as per safety data sheets (SDS).

6.2.2 Stock Solution Preparation

Individual stock solutions of each pharmaceutical compound and a stock mixture of the 14 PhCs, were prepared in methanol at 0.05 mg/mL. Stock solutions were stored in airtight containers at -20°C. A working solution of the PhC mixture was prepared (250 µg/L) by dilution of the stock solution in methanol. This was used to spike samples as required. These solutions were prepared on the day of analysis and stored in an airtight container at -18 °C for inter-day replicates.

A surrogate stock solution containing the four deuterated standards was prepared by diluting 100 µL of each solution in 2 mL of methanol (singular solution, 5000 µg/L). The working solution was prepared by further diluting the stock solution to a concentration of 500 µg/L. All biosolid samples were spiked with the working solution prior to extraction.

As this research is intended to be applied to non-targeted analysis in future applications phenanthrene was used as an internal standard following methods of Veenaas et al., 2018, Shareef et al., 2006 and Kumirska et al., 2013. An individual phenanthrene stock solution (0.5 mg/mL) and working solution (0.05 mg/mL) were prepared in ethyl acetate and stored at -20°C.

6.2.3 Biosolid Sample Collection and Preparation

Treated AngloScottish biosolid samples were collected in December 2017, September 2019 and August 2021 from James McCaig Farms located in Wester Jawcraig, Scotland. The samples will be referred to

as Biosolid 1, 2 and 3, respectively. Samples were freeze-dried and stored in the dark at room temperature until analysis.

On visual comparison, Biosolid 1 and 2 are spherical in nature, whereas Biosolid 3 is more cylindrical (Figure 6.3). Biosolid 1 samples are lighter brown in colour, compared to the others, and smaller in size than the Biosolid 2 samples. For extraction, all biosolid samples were ground with a mortar and pestle. Grinding the pellets increases the surface area for extraction. When ground, Biosolid 1 and 3 produced a flake-like powder, whereas Biosolid 2 produced a fine powder. Biosolid 2 samples were far denser than Biosolid 1 and 3, and therefore, a vast amount of force had to be applied to the pellets in order to break and grind them.



Figure 6.3: Biosolid 1, Biosolid 2 and Biosolid 3 Pellets as collected.

Prior to extraction, 1.0 g of all ground biosolid samples were spiked with 1 mL of 500 $\mu\text{g/L}$ surrogate standard. For spiked samples, 1 mL of 250 $\mu\text{g/L}$ PhC mixture was added to 1.0 g of ground biosolid samples (250 $\mu\text{g/kg}$). Samples were left in contact overnight, to allow for evaporation of the methanol. Extraction was completed the next day.

A composite sample was prepared by combining the three biosolid samples. Approximately 1.0 g of each ground biosolid was combined prior to extraction (CBE). The extraction was then performed as normal, with 1.0 g of the CBE sample (spiked with 1ml of 500 $\mu\text{g/L}$ surrogate standard).

6.2.4 Extraction Procedure

The optimised extraction method (see Chapter 5) followed an adapted version of the extraction method of Gago-Ferrero *et al.* (Gago-Ferrero *et al.*, 2015). A mass of biosolid (approx. 1.0 g) was accurately measured into a 10 mL vial. Aliquots (2 mL) of acidified methanol: water (50:50, pH 2.5, 0.1% formic acid) were added, the vial sealed, and the subsequent suspension vortexed for 1 minute. The vial was then added to the sonotrode device and ultrasound applied (40% pulse, 80% amplitude) for 5 minutes.

The vial was centrifuged at 5000 rpm for 10 mins, carefully decapped, and the supernatant collected in a separate 10 mL vial. This process was repeated twice more (three cycles in total) combining the supernatants each time. The resulting solution was then evaporated to dryness at a gentle heat (40 °C) on a hotplate overnight. After all solution had evaporated and vial had cooled to room temperature, an aliquot of ethyl acetate (100 µL) or methanol: water (30:70, not acidified, 1 mL) was added (for GC and LC analysis, respectively), the vial sealed, vortexed for 30 s and centrifuged for 5 mins at 5000 rpm. The ethyl acetate solution was transferred to a 300 µL sonication vial for derivatisation, prior to GC-MS and GCxGC-TOFMS analysis. The acidified methanol: water solution (30:70, pH 2.5, 0.1% formic acid) was filtered through a 0.2 µm nylon filters prior to LC-MS/MS analysis.

6.2.5 Derivatisation Procedure

The optimised derivatisation method (see Chapter 5) was used to derivatise samples for GC analysis. N-trimethylsilyl-N-methyltrifluoroacetamide (MSTFA) was used as the derivatisation agent. The optimal method is as follows. To the 100 µL ethyl acetate sample (from the extraction step), 25 µL of pyridine, 25 µL of the phenanthrene working solution (0.05 mg/mL) and 100 µL of MSTFA were added. Vials were capped and sonicated at 40% pulse, 60% amplitude for 30s.

6.2.6 Pellets

Individual pellets were analysed to determine homogeneity of samples. All pellets were less than 1.0 g in mass and differed in size and shape. To ensure comparison could be made, each pellet was ground with a mortar and pestle, and 100 mg weighed out for extraction. Samples were spiked with 1 mL of 250 µg/L PhC mixture (2500 µg/kg) prior to extraction. Extraction and derivatisation followed the same procedure as above.

6.2.7 Analysis Methods

6.2.7.1 LC-MS/MS

Analysis was conducted on Thermo Scientific Dionex Ultimate 3000 UHPLC system coupled to a Thermo Scientific Q-Exactive Orbitrap mass spectrometer. Aliquots (10 µL) of the extracted biosolid sample were analysed in reversed phase mode on a Waters XSelect HSS T3 XP chromatography column (2.5 µm particle size, 2.1 mm x 150 mm). Mobile phase composition was as follows: eluent A was acetonitrile, and eluent B was 10 mmol ammonium formate adjusted to pH 3.5 with formic acid. Initial composition was 1% A and 99% B for 2 mins, increasing to 30% A and 70% B at 5 mins, holding for 8 mins, and increasing further to 99% A and 1% B at 14 mins, holding for 6 mins and finally recalibrating back to 1% A and 99% B between 20 and 30 mins (illustrated in Appendix D). Flow rate set to was 0.2 mL/min to prevent high back pressure; and a total run time of 30 mins was observed. Samples were analysed in both positive and negative ion mode. Mass spectra were obtained in

electrospray ionisation mode (In-source CID = 0.0eV), in full scan mode (100-900 m/z positive and 50-750 m/z negative). Resolution was set to 17,500, the isolation window set to 2.0 m/z and the AGC target to 1×10^5 in both modes. Default charge state was set to 1 in both ionisation modes. An inclusion list was used in both methods for targeted analysis (Table 6-1), with the PhC standard used to identify preferred ionisation mode, retention time and specific precursor and product ions for each analyte PhC.

Table 6-1: Inclusion List: Retention times (mins), precursor and product ions (m/z) for the spiked PhCs – LC-MS/MS analysis

| Compound | RT (mins) | Precursor ion | Product ion | Ion mode |
|----------------|-----------|---------------|-------------|----------|
| Atenolol | 8.3 | 267.17032 | 190.0861 | POSITIVE |
| Dapsone | 11.2 | 249.06922 | 156.0113 | |
| Diclofenac | 17.8 | 296.02396 | 215.0493 | |
| Ketoprofen | 17.5 | 255.10157 | 209.0958 | |
| Metronidazole | 8.84 | 172.07167 | 128.0456 | |
| Paracetamol | 8.7 | 152.07061 | 110.0604 | |
| Sotalol | 8.06 | 273.12674 | 213.0691 | |
| Carbamazepine | 18.7 | 237.10279 | 194.0964 | |
| Clofibric Acid | 17.53 | 213.0324 | 126.9941 | NEGATIVE |
| Fluvastatin | 17.69 | 410.17731 | 210.0716 | |
| Ibuprofen | 17.82 | 205.1234 | 205.1225 | |
| Ketoprofen | 17.51 | 253.08702 | 209.1539 | |
| Salicylic Acid | 14.3 | 137.02442 | 93.0329 | |
| Triclosan | 18.01 | 286.94389 | 286.9435 | |
| Warfarin | 17.62 | 307.09758 | 161.0231 | |

6.2.7.2 GC-MS

Initial analysis was conducted using an Agilent 7890A gas chromatograph coupled to an Agilent 5975c quadrupole mass spectrometer. Aliquots (1 μ L) of sample were injected onto an Agilent DB-5 (5% phenyl and 95% methylpolysiloxane) capillary column (30 m x 0.25 mm x 0.25 μ m). Samples were analysed in splitless mode. The initial oven temperature was 100 °C, increasing by 10 °C/min to 300 °C, with a 10 min hold time, a total run time of 30 mins. Inlet and transfer line temperatures were set to 270 °C. Helium was used as the carrier gas at a flow rate of 1 mL/min. Mass spectra were obtained in electron ionisation mode (70 eV), in full scan mode (45-650 amu). MS source and quad temperatures were 230 °C and 150 °C, respectively.

6.2.7.3 GCxGC-TOFMS

Analysis was conducted on a LECO Pegasus 4D comprehensive two-dimensional gas chromatograph coupled to a LECO time of flight (TOF) mass spectrometer. Aliquots (1 μ L) of extracted biosolid sample were analysed in reversed phase mode. The first-dimension column was a DB-17MS (60 m x 0.25 mm x 0.25 μ m), and the second-dimension column a Rxi-5Sil column (2 m x 0.25 mm x 0.25 μ m – 0.1 m in modulator, 1.7 m in oven and 0.2 m in detector). Samples were analysed at in split mode (10:1). The initial oven temperature was 70 °C for 0.2 min, increasing by 5 °C/min to 300 °C, with a 20 min hold

time, a total run time of 66.2 mins. The secondary oven and modulator were set +10 °C and +20 °C to the primary oven, respectively. The modulation period was set to 4s. Inlet and transfer line temperatures were set to 300 °C and 280 °C, respectively. Mass spectra were obtained in electron ionisation mode (70 eV), in full scan mode (45-500 amu) at a rate of 200 spectra/s. MS source temperature was 230 °C and an acquisition delay of 600 s was applied. The number of samples required four non-consecutive days of analysis. Thus, 20 samples were analysed in a randomised order to prevent bias from unknown and uncontrollable factors (i.e., column/septa degradation or room temperature).

A second GCxGC method was made to be used as a ‘quick’ blank. The temperature program was set to 300 °C for 5 mins. The acquisition delay was 4 s. All other parameters remained the same. The shorter blank method was verified by running a longer blank after the short blank, to ensure no peaks were observed (see Appendix D).

6.2.7.4 ChromaTOF Tile Analysis

GCxGC-TOF MS samples were processed using ChromaTOF Tile. Optimised processing parameters were determined in this study. Tile size was calculated by measuring average peak width on ChromaTOF and using the auto-calculate feature on the ChromaTOF Tile software. A tile size of 3 modulations x 20 spectra (D1xD2) was used for all analysis. A S/N threshold of 10 was used on both ChromaTOF and ChromaTOF Tile. An F-ratio threshold of 20 was used for the majority of studies, reducing only when stated. An exclusion region of 2600-4000 s (D1) and 0-1.2 s (D2) was used to remove features which related to the solvent (see Figure 6.4). All targeted PhCs eluted within the included region.

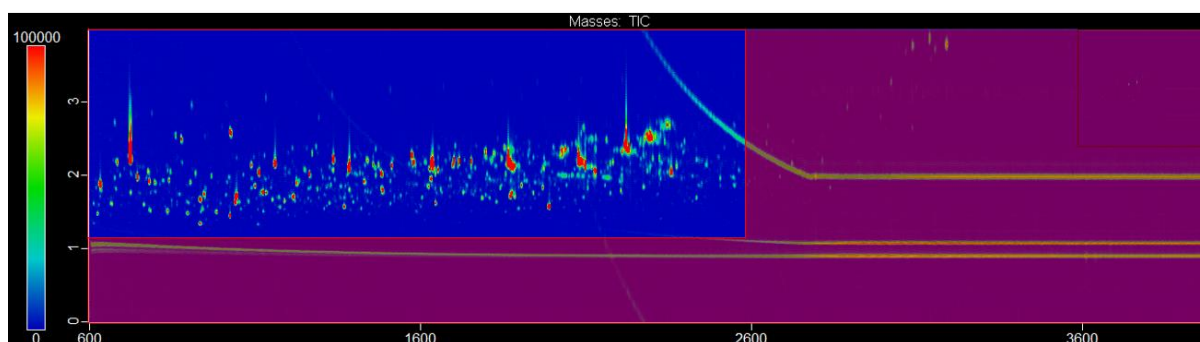


Figure 6.4: Excluded Areas from Tile Analysis - D1:2600-4000, D2: 0-1.2s – highlighted by red area on the chromatogram. Exclusions prevent solvent peaks being included in the analysis. All targeted PhCs eluted within this time frame.

6.2.8 Software

ChromaTOF 4.72.0.0 software was used for sample acquisition and analysis for GCxGC-TOFMS samples, with further analysis conducted on ChromaTOF Tile v1.01.00.0 software. LC-MS/MS analysis was conducted on Chromeleon, Xcalibur and Tracefinder software. Minitab 20.4.0.0 and RStudio v1.3.959 were used for statistical analysis.

6.3 Results and Discussion

6.3.1 Comparison to Gold Standard (LC-MS/MS) method

Various methods including the method of Gago-Ferrero *et al.*, on which this study is based, used LC-MS/MS for analysis of extracted sludge samples. Therefore, this is deemed the ‘Gold standard’ method to which the novel GCxGC-TOFMS method can be compared. Biosolid 1 and 2 were extracted using the optimised method and analysed by LC-MS/MS.

All 14 PhC peaks were detected in the PhC standard mixture (Table 6-2). All peaks with the exception of dapsone were detected in the spiked biosolid samples. As dapsone was detected at the same concentration (500 ng/L) in the PhC standard, matrix effects associated with the complex biosolid matrix may have hindered the detected response (6.3.1.1 Matrix effects)

Atenolol, paracetamol, carbamazepine, ibuprofen, ketoprofen, salicylic acid, and warfarin were detected in the non-spiked Biosolid 1 samples (43% of total compounds), and paracetamol, carbamazepine, ibuprofen, and salicylic acid were detected in non-spiked Biosolid 2 (29%). No other targeted PhCs were detected in the non-spiked samples.

Table 6-2: PhCs detected by targeted LC-MS/MS in non-spiked and spiked biosolid samples. Dapsone was the only PhC not detected in the spiked samples. Those highlighted green are identified in the corresponding sample, and those highlighted red are not. Bio1 and Bio2 refer to the Biosolid sample. NS = non-spiked, S = spiked with PhC mixture. PhC Std. refers to the standard mixture of PhCs.

| Compound | Bio1 NS | Bio1 S | Bio2 NS | Bio2 S | PhCStd. |
|------------------|---------|--------|---------|--------|---------|
| Atenolol | YES | YES | NO | YES | YES |
| Dapsone | NO | NO | NO | NO | YES |
| Diclofenac | NO | YES | NO | YES | YES |
| Metronidazole | NO | YES | NO | YES | YES |
| Paracetamol | YES | YES | YES | YES | YES |
| Sotalol | NO | YES | NO | YES | YES |
| Carbamazepine | YES | YES | YES | YES | YES |
| Clofibrilic Acid | NO | YES | NO | YES | YES |
| Fluvastatin | NO | YES | NO | YES | YES |
| Ibuprofen | YES | YES | YES | YES | YES |
| Ketoprofen | YES | YES | NO | YES | YES |
| Salicylic Acid | YES | YES | YES | YES | YES |
| Triclosan | NO | YES | NO | YES | YES |
| Warfarin | YES | YES | NO | YES | YES |

A heatmap was constructed to illustrate the difference between the two biosolids (Figure 6.5). The qualitative analysis shows a clear difference is visible between the two samples: Biosolid 1 samples

show a great number of dark green to red areas, whereas Biosolid 2 samples show mostly green with some darker areas, suggesting Biosolid 2 has less detected peaks than Biosolid 1. In terms of PhCs, this matches the results in Table 6-2 where Biosolid 1 has more detected PhCs than Biosolid 2. Although no quantitative results can be drawn from the heatmap, it indicates visually the differences between the biosolid samples in terms of the PhC load and shows the repeatability of the extraction.

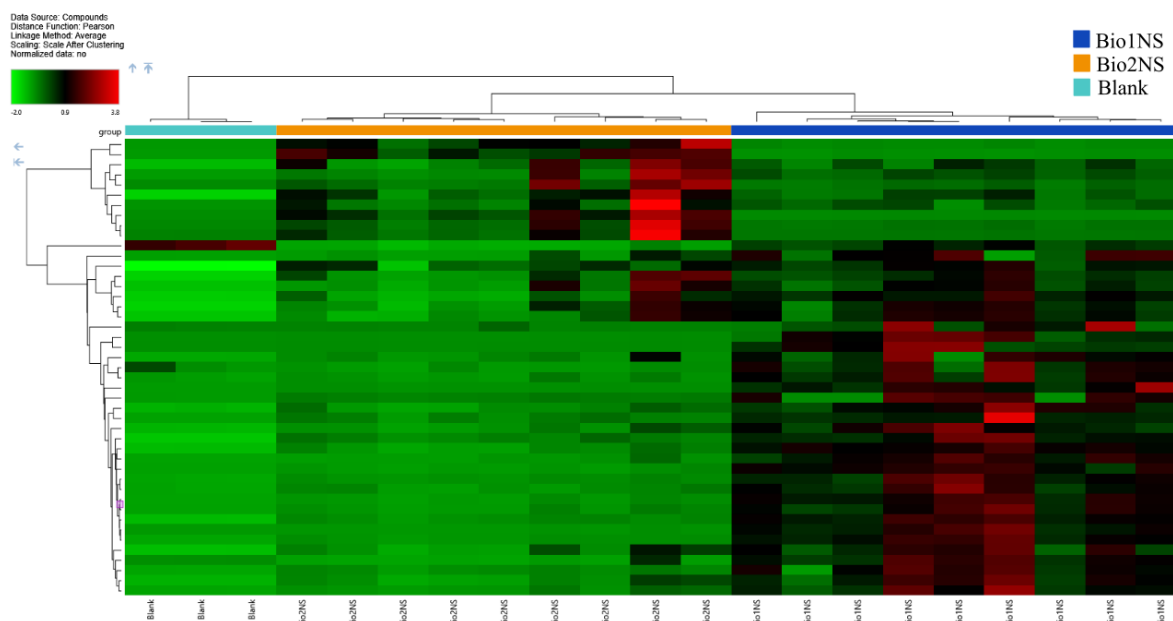


Figure 6.5: Heatmap of LC-MS/MS analysed non-spiked samples ($n=6$). Blank vs Biosolid 1 vs Biosolid 2. Colour indicates PhC peak detection, where dark green & red indicates increased detection. Sample blanks show no detected peaks, suggesting less contamination, in comparison to the Biosolid samples. Initial observations: Biosolid 2 is has less detected peaks than Biosolid 1.

6.3.1.1 Matrix effects

Matrix effects are defined as the “combined effect of all components of the sample other than the analyte on the measurement of the quantity” (IUPAC, 2014), in other words, the collective effect of the matrix on the analyte response. Environmental samples often have large matrix effects due to the ‘dirty’ nature of the samples, which can cause both ion suppression and enhancement when electrospray ionisation (ESI) is used.

To determine whether matrix effects were observed, deuterated surrogate standard PAs (atenolol-d7, carbamazepine-d10, clofibric acid-d4 and paracetamol-d4) were used to calculate the matrix effects. The calculation is shown in equation (6-4). A value of 100% signifies no matrix effect, a value below 100% indicates ion suppression and a value greater than 100% suggests ion enhancement. Values between 80 and 120% are considered acceptable, with responses outwith this range deemed significant (Carlton et al., 2015).

$$\text{Matrix Effect} = \left(\frac{\text{Analyte in Spiked Sample}}{\text{Analyte in Standard Solution}} \right) \times 100 \quad (6-4)$$

Significant matrix effects were calculated for all surrogates in both biosolid samples – all outwith the given acceptable range (see Table 6-3). Significant ion suppression was observed for carbamazepine-d10, atenolol-d7 and paracetamol-d4 (all <10%), and significant ion enhancement observed for clofibrac acid-d4 for all samples (>120%). No matrix effects could be calculated for the target PhCs as spiked concentrations differed from that of the PhC standard. Matrix effects can be reduced by introducing further sample preparation steps, though could potentially introduce selectivity to the analysis. These are discussed further in Section 6.3.3.2 Green Chemistry and Chapter 2.

Table 6-3: Calculated matrix effects for LC-MS/MS analysis of biosolids

| Biosolid Sample | Pharmaceutical | Calculated Matrix Effect (%) | Ion Suppression or Enhancement? |
|-----------------|-------------------|------------------------------|---------------------------------|
| Biosolid 1 | Atenolol-d7 | 5.39 | Suppression |
| | Carbamazepine-d10 | 1.55 | Suppression |
| | Clofibrac acid-d4 | 921.68 | Enhancement |
| | Paracetamol-d4 | 5.00 | Suppression |
| Biosolid 2 | Atenolol-d7 | 2.70 | Suppression |
| | Carbamazepine-d10 | 0.72 | Suppression |
| | Clofibrac acid-d4 | ND | ND |
| | Paracetamol-d4 | 2.94 | Suppression |

6.3.2 Translation from GC-MS to GCxGC-TOFMS

Previously (see Chapter 5), one-dimensional GC-MS was used to detect PhCs in biosolid samples. However, issues with sensitivity and co-eluting fatty acids arose. To overcome these issues, translation of the method from one-dimensional GC-MS to two-dimensional GCxGC-TOFMS was investigated.

Samples were derivatised prior to analysis; converting analyte PhCs to their TMS derivatives. Compounds were identified on GCxGC-TOFMS through retention times (determined by running PhC standard solutions) and confirmed by comparison of obtained spectra to NIST (national institute for science and technology) library spectra.

It should be noted that the NIST mass spectral library data was created using a quadrupole mass spectrometer. With GCxGC, a more sensitive TOF MS detector is used. The mass spectra formed using this detector can differ slightly to the NIST library. Therefore, the MS of each identified targeted PhC compound was checked manually to ensure accurate identification.

Resolution

A reversed phase column set-up (polar x non-polar) was used for analysis. The polar column on the first dimension, increases resolution of polar analytes (including PhCs); with the non-polar second dimension preventing co-elution with more non-polar analytes (i.e., fatty acids). GCxGC provides increased peak capacity, resolution, and sensitivity in comparison to one-dimensional GC – suggesting the technique is more compatible with non-targeted analysis.

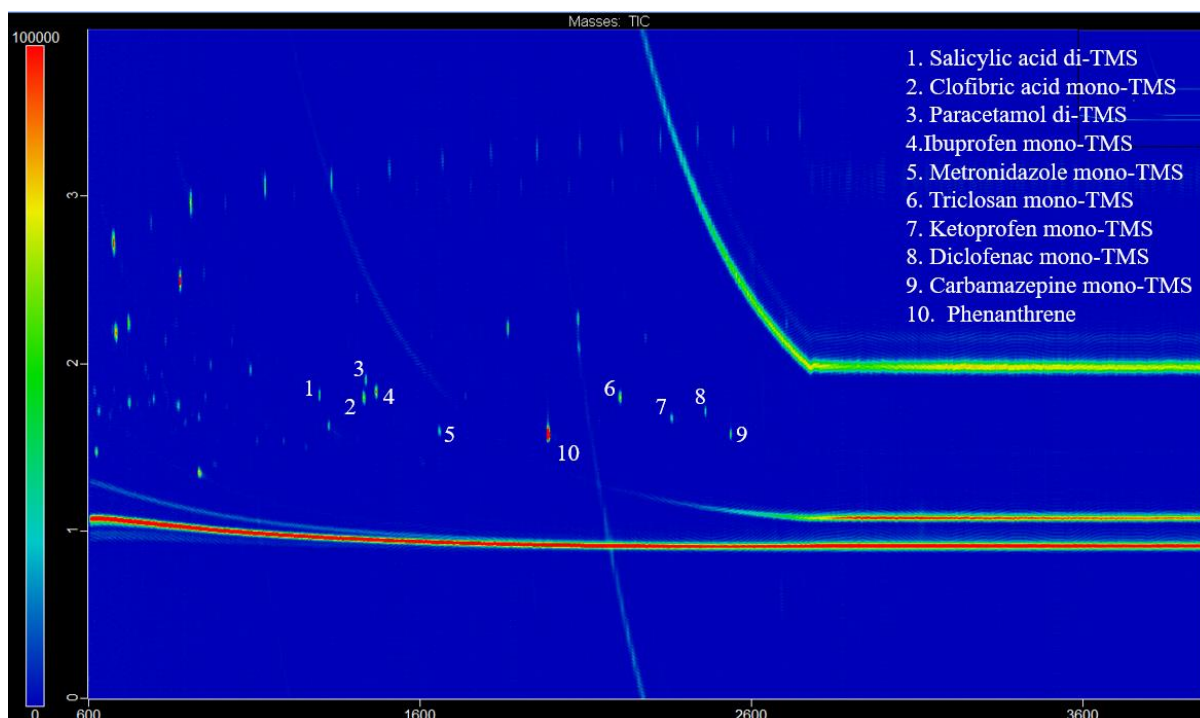


Figure 6.6: Annotated GCxGC Chromatogram for derivatised PhC Standard in ethyl acetate. Detected derivatised PhC peaks numbered and identified using mass spectra. 1 – Salicylic acid di-TMS (1296, 1.815); 2- Clofibric acid mono-TMS (1428, 1.805); 3 – Paracetamol di-TMS (1436, 1.910); 4 – Ibuprofen mono-TMS (1468, 1.835); 5 – Metronidazole mono-TMS (1656, 1.615); 6 – Triclosan mono-TMS (2204, 1.795); 7 – Ketoprofen mono-TMS (2360, 1.680); 8 – Diclofenac mono-TMS (2460, 1.715); 9- carbamazepine mono-TMS (2536, 1.590); 10 – Phenanthrene (1984, 1.585).

The orthogonal column set-up has the added advantage of structured elution – retention is related to physicochemical properties of analytes, allowing elution trends of homologous compounds to be established. Known as the ‘roof-tile effect’ (Shimadzu, 2012; von Mühlen et al., 2006), the elution order of similar compounds can often be predicted – retention increasing with increasing methyl groups for example (Marriott et al., 2004). This is observed for siloxanes and fatty acids (see Figure 6.7); where retention is increased with increasing alkyl chain length.

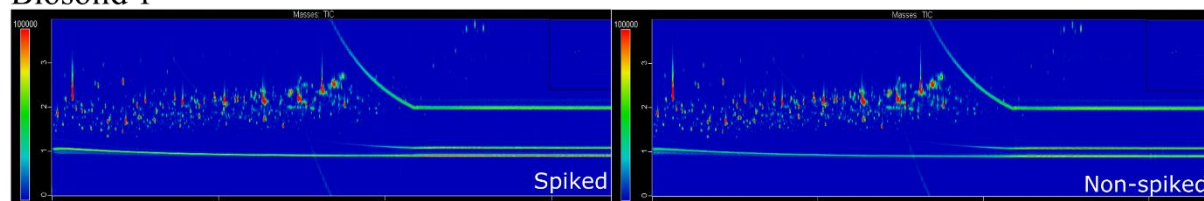


Figure 6.7: Two-dimensional gas chromatogram illustrating the 'roof-tile' structured elution of siloxanes and fatty acids; and the separation of peaks which co-elute on one-dimensional GC. The second-dimension separation prevents co-elution of metronidazole mono-TMS and ketoprofen mono-TMS with dodecanoic acid mono-TMS and sebacic acid di-TMS, respectively.

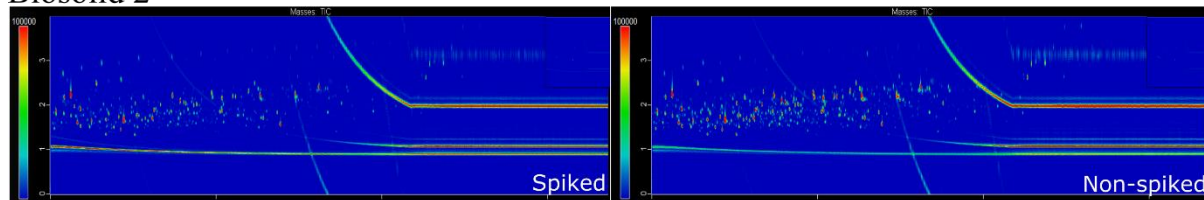
As stated in Chapter 5, when analysed on one-dimensional GC-MS, derivatised PhCs metronidazole mono-TMS and ketoprofen mono-TMS co-elute with derivatised fatty acids (dodecanoic acid mono-TMS and sebacic acid di-TMS, respectively). In two-dimensional GC, the secondary column provides separation on the second dimension, preventing co-elution. Metronidazole mono-TMS and ketoprofen mono-TMS are completely resolved from the respective fatty acids due to earlier elution in the second dimension (see Figure 6.7).

A qualitative comparison between the three biosolids highlights differences in the content of each sample - with Biosolid 1 having a greater number of peaks in comparison to Biosolid 2 and 3. Comparison of the spiked and non-spiked samples highlights little difference between spiked samples of the same biosolid. Non-spiked biosolid samples seem to have more peaks for Biosolid 2 and 3; though could be due to homogeneity of samples. The samples were spiked with 14 PhCs, though over 20,000 peaks were detected in each of the samples. Therefore, to illustrate the differences, extracted ion chromatograms (EICs) were used to identify PhCs (Figure 6.9). Detection was based on RT and MS. Ketoprofen mono-TMS and diclofenac mono-TMS were detected in the spiked sample, but not in the non-spiked sample, as expected. Whereas salicylic acid di-TMS was detected in both samples, though the peak area is smaller for the non-spiked sample. This suggests that the Biosolid sample likely contains the PhC salicylic acid.

Biosolid 1



Biosolid 2



Biosolid 3

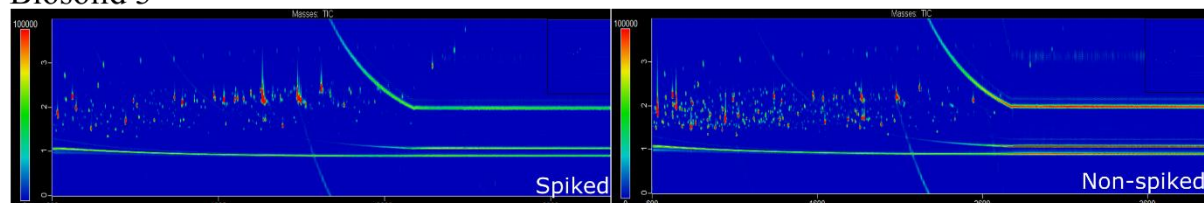
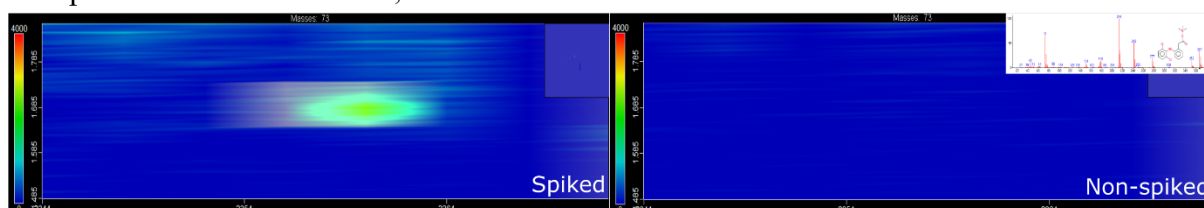
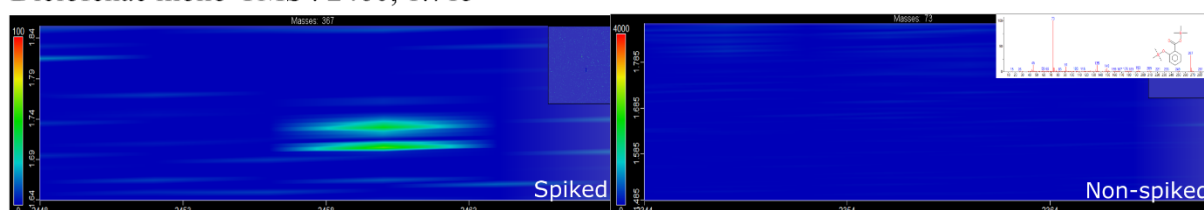


Figure 6.8: Comparison of spiked and non-spiked chromatograms for all biosolids – a) Biosolid 1 b) Biosolid 2 and c) Biosolid 3. Comparison made on total ion chromatogram (TIC) with the z-axis set to 100,000.

Ketoprofen mono-TMS : 2360, 1.680



Diclofenac mono-TMS : 2460, 1.715



Salicylic acid di-TMS : 1296, 1.815

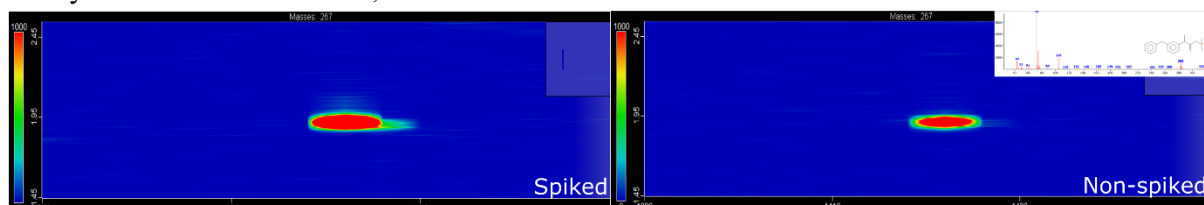


Figure 6.9: Comparison of spiked vs non-spiked Biosolid 1 samples for PhCs using extracted ion chromatograms (EIC) a) Ketoprofen mono-TMS (m/z 73) b) Diclofenac mono-TMS (m/z 367) and c) Salicylic acid di-TMS (m/z 267). Ions chosen from mass spectra (inset- NIST mass spectral database).

Overall, the reversed-phase set-up provides efficient separation of PhCs and prevents co-elution with fatty acids – suggesting the technique is more compatible with non-targeted analysis than one-dimensional GC.

6.3.3 Comparison of GCxGC-TOFMS vs LC-MS/MS

6.3.3.1 Biosolid PhC Load

Samples analysed on both LC-MS/MS and GCxGC-TOFMS were prepared using the same extraction method, only differing in reconstitution solvent and the derivatisation of GC samples. A qualitative comparison of detected PhCs was drawn between the two analysis methods to determine whether GCxGC-TOFMS method was suitable. The presence of the 14 targeted analyte PhCs in the non-spiked biosolid samples for Biosolid 1 and 2 are presented in Table 6-4.

Table 6-4: Comparison of analysis methods for identification of PhCs in non-spiked biosolid samples

| Pharmaceutical Identified* | Analysis Method | | | |
|----------------------------|-----------------|------|----------|------|
| | LC-MS/MS | | GCxGC-MS | |
| | Bio1 | Bio2 | Bio1 | Bio2 |
| Atenolol | ✓ | | | |
| Carbamazepine | ✓ | ✓ | ✓ | ✓ |
| Clofibric Acid | | | | |
| Dapsone | | | | |
| Diclofenac | | | | |
| Fluvastatin | | | | |
| Ibuprofen | ✓ | ✓ | ✓ | ✓ |
| Ketoprofen | ✓ | | | |
| Metronidazole | | | | |
| Paracetamol | ✓ | ✓ | ✓ | |
| Salicylic Acid | ✓ | ✓ | ✓ | ✓ |
| Sotalol | | | | |
| Triclosan | | | ✓ | ✓ |
| Warfarin | ✓ | | | |

*As the TMS derivative for the GCxGC method

Carbamazepine, ibuprofen, and salicylic acid were detected in all non-spiked biosolid samples using both analysis techniques. Additionally, atenolol, ketoprofen, paracetamol and warfarin were detected in Biosolid 1 using LC-MS/MS; with paracetamol also being detected in Biosolid 2. These compounds were not detected using the GCxGC-TOFMS method (with the exception of paracetamol in Biosolid 1). Issues with detection of these additional compounds may be attributed to two possibilities – PhC volatility and detector sensitivity. Atenolol and warfarin were not detected by GCxGC-TOFMS when analysing the PhC standard. Both compounds were analysed at high concentration (1000 µg/L); thus, a

peak was expected. However, both compounds near 400 g/mol when derivatised, suggesting that volatility of the PhCs prevents detection. Additionally, the difference in detector sensitivity (Orbitrap vs Time-of-flight); may prevent the detection of small concentrations of the paracetamol and ketoprofen derivatives. Both compounds were detected in the PhC standard; thus, may be at too low a concentration for the TOF detector. Therefore, this is a limitation to the GC method, though the addition of a more sensitive (higher resolution) detector may overcome sensitivity issues.

Triclosan was detected in both Biosolid 1 and 2 using the GCxGC method, though not detected in either biosolid when analysed by LC-MS/MS. This suggests that the derivatisation of triclosan aids in the detection and is more compatible with GCxGC-TOFMS method.

Matrix effects for the GCxGC-TOF method were calculated using the internal standard phenanthrene (as the PhC standard was at a different concentration to the spiked samples and deuterated surrogates were <LOD). Matrix effect was calculated to be 107% and 96% for Biosolid 1 and 2, respectively. Both are relatively close to 100% and so are deemed acceptable. It is widely accepted that matrix effects in GC analysis are often due to thermally labile or polar analytes (Anastassiades et al., 2003; Panuwet et al., 2016). In this method, analytes are converted to less polar, more thermally stable derivatives by silylation, reducing matrix effects. The reduction in matrix effects is an advantage to the GCxGC method.

However, competition for the derivatisation agent may also have prevented the detection of PhCs (i.e., paracetamol in Biosolid 2). Figure 6.8 suggests a difference in matrix content between the two biosolids – one Biosolid may contain more compounds with labile hydrogens which compete with the PhCs for MSTFA. With non-targeted analysis it is impossible to predict the number and type of compounds present in the sample. Thus, the number of labile hydrogens is unknown, and the molar ratio for the reaction cannot be calculated. From Chapter 4, a molar ratio of >100:1 is deemed beneficial for efficient silylation of PhCs; though in an unknown matrix, this ratio cannot be guaranteed. Therefore, the analyte compound may not be optimally derivatised prior to analysis, contributing to PhCs being falsely labelled as not present. Increasing the volume of derivatisation reagent to increase the likelihood of a 100:1 ratio will not guarantee the silylation of analyte compounds. As detailed in Chapter 4, the silylation reaction reaches an equilibrium; and whilst increasing the volume of reagent, will likely increase the response -competing reactions, and collision theory indicates that compounds in large concentration (such as fatty acids) are more likely to collide, and react with the derivatisation agent; than compounds in low concentrations (i.e., PhCs). This suggests that increasing the volume of reagent would, therefore, more likely increase the response of the fatty acids, than the response of the PhCs.

Thus, it seems that GCxGC-TOFMS analysis overcomes issues with matrix effects found in LC-MS/MS analysis, though presents new issues itself - primarily with robust derivatisation of unknown samples.

6.3.3.2 Green Chemistry

The main principle of green chemistry is to make chemistry ‘benign by design’ (Sheldon & Norton, 2020). Novel methods should adhere to the underlying 12 principles (see Chapter 3); ensuring environmental impact of the analysis is limited. A comparison between the advanced chromatographic methods with regards to the green chemistry principles was drawn.

Due to the physicochemical properties of the pharmaceuticals, coupled with the ionisation technique, the 14 targeted pharmaceutical analytes were only detected by the LC-MS/MS method when analysed in both positive and negative ion mode. Acidic pharmaceuticals (clofibrac acid, fluvastatin, ibuprofen, ketoprofen, salicylic acid, triclosan and warfarin) were visible only in negative ion mode, whereas more basic pharmaceuticals (atenolol, dapsone, diclofenac, metronidazole, paracetamol, sotalol and carbamazepine) were visible only in positive ion mode. Though, running samples in both positive and negative ion mode doubles analysis time, making the technique less efficient. As LC uses a liquid mobile phase, running samples in both ionisation modes doubles the LC solvent requirement, which increases the cost of analysis and produces more solvent waste. Gas chromatography methods only require one analysis mode per sample (EI ionisation), and uses helium as a carrier gas, eliminating the requirement for solvent, other than for sample preparation. Helium is an inert non-toxic gas, which has little environmental impact (BOC, 2021a), which aligns with the green chemistry principles. The liquid nitrogen used in the thermal modulator is also inert, with no expected adverse ecological effects (BOC, 2021b).

Additionally, matrix effects observed in LC-MS/MS analysis can lead to deviations in mass accuracy. To overcome this, ethylenediaminetetraacetic acid (EDTA) is often added to environmental samples (Gago-Ferrero et al., 2015). EDTA is a chelating agent which binds to mineral and metal ions in the sample preventing reaction with analyte molecules. However, EDTA has some environmental implications, including poor biodegradability (Oviedo & Rodríguez, 2003) and toxicity to fish, daphnia and other aquatic invertebrates (Sigma Aldrich, 2021). Therefore, the addition of this to the samples, even in small quantities would contradict the green chemistry principles of prevention, and safer solvents and auxiliaries (Anastas & Warner, 1998), particularly if a method which can be used without it is available.

Other options for overcoming the matrix effects are to dilute the sample, or ‘clean-up’ the sample. Dilution of the sample in a suitable medium will reduce the concentration injected into the instrument, and although this will reduce the matrix effects, it will also reduce the signal of the peak (concentration is proportionate to peak area/height). As the concentration of the PhCs is unknown in the sample, diluting the sample produces the possible risk of the analyte being <LOD in the analysis. Furthermore, if the solution is diluted in pure or mixed solvent (e.g., 1:1 MilliQ water), this will also increase the

solvent consumption. Sample ‘clean-up’ or preconcentration, using methods such as solid phase extraction (SPE), can reduce matrix effects by removing the interferents. This is often a step undertaken prior to analysis in literature with Oasis HLB, 600 mg being the SPE sorbent and cartridge (Gros et al., 2009; Söregård et al., 2019; Verlicchi et al., 2012). However, this can introduce a level of selectivity to the analysis – as the chosen SPE absorbent may remove some unknown unknown’s (potential analytes) from the sample, when undertaking non-targeted analysis. This goes against the ‘non-targeted’ or at least semi-targeted nature of this study. Adding a sample clean-up step to the sample preparation stage, would increase preparation time, but also increase the solvent consumption, as SPE requires cartridge conditioning, sample wash and elution stages.

Overall GC analysis vastly reduces solvent and energy consumption, and analysis time, with similar sensitivity to the LC analysis. Therefore, with respect to Green Chemistry, GC analysis is more suitable.

6.3.3.3 Identification of Optimal ChromaTOF Tile Parameters

The success of the data processing workflow for non-targeted analysis of biosolid samples is dependent on user identified parameters: tile size, S/N threshold and Fischer-ratio threshold. To identify these input parameters; PhC standards were used. The PhC standards were used to ‘calibrate’ the Tiles software for further analysis of biosolid samples. The use of three PhC concentrations highlights the sensitivity of the ChromaTOF Tile software.

Optimal Tile size was determined by measuring the first- and second-dimension peak width (at base) of four peaks which spanned the entire chromatographic run (D1 and D2 respectively), for the three PhC concentrations (see Appendix D). Two PhCs (ibuprofen mono-TMS and carbamazepine mono-TMS), and the internal standard (phenanthrene) were chosen as reference peaks. Average peak width was calculated to be 7.3 s x 0.1 s (D1 x D2); which corresponds to 3 modulations x 20 spectra when inputted in the Tile software. This Tile size was used for the remainder of the study.

S/N ratio threshold of 10 was determined by averaging the (software calculated) S/N ratios for the 9 PhC peaks at the concentration of 400 µg/L. All S/N ratios were based on TIC; and thus, could be compared. S/N ratios ranged from 4 to 22. The average was calculated to be 10.1; thus, a S/N ratio of 10 was used for the remainder of the study.

The optimal Tile Size and S/N threshold settings were used to identify the F-ratio threshold. F-ratio threshold altered from 5-100, at varying intervals; with number of detected features and PhCs recorded (Table 6-5). At each F-ratio studied, features were identified for all 9 targeted PhC compounds. As these were PhC standards, the only features present should relate to the PhCs and the internal standard (phenanthrene). Though far many more features are present in the analysis (Figure 6.6). These are likely to have arisen from the solvent (ethyl acetate), catalyst (pyridine) derivatisation reagent (MSTFA),

column or septa. As the features are present in all samples, they should be removed in future Tile applications. In total, 491 features should be removed - a list is detailed in the Appendix D.

Table 6-5: F-ratio threshold determination: Number of detected features and identified PhC features at varying F-ratio thresholds.

| F-ratio threshold | Number of Features | Number of PhCs |
|-------------------|--------------------|----------------|
| 5 | 1654 | 9 |
| 10 | 1027 | 9 |
| 20 | 500 | 9 |
| 30 | 318 | 9 |
| 50 | 178 | 9 |
| 100 | 78 | 9 |

The F-ratio threshold of 20 was chosen as the optimal. F-ratios lower than 20, produced a feature relating to phenanthrene (the internal standard), suggesting a significant difference in peak area. On closer inspection (see Figure 6.10), peak areas were similar ($n=6$), with an acceptable RSD calculated (2.5%). Increasing the F-ratio threshold >20 , decreased the number of features detected: which increases the risk of missing large differences in small peaks, which would have negative implications for non-targeted analysis.

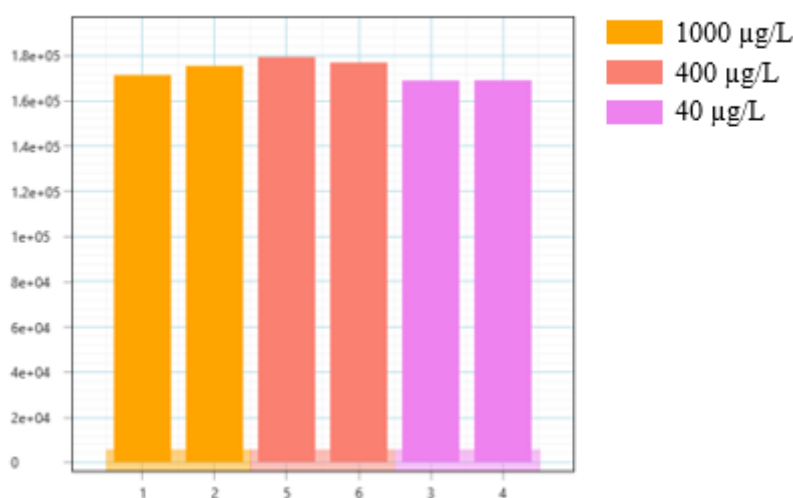


Figure 6.10: Phenanthrene peaks for three concentrations of PhC standards – little intra-class and inter-class difference. X = feature area and Y = sample number (2 replicates per sample) Tile parameters = F-ratio threshold 10; S/N threshold = 10, Tile Size = 3, 20.

6.3.3.4 Calibration of Tile Software

Using the determined optimal Tile parameters (Tile size = 3, 20; S/N threshold = 10 and F-ratio threshold = 20) principal component analysis (PCA) was applied to the identified features. As concentration was the only difference between the PhC standards, the samples were expected to only differ on one principal component (PC). This is shown in Figure 6.11a, where PC1 describes 99.48%

of the variance. PC1 is based mainly on the feature identified as ‘benzeneacetic acid, α -methyl-4-(2-methylpropyl)-, trimethylsilyl ester’ – also known as ibuprofen mono-TMS (corroborated through MS and RT – see Appendix D). PC2 is based mainly on carbamazepine mono-TMS and paracetamol di-TMS, though only describes 0.46% of the variance (Figure 6.11b). Individual F-ratios (i.e., ibuprofen mono-TMS = 7462) suggest little intra-sample variance, and large inter sample variance (Figure 6.11c), which is expected as the concentration is reduced from 1000 $\mu\text{g/L}$ to 40 $\mu\text{g/L}$.

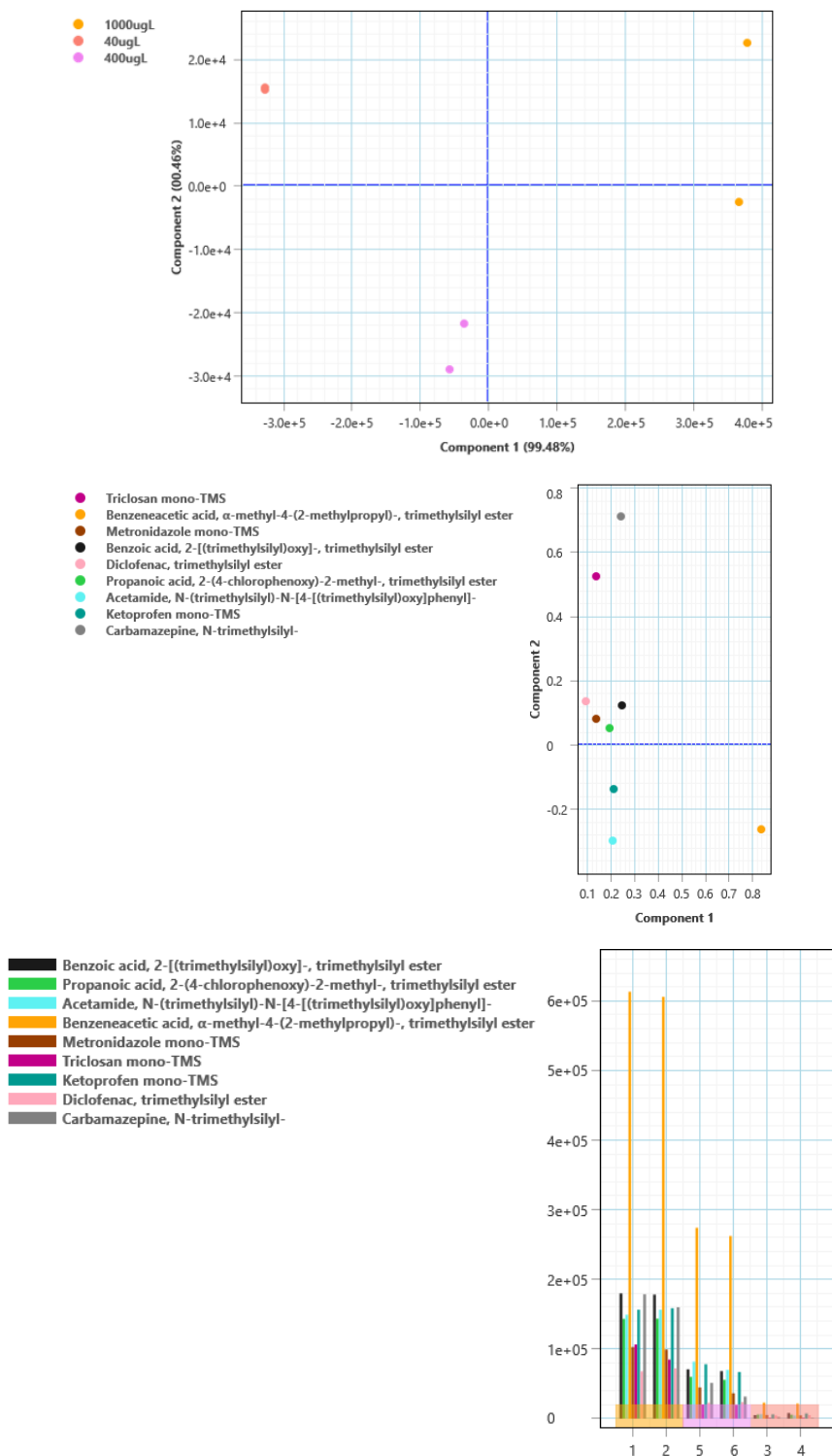


Figure 6.11: Comparison of Pharmaceutical standards at three different concentrations - multivariate analysis and inter and intra-sample variation analysis. Tile Size = 3, 20, S/N ratio = 10, Fischer Ratio = 20. a) Scores plot b) loadings plot c) bar chart of all PhCs

This also highlights the advantages of the ChromaTOF Tile software. At 40 $\mu\text{g/L}$, a PhC peak could not be detected ($<\text{LOD}$) when analysing each individual chromatogram on ChromaTOF. Though, when the chromatogram is divided into tiles, the Tile area is more sensitive to variation, and thus features are elucidated with more ease. For example, a feature is detected for carbamazepine mono-TMS at 40 $\mu\text{g/L}$, though no peak is visible on the EIC contour plot (Figure 6.12).

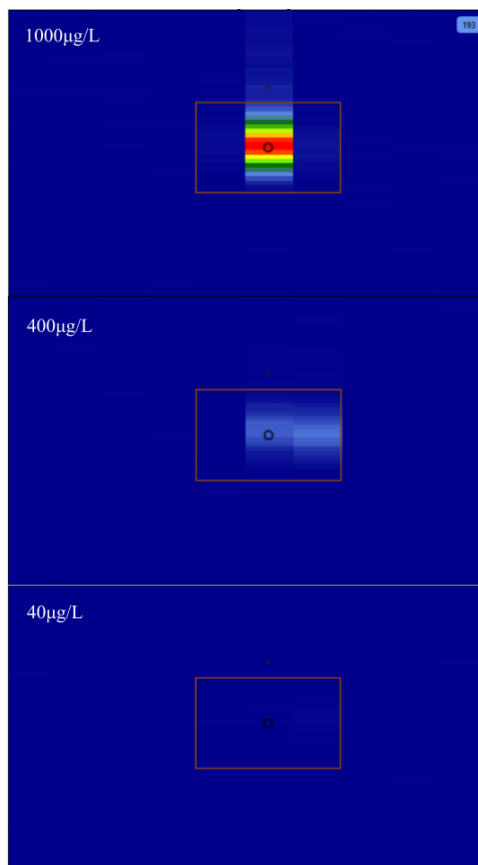


Figure 6.12: Contour plots highlighting carbamazepine mono-TMS peaks (m/z 193) in all three PhC concentrations

6.3.3.5 Robustness

In total, 42 samples were analysed in duplicate on the GCxGC-TOFMS. To prevent bias, the samples were run in a random order over 4 batches (on 4 different days – See Appendix D). Batches were labelled 1, 2, 4, and 5. To ensure all batches were similar and no instrumental variation was observed, all samples were compared using ChromaTOF Tile. Parameters were set to those determined above (Tile size: 3,20; S/N threshold: 10, F-ratio threshold: 20).

Low F-ratios are attributed to low within group (intra-) variation or high between (inter-) group variation. The F-ratio threshold of this analysis was set to 20, which is low. Therefore, intra-batch variation is expected to be as high as inter-batch variation, as samples are not homologous in each batch. This is illustrated in Figure 6.13.

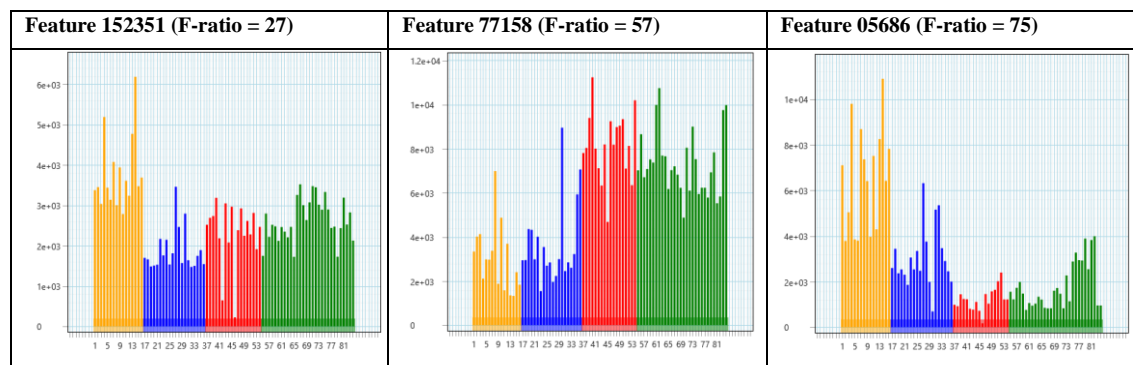


Figure 6.13: Bar charts illustrating feature areas for features over an F -ratio range of 20-81. Differences in feature areas within samples from the same batch suggest variance is intra-batch and not inter-batch. Batch 1 = yellow, batch 2 = blue, batch 4 = red and batch 5 = green.

In total, 754 features were obtained, though this was reduced to 692 features by removal of 62 features identified in the PhC Standards. No features corresponding to PhCs were identified. Data was log-transformed prior to multivariate analysis, where a mean-centred PCA was performed. The scores plot shows slight variation between the batches, where samples from each batch seem to group together (Figure 6.14a), as expected. However, all groupings are close to the origin, which suggests the variation is small.

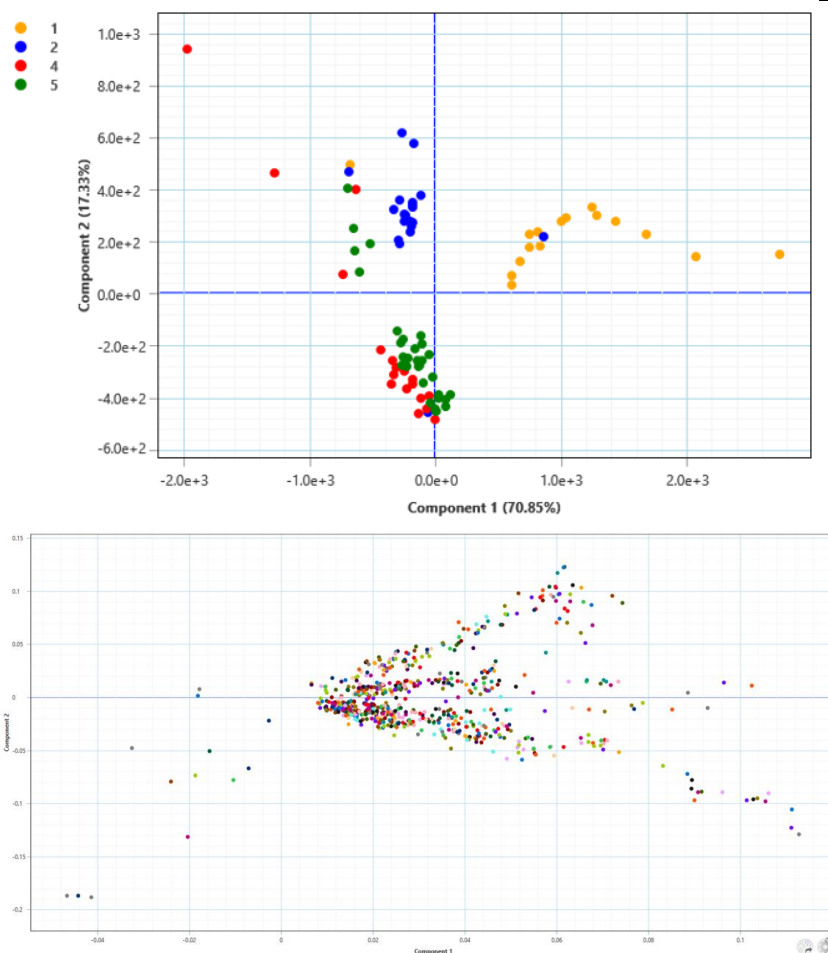


Figure 6.14: Multivariate analysis of samples from different batches. Batch 1 is represented in yellow, batch 2 in blue, batch 4 in red and batch 5 in green. Principal component analysis (PCA) applied to log-transformed data with interferent features removed. Features with F-ratio threshold of 20. a) scores plot of all features b) loadings plot of all features

The plots in Figure 6.14 show that PC1 describes 70.85% of the variance, based primarily on Feature 89943 and Feature 151147; and PC2 describes 17.33% of the variance and is described mainly on Feature 61006 and Feature 75867. These features are located mainly at the top of the chromatogram and are attributed to siloxanes. MS for these features can be found in the Appendix D. Siloxanes are generally linked to column or septa degradation; thus, akin to the features identified in ‘6.3.3.3 Identification of Optimal ChromaTOF Tile Parameters’; these features should be removed in all further analysis.

Sparse partial least squares discriminant analysis (sPLSDA) was also applied to the log-transformed data with the applied F-ratio threshold of 20. sPLSDA is a supervised method used to maximise inter-class variance. It highlights discrimination between variables, giving a more efficient separation, in comparison to PCA (an unsupervised method). Akin to PCA; all batches are grouped around the origin, suggesting the inter-batch variation is minimal (Figure 6.15).

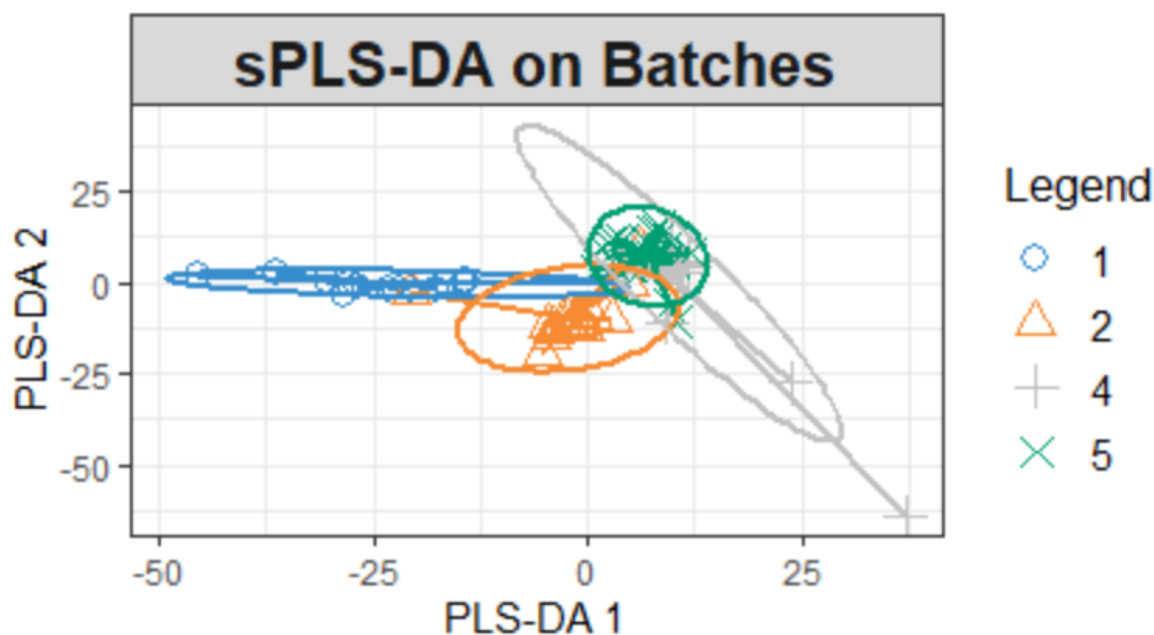


Figure 6.15: Partial least squares discriminant analysis (PLSDA) of log transformed Batch data. F-ratio threshold = 20. Interferent compounds removed. Batch 1 is represented in blue, batch 2 in orange, batch 4 in grey and batch 5 in green.

As little variance was observed between the batches, it suggests that the random run order prevents bias from uncontrollable conditions. Therefore, it is recommended that all future samples should be analysed in a random order.

6.3.3.6 Sensitivity

Biosolids were analysed as both non-spiked and (PhC) spiked samples (250 $\mu\text{g}/\text{kg}$). To determine if the difference in PhC concentration (between spiked vs non-spiked) is picked up by the software; three extractions of each were completed and analysed in duplicate ($n=6$).

Using the parameters determined above; Biosolid 1 generated only 2 features, Biosolid 2 - no features, and Biosolid 3 - 1 feature, when the non-spiked and spiked samples were compared. This would suggest no variance is detected between the non-spiked and spiked samples. Therefore, the F-ratio threshold was reduced to increase the sensitivity of the analysis. At an F-ratio threshold of 5, Biosolid 1 generated 13 hits, 2 of which were identified as target PhCs, though the threshold had to be reduced to 1 to identify 3 PhC peaks in Biosolid 1 and 3 (see Table 6-6).

Table 6-6: Sensitivity analysis of ChromaTOF Tile software: non-spiked vs spiked biosolid samples

| Biosolid Sample | F-Ratio | No of Features | No of Identified PhCs | PhCs identified |
|-----------------|---------|----------------|-----------------------|---|
| 1 | 20 | 2 | 0 | - |
| | 5 | 13 | 2 | Ibuprofen mono-TMS Carbamazepine mono-TMS |
| | 1 | 4048 | 3 | Paracetamol di-TMS Ibuprofen mono-TMS Carbamazepine mono-TMS |
| 2 | 20 | 0 | 0 | - |
| | 5 | 144 | 0 | - |
| | 1 | 2497 | 1 | Triclosan mono-TMS |
| 3 | 20 | 1 | 0 | - |
| | 5 | 931 | 2 | Ibuprofen mono-TMS Carbamazepine mono-TMS |
| | 1 | 4905 | 3 | Salicylic acid di-TMS Ibuprofen mono-TMS Carbamazepine mono-TMS |

As shown previously (see 6.3.3.4 Calibration of Tile Software) differences in PhCs are observed when PhC standards are analysed. The identification of only 3 PhCs (out of 9) in Biosolid 1 and 3 at the F-ratio threshold of 1 would suggest that the complex matrix may be influencing method sensitivity. Only one feature was identified in Biosolid 2, which further verifies this theory. The matrix components may differ between Biosolids, and thus derivatisation of different analytes may take place. The increased number of compounds which can undergo silylation will reduce the sensitivity of the method as PhCs will compete with the other compounds for MSTFA.

Regardless, PCA was applied to the features produced for Biosolid 1 with an F-ratio threshold of 5 and 1 (Figure 6.16). A difference can be observed between samples at an F-ratio of 5, though the non-spiked and spiked samples do not group closely to another. All samples are close to the origin, which suggests little inter-sample variance. At an F-ratio threshold of 1; no pattern is observed, and no groups can be identified.

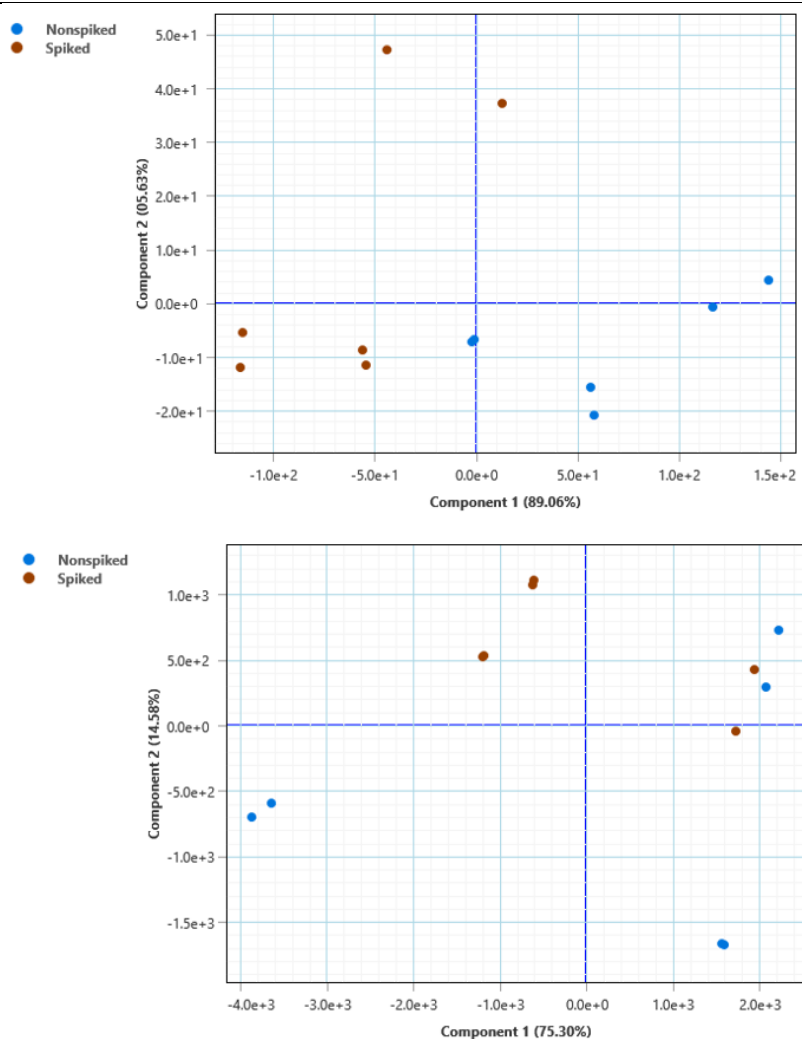


Figure 6.16: PCA analysis for non-spiked vs spiked Biosolid 1 samples a) scores plot for F-ratio threshold 5 b) scores plot for F-ratio threshold 1. No grouping suggests little variance between the samples.

The F-ratio thresholds of 5 and 1 are very low, suggesting either high intra-sample or low inter-sample variance. To evaluate this, bar charts of identified PhC features were produced (Figure 6.17). Inter-sample variance is observed - spiked samples (brown) generally giving larger bars than non-spiked samples (blue). Intra-sample variance is also observed. The bar heights for replicates of the spiked and non-spiked samples vary greatly. A larger difference in bar height would have been expected between the non-spiked and spiked samples. Therefore, with such low feature F-ratios, it is more likely that this is attributed to intra-sample variance. This intra-sample variance was also illustrated in the majority of features detected in the three biosolid samples (see Figure 6.17d). This suggests that the method is not sensitive enough to differentiate between spiked and non-spiked samples, though indicates repeatability of the extraction method.

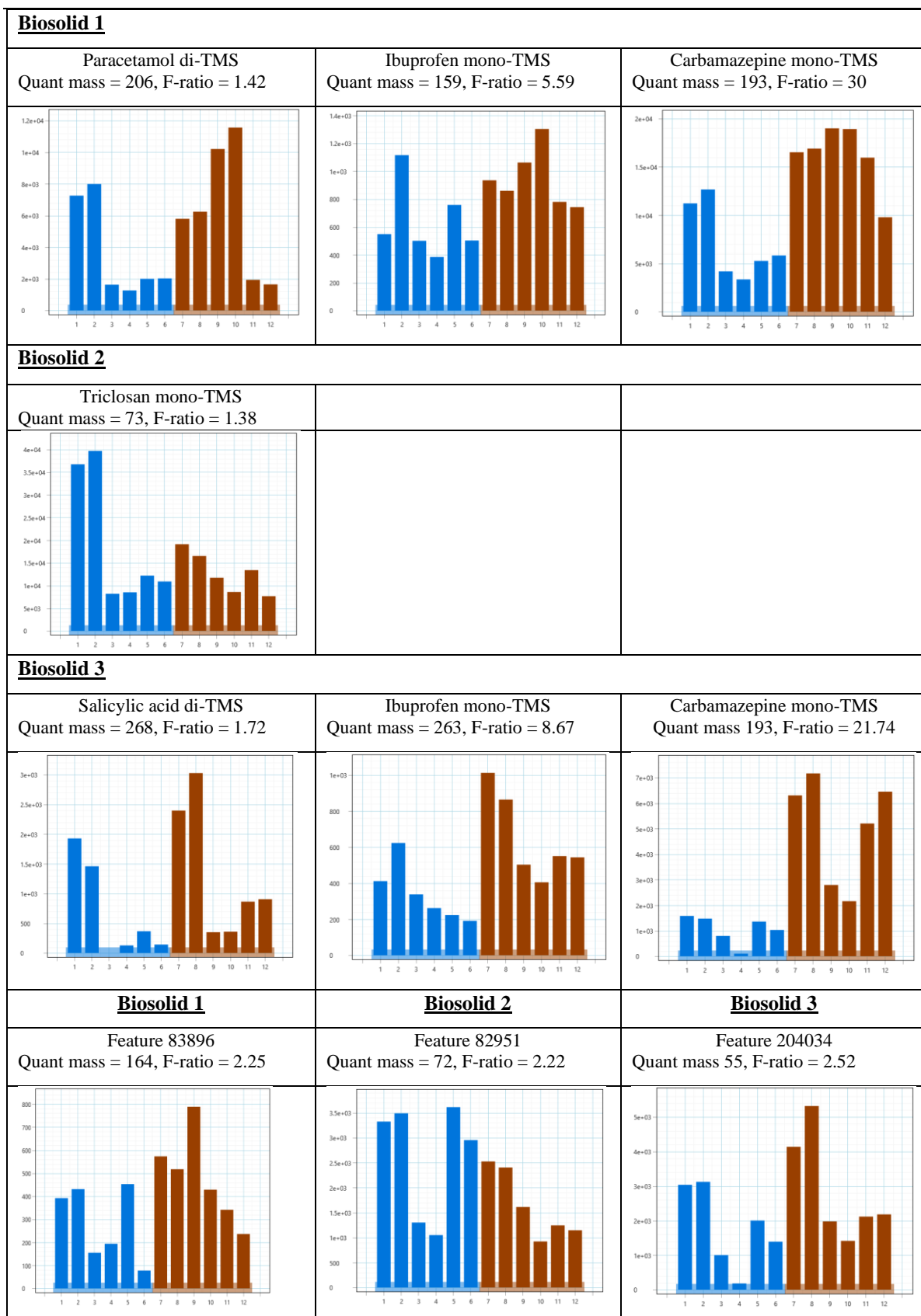


Figure 6.17: Comparison of non-spiked (blue) and spiked (brown) samples for Identified PhCs in a) Biosolid 1 b) Biosolid 2 c) Biosolid 3 and d) Random Features from Biosolid 1, 2 and 3. F-ratio threshold of 1. Charts suggest intrasample variation attributes to the variance more than inter-sample variance.

6.3.3.7 Repeatability

In this study, biosolid pellets were ground prior to weighing, to increase the surface area for extraction, but also to ensure a homogenous sample was analysed. It was hypothesised that biosolid pellets which belong to the same batch (Biosolid 1, 2 or 3) would have similar characteristic load. To determine if biosolid pellets were homogenous; 6 individual pellets of Biosolid 1 were extracted and analysed using the optimised method, before comparison of raw data via ChromaTOF Tile. Each pellet weighed less than 1.0 g (optimised mass); and so, the mass was reduced to 100 mg.

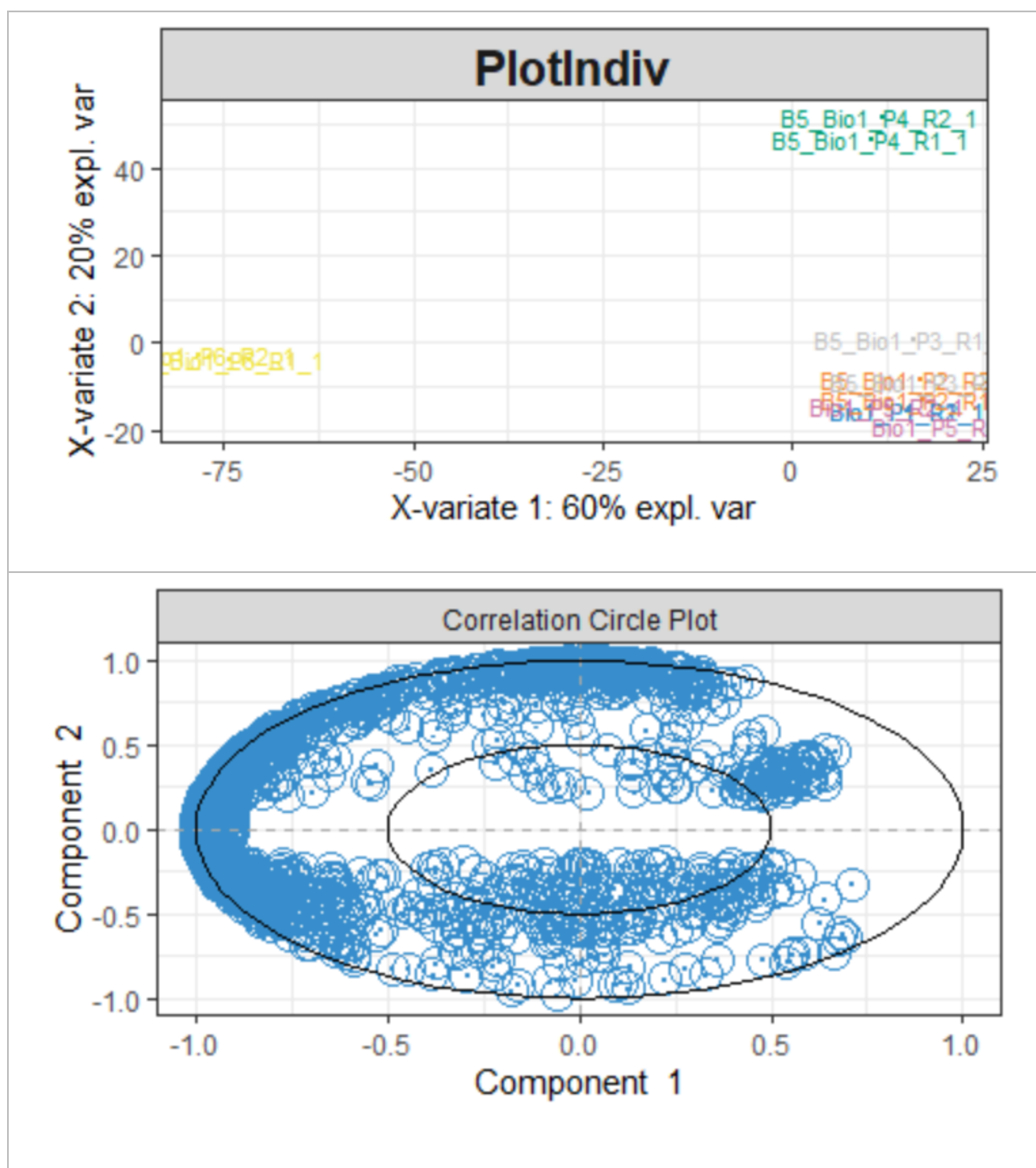


Figure 6.18: Homogeneity of Pellets - Biosolid 1: a) SPLSDA scores plot b) SPLSDA loadings plot

With an F-ratio threshold of 20, 3032 features were observed for the 6 pellets of Biosolid 1. A distinct difference between the pellets is visible when sPLSDA was applied to the data (Figure 6.18a). Four Pellets (1, 2, 3 and 5) group together on the scores chart, though Pellet 6 and Pellet 4 group further away from the other biosolid pellets. This indicates differences in the load of individual pellets which is corroborated by bar charts of four features picked at random (Figure 6.19). The sPLSDA loadings chart shows identified features are distributed mainly to the left-hand side of the chart (Figure 6.20) - suggesting these features are primarily found in Pellet 6. However, the top 2 features which influence the sPLSDA were identified as Feature 53649 and Feature 80729. Bar charts produced for these features indicate that they are more prominent in Pellet 4, and so explain the separation on the y-axis (Figure 6.19). All features present in Figure 6.19 have individual F-ratios of >400 which suggests variance is attributed to between pellets, and pellets are not homogenous.

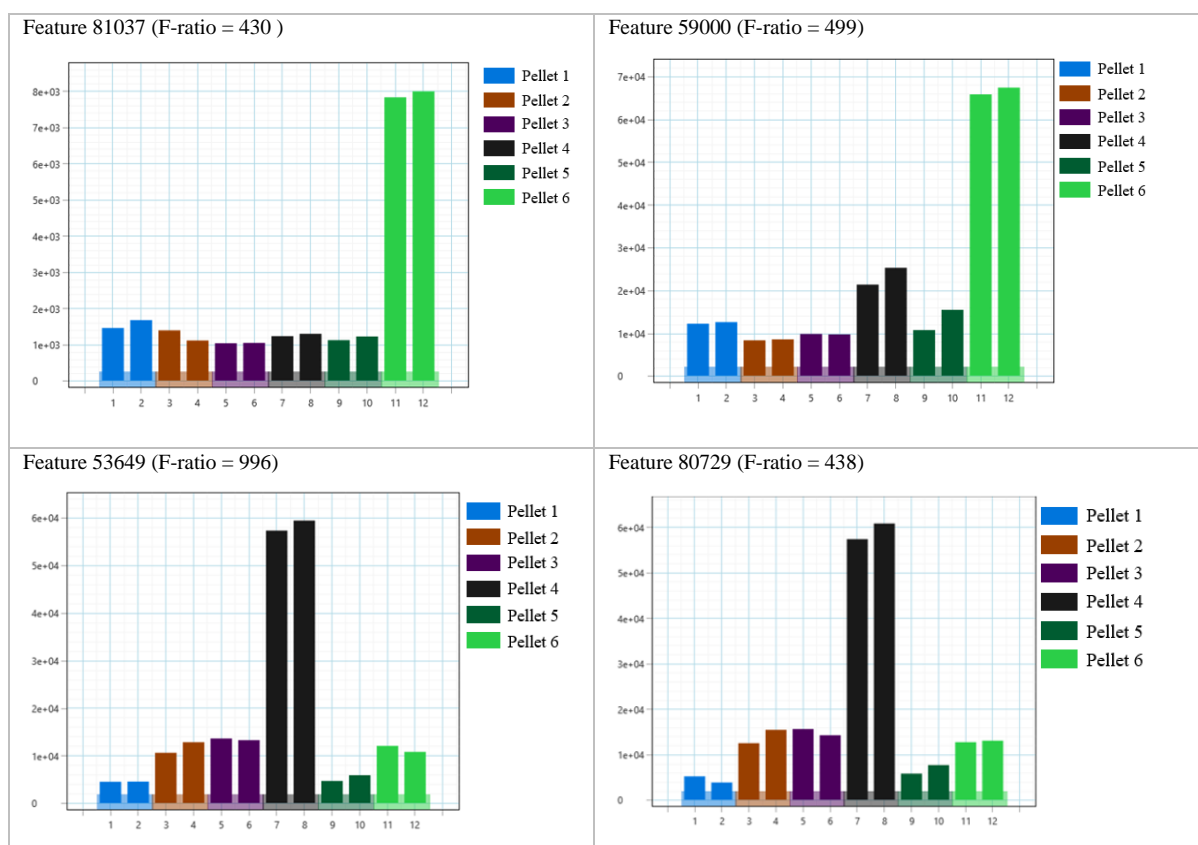


Figure 6.19: Homogeneity of Pellets – Biosolid 1: Bar charts describe inter-pellet variance.

The analysis was repeated for 6 pellets of all three biosolid samples. At the F-ratio threshold of 20, 783 features were produced. A distinct difference between Biosolid samples (1, 2 and 3) was observed when sPLSDA was applied, suggesting the biosolid loads differs between the sample (Figure 6.20). Biosolid 1 pellets group the closest together: suggesting the least variance between the individual pellets. Pellets for Biosolid 2 and 3, have a larger separation between the pellets suggesting a greater intra-group

variance. This was confirmed using PCA; where a separation was observed between pellets for both Biosolids (see Appendix D).

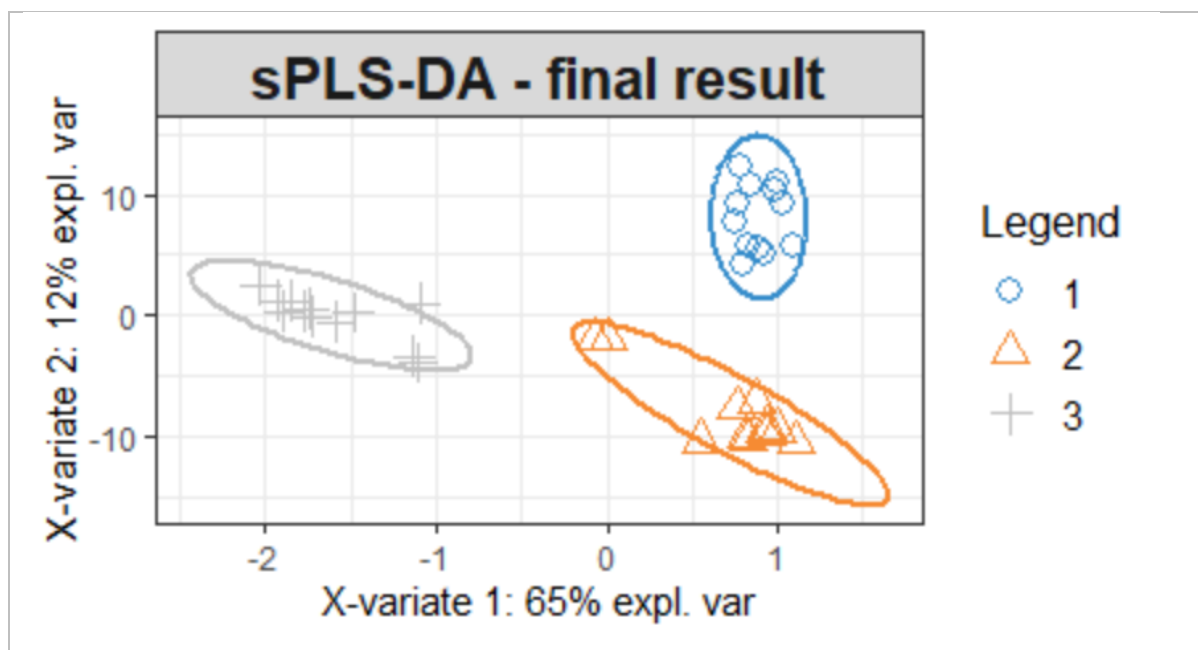


Figure 6.20: Comparison of pellets from 3 different biosolid samples ($n=6$). sPLSDA score plot suggests variance between the Biosolid samples, and between pellets of the same sample.

Therefore, as the F-ratios attributed with the identified features in Biosolid 1 suggest large variance between pellets of the same biosolid, and differences in pellets is observed for all three biosolid samples - it is recommended that several pellets are ground together, prior to extraction, to produce a homogenous sample.

6.3.3.8 Selectivity

Analysis of the Biosolid Pellets indicated a difference between the three Biosolid samples. To determine if the biosolid load was similar within the three biosolid samples, a comparison was made of the non-spiked samples for each of the biosolids. The composite sample (CBE - a mixture of the 3 biosolid samples) was added as a comparison.

With an F-ratio of 20, 156 features were produced. This is very low, as over 25,000 peaks were detected for each biosolid. sPLSDA analysis was conducted, where a difference between the three biosolids was observed. A clear separation of Biosolid 1 from the other Biosolids is obtained - suggesting Biosolid 1 differs significantly from the other samples (Figure 6.21a). Biosolids 2 and 3 group more closely together, suggesting less variation between these biosolids. Further investigation (Figure 6.21b) indicates that the separation is based primarily Feature 04871. This feature is prominent in Biosolid 2 samples, and the CBE samples (Figure 6.21c), which explains the grouping on the scores plot. Removal

of this Feature does not have a large effect on the Biosolid groupings, suggesting that variance is identified between the three biosolid samples.

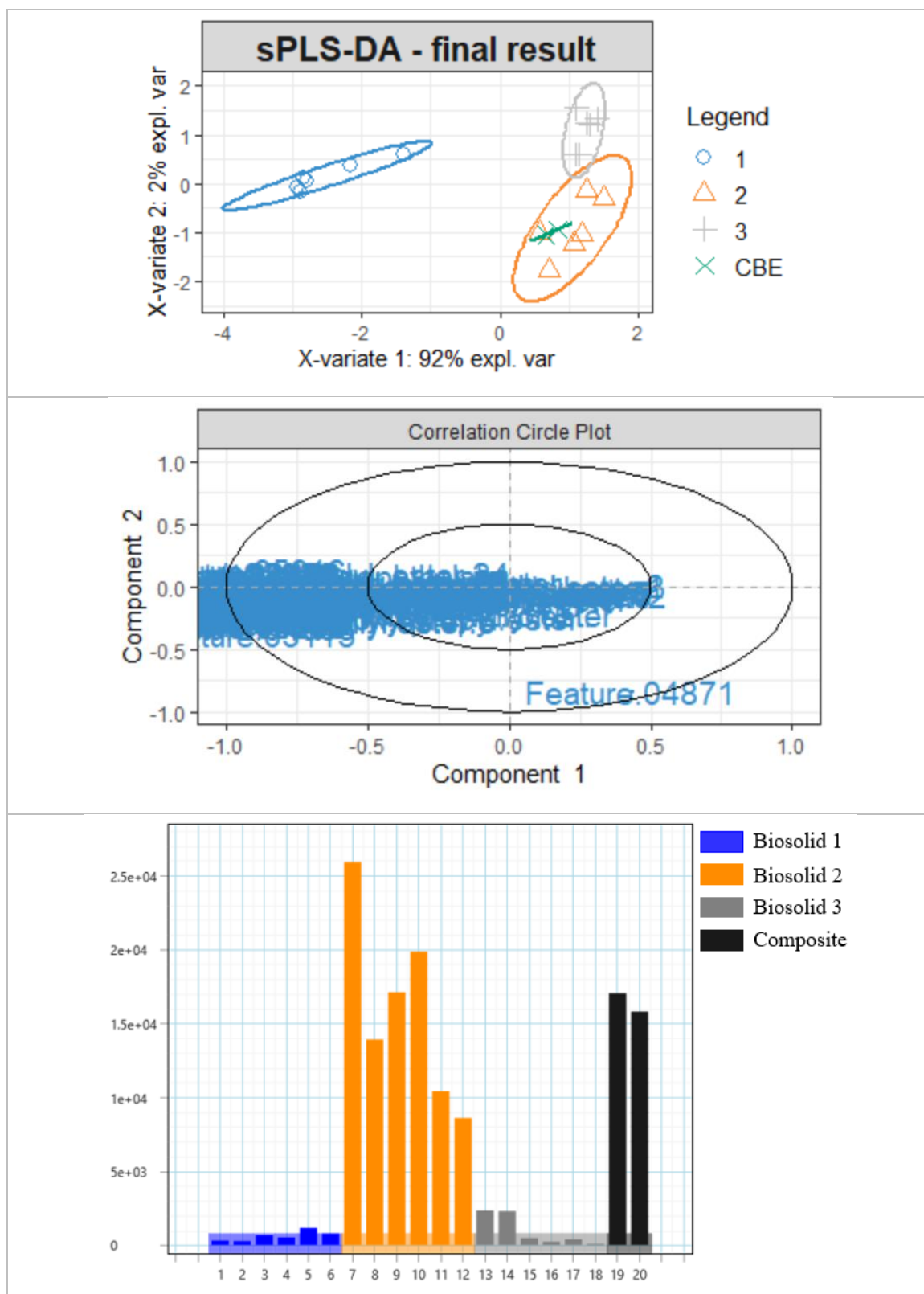


Figure 6.21: Comparison of Biosolids (Biosolid 1, 2 and 3) a) scores plot from PCA b) scores plot from sPLSDA c) bar charts for Feature 04871 (individual F-ratio = 29).

Therefore, overall, a difference between three different biosolid samples was observed through the use of ChromaTOF Tile. Repeatability, selectivity, and robustness were sufficient for the method, though issues with sensitivity were observed.

6.4 Conclusion

In conclusion, the GCxGC-TOF-MS method successfully identified 5 targeted PhCs within biosolid samples. The reversed phase column set-up provided efficient separation of PhCs, preventing co-elution with derivatised fatty acids. The GCxGC-TOFMS method identified less PhCs in the non-spiked biosolids than the LC-MS/MS method, though this was expected due to the sensitivity of the tandem MS detector attached to the LC. Matrix effects were reduced with GC analysis, though issues with derivatisation of unknown samples were observed. Overall, the GCxGC method was comparable to LC-MS/MS method, though reduced solvent and energy consumption. ChromaTOF Tile was used to explore non-targeted analysis of three Biosolid samples. The method was deemed sufficient in terms of repeatability, robustness, and selectivity, though sensitivity was an issue. Regardless, differences between Biosolid samples were observed, with Biosolid 1 differing greatly from Biosolid 2 and 3. In future analysis, it is recommended that samples are homogenised prior to extraction and analysed in a random order.

Chapter 7: Conclusions and recommendations

7.1 Restatement of Research Objectives

7.1.1 Research Aims and Objectives

The aim of this research is to investigate the use of ultrasonic assisted techniques and a two-dimensional gas chromatography method in the non-targeted characterisation of pharmaceuticals in biosolids, with respect to Green Chemistry principles. To achieve the aims of this project, the following objectives were identified:

- To evaluate and optimise a derivatisation method suitable for a range of pharmaceutical compounds.
- To develop and evaluate the novel use of a sonotrode device for optimal ultrasonic assisted extraction and derivatisation of pharmaceutical compounds in biosolid samples.
- To evaluate the use of a two-dimensional gas chromatography method compared with the ‘gold standard’ liquid chromatography method for analysis of pharmaceutical compounds in biosolids.
- To investigate the use of two-dimensional gas chromatography method with an associated data processing workflow for non-targeted characterisation of pharmaceuticals in biosolid samples.

7.2 Summary Details of Key Findings for Chapter 4 to Chapter 6

7.2.1 Understanding and optimising conventional silylation for exhaustive derivatisation of pharmaceutical compounds

A derivatisation method suitable for derivatising a range of pharmaceuticals (PhCs) prior to gas chromatography mass spectrometry (GC-MS) analysis was investigated. Silylation was found to produce desired trimethylsilyl (TMS) derivatives, more compatible with GC-MS analysis - increasing the number of detected PhC compounds. Evaluation of derivatisation reagents, indicated that silylation using N-Methyl-N-(Trimethylsilyl)trifluoroacetamide (MSTFA) was found to be more effective, producing a greater molar ratio, with smaller volume of reagent. Pyridine was found to catalyse the reaction, though competing reactions indicated derivatisation was hindered for some compounds when analysed in a mixture. The silylation reaction was deemed to be in dynamic equilibrium, where increasing the MSTFA volume, increased the TMS response. Conventional silylation conditions (time and temperature) were optimised through design of experiment (DOE). Derivatising samples by heating to 50 °C for 40 mins maximised PhC derivative response and minimised PhC parent response; with acceptable relative standard deviations (RSDs <10%) obtained across five targeted PhCs.

7.2.2 Investigation into the use of ultrasonication for the extraction and derivatisation of pharmaceutical compounds from biosolid samples

The application of ultrasound to facilitate extraction and derivatisation of PhCs from biosolid samples was investigated. The novel use of a sonotrode was found to effectively apply ultrasound to samples without the risk of contamination or sample loss. A suitable ultrasonic assisted extraction (UAE) and derivatisation (UAD) method was designed to facilitate the extraction and derivatisation processes. Absolute recoveries of spiked PhCs ranged from 8-64%, with RSDs ranging from 5-29% for the UAE method. The optimised UAD method showed no statistically significant difference in response to the optimised oven method (Chapter 4); though RSDs were far higher (~30%). This suggests that the stability of TMS derivatives may be lower with the application of ultrasound. The optimised method showed major reductions in derivatisation time (99% decrease), overall sample preparation time (37% decrease) and solvent consumption (97% decrease) when compared to the method of Gago-Ferrero *et al.*, and the optimised oven derivatisation method in Chapter 4. Four PhCs were identified in non-spiked Biosolid samples (salicylic acid, ibuprofen, paracetamol, and carbamazepine) extracted using the optimised method, though co-elution with fatty acids prevented the detection of some PhCs. GC-MS was therefore deemed unsuitable for non-targeted analysis of PhCs in biosolid samples.

7.2.3 Application of advanced chromatographic techniques in the non-targeted analysis of pharmaceutical compounds in biosolid samples

Characterisation of PhCs in three biosolids through advanced chromatographic techniques was investigated. Two-dimensional gas chromatography coupled to a time-of-flight MS detector (GCxGC-TOFMS) overcame issues with co-elution observed with one dimensional GC-MS. Salicylic acid, paracetamol, ibuprofen, triclosan and carbamazepine were identified in biosolid samples using the optimised GCxGC-TOF MS method. Comparison to the 'gold standard' liquid chromatography tandem mass spectrometry (LC-MS/MS) method, highlighted similarities in PhC detection, though illustrated differences in sensitivity, however this is likely attributed to the high resolution orbitrap detector used with LC. Non-targeted screening of biosolid samples was applied using a tile-based data processing workflow. Repeatability, selectivity, and robustness were successfully validated, though limitations in method sensitivity were observed. Differences in the composition of the three biosolids was illustrated, with inter-pellet variance also observed. To increase repeatability and minimise bias, it is recommended that samples be homogenised through grinding prior to extraction and analysed in a random order.

7.3 Conclusions and Recommendations for Future Work

In literature, liquid chromatography (LC) based methods are considered the ideal technique for analysis of PhCs in complex matrices, such as wastewater and sludge. However, this thesis showcases the applicability of gas chromatography as a 'greener' alternative to the traditional methods. The

development of a non-targeted method for identification of PhCs in biosolid samples is described in this thesis; using ultrasound assisted extraction and derivatisation techniques, and semi-targeted data analysis.

This thesis introduces several novelties in the field of analytical and environmental/Green chemistry. First, is the use of molar ratio as a tool for silylation. Although it is widely acknowledged that a 2:1 ratio is required for silylation, no study has attributed their reagent choice to molar ratio, instead basing the reagent choice solely on the yield of TMS derivative. This thesis introduces the idea that the reaction reaches a dynamic equilibrium, where increasing the volume of reagent (thus, increasing the molar ratio), will push the equilibrium to the product side, and a proportional increase in TMS derivative will be observed. Therefore, increasing the volume of derivatisation reagent will always give an increased response, though the number of atoms wasted will also increase tremendously. Calculating the molar ratio would reduce the associated atom wastage; aligning with the Green Chemistry principles of 'Prevention', 'Atom Economy' and 'Reduce Derivatives'. Therefore, it is recommended, where possible, to calculate the molar ratio of the proposed reaction to improve atom economy. It is likely that a volume of 100 μL MSTFA will provide a molar ratio of $> 100:1$; where the reaction is facilitated though waste is reduced. Although, this thesis acknowledges that calculating the molar ratio in non-targeted analysis is near impossible, as the content of the sample is not known. In this instance, it is recommended that three volumes of reagent are trialled (e.g., 50 μL , 100 μL , 150 μL), and three analyte responses compared at the three volumes. An increase in TMS response is expected, though differences in number and location of derivatised peaks should be taken into consideration, as this will highlight any changes caused by the increased reagent volume. The lowest acceptable volume should always be used.

This thesis also introduces the use of a sonotrode device, as a means of facilitating reactions and reducing sample preparation time. The sonotrode has the advantage of uniform indirect sonication, without the possibility of sample loss or contamination, or energy loss associated with traditional sonication techniques. The device was used to implement ultrasound in extraction (UAE) and derivatisation (UAD); showing to facilitate both sample preparation stages. Low recoveries (8-64%) and high RSDs (5-29%) are thought to be attributed the stability of the TMS derivative post-sonication. In both techniques, the optimisation was based on TMS yield. The stability of the TMS derivative was shown to reduce when optimised sonication parameters were applied, thus large RSDs were obtained. Therefore, it is recommended that the optimisation of the UAD method be repeated, with RSD as the desired response. This would reduce the variation attributed to the UAD method and identify sonication parameters which increase the stability of the TMS derivatives.

Additionally, in this study, ultrasound is only applied to one sample at a time, though the sonotrode has the ability to hold up to five samples. Therefore, it is recommended that the possibility of multi-sample

sonication is investigated for UAE and UAD. Provided the ultrasound applied to all vials is uniform, recoveries are acceptable, and optimised RSDs are <10%; the sample preparation time could be further reduced by up to 5x. This would also reduce costs and energy consumption – aligning with Green Chemistry Principle of “Design for Energy Efficiency”.

Lastly, this thesis introduces the use of a tile-based data processing workflow (using ChromaTOF Tile) for the non-targeted characterisation of biosolid samples. The method allows for a one-step data analysis workflow, reducing data processing time and highlighting inter and intra-sample variance through easily applied multi-variate analysis. However, issues with sensitivity were observed with the tile-based approach in Chapter 6, with no significant difference detected between non-spiked and spiked biosolid samples (14 PhCs at 250 µg/kg). Therefore, it seems that large differences in small peaks may not be detected, though small differences in large peaks are. This causes issues for PhC identification, as these compounds are generally at low levels (ng/kg). Further analysis into the F-ratio threshold using a null-distribution approach may increase the sensitivity of the analysis by increasing the number of true-positives and reducing the number of false-positive results (Watson et al., 2016). Though it is recommended that this should be conducted after the derivatisation method has been optimised in relation to RSD (Chapter 5); as differences in the derivatisation (dependant on other compounds in the sample) may make multi-variate comparison difficult.

Additionally, it is recommended that the removal of fatty acids be investigated. The fatty acids caused two issues in this study: co-elution with PhC peaks, and competition for derivatisation reagent. Co-elution issues were resolved with the application of the second-dimension separation associated with GCxGC, though the derivatisation competition remains an issue. Ideally, removal of these interferents prior to derivatisation would prevent this issue, either during extraction or as a sample clean-up step. An interesting possibility could be the use of QuEChERs (Quick, Easy, Cheap, Effective, Rugged and Safe) as the extraction technique; which has shown to overcome issues with fatty acids when analysing pesticides in pecan nuts (Barci et al., 2020). Benefits of the technique include the reductions in extraction time, extraction costs and solvent use in comparison to traditional techniques (e.g., Soxhlet or liquid-liquid extraction), thus aligning with the Green Chemistry principles discussed in this thesis. QuEChERs utilises a dispersive solid phase extraction (d-SPE) clean-up step which may add bias to the analysis and thus a reduction from non-targeted to semi-targeted analysis may be observed. This is a limitation which has to be taken into consideration. In this thesis, no clean-up step was applied to encapsulate as many PhCs as possible, though the addition of an SPE or d-SPE step post UAE, may provide additional benefits, such as a reduction in matrix interferents; and thus, the addition of a sample clean-up stage could be considered. It would be interesting to compare a QuEChERs method to the optimised UAE method, in terms of extraction yield, recovery and precision, but also in sample preparation time, solvent consumption and energy consumption.

With the addition of these suggestions, the method would be suitable for monitoring of emerging PhCs in biosolid matrices. Non-targeted characterisation of these samples would allow for elucidation of a pathway of recalcitrant PhCs, from source to the environment, with a one-step visual comparison. Environmental researchers could use this method to study the presence, recalcitrance, root-uptake, and possible bioaccumulation of PhCs in the environment after biosolid application as the method could be used for a variety of solid matrices, including untreated/treated sludge, soil, sediment, or a range of animal faeces. The findings could be used by monitoring bodies like SEPA, to help implement new legislation governing the removal and release of PhCs by WWTPs. This would be extremely beneficial for point-source locations such as hospitals, where the addition of further treatment to remove high concentrations of PhCs is desirable. The developed method could also be expanded to include a large range of analyses, by altering the extraction solvent, and GCxGC chromatographic conditions. It would be interesting to apply the developed method to other emerging contaminants such as personal care products; or polyaromatic hydrocarbons (PAHs) by changing the extraction solvents from water: methanol, to more non-polar solvents like hexane or cyclopentyl-methyl ether (CPME). Altering the extraction solvents will alter the extracted analytes, adapting the focus of the study. Thus, this research could be used as the basis for monitoring of many emerging organic contaminants.

Appendix A – Chapter 3

Electron impact ionisation (EI)

Table S8-1: Common loss fragments from a molecular ion - electron impact ionisation

| Loss of x a.m.u. | Radicals/Neutral Fragments Lost | Interpretation |
|------------------|---|---|
| 1 | H [•] | Often major ion in amines and aldehydes |
| 15 | CH ₃ [•] | Often lost from quaternary carbons |
| 17 | OH [•] or NH ₃ | - |
| 18 | H ₂ O | Often lost from 2° or 3° alcohols |
| 28 | CO | Ketone or acid |
| 29 | C ₂ H ₅ [•] | - |
| 32 | CH ₃ OH | Methyl ester |
| 35/36 | Cl [•] /HCl | Chloride |
| 44 | CO ₂ | Ester |
| 45 | COOH [•] | Carboxylic acid |
| 60 | CH ₃ COOH | Acetate |
| 73 | (CH ₃) ₃ Si [•] | TMS |
| 77 | C ₆ H ₅ [•] | Benzene |
| 90 | (CH ₃) ₃ SiOH | TMS |

Electrospray ionisation (ESI)

Table S8-2: Common observed additions to molecular ions, forming adducts in ESI

| Addition to + ^{ve} ion | Radicals/Neutral Fragments Lost | Interpretation |
|------------------------------------|--|--|
| 18 | NH ₄ ⁺ | Occurs with ammonium in mobile phase |
| 20 | H ⁺ /K ⁺ or Ca ²⁺ | Doubly charged ion |
| 22 | Na ⁺ | Forms without the presence of Na in the mobile phase |
| 32 | CH ₃ OH | Methanol in the mobile phase |
| 39 | K ⁺ | Forms without K in the mobile phase, although less common than Na ⁺ |
| 41 | CH ₃ CN | Acetonitrile in the mobile phase |
| 54 | CH ₃ OH/Na ⁺ | Methanol in the mobile phase |
| 63 | CH ₃ CN/Na ⁺ | Acetonitrile in the mobile phase |
| Addition to - ^{ve} ion | Radicals/Neutral Fragments Lost | Interpretation |
| 35 | Cl ⁻ | - |
| 46 | HCOOH | Formic acid in the mobile phase |
| 60 | CH ₃ COOH | Acetic acid in the mobile phase |

Appendix B – Chapter 4

2.2 Pharmaceutical Compound Selection

The 14 representative compounds were chosen based on LogP and MW; from a list of over 150 PhCs. These compounds can be found at the link below.

https://gla-my.sharepoint.com/:x:/g/personal/k_fell_1_research_gla_ac_uk/EU1oLVtmrxRAoV3iaVfnH9ABR42SWdLmProyGa1FBBGyPw?e=xODo8s

2.4.2 Derivatisation Procedure



Figure S9.1: Vials used for GC derivatisation. a) 2ml GC vial b) 200µl vial insert and c) 300µl sonication vial (Thermo Fischer Scientific Inc., 2022).

2.5.1 Dilution Factor Calculation – Worked Example

To a 200µl sample, varying volumes of derivatisation reagent are added. These volumes are 10, 20, 50, 100µl. The final volume of each sample is therefore 210, 220, 250 and 300µl, respectively. The dilution factor for the first sample (addition of 10µl of derivatisation reagent) is calculated as follows:

$$\text{Dilution Factor} = \frac{\text{Total volume of sample } (\mu\text{l})}{\text{Total volume of greatest dilution } (\mu\text{l})}$$

$$\text{Dilution Factor} = \frac{210 (\mu\text{l})}{300 (\mu\text{l})}$$

$$\text{Dilution Factor} = \frac{210 (\mu\text{l})}{300 (\mu\text{l})}$$

$$\text{Dilution Factor} = 0.7$$

Table S9-1: Calculation of dilution factor - worked example.

| Volume of Derivatisation Reagent Added (μl) | Total Sample Volume (μl) | Calculated Dilution Factor |
|--|---------------------------------------|----------------------------|
| 10 | 210 | 0.70 |
| 20 | 220 | 0.73 |
| 50 | 250 | 0.83 |
| 100 | 300 | 1.0 |

3.1.1 Solvent Comparison

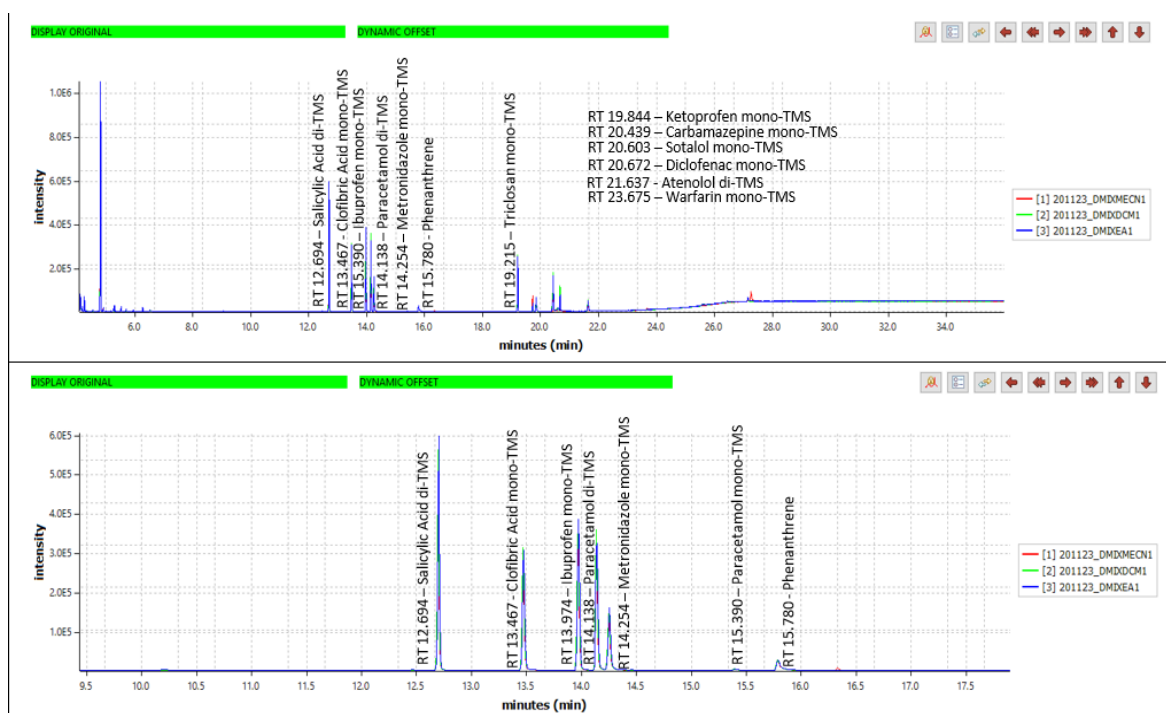


Figure S9.2: Comparison of reconstitution solvents, with identified PhCs and RTs. A) full chromatogram, b) magnified chromatogram showing RT 9.5 to 18 mins. Ethyl acetate and dichloromethane had comparable results, whereas acetonitrile had consistently lower peak area ratios and incomplete silylation of diclofenac. Ethyl acetate was chosen as the reconstitution solvent, due to its increased performance and decreased toxicity when compared to dichloromethane.

3.1.3 Log Transformation of Phenanthrene Data

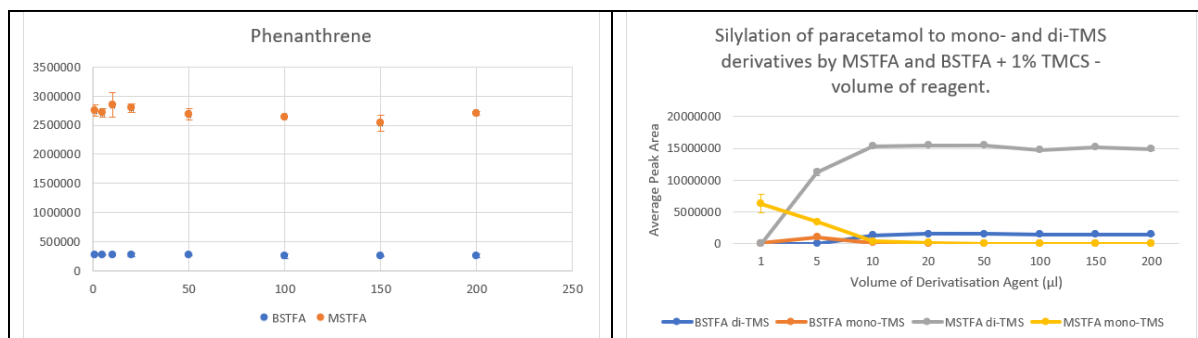


Figure S9.3: Peak areas for a) phenanthrene and b) paracetamol mono- and di-TMS derivatives for MSTFA vs BSTFA + 1% TMCS prior to log transformation. Peak areas were significantly lower for all peaks for BSTFA + 1% TMCS.

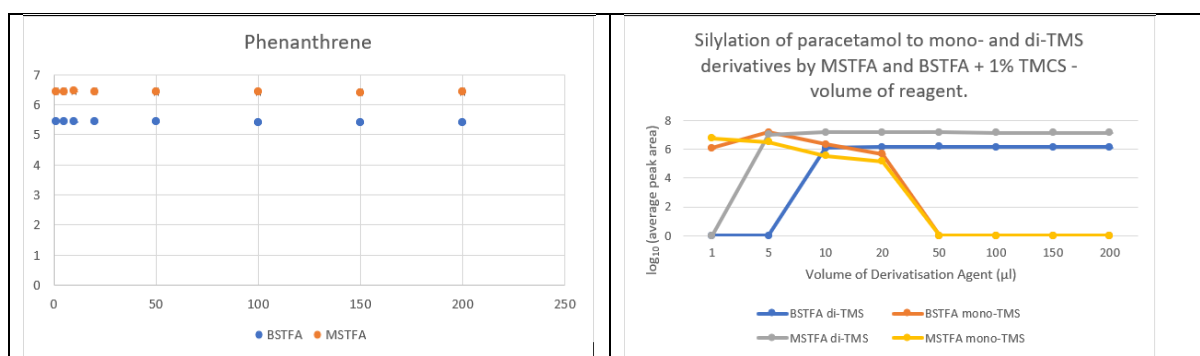


Figure S9.4: Peak areas for a) phenanthrene and b) paracetamol mono- and di-TMS derivatives for MSTFA vs BSTFA + 1% TMCS after log transformation. Peak areas were similar and more appropriate for comparison.

3.2.1 Comparative study of silylation reagents: BSTFA + 1% TMCS vs MSTFA

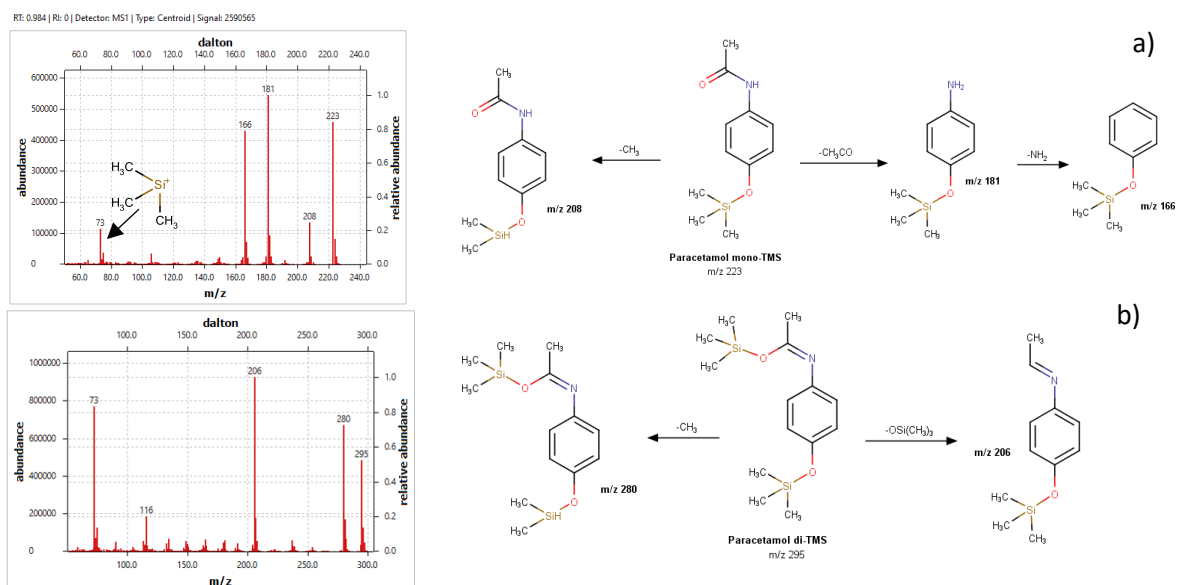


Figure S9.5: Observed mass spectra and related fragmentation patterns for paracetamol a) mono-TMS and b) di-TMS. Fragmentation patterns determined by the mass spectrometry. Beta-fragmentation for di-TMS suggesting silylation of the oxygen on the amide group, as reported by Caban and Stepnowski (Caban & Stepnowski, 2018). Characteristic ion at m/z 73 is highlighted in a) which corresponds to the trimethylsilyl (TMS) group.

3.2.1.1 Molar Ratio

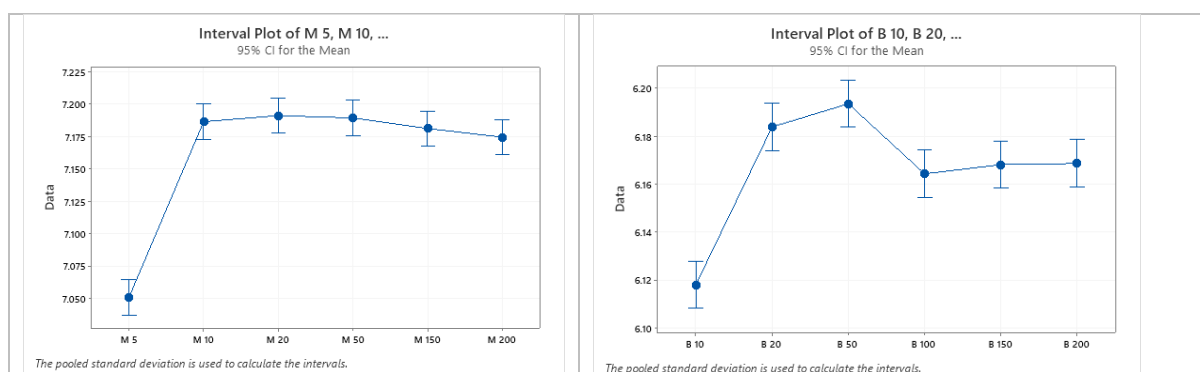


Figure S9.6: Interval plot for ANOVA analysis of a) MSTFA and b) BSTFA + 1% TMCS. ANOVA concluded that a plateau was formed from 20 μl for MSTFA and 150 μl for BSTFA + 1% TMCS ($n=3$, p -value = 0.05).

Atom Economy

Highlighted in red are the reactant atoms which make up the desired product (paracetamol di-TMS - blue), and those in black are wasted.

MSTFA reaction:



BSTFA reaction:



3.2.3 Addition of a catalyst

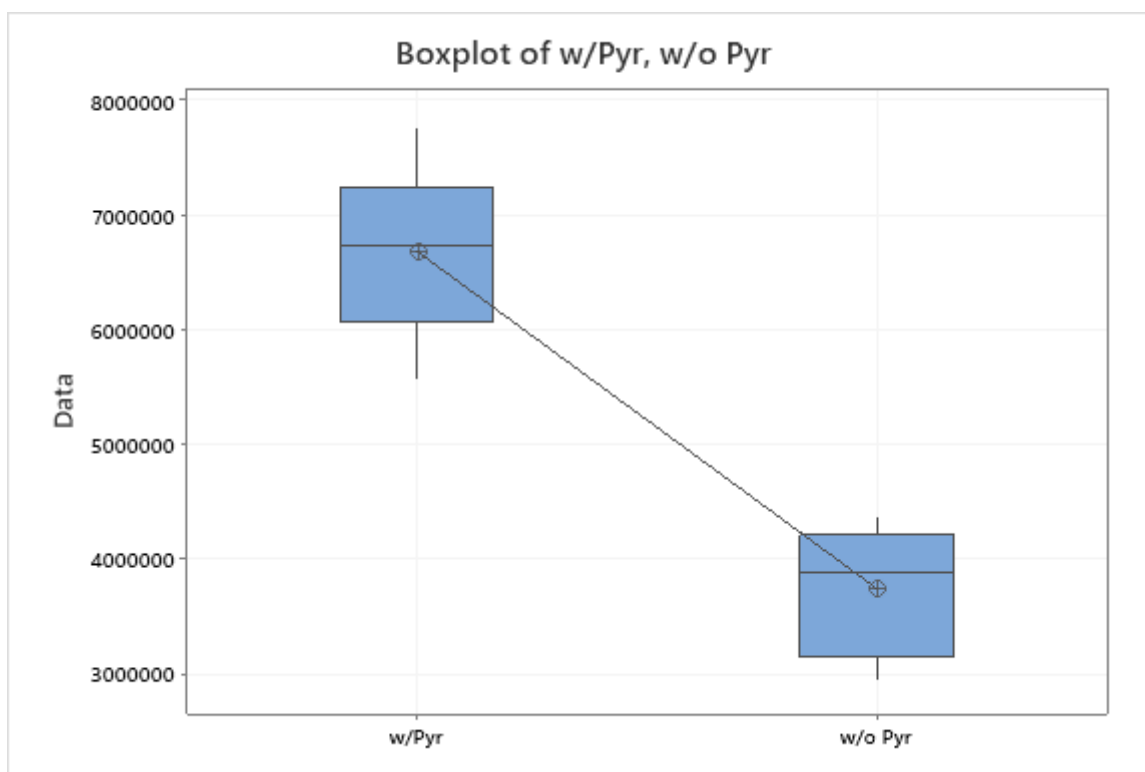


Figure S9.7: Effect of pyridine on average PA for carbamazepine mono-TMS. 2-sample *t*-test (*p*-value = 0.000, *n*=6). W Pyr = with pyridine and wo Pyr = without pyridine. A clear statistically significant difference is observed between the two samples.

3.2.4 Competing Reactions

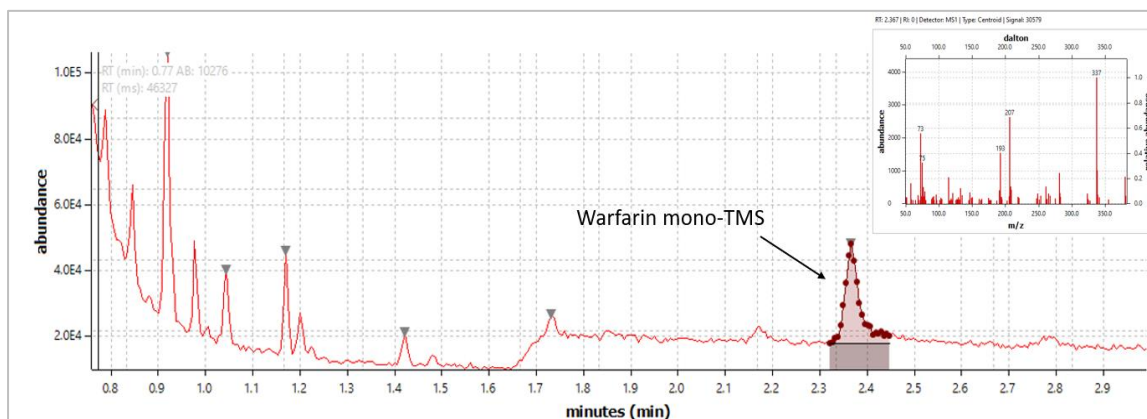


Figure S9.8: Warfarin mono-TMS. Chromatogram and MS (inset) for warfarin when analysed individually. Warfarin mono-silylates on the oxygen atom of the COOH.

3.2.5.2 DOE Response Optimisation

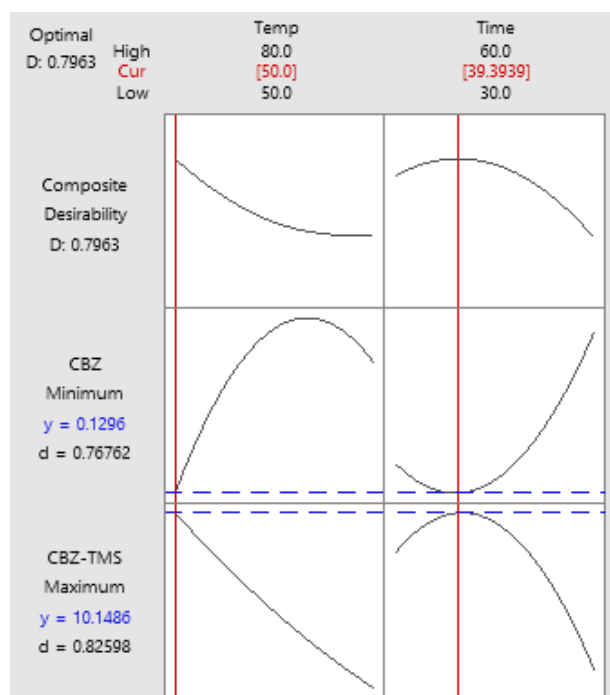


Figure S9.9: Response Optimisation Chart for carbamazepine silylation. Software is programmed to generate the exact parameters (time and temperature) where the CBZ response is minimised and CBZ-TMS response is maximised. Optimal responses are 50oC for 39.39 mins.

Appendix C – Chapter 5

2.3.1 Sample Collection

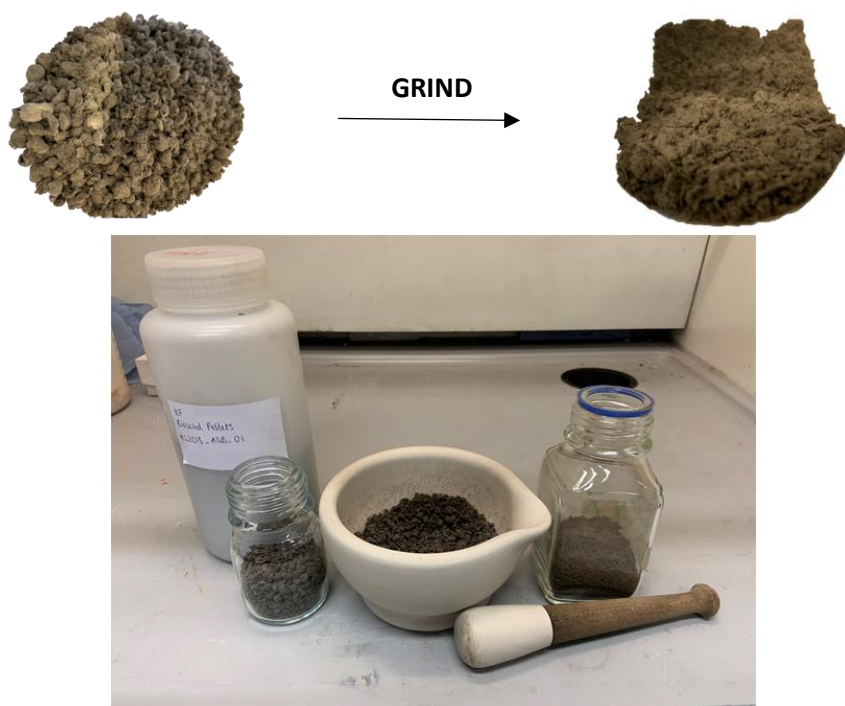


Figure S10.1: Biosolid Samples – top: biosolid pre- and post-grinding. bottom: L-R whole, partially ground and completely ground sample with apparatus (mortar and pestle)

2.3.2 Optimised Extraction Procedure

Post Sonication:



Post Centrifugation:



Post Reconstitution*:



* In ethyl acetate

Figure S10.2: Biosolid samples - extraction and reconstitution with optimised method. Reconstitution in 1ml of Ethyl Acetate

2.4 Sonotrode Device

The sonotrode was operated in a soundproof box. The box was placed in a fume hood (sash fully down when in operation) for safety. Sonotrode parameters were altered using the attached control panel. Vials were placed in the VialPress; and the sonotrode device placed on a piece of tinfoil. The tin foil base was used for easy clean-up if the vial were to shatter.



Figure S10.3: Sonotrode set-up. Top: Sonotrode operated in soundproof box, placed in a fume hood. Fume hood sash was fully down whilst in operation. Sonotrode controlled by the control panel (silver device to the LHS of photo). Bottom: Sonotrode device with a 10ml headspace vial attached in the VialPress.

3.2.4 Comparison to the optimised conventional oven method

Test

Null hypothesis $H_0: \mu_1 - \mu_2 = 0$

Alternative hypothesis $H_1: \mu_1 - \mu_2 \neq 0$

| T-Value | DF | P-Value |
|---------|----|---------|
| 1.19 | 10 | 0.262 |



Figure S10.4: Two-sample *t*-test output for the comparison of optimised conventional oven and sonication methods. *p*-value = 0.262. No statistically significant difference observed.

Appendix D – Chapter 6

2.7.1 LC-MS/MS

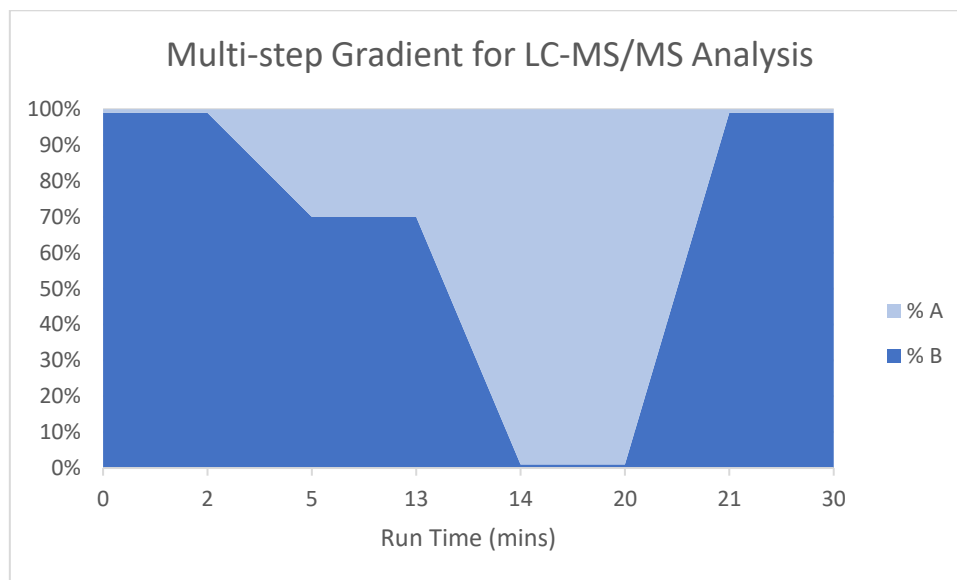
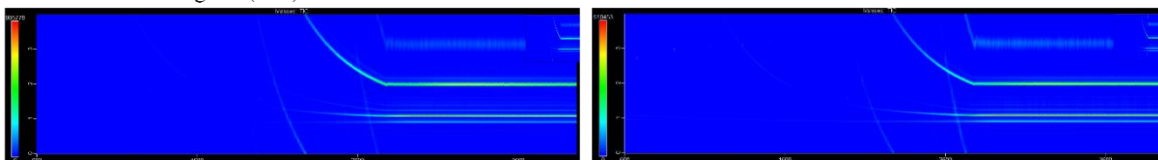


Figure S11.1: Plot illustrating the multi-step gradient for LC-MS/MS analysis. Reversed phase analysis mode. A = acetonitrile and B = 10mmol ammonium formate adjusted to pH 3.5 with formic acid.

2.7.3 GCxGC-TOFMS

Total Ion Chromatogram (TIC):



Extracted Ion Chromatogram (EIC) for m/z 73:

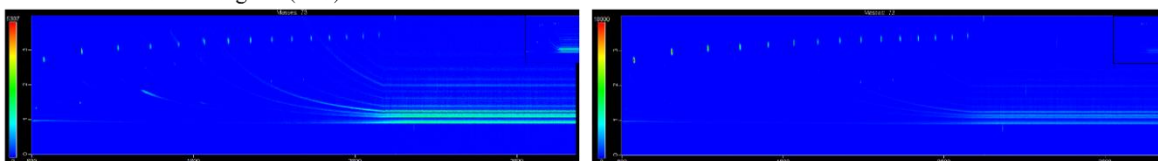


Figure S11.2: Total Ion Chromatograms and Extracted ion chromatograms (m/z 73) for blank ethyl acetate analysed before sample (left), and blank ethyl acetate analysed after a short (5 min) blank sample – analysed immediately after a biosolid sample (right). This shows that no carryover from the biosolid sample occurred, and that the short blank method was sufficient for between samples.

3.3.3 Identification of Optimal ChromaTOF Tile Parameters

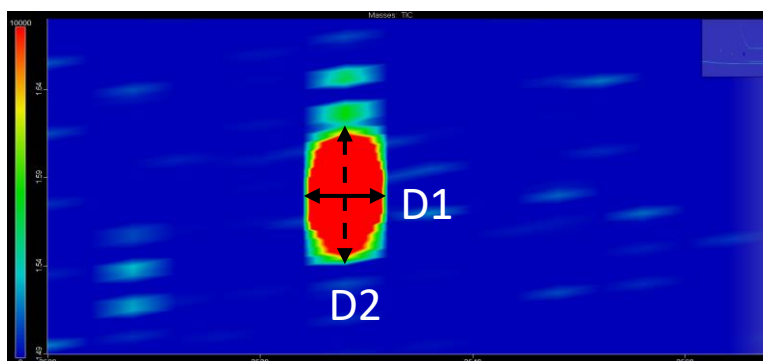


Figure S11.3: Measurement of first- and second-dimension peak width for optimal tile size calculation. Carbamazepine mono-TMS peak (2536s, 1.580s).

Features to be removed from further Tiles analysis can be found in the link below:

https://gla-my.sharepoint.com/:x/g/personal/k_fell_1_research_gla_ac_uk/EWN8DXG5uOBKgQUgTeNkcEcBAxrgPbSxuaAz1xqj4MM7jA?e=ScwcTc

3.3.4 Calibration of Tile Software

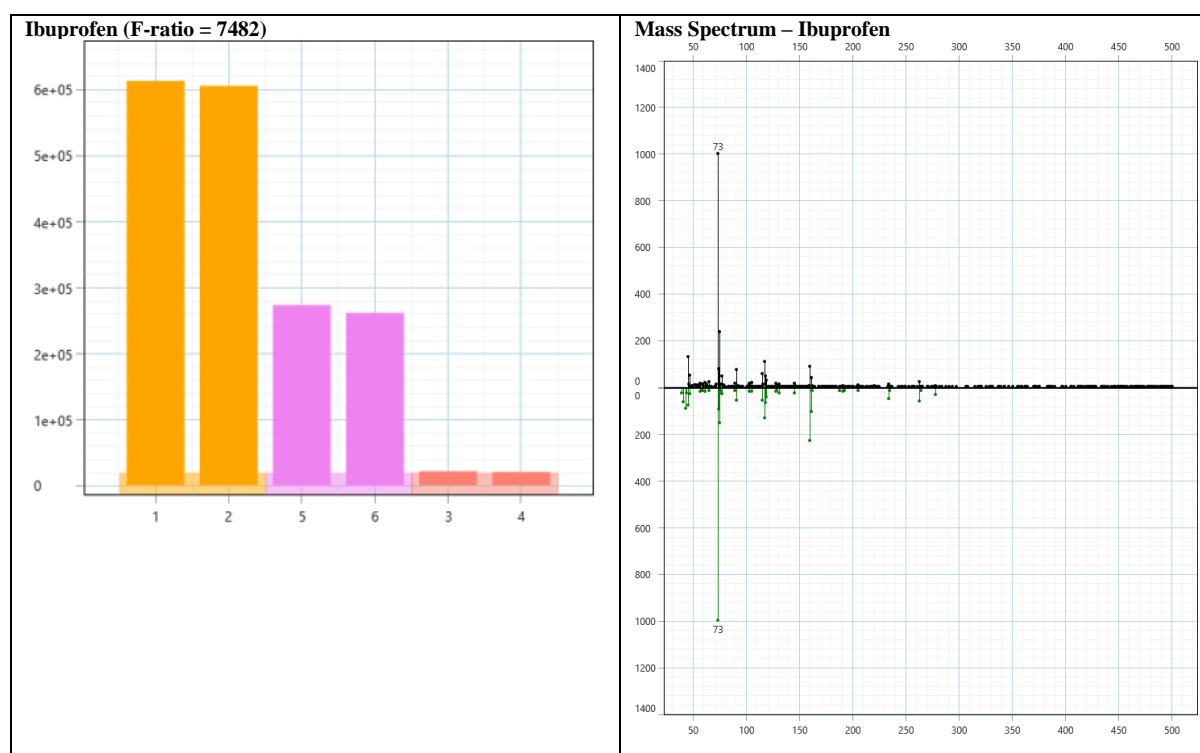


Figure 11.4: Ibuprofen mono-TMS in PhC standards. a) Feature area decreases from 1000-40 ug/L. b) MS for identified feature (top) which matches MS from NIST database (bottom)

3.3.5 Robustness

Table S11-1: List of samples analysed in batch. Samples and order randomised on Minitab. Randomisation used to prevent bias. All samples analysed in duplicate.

| Batch 1 | Batch 2 | Batch 4 | Batch 5 |
|--------------------------|------------------------------------|--------------------------|--------------------------|
| Non-spiked Biosolid 2 R1 | Non-spiked Biosolid 1 R3 | Spiked Biosolid 1 R1 | Spiked Biosolid 1 R3 |
| Spiked Biosolid 2 R1 | Spiked Biosolid 1 R2 | Non-spiked Biosolid 2 R3 | Non-spiked Biosolid 1 R1 |
| Non-spiked Biosolid 3 R1 | Spiked Biosolid 3 R3 | Spiked Biosolid 2 R2 | Non-spiked Biosolid 1 R2 |
| Biosolid 2 Pellet 2 | Composite Sample | Spiked Biosolid 2 R3 | Non-spiked Biosolid 2 R2 |
| Biosolid 2 Pellet 3 | Biosolid 1 Pellet 1 | Non-spiked Biosolid 3 R3 | Non-spiked Biosolid 3 R2 |
| PhC Standard – 40µg/L | Biosolid 2 Pellet 1 | Spiked Biosolid 3 R1 | Biosolid 1 Pellet 2 |
| PhC Standard – 400µg/L | Biosolid 2 Pellet 4 | Spiked Biosolid 3 R2 | Biosolid 1 Pellet 3 |
| | Biosolid 3 Pellet 5 | Biosolid 1 Pellet 5 | Biosolid 1 Pellet 4 |
| | Biosolid 3 Pellet 6 | | Biosolid 1 Pellet 6 |
| | Deuterated Surrogates – 100µg/L | | Biosolid 2 Pellet 6 |
| | | | Biosolid 3 Pellet 1 |
| | | | Biosolid 3 Pellet 2 |
| | | | Biosolid 3 Pellet 3 |
| | | | Biosolid 3 Pellet 4 |
| | | | PhC Standard – 1000µg/L |

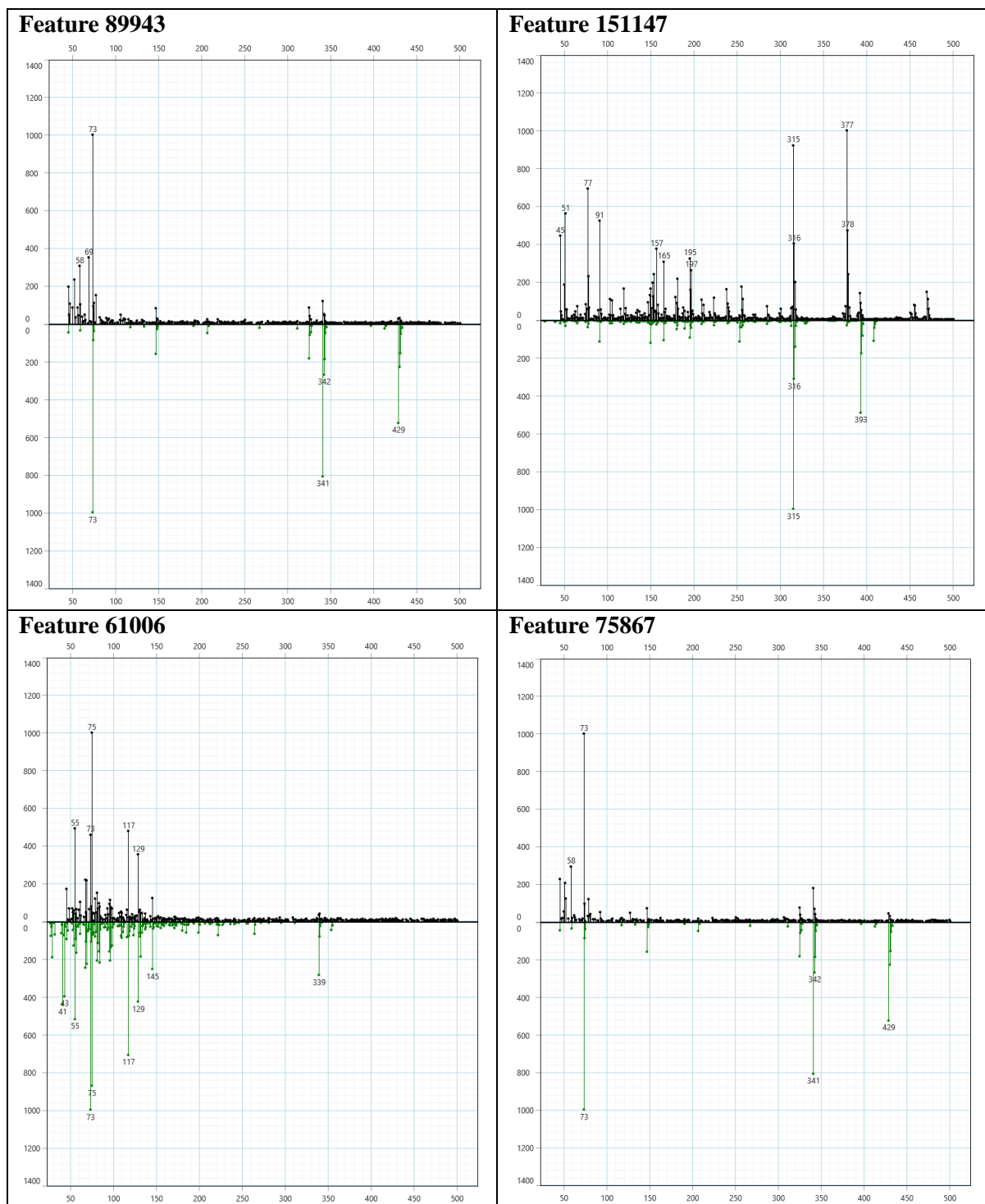


Figure S11.5: MS obtained for the four features which PC1 and PC2 are based.

3.3.7 Repeatability

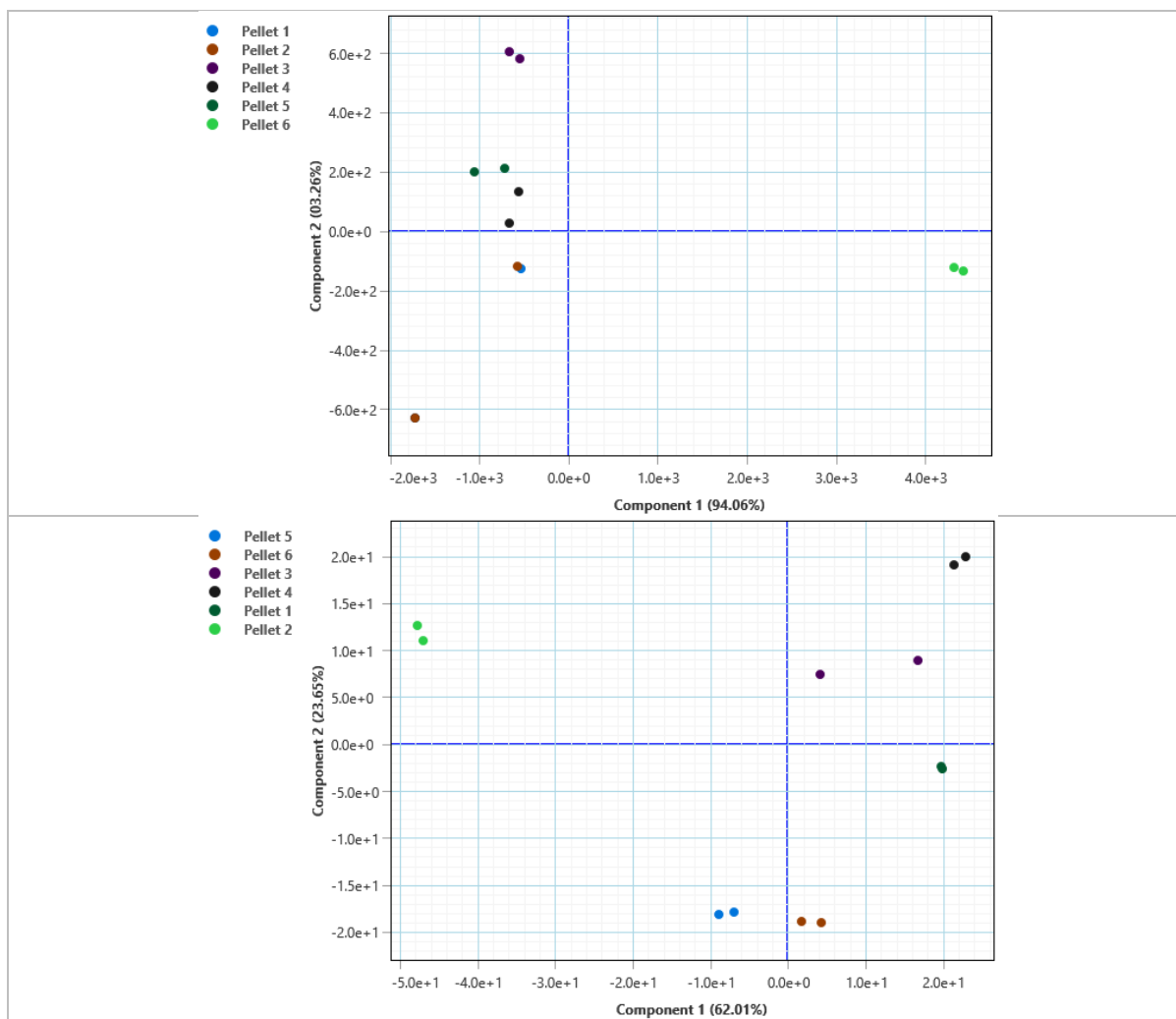


Figure S11.6: PCA scores plots for a) Biopellets 2 and b) Biopellets 3 – a clear difference is observed between biopellets of the same biosolid sample. This suggests pellets are not homogenous – thus it is recommended to combine numerous pellets and grind before extraction.

References

- Albero, B., Sánchez-Brunete, C., Miguel, E., Aznar, R., Tadeo, J.L., 2014. Determination of selected pharmaceutical compounds in biosolids by supported liquid extraction and gas chromatography–tandem mass spectrometry. *Journal of Chromatography A* 1336, 52–58. <https://doi.org/10.1016/j.chroma.2014.02.020>
- Albero, B., Tadeo, J.L., Pérez, R.A., 2019. Ultrasound-assisted extraction of organic contaminants. *TrAC Trends in Analytical Chemistry* 118, 739–750. <https://doi.org/10.1016/j.trac.2019.07.007>
- Alder, C.M., Hayler, J.D., Henderson, R.K., Redman, A.M., Shukla, L., Shuster, L.E., Sneddon, H.F., 2016. Updating and further expanding GSK’s solvent sustainability guide. *Green Chem.* 18, 3879–3890. <https://doi.org/10.1039/C6GC00611F>
- Al-Khazrajy, O.S.A., Boxall, A.B.A., 2017. Determination of pharmaceuticals in freshwater sediments using ultrasonic-assisted extraction with SPE clean-up and HPLC-DAD or LC-ESI-MS/MS detection. *Analytical Methods* 9, 4190–4200. <https://doi.org/10.1039/C7AY00650K>
- Almakki, A., Jumas-Bilak, E., Marchandin, H., Licznar-Fajardo, P., 2019. Antibiotic resistance in urban runoff. *Science of The Total Environment* 667, 64–76. <https://doi.org/10.1016/j.scitotenv.2019.02.183>
- Alvarez-Rivera, G., Bueno, M., Ballesteros-Vivas, D., Mendiola, J.A., Ibañez, E., 2020. Chapter 13 - Pressurized Liquid Extraction, in: Poole, C.F. (Ed.), *Liquid-Phase Extraction, Handbooks in Separation Science*. Elsevier, pp. 375–398. <https://doi.org/10.1016/B978-0-12-816911-7.00013-X>
- Amendola, L., Colamonici, C., Mazzarino, M., Botrè, F., 2003. Rapid determination of diuretics in human urine by gas chromatography–mass spectrometry following microwave assisted derivatization. *Analytica Chimica Acta* 475, 125–136. [https://doi.org/10.1016/S0003-2670\(02\)01223-0](https://doi.org/10.1016/S0003-2670(02)01223-0)

- American Chemical Society, 2022. What Is Green Chemistry? [WWW Document]. American Chemical Society. URL <https://www.acs.org/content/acs/en/greenchemistry/what-is-green-chemistry.html> (accessed 2.5.21).
- American Chemical Society, 2020. 12 Principles of Green Chemistry [WWW Document]. American Chemical Society. URL <https://www.acs.org/content/acs/en/greenchemistry/principles/12-principles-of-green-chemistry.html> (accessed 2.5.21).
- Anand, U., Reddy, B., Singh, V.K., Singh, A.K., Kesari, K.K., Tripathi, P., Kumar, P., Tripathi, V., Simal-Gandara, J., 2021. Potential Environmental and Human Health Risks Caused by Antibiotic-Resistant Bacteria (ARB), Antibiotic Resistance Genes (ARGs) and Emerging Contaminants (ECs) from Municipal Solid Waste (MSW) Landfill. *Antibiotics (Basel)* 10, 374. <https://doi.org/10.3390/antibiotics10040374>
- Anastas, P.T., Warner, J.C., 1998. *Green Chemistry: Theory and Practice*. Oxford University Press.
- Anastassiades, M., Maštovská, K., Lehotay, S.J., 2003. Evaluation of analyte protectants to improve gas chromatographic analysis of pesticides. *Journal of Chromatography A* 1015, 163–184. [https://doi.org/10.1016/S0021-9673\(03\)01208-1](https://doi.org/10.1016/S0021-9673(03)01208-1)
- Andreozzi, R., Raffaele, M., Nicklas, P., 2003. Pharmaceuticals in STP effluents and their solar photodegradation in aquatic environment. *Chemosphere* 50, 1319–1330. [https://doi.org/10.1016/S0045-6535\(02\)00769-5](https://doi.org/10.1016/S0045-6535(02)00769-5)
- Antonić, J., Heath, E., 2007. Determination of NSAIDs in river sediment samples. *Anal Bioanal Chem* 387, 1337–1342. <https://doi.org/10.1007/s00216-006-0947-7>
- Argoti, D., 2008. *Liquid chromatography : mass spectrometry for detection and characterization of DNA biomarkers and reactive metabolites*. Northeastern University.
- Azzouz, A., Ballesteros, E., 2013. Influence of seasonal climate differences on the pharmaceutical, hormone and personal care product removal efficiency of a drinking water treatment plant. *Chemosphere* 93, 2046–2054. <https://doi.org/10.1016/j.chemosphere.2013.07.037>
- Babushok, V.I., 2015. Chromatographic retention indices in identification of chemical compounds. *TrAC Trends in Analytical Chemistry* 69, 98–104. <https://doi.org/10.1016/j.trac.2015.04.001>

- Ballin, N.Z., Laursen, K.H., 2019. To target or not to target? Definitions and nomenclature for targeted versus non-targeted analytical food authentication. *Trends in Food Science & Technology* 86, 537–543. <https://doi.org/10.1016/j.tifs.2018.09.025>
- Bannan, C.C., Calabró, G., Kyu, D.Y., Mobley, D.L., 2016. Calculating partition coefficients of small molecules in octanol/water and cyclohexane/water. *J Chem Theory Comput* 12, 4015–4024. <https://doi.org/10.1021/acs.jctc.6b00449>
- Barber, W.P.F., 2016. Thermal hydrolysis for sewage treatment: A critical review. *Water Research* 104, 53–71. <https://doi.org/10.1016/j.watres.2016.07.069>
- Barci, P.E.P., Alves, L. da S., Avellar, Á.A.S., Cendon, L.R., dos Santos, P.J., Stringhini, F.M., Prestes, O.D., Zanella, R., 2020. Modified QuEChERS Method for Multiresidue Determination of Pesticides in Pecan Nuts by Liquid Chromatography Tandem Mass Spectrometry. *Food Anal. Methods* 13, 793–801. <https://doi.org/10.1007/s12161-019-01696-0>
- Barreto, E.F., Larson, T.R., Koubek, E.J., 2021. Drug Excretion, in: *Reference Module in Biomedical Sciences*. Elsevier. <https://doi.org/10.1016/B978-0-12-820472-6.99999-7>
- Barron, L., Tobin, J., Paull, B., 2008. Multi-residue determination of pharmaceuticals in sludge and sludge enriched soils using pressurized liquid extraction, solid phase extraction and liquid chromatography with tandem mass spectrometry. *J. Environ. Monit.* 10, 353–361. <https://doi.org/10.1039/B717453E>
- Bayer HealthCare Pharmaceuticals Inc., 2011. *CLINICAL PHARMACOLOGY* 25.
- Beldean-Galea, M.S., Coman, V., Copaciu, F., Thiébaud, D., Vial, J., 2014. SIMULTANEOUS IDENTIFICATION OF FENTON DEGRADATION BY-PRODUCTS OF DICLOFENAC, IBUPROFEN AND KETOPROFEN IN AQUATIC MEDIA BY COMPREHENSIVE TWO-DIMENSIONAL GAS CHROMATOGRAPHY COUPLED WITH MASS SPECTROMETRY 59, 1021–1027.
- Bergslien, E., 2012. *An Introduction to Forensic Geoscience*. John Wiley & Sons.
- Betts, J.N., Johnson, M.G., Rygiewicz, P.T., King, G.A., Andersen, C.P., 2013. Potential for metal contamination by direct sonication of nanoparticle suspensions. *Environmental Toxicology and Chemistry* 32, 889–893. <https://doi.org/10.1002/etc.2123>

- Biel-Maeso, M., Corada-Fernández, C., Lara-Martín, P.A., 2019. Removal of personal care products (PCPs) in wastewater and sludge treatment and their occurrence in receiving soils. *Water Research* 150, 129–139. <https://doi.org/10.1016/j.watres.2018.11.045>
- Bisceglia, K.J., Yu, J.T., Coelhan, M., Bouwer, E.J., Roberts, A.L., 2010. Trace determination of pharmaceuticals and other wastewater-derived micropollutants by solid phase extraction and gas chromatography/mass spectrometry. *Journal of Chromatography A* 1217, 558–564. <https://doi.org/10.1016/j.chroma.2009.11.062>
- Blair, R.M., Waldron, S., Gauchotte-Lindsay, C., 2019. Average daily flow of microplastics through a tertiary wastewater treatment plant over a ten-month period. *Water Research* 163, 114909. <https://doi.org/10.1016/j.watres.2019.114909>
- Blau, K., Halket, J.M., 1993. *Handbook of derivatives for chromatography*. Wiley.
- Blau, K., King, G.S., 1978. *Handbook of Derivatives for Chromatography*. Heyden.
- Bloom, 2019. Diazomethane: A Deadly, Explosive, Carcinogenic Gas Made From Another Carcinogen. Aside From That It's Fine. [WWW Document]. American Council on Science and Health. URL <https://www.acsh.org/news/2019/11/04/diazomethane-deadly-explosive-carcinogenic-gas-made-another-carcinogen-aside-its-fine-14374> (accessed 2.2.22).
- Blum, K.M., Andersson, P.L., Renman, G., Ahrens, L., Gros, M., Wiberg, K., Haglund, P., 2017. Non-target screening and prioritization of potentially persistent, bioaccumulating and toxic domestic wastewater contaminants and their removal in on-site and large-scale sewage treatment plants. *Science of The Total Environment* 575, 265–275. <https://doi.org/10.1016/j.scitotenv.2016.09.135>
- BOC, 2021a. Helium (Compressed).
- BOC, 2021b. Nitrogen, refrigerated liquid 13.
- Bootman, 2021. *Liquid Chromatography vs Gas Chromatography*. LC Services. URL <https://www.lcservicesltd.co.uk/liquid-chromatography-vs-gas-chromatography/> (accessed 8.20.21).

- Bossio, J.P., Harry, J., Kinney, C.A., 2008. Application of ultrasonic assisted extraction of chemically diverse organic compounds from soils and sediments. *Chemosphere* 70, 858–864.
<https://doi.org/10.1016/j.chemosphere.2007.06.088>
- Bound, J.P., Voulvoulis, N., 2005. Household disposal of pharmaceuticals as a pathway for aquatic contamination in the United kingdom. *Environ Health Perspect* 113, 1705–1711.
<https://doi.org/10.1289/ehp.8315>
- Britannica Encyclopedia, n.d. wastewater treatment - Sludge treatment and disposal | Britannica [WWW Document]. URL <https://www.britannica.com/technology/wastewater-treatment/Sludge-treatment-and-disposal> (accessed 1.30.22).
- Brooks, B.W., 2019. Greening chemistry and ecotoxicology towards sustainable environmental quality. *Green Chem.* 21, 2575–2582. <https://doi.org/10.1039/C8GC03893G>
- Brunelli, C., Bicchi, C., Stilo, A.D., Salomone, A., Vincenti, M., 2006. High-speed gas chromatography in doping control: Fast-GC and fast-GC/MS determination of β -adrenoceptor ligands and diuretics. *Journal of Separation Science* 29, 2765–2771.
<https://doi.org/10.1002/jssc.200500387>
- Brunetto, M. del R., Clavijo, S., Delgado, Y., Orozco, W., Gallignani, M., Ayala, C., Cerdà, V., 2015. Development of a MSFIA sample treatment system as front end of GC–MS for atenolol and propranolol determination in human plasma. *Talanta* 132, 15–22.
<https://doi.org/10.1016/j.talanta.2014.08.056>
- Budzinski, H., Devier, M.H., Labadie, P., Togola, A., 2006. Analysis of hormonal steroids in fish plasma and bile by coupling solid-phase extraction to GC/MS. *Anal Bioanal Chem* 386, 1429–1439. <https://doi.org/10.1007/s00216-006-0686-9>
- Butts, W.C., 1972. Two-column gas chromatography of trimethylsilyl derivatives of biochemically significant compounds. *Analytical Biochemistry* 46, 187–199. [https://doi.org/10.1016/0003-2697\(72\)90411-3](https://doi.org/10.1016/0003-2697(72)90411-3)
- Byrne, F.P., Jin, S., Paggiola, G., Petchey, T.H.M., Clark, J.H., Farmer, T.J., Hunt, A.J., Robert McElroy, C., Sherwood, J., 2016. Tools and techniques for solvent selection: green solvent selection guides. *Sustain Chem Process* 4, 7. <https://doi.org/10.1186/s40508-016-0051-z>

- Caban, M., Lis, E., Kumirska, J., Stepnowski, P., 2015. Determination of pharmaceutical residues in drinking water in Poland using a new SPE-GC-MS(SIM) method based on Speedisk extraction disks and DIMETRIS derivatization. *Science of The Total Environment* 538, 402–411. <https://doi.org/10.1016/j.scitotenv.2015.08.076>
- Caban, M., Mioduszevska, K., Łukaszewicz, P., Migowska, N., Stepnowski, P., Kwiatkowski, M., Kumirska, J., 2014. A new silylating reagent – dimethyl(3,3,3-trifluoropropyl)silyldiethylamine – for the derivatisation of non-steroidal anti-inflammatory drugs prior to gas chromatography–mass spectrometry analysis. *Journal of Chromatography A* 1346, 107–116. <https://doi.org/10.1016/j.chroma.2014.04.054>
- Caban, M., Mioduszevska, K., Stepnowski, P., Kwiatkowski, M., Kumirska, J., 2013. Dimethyl(3,3,3-trifluoropropyl)silyldiethylamine—A new silylating agent for the derivatization of β -blockers and β -agonists in environmental samples. *Analytica Chimica Acta* 782, 75–88. <https://doi.org/10.1016/j.aca.2013.04.018>
- Caban, M., Stepnowski, P., 2018. Silylation of acetaminophen by trifluoroacetamide-based silylation agents. *Journal of Pharmaceutical and Biomedical Analysis* 154, 433–437. <https://doi.org/10.1016/j.jpba.2018.03.037>
- Caban, M., Stepnowski, P., Kwiatkowski, M., Migowska, N., Kumirska, J., 2011. Determination of β -blockers and β -agonists using gas chromatography and gas chromatography–mass spectrometry – A comparative study of the derivatization step. *Journal of Chromatography A* 1218, 8110–8122. <https://doi.org/10.1016/j.chroma.2011.08.093>
- Cann, 2021. Green Chemistry | English | Green Chemistry [WWW Document]. URL <https://www.scranton.edu/faculty/cannm/green-chemistry/english/organicmodule.shtml> (accessed 7.26.21).
- Carballa, M., Omil, F., Alder, A.C., Lema, J.M., 2006. Comparison between the conventional anaerobic digestion of sewage sludge and its combination with a chemical or thermal pre-treatment concerning the removal of pharmaceuticals and personal care products. *Water Science and Technology* 53, 109–117. <https://doi.org/10.2166/wst.2006.241>

- Carballa, M., Omil, F., Lema, J.M., Llompart, M., García-Jares, C., Rodríguez, I., Gómez, M., Ternes, T., 2004. Behavior of pharmaceuticals, cosmetics and hormones in a sewage treatment plant. *Water Research* 38, 2918–2926. <https://doi.org/10.1016/j.watres.2004.03.029>
- Carlton, D.D., Fontenot, B.E., Hildenbrand, Z.L., Davis, T.M., Walton, J.L., Schug, K.A., 2015. Varying matrix effects for elemental analysis identified from groundwater in the Barnett Shale. *Int. J. Environ. Sci. Technol.* 12, 3665–3674. <https://doi.org/10.1007/s13762-015-0803-4>
- Casals, G., Marcos, J., Pozo, O.J., Alcaraz, J., Martínez de Osaba, M.J., Jiménez, W., 2014. Microwave-assisted derivatization: Application to steroid profiling by gas chromatography/mass spectrometry. *Journal of Chromatography B* 960, 8–13. <https://doi.org/10.1016/j.jchromb.2014.04.015>
- Chatel, G., 2018. How sonochemistry contributes to green chemistry? *Ultrasonics Sonochemistry*, SI: ESS-15, 2016, Istanbul 40, 117–122. <https://doi.org/10.1016/j.ultsonch.2017.03.029>
- Chen, Y., Cheng, J.J., Creamer, K.S., 2008. Inhibition of anaerobic digestion process: A review. *Bioresource Technology* 99, 4044–4064. <https://doi.org/10.1016/j.biortech.2007.01.057>
- Chenxi, W., Spongberg, A.L., Witter, J.D., 2008a. Determination of the persistence of pharmaceuticals in biosolids using liquid-chromatography tandem mass spectrometry. *Chemosphere* 73, 511–518. <https://doi.org/10.1016/j.chemosphere.2008.06.026>
- Chenxi, W., Spongberg, A.L., Witter, J.D., 2008b. Determination of the persistence of pharmaceuticals in biosolids using liquid-chromatography tandem mass spectrometry. *Chemosphere* 73, 511–518. <https://doi.org/10.1016/j.chemosphere.2008.06.026>
- Clark, 2015. equilibrium constants - Kc [WWW Document]. URL <http://www.chemguide.co.uk/physical/equilibria/kc.html> (accessed 1.5.22).
- Cohen, J.M., Beltran-Huarac, J., Pyrgiotakis, G., Demokritou, P., 2018. Effective delivery of sonication energy to fast settling and agglomerating nanomaterial suspensions for cellular studies: Implications for stability, particle kinetics, dosimetry and toxicity. *NanoImpact* 10, 81–86. <https://doi.org/10.1016/j.impact.2017.12.002>

- Cravotto, G., Cintas, P., 2006. Power ultrasound in organic synthesis: moving cavitation chemistry from academia to innovative and large-scale applications. *Chem. Soc. Rev.* 35, 180–196.
<https://doi.org/10.1039/B503848K>
- Daughton, C.G., Ternes, T.A., 1999. Pharmaceuticals and personal care products in the environment: agents of subtle change? *Environ Health Perspect* 107, 907–938.
- de Albuquerque Cavalcanti, G., Rodrigues, L.M., dos Santos, L., Zheng, X., Gujar, A., Cole, J., Padilha, M.C., de Aquino Neto, F.R., 2018. Non-targeted acquisition strategy for screening doping compounds based on GC-EI-hybrid quadrupole-Orbitrap mass spectrometry: A focus on exogenous anabolic steroids. *Drug Testing and Analysis* 10, 507–517.
<https://doi.org/10.1002/dta.2227>
- de Zeeuw, 2017. Impact of GC Parameters on The Separation.
- Deblonde, T., Cossu-Leguille, C., Hartemann, P., 2011. Emerging pollutants in wastewater: A review of the literature. *International Journal of Hygiene and Environmental Health*, The second European PhD students workshop: Water and health ? Cannes 2010 214, 442–448.
<https://doi.org/10.1016/j.ijheh.2011.08.002>
- DEFRA, 2012. Waste water treatment in the United Kingdom - 2012.
- Delgado-Povedano, M.M., Luque de Castro, M.D., 2013. Ultrasound-assisted extraction and in situ derivatization. *Journal of Chromatography A, Microreactions in Separation Science: Reagents and Techniques* 1296, 226–234. <https://doi.org/10.1016/j.chroma.2013.04.004>
- Deng, C., Yin, X., Zhang, L., Zhang, X., 2005. Development of microwave-assisted derivatization followed by gas chromatography/mass spectrometry for fast determination of amino acids in neonatal blood samples. *Rapid Communications in Mass Spectrometry* 19, 2227–2234.
<https://doi.org/10.1002/rcm.2052>
- Dey, S., Bano, F., Malik, A., 2019. 1 - Pharmaceuticals and personal care product (PPCP) contamination—a global discharge inventory, in: Prasad, M.N.V., Vithanage, M., Kapley, A. (Eds.), *Pharmaceuticals and Personal Care Products: Waste Management and Treatment Technology*. Butterworth-Heinemann, pp. 1–26. <https://doi.org/10.1016/B978-0-12-816189-0.00001-9>

- Díaz, A., Peña-Alvarez, A., 2017. A Simple Method for the Simultaneous Determination of Pharmaceuticals and Personal Care Products in River Sediment by Ultrasound-Assisted Extraction Followed by Solid-Phase Microextraction Coupled with Gas Chromatography–Mass Spectrometry. *J Chromatogr Sci* 55, 946–953. <https://doi.org/10.1093/chromsci/bmx058>
- Ding, Y., Zhang, W., Gu, C., Xagorarakis, I., Li, H., 2011. Determination of pharmaceuticals in biosolids using accelerated solvent extraction and liquid chromatography/tandem mass spectrometry. *Journal of Chromatography A* 1218, 10–16. <https://doi.org/10.1016/j.chroma.2010.10.112>
- Djatkina, R., Ding, W.-H., 2016. Optimization of Silylation for Parabens Determination by Gas Chromatography-Mass Spectrometry. *AI* 5, 55. <https://doi.org/10.18860/al.v5i2.3743>
- Doktycz, S.J., Suslick, K.S., 1990. Interparticle Collisions Driven by Ultrasound. *Science*. <https://doi.org/10.1126/science.2309118>
- Drewes, J.E., 2007. Analysis, fate and removal of pharmaceuticals in the water cycle. *Wilson & Wilsons*. Elsevier, Amsterdam 427–446.
- Drugbank, 2005a. Atenolol [WWW Document]. URL <https://go.drugbank.com/drugs/DB00335> (accessed 1.7.22).
- Drugbank, 2005b. Sotalol [WWW Document]. URL <https://go.drugbank.com/drugs/DB00489> (accessed 11.12.21).
- Electron Impact - an overview | ScienceDirect Topics [WWW Document], n.d. URL <https://www.sciencedirect.com/topics/earth-and-planetary-sciences/electron-impact> (accessed 10.26.21).
- Encyclopedia Britannica, 2020. chloral hydrate | drug | Britannica [WWW Document]. URL <https://www.britannica.com/science/chloral-hydrate> (accessed 11.14.21).
- Eriksson, E., Auffarth, K., Henze, M., Ledin, A., 2002. Characteristics of grey wastewater. *Urban Water* 4, 85–104. [https://doi.org/10.1016/S1462-0758\(01\)00064-4](https://doi.org/10.1016/S1462-0758(01)00064-4)
- Erythropel, H.C., Zimmerman, J.B., Winter, T.M. de, Petitjean, L., Melnikov, F., Lam, C.H., Lounsbury, A.W., Mellor, K.E., Janković, N.Z., Tu, Q., Pincus, L.N., Falinski, M.M., Shi, W., Coish, P., Plata, D.L., Anastas, P.T., 2018. The Green ChemisTREE: 20 years after

- taking root with the 12 principles. *Green Chem.* 20, 1929–1961.
<https://doi.org/10.1039/C8GC00482J>
- European Commission, 2014. Introduction to the EU Water Framework Directive - Environment - European Commission [WWW Document]. URL
https://ec.europa.eu/environment/water/water-framework/info/intro_en.htm (accessed 7.16.20).
- European Commission. Joint Research Centre., 2020. Selection of substances for the 3rd Watch List under the Water Framework Directive. Publications Office, LU.
- Farré, M. la, Pérez, S., Kantiani, L., Barceló, D., 2008. Fate and toxicity of emerging pollutants, their metabolites and transformation products in the aquatic environment. *TrAC Trends in Analytical Chemistry, Advanced MS Analysis of Metabolites and Degradation Products - II* 27, 991–1007. <https://doi.org/10.1016/j.trac.2008.09.010>
- Farré, M., Ferrer, I., Ginebreda, A., Figueras, M., Olivella, L., Tirapu, L., Vilanova, M., Barceló, D., 2001. Determination of drugs in surface water and wastewater samples by liquid chromatography–mass spectrometry: methods and preliminary results including toxicity studies with *Vibrio fischeri*. *Journal of Chromatography A, 10th Symposium on Handling of Environmental and Biological Samples in Chromatography* 938, 187–197.
[https://doi.org/10.1016/S0021-9673\(01\)01154-2](https://doi.org/10.1016/S0021-9673(01)01154-2)
- Fatta, D., Achilleos, A., Nikolaou, A., Meriç, S., 2007. Analytical methods for tracing pharmaceutical residues in water and wastewater. *TrAC Trends in Analytical Chemistry, Pharmaceutical-residue analysis* 26, 515–533. <https://doi.org/10.1016/j.trac.2007.02.001>
- Fatta-Kassinos, D., Meric, S., Nikolaou, A., 2011. Advances in Analytical Methods for the Determination of Pharmaceutical Residues in Waters and Wastewaters, in: Nriagu, J.O. (Ed.), *Encyclopedia of Environmental Health*. Elsevier, Burlington, pp. 9–16.
<https://doi.org/10.1016/B978-0-444-52272-6.00426-8>
- Felis, E., Kalka, J., Sochacki, A., Kowalska, K., Bajkacz, S., Harnisz, M., Korzeniewska, E., 2020. Antimicrobial pharmaceuticals in the aquatic environment - occurrence and environmental

- implications. *European Journal of Pharmacology* 866, 172813.
<https://doi.org/10.1016/j.ejphar.2019.172813>
- Fiamegos, Y.C., Nanos, C.G., Stalikas, C.D., 2004. Ultrasonic-assisted derivatization reaction of amino acids prior to their determination in urine by using single-drop microextraction in conjunction with gas chromatography. *Journal of Chromatography B* 813, 89–94.
<https://doi.org/10.1016/j.jchromb.2004.09.013>
- Filigenzi, M., 2017. What are the advantages of gas chromatography–mass spectrometry (GC-MS)? - Quora [WWW Document]. What are the advantages of gas chromatography-mass spectrometry (GC-MS)? URL <https://www.quora.com/What-are-the-advantages-of-gas-chromatography%E2%80%93mass-spectrometry-GC-MS> (accessed 9.18.18).
- Fisher, C.M., Croley, T.R., Knolhoff, A.M., 2021. Data processing strategies for non-targeted analysis of foods using liquid chromatography/high-resolution mass spectrometry. *TrAC Trends in Analytical Chemistry* 136, 116188. <https://doi.org/10.1016/j.trac.2021.116188>
- Frédéric, O., Yves, P., 2014. Pharmaceuticals in hospital wastewater: Their ecotoxicity and contribution to the environmental hazard of the effluent. *Chemosphere*, PHARMACEUTICAL PRODUCTS IN THE ENVIRONMENT: FOR A MORE RELIABLE RISK ASSESSMENT 115, 31–39. <https://doi.org/10.1016/j.chemosphere.2014.01.016>
- Freye, C., Bowden, P., Greenfield, M., Tappan, B., 2019. Non-targeted discovery-based analysis for gas chromatography with mass spectrometry: A comparison of peak table, tile, and pixel-based Fisher ratio analysis. *Talanta* 211, 120668.
<https://doi.org/10.1016/j.talanta.2019.120668>
- Gago-Ferrero, P., Viola, Dasenaki, M.E., Thomaidis, N.S., 2015. Simultaneous determination of 148 pharmaceuticals and illicit drugs in sewage sludge based on ultrasound-assisted extraction and liquid chromatography–tandem mass spectrometry. *Analytical and Bioanalytical Chemistry* 407, 4287–4297. <https://doi.org/10.1007/s00216-015-8540-6>
- Gałuszka, A., Migaszewski, Z., Namieśnik, J., 2013. The 12 principles of green analytical chemistry and the SIGNIFICANCE mnemonic of green analytical practices. *TrAC Trends in Analytical Chemistry* 50, 78–84. <https://doi.org/10.1016/j.trac.2013.04.010>

- Gerriets, V., Anderson, J., Nappe, T.M., 2021. Acetaminophen, in: StatPearls. StatPearls Publishing, Treasure Island (FL).
- Giandomenico, S., Cardellicchio, N., Annicchiarico, C., Lopez, L., Maggi, M., Spada, L., Di Leo, A., 2011. Simultaneous determination of pharmaceutical compounds in environmental samples by solid-phase extraction and gas chromatography–mass spectrometry. *Chemistry and Ecology* 27, 127–136. <https://doi.org/10.1080/02757540.2011.625936>
- Giordano, A., Vásquez, J., Retamal, M., Ascar, L., Giordano, A., Vásquez, J., Retamal, M., Ascar, L., 2016. Ibuprofen, Carbamazepine and β -Estradiol Determination Using Thin-Film Microextraction and Gas Chromatography-Mass Spectrometry. *Journal of the Brazilian Chemical Society* 27, 1744–1749. <https://doi.org/10.5935/0103-5053.20160055>
- Golet, E.M., Strehler, A., Alder, A.C., Giger, W., 2002. Determination of Fluoroquinolone Antibacterial Agents in Sewage Sludge and Sludge-Treated Soil Using Accelerated Solvent Extraction Followed by Solid-Phase Extraction. *Anal. Chem.* 74, 5455–5462. <https://doi.org/10.1021/ac025762m>
- Goñi-Urriza, M., Capdepuy, M., Arpin, C., Raymond, N., Caumette, P., Quentin, C., 2000. Impact of an Urban Effluent on Antibiotic Resistance of Riverine Enterobacteriaceae and *Aeromonas* spp. *Appl Environ Microbiol* 66, 125–132.
- González, A., Avivar, J., Cerdà, V., 2015. Estrogens determination in wastewater samples by automatic in-syringe dispersive liquid–liquid microextraction prior silylation and gas chromatography. *Journal of Chromatography A* 1413, 1–8. <https://doi.org/10.1016/j.chroma.2015.08.031>
- González-Gaya, B., Lopez-Herguedas, N., Bilbao, D., Mijangos, L., Iker, A.M., Etxebarria, N., Irazola, M., Prieto, A., Olivares, M., Zuloaga, O., 2021. Suspect and non-target screening: the last frontier in environmental analysis. *Anal. Methods* 13, 1876–1904. <https://doi.org/10.1039/D1AY00111F>
- Gravert, T.K.O., Vuaille, J., Magid, J., Hansen, M., 2021. Non-target analysis of organic waste amended agricultural soils: Characterization of added organic pollution. *Chemosphere* 280, 130582. <https://doi.org/10.1016/j.chemosphere.2021.130582>

- Gros, M., Petrović, M., Barceló, D., 2009. Tracing Pharmaceutical Residues of Different Therapeutic Classes in Environmental Waters by Using Liquid Chromatography/Quadrupole-Linear Ion Trap Mass Spectrometry and Automated Library Searching. *Anal. Chem.* 81, 898–912. <https://doi.org/10.1021/ac801358e>
- Gros, M., Petrović, M., Ginebreda, A., Barceló, D., 2010. Removal of pharmaceuticals during wastewater treatment and environmental risk assessment using hazard indexes. *Environment International* 36, 15–26. <https://doi.org/10.1016/j.envint.2009.09.002>
- Guerra, P., Kim, M., Shah, A., Alaei, M., Smyth, S.A., 2014. Occurrence and fate of antibiotic, analgesic/anti-inflammatory, and antifungal compounds in five wastewater treatment processes. *Science of The Total Environment* 473–474, 235–243. <https://doi.org/10.1016/j.scitotenv.2013.12.008>
- Gumbi, B.P., Moodley, B., Birungi, G., Ndungu, P.G., 2017. Detection and quantification of acidic drug residues in South African surface water using gas chromatography-mass spectrometry. *Chemosphere* 168, 1042–1050. <https://doi.org/10.1016/j.chemosphere.2016.10.105>
- Hajeb, P., Zhu, L., Bossi, R., Vorkamp, K., 2022. Sample preparation techniques for suspect and non-target screening of emerging contaminants. *Chemosphere* 287, 132306. <https://doi.org/10.1016/j.chemosphere.2021.132306>
- Halket, J., Zaikin, V., 2004. Derivatization in Mass Spectrometry– 3. Alkylation (Arylation). *European journal of mass spectrometry (Chichester, England)* 10, 1–19. <https://doi.org/10.1255/ejms.619>
- Hall, T., Smukste, I., R., K., Wang, Y., McKearn, D., E., R., 2012. Identifying and Overcoming Matrix Effects in Drug Discovery and Development, in: Prasain, J. (Ed.), *Tandem Mass Spectrometry - Applications and Principles*. InTech. <https://doi.org/10.5772/32108>
- Hamscher, G., Sczesny, S., Höper, H., Nau, H., 2002. Determination of Persistent Tetracycline Residues in Soil Fertilized with Liquid Manure by High-Performance Liquid Chromatography with Electrospray Ionization Tandem Mass Spectrometry. *Anal. Chem.* 74, 1509–1518. <https://doi.org/10.1021/ac015588m>

- Harvey, D.J., Vouros, P., 2020. Mass Spectrometric Fragmentation of Trimethylsilyl and Related Alkylsilyl Derivatives. *Mass Spectrometry Reviews* 39, 105–211. <https://doi.org/10.1002/mas.21590>
- Helmenstine, 2019. Understand the Significance of the Equilibrium Constant [WWW Document]. ThoughtCo. URL <https://www.thoughtco.com/equilibrium-constant-606794> (accessed 1.5.22).
- Henderson, R.K., Jiménez-González, C., Constable, D.J.C., Alston, S.R., Inglis, G.G.A., Fisher, G., Sherwood, J., Binks, S.P., Curzons, A.D., 2011. Expanding GSK's solvent selection guide – embedding sustainability into solvent selection starting at medicinal chemistry. *Green Chem.* 13, 854–862. <https://doi.org/10.1039/C0GC00918K>
- Hielscher, 2020a. Ultrasonic Crystallization and Precipitation [WWW Document]. Hielscher Ultrasound Technology. URL <https://www.hielscher.com/ultrasonic-crystallization-and-precipitation.htm> (accessed 5.18.20).
- Hielscher, 2020b. Ultrasonic Cavitation in Liquids [WWW Document]. Hielscher Ultrasound Technology. URL <https://www.hielscher.com/ultrasonic-cavitation-in-liquids-2.htm> (accessed 4.23.20).
- Hielscher, 2020c. Ultrasonic Laboratory Devices [WWW Document]. Hielscher Ultrasound Technology. URL <https://www.hielscher.com/lab.htm> (accessed 6.11.21).
- Hielscher, 2020d. Ultrasonic Sonotrodes, Flow Cells & Accessories [WWW Document]. Hielscher Ultrasound Technology. URL <https://www.hielscher.com/ultrasonic-sonotrodes-flow-cells-accessories.htm> (accessed 2.5.21).
- Hielscher Ultrasound Technology, 2022. Probe-Type Sonication vs. Ultrasonic Bath: An Efficiency Comparison [WWW Document]. Hielscher Ultrasound Technology. URL <https://www.hielscher.com/probe-type-sonication-vs-ultrasonic-bath-an-efficiency-comparison.htm> (accessed 12.29.21).
- H. Langford, K., Reid, M., V. Thomas, K., 2011. Multi-residue screening of prioritised human pharmaceuticals, illicit drugs and bactericides in sediments and sludge. *Journal of Environmental Monitoring* 13, 2284–2291. <https://doi.org/10.1039/C1EM10260E>

- Huber, S., Remberger, M., Kaj, L., Schlabach, M., Jörundsdóttir, H.Ó., Vester, J., Arnórsson, M., Mortensen, I., Schwartzon, R., Dam, M., 2016. A first screening and risk assessment of pharmaceuticals and additives in personal care products in waste water, sludge, recipient water and sediment from Faroe Islands, Iceland and Greenland. *Science of The Total Environment* 562, 13–25. <https://doi.org/10.1016/j.scitotenv.2016.03.063>
- Huggett, D.B., Khan, I.A., Foran, C.M., Schlenk, D., 2003. Determination of beta-adrenergic receptor blocking pharmaceuticals in united states wastewater effluent. *Environmental Pollution* 121, 199–205. [https://doi.org/10.1016/S0269-7491\(02\)00226-9](https://doi.org/10.1016/S0269-7491(02)00226-9)
- Ihme, 2020. Ethyl acetate [WWW Document]. SEKAB. URL <https://www.sekab.com/en/products-services/product/ethyl-acetate/> (accessed 5.21.21).
- IUPAC, 2014. *Compendium of Chemical Terminology*, 2nd ed. <https://doi.org/10.1351/goldbook.M03759>
- Jacobsson, S.-E., Jönsson, S., Lindberg, C., Svensson, L.-Å., 1980. Determination of terbutaline in plasma by gas chromatography chemical ionization mass spectrometry. *Biomedical Mass Spectrometry* 7, 265–268. <https://doi.org/10.1002/bms.1200070608>
- Jayampathi, T., Atugoda, T., Jayasinghe, C., 2019. 4 - Uptake and accumulation of pharmaceuticals and personal care products in leafy vegetables, in: Prasad, M.N.V., Vithanage, M., Kapley, A. (Eds.), *Pharmaceuticals and Personal Care Products: Waste Management and Treatment Technology*. Butterworth-Heinemann, pp. 87–113. <https://doi.org/10.1016/B978-0-12-816189-0.00004-4>
- Jelic, A., Gros, M., Ginebreda, A., Cespedes-Sánchez, R., Ventura, F., Petrovic, M., Barcelo, D., 2011. Occurrence, partition and removal of pharmaceuticals in sewage water and sludge during wastewater treatment. *Water Research* 45, 1165–1176. <https://doi.org/10.1016/j.watres.2010.11.010>
- Jones, A.W., 2011. Early drug discovery and the rise of pharmaceutical chemistry. *Drug Testing and Analysis* 3, 337–344. <https://doi.org/10.1002/dta.301>
- Joseph, S., n.d. *Mass Spectrometry Solutions from LECO* 34.
- JSB International, 2015. *OUR GC×GC MODULATORS: AN OVERVIEW*.

- Jux, U., Baginski, R.M., Arnold, H.-G., Krönke, M., Seng, P.N., 2002. Detection of pharmaceutical contaminations of river, pond, and tap water from Cologne (Germany) and surroundings. *International Journal of Hygiene and Environmental Health* 205, 393–398.
<https://doi.org/10.1078/1438-4639-00166>
- Kashutina, M.V., Ioffe, S.L., Tartakovskii, V.A., 1975. Silylation of Organic Compounds. *Russ. Chem. Rev.* 44, 733. <https://doi.org/10.1070/RC1975v044n09ABEH002373>
- Kataoka, H., 2014. Amines: Gas Chromatography☆☆Change History: October 2013. H Kataoka added derivatization methods and detectors for the determination of underivatized and derivatized amines in the text. Deleted Tables 1, 2 and Figures 1–6, since they are information of more than 10 years ago. Added new table, including derivatizing reagents and derivatization reactions for gas chromatography of amines. Replaced the section of ‘Further Reading’ with new references., in: *Reference Module in Chemistry, Molecular Sciences and Chemical Engineering*. Elsevier. <https://doi.org/10.1016/B978-0-12-409547-2.10941-2>
- Kermia, A.E.B., Fouial-Djebbar, D., Trari, M., 2016. Occurrence, fate and removal efficiencies of pharmaceuticals in wastewater treatment plants (WWTPs) discharging in the coastal environment of Algiers. *Comptes Rendus Chimie* 19, 963–970.
<https://doi.org/10.1016/j.crci.2016.05.005>
- Kirch, W., Görg, K.G., 1982. Clinical pharmacokinetics of atenolol--a review. *Eur J Drug Metab Pharmacokinet* 7, 81–91. <https://doi.org/10.1007/BF03188723>
- Knapp, 1979. *Handbook of analytical derivatization reactions*. By DANIEL R. KNAPP. Wiley, One Wiley Drive, Somerset, NJ 08873. 1979. 741 pp. 15 × 23 cm. Price \$34.95 - 1980 - *Journal of Pharmaceutical Sciences* - Wiley Online Library [WWW Document]. URL <https://onlinelibrary.wiley.com/doi/abs/10.1002/jps.2600690549> (accessed 3.5.20).
- Kokosa, J.M., 2019. Selecting an extraction solvent for a greener liquid phase microextraction (LPME) mode-based analytical method. *TrAC Trends in Analytical Chemistry* 118, 238–247.
<https://doi.org/10.1016/j.trac.2019.05.012>

- Kopperi, M., Ruiz-Jiménez, J., Hukkinen, J.I., Riekkola, M.-L., 2013. New way to quantify multiple steroidal compounds in wastewater by comprehensive two-dimensional gas chromatography–time-of-flight mass spectrometry. *Analytica Chimica Acta* 761, 217–226.
<https://doi.org/10.1016/j.aca.2012.11.059>
- Kostopoulou, M., Nikolaou, A., 2008. Analytical problems and the need for sample preparation in the determination of pharmaceuticals and their metabolites in aqueous environmental matrices. *TrAC Trends in Analytical Chemistry, Advanced MS Analysis of Metabolites and Degradation Products - II* 27, 1023–1035. <https://doi.org/10.1016/j.trac.2008.09.011>
- Kotowska, U., Kapelewska, J., Sturgulewska, J., 2014. Determination of phenols and pharmaceuticals in municipal wastewaters from Polish treatment plants by ultrasound-assisted emulsification–microextraction followed by GC–MS. *Environ Sci Pollut Res* 21, 660–673.
<https://doi.org/10.1007/s11356-013-1904-6>
- Kovalova, L., Siegrist, H., Singer, H., Wittmer, A., McArdell, C.S., 2012. Hospital Wastewater Treatment by Membrane Bioreactor: Performance and Efficiency for Organic Micropollutant Elimination. *Environ. Sci. Technol.* 46, 1536–1545. <https://doi.org/10.1021/es203495d>
- Kumirska, J., Łukaszewicz, P., Caban, M., Migowska, N., Plenis, A., Białk-Bielińska, A., Czerwicka, M., Qi, F., Piotr, S., 2019. Determination of twenty pharmaceutical contaminants in soil using ultrasound-assisted extraction with gas chromatography-mass spectrometric detection. *Chemosphere* 232, 232–242. <https://doi.org/10.1016/j.chemosphere.2019.05.164>
- Kumirska, J., Plenis, A., Łukaszewicz, P., Caban, M., Migowska, N., Białk-Bielińska, A., Czerwicka, M., Stepnowski, P., 2013. Chemometric optimization of derivatization reactions prior to gas chromatography–mass spectrometry analysis. *Journal of Chromatography A, Microreactions in Separation Science: Reagents and Techniques* 1296, 164–178.
<https://doi.org/10.1016/j.chroma.2013.04.079>
- Kummerer, 2010. Pharmaceuticals in the Environment | Annual Review of Environment and Resources. *Annual Review of Environment and Resources* 35, 57–75.
<https://doi.org/10.1146/annurev-environ-052809-161223>

- Kummerer, K., 2004. Resistance in the environment. *Journal of Antimicrobial Chemotherapy* 54, 311–320. <https://doi.org/10.1093/jac/dkh325>
- Kunzelmann, M., Winter, M., Åberg, M., Hellenäs, K.-E., Rosén, J., 2018. Non-targeted analysis of unexpected food contaminants using LC-HRMS. *Anal Bioanal Chem* 410, 5593–5602. <https://doi.org/10.1007/s00216-018-1028-4>
- Kurkiewicz, S., Dzierzega-Leczna, A., Stępień, K., 2010. Comparison of the efficiency of silylating agents in GC/MS analysis of non-steroidal anti-inflammatory drugs. *Farmaceutyczny Przegląd Naukowy* 7, 28–32.
- Kuster, M., López de Alda, M.J., Hernando, M.D., Petrovic, M., Martín-Alonso, J., Barceló, D., 2008. Analysis and occurrence of pharmaceuticals, estrogens, progestogens and polar pesticides in sewage treatment plant effluents, river water and drinking water in the Llobregat river basin (Barcelona, Spain). *Journal of Hydrology* 358, 112–123. <https://doi.org/10.1016/j.jhydrol.2008.05.030>
- Kyle, P.B., 2017. Chapter 7 - Toxicology: GCMS, in: Nair, H., Clarke, W. (Eds.), *Mass Spectrometry for the Clinical Laboratory*. Academic Press, San Diego, pp. 131–163. <https://doi.org/10.1016/B978-0-12-800871-3.00007-9>
- Lacina, P., Mravcová, L., Vávrová, M., 2013. Application of comprehensive two-dimensional gas chromatography with mass spectrometric detection for the analysis of selected drug residues in wastewater and surface water. *Journal of Environmental Sciences* 25, 204–212. [https://doi.org/10.1016/S1001-0742\(12\)60006-0](https://doi.org/10.1016/S1001-0742(12)60006-0)
- Lai, Z., Fiehn, O., 2018. Mass spectral fragmentation of trimethylsilylated small molecules. *Mass Spectrometry Reviews* 37, 245–257. <https://doi.org/10.1002/mas.21518>
- Lajeunesse, A., Gagnon, C., 2007. Determination of acidic pharmaceutical products and carbamazepine in roughly primary-treated wastewater by solid-phase extraction and gas chromatography–tandem mass spectrometry. *International Journal of Environmental Analytical Chemistry* 87, 565–578. <https://doi.org/10.1080/03067310701189083>
- Latham, J.L., Burgess, A.E., 1977. *Elementary Reaction Kinetics*. Butterworths.

- Lavén, M., Alsberg, T., Yu, Y., Adolfsson-Erici, M., Sun, H., 2009. Serial mixed-mode cation- and anion-exchange solid-phase extraction for separation of basic, neutral and acidic pharmaceuticals in wastewater and analysis by high-performance liquid chromatography–quadrupole time-of-flight mass spectrometry. *Journal of Chromatography A* 1216, 49–62. <https://doi.org/10.1016/j.chroma.2008.11.014>
- Lawson, Lower, 2013. 6.1.6: The Collision Theory [WWW Document]. Chemistry LibreTexts. URL [https://chem.libretexts.org/Bookshelves/Physical_and_Theoretical_Chemistry_Textbook_Maps/Supplemental_Modules_\(Physical_and_Theoretical_Chemistry\)/Kinetics/06%3A_Modeling_Reaction_Kinetics/6.01%3A_Collision_Theory/6.1.06%3A_The_Collision_Theory](https://chem.libretexts.org/Bookshelves/Physical_and_Theoretical_Chemistry_Textbook_Maps/Supplemental_Modules_(Physical_and_Theoretical_Chemistry)/Kinetics/06%3A_Modeling_Reaction_Kinetics/6.01%3A_Collision_Theory/6.1.06%3A_The_Collision_Theory) (accessed 2.2.22).
- Lechner, 2021. 10.4 Experimental design [WWW Document]. URL https://sisu.ut.ee/lcms_method_validation/104-experimental-design (accessed 12.1.21).
- LECO, 2021. ChromaTOF® Tile Analytical Software.
- LECO, 2020. ChromaTOF Tile Guidance Document.
- Lee, 2020. Dynamic equilibrium [WWW Document]. Chemistry LibreTexts. URL [https://chem.libretexts.org/Bookshelves/Physical_and_Theoretical_Chemistry_Textbook_Maps/Supplemental_Modules_\(Physical_and_Theoretical_Chemistry\)/Equilibria/Chemical_Equilibria/Principles_of_Chemical_Equilibria/Dynamic_equilibrium](https://chem.libretexts.org/Bookshelves/Physical_and_Theoretical_Chemistry_Textbook_Maps/Supplemental_Modules_(Physical_and_Theoretical_Chemistry)/Equilibria/Chemical_Equilibria/Principles_of_Chemical_Equilibria/Dynamic_equilibrium) (accessed 1.5.22).
- Leeson, P.D., 2016. Molecular inflation, attrition and the rule of five. *Advanced Drug Delivery Reviews*, Understanding the challenges of beyond-rule-of-5 compounds 101, 22–33. <https://doi.org/10.1016/j.addr.2016.01.018>
- Lewis, S.W., 2009. 11 - Analysis of dyes using chromatography, in: Houck, M.M. (Ed.), *Identification of Textile Fibers*, Woodhead Publishing Series in Textiles. Woodhead Publishing, pp. 203–223. <https://doi.org/10.1533/9781845695651.2.203>
- Li, 2014. Occurrence, sources, and fate of pharmaceuticals in aquatic environment and soil. *Environmental Pollution* 187, 193–201. <https://doi.org/10.1016/j.envpol.2014.01.015>

- Li, S., 2017. Chapter 2 - Fundamentals of Reaction Kinetics, in: Li, S. (Ed.), *Reaction Engineering*. Butterworth-Heinemann, Boston, pp. 25–93. <https://doi.org/10.1016/B978-0-12-410416-7.00002-1>
- Li, Sabourin, L., Renaud, J., Halloran, S., Singh, A., Sumarah, M., Dagnew, M., Ray, M.B., 2021. Simultaneous quantification of five pharmaceuticals and personal care products in biosolids and their fate in thermo-alkaline treatment. *Journal of Environmental Management* 278, 111404. <https://doi.org/10.1016/j.jenvman.2020.111404>
- Li, Ye, Q., Gan, J., 2014. Degradation and transformation products of acetaminophen in soil. *Water Research* 49, 44–52. <https://doi.org/10.1016/j.watres.2013.11.008>
- Lima, M.L., Luís, S., Poggio, L., Aragonés, J.I., Courtier, A., Roig, B., Calas-Blanchard, C., 2020. The importance of household pharmaceutical products disposal and its risk management: Example from Southwestern Europe. *Waste Management* 104, 139–147. <https://doi.org/10.1016/j.wasman.2020.01.008>
- Lindberg, C., Jönsson, S., 1982. Simultaneous determination of terbutaline and salbutamol in plasma by selected ion monitoring. *Biomedical Mass Spectrometry* 9, 493–494. <https://doi.org/10.1002/bms.1200091107>
- Lipinski, C.A., Lombardo, F., Dominy, B.W., Feeney, P.J., 1997. Experimental and computational approaches to estimate solubility and permeability in drug discovery and development settings. *Advanced Drug Delivery Reviews, In Vitro Models for Selection of Development Candidates* 23, 3–25. [https://doi.org/10.1016/S0169-409X\(96\)00423-1](https://doi.org/10.1016/S0169-409X(96)00423-1)
- Little, J.L., 1999. Artifacts in trimethylsilyl derivatization reactions and ways to avoid them. *Journal of Chromatography A* 844, 1–22. [https://doi.org/10.1016/S0021-9673\(99\)00267-8](https://doi.org/10.1016/S0021-9673(99)00267-8)
- Löffler, D., Ternes, T.A., 2003. Determination of acidic pharmaceuticals, antibiotics and ivermectin in river sediment using liquid chromatography–tandem mass spectrometry. *Journal of Chromatography A* 1021, 133–144. <https://doi.org/10.1016/j.chroma.2003.08.089>
- Logarinho, F., Rosado, T., Lourenço, C., Barroso, M., Araujo, A.R.T.S., Gallardo, E., 2016. Determination of antipsychotic drugs in hospital and wastewater treatment plant samples by

- gas chromatography/tandem mass spectrometry. *Journal of Chromatography B* 1038, 127–135. <https://doi.org/10.1016/j.jchromb.2016.10.031>
- López Zavala, M.Á., Reynoso-Cuevas, L., 2015. Simultaneous extraction and determination of four different groups of pharmaceuticals in compost using optimized ultrasonic extraction and ultrahigh pressure liquid chromatography–mass spectrometry. *Journal of Chromatography A* 1423, 9–18. <https://doi.org/10.1016/j.chroma.2015.10.051>
- Lua, L., Murphy, Blanchard, 2013. 2.8: Second-Order Reactions [WWW Document]. Chemistry LibreTexts. URL [https://chem.libretexts.org/Bookshelves/Physical_and_Theoretical_Chemistry_Textbook_Maps/Supplemental_Modules_\(Physical_and_Theoretical_Chemistry\)/Kinetics/02%3A_Reaction_Rates/2.08%3A_Second-Order_Reactions](https://chem.libretexts.org/Bookshelves/Physical_and_Theoretical_Chemistry_Textbook_Maps/Supplemental_Modules_(Physical_and_Theoretical_Chemistry)/Kinetics/02%3A_Reaction_Rates/2.08%3A_Second-Order_Reactions) (accessed 3.12.21).
- Lund Research Ltd., 2018. One-way ANOVA in Minitab | Procedure, output and interpretation of the output using a relevant example. [WWW Document]. URL <https://statistics.laerd.com/minitab-tutorials/one-way-anova-using-minitab.php> (accessed 7.14.21).
- Luque de Castro, M.D., Priego-Capote, F., Peralbo-Molina, A., 2011. The role of ultrasound in analytical derivatizations. *Journal of Chromatography B, ENHANCEMENT OF ANALYSIS BY ANALYTICAL DERIVATIZATION* 879, 1189–1195. <https://doi.org/10.1016/j.jchromb.2010.09.002>
- Macherius, A., Eggen, T., Lorenz, W., Moeder, M., Ondruschka, J., Reemtsma, T., 2012. Metabolization of the Bacteriostatic Agent Triclosan in Edible Plants and its Consequences for Plant Uptake Assessment. *Environ. Sci. Technol.* 46, 10797–10804. <https://doi.org/10.1021/es3028378>
- Marriott, P.J., Massil, T., Hügel, H., 2004. Molecular structure retention relationships in comprehensive two-dimensional gas chromatography. *Journal of Separation Science* 27, 1273–1284. <https://doi.org/10.1002/jssc.200401917>

- Marsik, P., Rezek, J., Židková, M., Kramulová, B., Tauchen, J., Vaněk, T., 2017. Non-steroidal anti-inflammatory drugs in the watercourses of Elbe basin in Czech Republic. *Chemosphere* 171, 97–105. <https://doi.org/10.1016/j.chemosphere.2016.12.055>
- Martín, J., Santos, J.L., Aparicio, I., Alonso, E., 2010. Multi-residue method for the analysis of pharmaceutical compounds in sewage sludge, compost and sediments by sonication-assisted extraction and LC determination. *Journal of Separation Science* 33, 1760–1766. <https://doi.org/10.1002/jssc.200900873>
- Matamoros, V., Jover, E., Bayona, J.M., 2010. Part-per-Trillion Determination of Pharmaceuticals, Pesticides, and Related Organic Contaminants in River Water by Solid-Phase Extraction Followed by Comprehensive Two-Dimensional Gas Chromatography Time-of-Flight Mass Spectrometry. *Anal. Chem.* 82, 699–706. <https://doi.org/10.1021/ac902340e>
- McClellan, K., Halden, R.U., 2010. Pharmaceuticals and personal care products in archived U.S. biosolids from the 2001 EPA national sewage sludge survey. *Water Research, Emerging Contaminants in water: Occurrence, fate, removal and assessment in the water cycle (from wastewater to drinking water)* 44, 658–668. <https://doi.org/10.1016/j.watres.2009.12.032>
- Mehinto, A.C., Hill, E.M., Tyler, C.R., 2010. Uptake and Biological Effects of Environmentally Relevant Concentrations of the Nonsteroidal Anti-inflammatory Pharmaceutical Diclofenac in Rainbow Trout (*Oncorhynchus mykiss*). *Environ. Sci. Technol.* 44, 2176–2182. <https://doi.org/10.1021/es903702m>
- Meredith, T.J., Goulding, R., 1980. Paracetamol. *Postgrad Med J* 56, 459–473.
- Migowska, N., Caban, M., Stepnowski, P., Kumirska, J., 2012. Simultaneous analysis of non-steroidal anti-inflammatory drugs and estrogenic hormones in water and wastewater samples using gas chromatography–mass spectrometry and gas chromatography with electron capture detection. *Science of The Total Environment* 441, 77–88. <https://doi.org/10.1016/j.scitotenv.2012.09.043>
- Mikulic, 2021. Topic: Global pharmaceutical industry [WWW Document]. Statista. URL <https://www.statista.com/topics/1764/global-pharmaceutical-industry/> (accessed 11.14.21).

- Milman, B.L., Zhurkovich, I.K., 2017. The chemical space for non-target analysis. *TrAC Trends in Analytical Chemistry* 97, 179–187. <https://doi.org/10.1016/j.trac.2017.09.013>
- Minitab Inc, 2022a. Interpret the key results for Analyze Factorial Design [WWW Document]. URL <https://support.minitab.com/en-us/minitab/18/help-and-how-to/modeling-statistics/doe/how-to/factorial/analyze-factorial-design/interpret-the-results/key-results/> (accessed 11.11.20).
- Minitab Inc, 2022b. What is response optimization? [WWW Document]. URL <https://support.minitab.com/en-us/minitab/18/help-and-how-to/modeling-statistics/using-fitted-models/supporting-topics/response-optimization/what-is-response-optimization/> (accessed 11.12.20).
- Minitab Inc., 2021a. Overview for Contour Plot [WWW Document]. URL <https://support.minitab.com/en-us/minitab/18/help-and-how-to/modeling-statistics/using-fitted-models/how-to/contour-plot/before-you-start/overview/> (accessed 12.27.21).
- Minitab Inc, 2021. What is an optimization plot? [WWW Document]. URL <https://support.minitab.com/en-us/minitab/18/help-and-how-to/modeling-statistics/using-fitted-models/supporting-topics/response-optimization/what-is-an-optimization-plot/> (accessed 12.27.21).
- Minitab Inc., 2021b. Data considerations for 2-Sample t [WWW Document]. URL <https://support.minitab.com/en-us/minitab-express/1/help-and-how-to/basic-statistics/inference/how-to/two-samples/2-sample-t/before-you-start/data-considerations/> (accessed 7.14.21).
- Minitab Inc., 2021c. Methods and formulas for 2-Sample t [WWW Document]. URL <https://support.minitab.com/en-us/minitab-express/1/help-and-how-to/basic-statistics/inference/how-to/two-samples/2-sample-t/methods-and-formulas/methods-and-formulas/> (accessed 7.14.21).
- Minitab Inc., 2020. Effects plots for Analyze Factorial Design [WWW Document]. URL <https://support.minitab.com/en-us/minitab/18/help-and-how-to/modeling-statistics/doe/how-to/factorial/analyze-factorial-design/interpret-the-results/all-statistics-and-graphs/effects-plots/> (accessed 11.11.20).

- Minitab Inc, 2019. Interpret the key results for Contour Plot [WWW Document]. URL <https://support.minitab.com/en-us/minitab/18/help-and-how-to/modeling-statistics/using-fitted-models/how-to/contour-plot/interpret-the-results/key-results/> (accessed 12.27.21).
- Minitab Inc., 2017a. Design of Experiments (DOE).
- Minitab Inc., 2017b. What are individual desirability and composite desirability? [WWW Document]. URL <https://support.minitab.com/en-us/minitab/18/help-and-how-to/modeling-statistics/using-fitted-models/supporting-topics/response-optimization/what-are-individual-desirability-and-composite-desirability/> (accessed 5.24.21).
- Mohapatra, D.P., Cledón, M., Brar, S.K., Surampalli, R.Y., 2016. Application of Wastewater and Biosolids in Soil: Occurrence and Fate of Emerging Contaminants. *Water Air Soil Pollut* 227, 77. <https://doi.org/10.1007/s11270-016-2768-4>
- Moldoveanu and David, 2014. *Modern Sample Preparation for Chromatography*. Elsevier.
- Müller, A., Schulz, W., Ruck, W.K.L., Weber, W.H., 2011. A new approach to data evaluation in the non-target screening of organic trace substances in water analysis. *Chemosphere* 85, 1211–1219. <https://doi.org/10.1016/j.chemosphere.2011.07.009>
- National Institute of Standards and Technology, 2013. 5.3.1. What are the objectives? [WWW Document]. URL <https://www.itl.nist.gov/div898/handbook/pri/section3/pri31.htm> (accessed 11.12.20).
- National Institute of Standards and Technology, 2012a. 4.3.1. What is design of experiments (DOE)? [WWW Document]. e-Handbook of Statistical Methods. URL <https://www.itl.nist.gov/div898/handbook/pmd/section3/pmd31.htm> (accessed 11.17.21).
- National Institute of Standards and Technology, 2012b. 5.3.3.4.6. Screening designs [WWW Document]. e-Handbook of Statistical Methods. URL <https://www.itl.nist.gov/div898/handbook/pri/section3/pri3346.htm> (accessed 11.11.20).
- National Institute of Standards and Technology, 2009. Electron Ionization Library Component of the NIST/EPA/NIH Mass Spectral Library and NIST GC Retention Index Database [WWW Document]. NIST. URL <https://www.nist.gov/programs-projects/electron-ionization-library-component-nistepanih-mass-spectral-library-and-nist-gc> (accessed 10.28.21).

- Nebot, C., Falcon, R., Boyd, K.G., Gibb, S.W., 2015. Introduction of human pharmaceuticals from wastewater treatment plants into the aquatic environment: a rural perspective. *Environ Sci Pollut Res* 22, 10559–10568. <https://doi.org/10.1007/s11356-015-4234-z>
- NHS Digital, 2018. Practice level prescribing - glossary of terms [WWW Document]. NHS Digital. URL <https://digital.nhs.uk/data-and-information/areas-of-interest/prescribing/practice-level-prescribing-in-england-a-summary/practice-level-prescribing-glossary-of-terms> (accessed 8.6.20).
- NHS Inform, 2021a. Paracetamol [WWW Document]. URL <https://www.nhsinform.scot/tests-and-treatments/medicines-and-medical-aids/types-of-medicine/paracetamol> (accessed 11.13.21).
- NHS Inform, 2021b. Ibuprofen uses and side effects [WWW Document]. URL <https://www.nhsinform.scot/tests-and-treatments/medicines-and-medical-aids/types-of-medicine/ibuprofen> (accessed 11.13.21).
- Nikolin, B., Imamović, B., Medanhodžić-Vuk, S., Sober, M., 2004. HIGH PERFORMANCE LIQUID CHROMATOGRAPHY IN PHARMACEUTICAL ANALYSES. *Bosn J Basic Med Sci* 4, 5–9.
- Noctor, G., Bergot, G., Mauve, C., Thominet, D., Lelarge-Trouverie, C., Prioul, J.-L., 2007. A comparative study of amino acid measurement in leaf extracts by gas chromatography-time of flight-mass spectrometry and high performance liquid chromatography with fluorescence detection. *Metabolomics* 3, 161–174. <https://doi.org/10.1007/s11306-007-0057-3>
- NursingNotes, 2017. Top 100 Most-Prescribed Medications in UK Hospitals [WWW Document]. NursingNotes. URL <https://nursingnotes.co.uk/the-100-most-common-medications-in-uk-hospitals/> (accessed 6.1.18).
- Ohoru, C.R., Adeniji, A.O., Okoh, A.I., Okoh, O.O., 2019. Distribution and Chemical Analysis of Pharmaceuticals and Personal Care Products (PPCPs) in the Environmental Systems: A Review. *Int J Environ Res Public Health* 16, 3026. <https://doi.org/10.3390/ijerph16173026>
- Öllers, S., Singer, H.P., Fässler, P., Müller, S.R., 2001. Simultaneous quantification of neutral and acidic pharmaceuticals and pesticides at the low-ng/l level in surface and waste water. *Journal of Chromatography A* 911, 225–234. [https://doi.org/10.1016/S0021-9673\(01\)00514-3](https://doi.org/10.1016/S0021-9673(01)00514-3)

- Ong, S.G.M., Chitneni, M., Lee, K.S., Ming, L.C., Yuen, K.H., 2016. Evaluation of Extrusion Technique for Nanosizing Liposomes. *Pharmaceutics* 8, 36.
<https://doi.org/10.3390/pharmaceutics8040036>
- Orata, F., 2012. Derivatization Reactions and Reagents for Gas Chromatography Analysis. *Advanced Gas Chromatography - Progress in Agricultural, Biomedical and Industrial Applications* 27.
- Orozco-Solano, M., Ruiz-Jiménez, J., Luque de Castro, M.D., 2010. Ultrasound-assisted extraction and derivatization of sterols and fatty alcohols from olive leaves and drupes prior to determination by gas chromatography–tandem mass spectrometry. *Journal of Chromatography A* 1217, 1227–1235. <https://doi.org/10.1016/j.chroma.2009.12.040>
- Ouellette, R.J., Rawn, J.D., 2015. 7 - Nucleophilic Substitution and Elimination Reactions, in: Ouellette, R.J., Rawn, J.D. (Eds.), *Principles of Organic Chemistry*. Elsevier, Boston, pp. 189–208. <https://doi.org/10.1016/B978-0-12-802444-7.00007-0>
- Oviedo, C., Rodríguez, J., 2003. EDTA: The chelating agent under environmental scrutiny. *Química Nova* 26, 901–905. <https://doi.org/10.1590/S0100-40422003000600020>
- Pan, Z., Qu, W., Ma, H., Atungulu, G.G., McHugh, T.H., 2012. Continuous and pulsed ultrasound-assisted extractions of antioxidants from pomegranate peel. *Ultrasonics Sonochemistry* 19, 365–372. <https://doi.org/10.1016/j.ultsonch.2011.05.015>
- Panuwet, P., Hunter, R.E., D'Souza, P.E., Chen, X., Radford, S.A., Cohen, J.R., Marder, M.E., Kartavenka, K., Ryan, P.B., Barr, D.B., 2016. Biological Matrix Effects in Quantitative Tandem Mass Spectrometry-Based Analytical Methods: Advancing Biomonitoring. *Crit Rev Anal Chem* 46, 93–105. <https://doi.org/10.1080/10408347.2014.980775>
- Parkinson, D.R., 2012. 2.26 - Analytical Derivatization Techniques, in: Pawliszyn, J. (Ed.), *Comprehensive Sampling and Sample Preparation*. Academic Press, Oxford, pp. 559–595.
<https://doi.org/10.1016/B978-0-12-381373-2.00060-0>
- Parsons, B.A., Marney, L.C., Siegler, W.C., Hoggard, J.C., Wright, B.W., Synovec, R.E., 2015. Tile-Based Fisher Ratio Analysis of Comprehensive Two-Dimensional Gas Chromatography Time-of-Flight Mass Spectrometry (GC × GC–TOFMS) Data Using a Null Distribution Approach. *Anal. Chem.* 87, 3812–3819. <https://doi.org/10.1021/ac504472s>

- Pawlowski, S., van Aerle, R., Tyler, C.R., Braunbeck, T., 2004. Effects of 17 α -ethinylestradiol in a fathead minnow (*Pimephales promelas*) gonadal recrudescence assay. *Ecotoxicology and Environmental Safety* 57, 330–345. <https://doi.org/10.1016/j.ecoenv.2003.07.019>
- Pereira, R.O., Postigo, C., de Alda, M.L., Daniel, L.A., Barceló, D., 2011. Removal of estrogens through water disinfection processes and formation of by-products. *Chemosphere* 82, 789–799. <https://doi.org/10.1016/j.chemosphere.2010.10.082>
- Pérez-Lemus, N., López-Serna, R., Pérez-Elvira, S.I., Barrado, E., 2019. Analytical methodologies for the determination of pharmaceuticals and personal care products (PPCPs) in sewage sludge: A critical review. *Analytica Chimica Acta* 1083, 19–40. <https://doi.org/10.1016/j.aca.2019.06.044>
- Petrović, M., Gonzalez, S., Barceló, D., 2003. Analysis and removal of emerging contaminants in wastewater and drinking water. *TrAC Trends in Analytical Chemistry* 22, 685–696. [https://doi.org/10.1016/S0165-9936\(03\)01105-1](https://doi.org/10.1016/S0165-9936(03)01105-1)
- Peysson, W., Vulliet, E., 2013. Determination of 136 pharmaceuticals and hormones in sewage sludge using quick, easy, cheap, effective, rugged and safe extraction followed by analysis with liquid chromatography–time-of-flight-mass spectrometry. *Journal of Chromatography A* 1290, 46–61. <https://doi.org/10.1016/j.chroma.2013.03.057>
- Phillips, P.J., Schubert, C., Argue, D., Fisher, I., Furlong, E.T., Foreman, W., Gray, J., Chalmers, A., 2015. Concentrations of hormones, pharmaceuticals and other micropollutants in groundwater affected by septic systems in New England and New York. *Science of The Total Environment* 512–513, 43–54. <https://doi.org/10.1016/j.scitotenv.2014.12.067>
- Pierce, 2004. *GC Derivatization*.
- Pierce, A.E., 1968. *Silylation of Organic Compounds: a technique for gas-phase analysis*. Pierce Chemical Co., Rockford, Illinois.
- Pietrogrande, M.C., Manarini, F., Quintana, J.B., Rodil, R., Villaverde-de-Sáa, E., Visentin, M., 2017. Optimization of an ultrasound-assisted derivatization for GC/MS analysis of oxygenated organic species in atmospheric aerosol. *Anal Bioanal Chem* 409, 4279–4291. <https://doi.org/10.1007/s00216-017-0379-6>

- Pitt, J.J., 2009. Principles and Applications of Liquid Chromatography-Mass Spectrometry in Clinical Biochemistry. *Clin Biochem Rev* 30, 19–34.
- Prebihalo, S., Brockman, A., Cochran, J., Dorman, F.L., 2015. Determination of emerging contaminants in wastewater utilizing comprehensive two-dimensional gas-chromatography coupled with time-of-flight mass spectrometry. *Journal of Chromatography A* 1419, 109–115. <https://doi.org/10.1016/j.chroma.2015.09.080>
- Prebihalo, S.E., 2020. Advanced chemometrics and fundamental considerations for non-targeted analysis with comprehensive multidimensional gas chromatography coupled with time-of-flight mass spectrometry (Thesis).
- Preisner, M., Neverova-Dziopak, E., Kowalewski, Z., 2021. Mitigation of eutrophication caused by wastewater discharge: A simulation-based approach. *Ambio* 50, 413–424. <https://doi.org/10.1007/s13280-020-01346-4>
- Prozorov, T., Prozorov, R., Suslick, K.S., 2004. High Velocity Interparticle Collisions Driven by Ultrasound. *J. Am. Chem. Soc.* 126, 13890–13891. <https://doi.org/10.1021/ja049493o>
- Radjenović, J., Jelić, A., Petrović, M., Barceló, D., 2009. Determination of pharmaceuticals in sewage sludge by pressurized liquid extraction (PLE) coupled to liquid chromatography-tandem mass spectrometry (LC-MS/MS). *Anal Bioanal Chem* 393, 1685–1695. <https://doi.org/10.1007/s00216-009-2604-4>
- Rakitzis, E.T., Papandreou, P., 1999. Kinetic Analysis of Parallel Reactions, the Initial Reactant of which Presents with two Interconvertible Isomeric Forms (hydrolysis and hydroxylaminolysis of 6-phosphogluconolactone). *Journal of Theoretical Biology* 200, 427–434. <https://doi.org/10.1006/jtbi.1999.1006>
- Rao, P., Knaus, E.E., 2008. Evolution of nonsteroidal anti-inflammatory drugs (NSAIDs): cyclooxygenase (COX) inhibition and beyond. *J Pharm Pharm Sci* 11, 81s–110s. <https://doi.org/10.18433/j3t886>
- Rodriguez-Mozaz, S., Chamorro, S., Marti, E., Huerta, B., Gros, M., Sánchez-Melsió, A., Borrego, C.M., Barceló, D., Balcázar, J.L., 2015. Occurrence of antibiotics and antibiotic resistance

- genes in hospital and urban wastewaters and their impact on the receiving river. *Water Research* 69, 234–242. <https://doi.org/10.1016/j.watres.2014.11.021>
- Rogowska, J., Cieszyńska-Semenowicz, M., Ratajczyk, W., Wolska, L., 2020. Micropollutants in treated wastewater. *Ambio* 49, 487–503. <https://doi.org/10.1007/s13280-019-01219-5>
- Rosenfeld, P.E., Feng, L.G.H., 2011. 16 - Emerging Contaminants, in: Rosenfeld, P.E., Feng, L.G.H. (Eds.), *Risks of Hazardous Wastes*. William Andrew Publishing, Boston, pp. 215–222. <https://doi.org/10.1016/B978-1-4377-7842-7.00016-7>
- Royal Society of Chemistry, 2019. *Green Chemistry – The atom economy*.
- Sacher, F., Lange, F.T., Brauch, H.-J., Blankenhorn, I., 2001. Pharmaceuticals in groundwaters: Analytical methods and results of a monitoring program in Baden-Württemberg, Germany. *Journal of Chromatography A, 10th Symposium on Handling of Environmental and Biological Samples in Chromatography* 938, 199–210. [https://doi.org/10.1016/S0021-9673\(01\)01266-3](https://doi.org/10.1016/S0021-9673(01)01266-3)
- Samaras, Thomaidis, N., Stasinakis, A., Gatidou, G., Lekkas, T., 2010. Determination of selected non-steroidal anti-inflammatory drugs in wastewater by gas chromatography – mass spectrometry. *International Journal of Environmental Analytical Chemistry* 90, 219–229. <https://doi.org/10.1080/03067310903243936>
- Samaras, Thomaidis, N.S., Stasinakis, A.S., Lekkas, T.D., 2011. An analytical method for the simultaneous trace determination of acidic pharmaceuticals and phenolic endocrine disrupting chemicals in wastewater and sewage sludge by gas chromatography-mass spectrometry. *Anal Bioanal Chem* 399, 2549–2561. <https://doi.org/10.1007/s00216-010-4607-6>
- Samaras, V.G., Stasinakis, A.S., Mamais, D., Thomaidis, N.S., Lekkas, T.D., 2013. Fate of selected pharmaceuticals and synthetic endocrine disrupting compounds during wastewater treatment and sludge anaerobic digestion. *Journal of Hazardous Materials* 244–245, 259–267. <https://doi.org/10.1016/j.jhazmat.2012.11.039>
- Sampsonidis, I., 2019. *Semi-volatile organic compounds in underground coal gasification effluents: from sample preparation to data analysis (PhD)*. University of Glasgow.

- Sánchez Ávila, N., Priego Capote, F., Luque de Castro, M.D., 2007. Ultrasound-assisted extraction and silylation prior to gas chromatography–mass spectrometry for the characterization of the triterpenic fraction in olive leaves. *Journal of Chromatography A* 1165, 158–165.
<https://doi.org/10.1016/j.chroma.2007.07.039>
- Santos, Gros, M., Rodriguez-Mozaz, S., Delerue-Matos, C., Pena, A., Barceló, D., Montenegro, M.C.B.S.M., 2013. Contribution of hospital effluents to the load of pharmaceuticals in urban wastewaters: Identification of ecologically relevant pharmaceuticals. *Science of The Total Environment* 461–462, 302–316. <https://doi.org/10.1016/j.scitotenv.2013.04.077>
- Santos, H.M., Capelo, J.L., 2007. Trends in ultrasonic-based equipment for analytical sample treatment. *Talanta* 73, 795–802. <https://doi.org/10.1016/j.talanta.2007.05.039>
- Sartorius, 2020. What is DOE? Design of Experiments Basics for Beginners [WWW Document]. Sartorius. URL <https://www.sartorius.com/en/knowledge/science-snippets/what-is-doe-design-of-experiments-basics-for-beginners-507170> (accessed 11.17.21).
- Schulman, L.J., Sargent, E.V., Naumann, B.D., Faria, E.C., Dolan, D.G., Wargo, J.P., 2002. A Human Health Risk Assessment of Pharmaceuticals in the Aquatic Environment. *Human and Ecological Risk Assessment: An International Journal* 8, 657–680.
<https://doi.org/10.1080/20028091057141>
- Scottish Government, 2021. Sewage sludge processing systems in Scotland.
- Sebők, Á., Vasánits-Zsigrai, A., Palkó, Gy., Záray, Gy., Molnár-Perl, I., 2008. Identification and quantification of ibuprofen, naproxen, ketoprofen and diclofenac present in waste-waters, as their trimethylsilyl derivatives, by gas chromatography mass spectrometry. *Talanta* 76, 642–650. <https://doi.org/10.1016/j.talanta.2008.04.008>
- Seidi, S., Yamini, Y., 2012. Analytical sonochemistry; developments, applications, and hyphenations of ultrasound in sample preparation and analytical techniques. *Open Chemistry* 10.
<https://doi.org/10.2478/s11532-011-0160-1>
- Seoud, O.A.E., Baader, W.J., Bastos, E.L., 2016. Practical Chemical Kinetics in Solution, in: *Encyclopedia of Physical Organic Chemistry*. American Cancer Society, pp. 1–68.
<https://doi.org/10.1002/9781118468586.epoc1012>

- SepSolve Analytical, 2016. Technical note: Comprehensive two-dimensional gas chromatography.
- Serre, J., 1984. Theoretical approach of the chemical reactivity: The SN2 reaction. *International Journal of Quantum Chemistry* 26, 593–605. <https://doi.org/10.1002/qua.560260504>
- Shanmugam, G., Ramaswamy, B.R., Radhakrishnan, V., Tao, H., 2010. GC–MS method for the determination of paraben preservatives in the human breast cancerous tissue. *Microchemical Journal, Polar Chemistry* 96, 391–396. <https://doi.org/10.1016/j.microc.2010.07.005>
- Shareef, A., Angove, M.J., Wells, J.D., 2006. Optimization of silylation using N-methyl-N-(trimethylsilyl)-trifluoroacetamide, N,O-bis-(trimethylsilyl)-trifluoroacetamide and N-(tert-butyl-dimethylsilyl)-N-methyltrifluoroacetamide for the determination of the estrogens estrone and 17 α -ethinyloestradiol by gas chromatography–mass spectrometry. *Journal of Chromatography A* 1108, 121–128. <https://doi.org/10.1016/j.chroma.2005.12.098>
- Sheldon, R.A., 2017. The E factor 25 years on: the rise of green chemistry and sustainability. *Green Chem.* 19, 18–43. <https://doi.org/10.1039/C6GC02157C>
- Sheldon, R.A., Norton, M., 2020. Green chemistry and the plastic pollution challenge: towards a circular economy. *Green Chem.* 22, 6310–6322. <https://doi.org/10.1039/D0GC02630A>
- Shimadzu, 2020a. About Resolution, Part 1 : SHIMADZU (Shimadzu Corporation) [WWW Document]. URL <https://www.shimadzu.com/an/hplc/support/lib/ictalk/resol-1.html> (accessed 6.23.20).
- Shimadzu, 2020b. 2. Analysis Results [WWW Document]. URL <https://www.shimadzu.com/an/service-support/technical-support/analysis-basics/fundamentals/results.html> (accessed 7.12.21).
- Shimadzu, 2012. GC \times GC Handbook Fundamental Principles of Comprehensive 2D GC 31.
- Sigma Aldrich, 2021. Ethylenediaminetetraacetic acid 99% | 60-00-4.
- Sigma Aldrich, 2018. Product Information 69479 N-Methyl-N-(trimethylsilyl)trifluoroacetamide for GC derivatization, LiChropur®.
- Sigma Aldrich, 2011. Derivatization Reagents.
- Sigma Aldrich, 1997a. BSTFA + TMCS - Product Specification.
- Sigma Aldrich, 1997b. Guide to Derivatization Reagents for GC.

- Sigma-Aldrich, 2007. Harnessing the Power of Chromatographic Selectivity [WWW Document].
Sigma-Aldrich. URL <https://www.sigmaaldrich.com/analytical-chromatography/hplc/learning-center/chromatographic-selectivity.html> (accessed 6.23.20).
- Smith, 2019. Dynamic Equilibrium | What Is It, Examples, Definition. URL
<https://chemdictionary.org/dynamic-equilibrium/> (accessed 1.5.22).
- Smith, 2017. Le Chatelier's Principle Definition And Examples | Chemistry Dictionary. URL
<https://chemdictionary.org/le-chateliers-principle/> (accessed 1.5.22).
- Sobolevsky, T.G., Revelsky, A.I., Miller, B., Oriedo, V., Chernetsova, E.S., Revelsky, I.A., 2003.
Comparison of silylation and esterification/acylation procedures in GC-MS analysis of amino acids. *Journal of Separation Science* 26, 1474–1478. <https://doi.org/10.1002/jssc.200301492>
- Söderholm, S.L., Damm, M., Kappe, C.O., 2010. Microwave-assisted derivatization procedures for gas chromatography/mass spectrometry analysis. *Mol Divers* 14, 869–888.
<https://doi.org/10.1007/s11030-010-9242-9>
- Song, S.M., Marriott, P., Kotsos, A., Drummer, O.H., Wynne, P., 2004. Comprehensive two-dimensional gas chromatography with time-of-flight mass spectrometry (GC × GC-TOFMS) for drug screening and confirmation. *Forensic Science International, Excerpts from TIAFT* 2003, Melbourne 143, 87–101. <https://doi.org/10.1016/j.forsciint.2004.02.042>
- Söregård, M., Campos-Pereira, H., Ullberg, M., Lai, F.Y., Golovko, O., Ahrens, L., 2019. Mass loads, source apportionment, and risk estimation of organic micropollutants from hospital and municipal wastewater in recipient catchments. *Chemosphere* 234, 931–941.
<https://doi.org/10.1016/j.chemosphere.2019.06.041>
- Sparkman, O.D., Penton, Z.E., Kitson, F.G. (Eds.), 2011. Appendix H - Points of Comparison of LC/MS vs GC/MS, in: *Gas Chromatography and Mass Spectrometry (Second Edition)*. Academic Press, Amsterdam, pp. 459–462. <https://doi.org/10.1016/B978-0-12-373628-4.00044-7>
- Speight, J.G., 2020. 5 - Sources of water pollution, in: Speight, J.G. (Ed.), *Natural Water Remediation*. Butterworth-Heinemann, pp. 165–198. <https://doi.org/10.1016/B978-0-12-803810-9.00005-X>

- Stalling, D.L., Gehrke, C.W., Zumwalt, R.W., 1968. A new silylation reagent for amino acids bis (trimethylsilyl)trifluoroacetamide (BSTFA). *Biochemical and Biophysical Research Communications* 31, 616–622. [https://doi.org/10.1016/0006-291X\(68\)90523-8](https://doi.org/10.1016/0006-291X(68)90523-8)
- Statista, 2022. Granted patents in pharmaceuticals Europe 2009-2020 [WWW Document]. Statista. URL <https://www.statista.com/statistics/999563/granted-patents-in-pharmaceuticals-europe/> (accessed 1.12.22).
- Stewart, C., 2021. Topic: Contraception in the United Kingdom [WWW Document]. Statista. URL <https://www.statista.com/topics/3238/contraception-in-the-united-kingdom/> (accessed 1.12.22).
- Stupak, M., Goodall, I., Tomaniova, M., Pulkrabova, J., Hajslova, J., 2018. A novel approach to assess the quality and authenticity of Scotch Whisky based on gas chromatography coupled to high resolution mass spectrometry. *Analytica Chimica Acta* 1042, 60–70. <https://doi.org/10.1016/j.aca.2018.09.017>
- Sunartio, D., Ashokkumar, M., Grieser, F., 2007. Study of the Coalescence of Acoustic Bubbles as a Function of Frequency, Power, and Water-Soluble Additives. *J. Am. Chem. Soc.* 129, 6031–6036. <https://doi.org/10.1021/ja068980w>
- Tahrani, L., Van Loco, J., Ben Mansour, H., Reynolds, T., 2015. Occurrence of antibiotics in pharmaceutical industrial wastewater, wastewater treatment plant and sea waters in Tunisia. *Journal of Water and Health* 14, 208–213. <https://doi.org/10.2166/wh.2015.224>
- Tao, T., He, T., Mao, H., Wu, X., Liu, X., 2020. Non-Targeted Metabolomic Profiling of Coronary Heart Disease Patients With Taohong Siwu Decoction Treatment. *Front Pharmacol* 11, 651. <https://doi.org/10.3389/fphar.2020.00651>
- Ternes, T.A., 2001. Analytical methods for the determination of pharmaceuticals in aqueous environmental samples. *TrAC Trends in Analytical Chemistry* 20, 419–434. [https://doi.org/10.1016/S0165-9936\(01\)00078-4](https://doi.org/10.1016/S0165-9936(01)00078-4)
- Ternes, T.A., Bonerz, M., Herrmann, N., Löffler, D., Keller, E., Lacida, B.B., Alder, A.C., 2005. Determination of pharmaceuticals, iodinated contrast media and musk fragrances in sludge by

- LC tandem MS and GC/MS. *Journal of Chromatography A, Mass Spectrometry: Innovation and Application. Part IV 1067*, 213–223. <https://doi.org/10.1016/j.chroma.2004.10.096>
- Tetko, I.V., Livingstone, D.J., 2007. 5.27 - Rule-Based Systems to Predict Lipophilicity, in: Taylor, J.B., Trigg, D.J. (Eds.), *Comprehensive Medicinal Chemistry II*. Elsevier, Oxford, pp. 649–668. <https://doi.org/10.1016/B0-08-045044-X/00144-9>
- Themes, U.F.O., 2016. Mass spectrometry. *Basicmedical Key*. URL <https://basicmedicalkey.com/mass-spectrometry/> (accessed 10.27.21).
- Thermo Fischer Scientific Inc., 2022. Chromacol™ GOLD-Grade Inert Vials and Inserts [WWW Document]. URL <https://www.thermofisher.com/order/catalog/product/01-CVG> (accessed 2.3.22).
- Thermo Fischer Scientific Inc., 2008. BSTFA + TMCS.
- Thermo Fisher Scientific, 2016. Q Exactive Plus Orbitrap LC-MS/MS System - Characterize, quantify and confirm with unmatched confidence 4.
- Tiwari, B.K., 2015a. Ultrasound: A clean, green extraction technology. *TrAC Trends in Analytical Chemistry, Green Extraction Techniques 71*, 100–109. <https://doi.org/10.1016/j.trac.2015.04.013>
- Tiwari, B.K., 2015b. Ultrasound: A clean, green extraction technology. *TrAC Trends in Analytical Chemistry, Green Extraction Techniques 71*, 100–109. <https://doi.org/10.1016/j.trac.2015.04.013>
- TOFWERK, 2020. Advantages of Time-of-Flight Mass Spectrometry Over Quadrupole MS. TOFWERK. URL <https://www.tofwerk.com/advantages-time-of-flight-mass-spectrometry-over-quadrupole-ms/> (accessed 11.8.21).
- Tuckerman, M., 2015. 9.4: More Complex Reactions [WWW Document]. *Chemistry LibreTexts*. URL [https://chem.libretexts.org/Bookshelves/Physical_and_Theoretical_Chemistry_Textbook_Maps/Map%3A_Physical_Chemistry_for_the_Biosciences_\(Chang\)/09%3A_Chemical_Kinetics/9.04%3A_More_Complex_Reactions](https://chem.libretexts.org/Bookshelves/Physical_and_Theoretical_Chemistry_Textbook_Maps/Map%3A_Physical_Chemistry_for_the_Biosciences_(Chang)/09%3A_Chemical_Kinetics/9.04%3A_More_Complex_Reactions) (accessed 8.23.21).

- Ukaogo, P.O., Ewuzie, U., Onwuka, C.V., 2020. 21 - Environmental pollution: causes, effects, and the remedies, in: Chowdhary, P., Raj, A., Verma, D., Akhter, Y. (Eds.), *Microorganisms for Sustainable Environment and Health*. Elsevier, pp. 419–429. <https://doi.org/10.1016/B978-0-12-819001-2.00021-8>
- Ultrasonic baths, Elmasonic P series [WWW Document], n.d. . VWR. URL <https://uk.vwr.com/store/product/6509341/ultrasonic-baths-elmasonic-p-series> (accessed 11.4.21).
- US EPA, 2007. Method 1694: Pharmaceuticals and Personal Care Products in Water, Soil, Sediment, and Biosolids by HPLC/MS/MS 77.
- US EPA, 2003. Protecting Water Quality from Urban Runoff.
- US EPA, O., 2016. Basic Information about Biosolids [WWW Document]. URL <https://www.epa.gov/biosolids/basic-information-about-biosolids> (accessed 1.12.22).
- US EPA, O., 2013. Basics of Green Chemistry [WWW Document]. US EPA. URL <https://www.epa.gov/greenchemistry/basics-green-chemistry> (accessed 4.19.21).
- U.S. Food and Drug Administration, 2021. Fact Sheet: FDA at a Glance. FDA.
- Valett, H.M., Sheibley, R.W., 2009. Ground Water and Surface Water Interaction, in: Likens, G.E. (Ed.), *Encyclopedia of Inland Waters*. Academic Press, Oxford, pp. 691–702. <https://doi.org/10.1016/B978-012370626-3.00019-3>
- Vallejo, A., Usobiaga, A., Martinez-Arkarazo, I., Prieto, A., Etxebarria, N., Zuloaga, O., Fernández, L.A., 2010. Ultrasonic-assisted derivatization of estrogenic compounds in a cup horn booster and determination by GC-MS. *Journal of Separation Science* 33, 104–111. <https://doi.org/10.1002/jssc.200900449>
- Vannini, C., Domingo, G., Marsoni, M., De Mattia, F., Labra, M., Castiglioni, S., Bracale, M., 2011. Effects of a complex mixture of therapeutic drugs on unicellular algae *Pseudokirchneriella subcapitata*. *Aquatic Toxicology* 101, 459–465. <https://doi.org/10.1016/j.aquatox.2010.10.011>
- Veenaas, C., Bignert, A., Liljelind, P., Haglund, P., 2018. Nontarget Screening and Time-Trend Analysis of Sewage Sludge Contaminants via Two-Dimensional Gas Chromatography–High

- Resolution Mass Spectrometry. *Environmental Science & Technology* 52, 7813–7822.
<https://doi.org/10.1021/acs.est.8b01126>
- Veenas, C., Haglund, P., 2017. Methodology for non-target screening of sewage sludge using comprehensive two-dimensional gas chromatography coupled to high-resolution mass spectrometry. *Anal Bioanal Chem* 409, 4867–4883. <https://doi.org/10.1007/s00216-017-0429-0>
- Verenitch, S.S., Lowe, C.J., Mazumder, A., 2006. Determination of acidic drugs and caffeine in municipal wastewaters and receiving waters by gas chromatography–ion trap tandem mass spectrometry. *Journal of Chromatography A* 1116, 193–203.
<https://doi.org/10.1016/j.chroma.2006.03.005>
- Verlicchi, P., Al Aukidy, M., Galletti, A., Petrovic, M., Barceló, D., 2012. Hospital effluent: Investigation of the concentrations and distribution of pharmaceuticals and environmental risk assessment. *Science of The Total Environment* 430, 109–118.
<https://doi.org/10.1016/j.scitotenv.2012.04.055>
- Verlicchi, P., Al Aukidy, M., Zambello, E., 2015. What have we learned from worldwide experiences on the management and treatment of hospital effluent? — An overview and a discussion on perspectives. *Science of The Total Environment* 514, 467–491.
<https://doi.org/10.1016/j.scitotenv.2015.02.020>
- von Mühlen, C., Khummueng, W., Alcaraz Zini, C., Bastos Caramão, E., Marriott, P.J., 2006. Detector technologies for comprehensive two-dimensional gas chromatography. *Journal of Separation Science* 29, 1909–1921. <https://doi.org/10.1002/jssc.200500443>
- Wagner, J.R., Mount, E.M., Giles, H.F., 2014. 25 - Design of Experiments, in: Wagner, J.R., Mount, E.M., Giles, H.F. (Eds.), *Extrusion (Second Edition)*, *Plastics Design Library*. William Andrew Publishing, Oxford, pp. 291–308. <https://doi.org/10.1016/B978-1-4377-3481-2.00025-9>
- Walters, E., McClellan, K., Halden, R.U., 2010. Occurrence and loss over three years of 72 pharmaceuticals and personal care products from biosolids–soil mixtures in outdoor mesocosms. *Water Research* 44, 6011–6020. <https://doi.org/10.1016/j.watres.2010.07.051>

- Wang, N., Zhou, X., Wang, W., Wang, L., Jiang, L., Liu, T., Yu, D., 2021. Effect of high intensity ultrasound on the structure and solubility of soy protein isolate-pectin complex. *Ultrasonics Sonochemistry* 80, 105808. <https://doi.org/10.1016/j.ultsonch.2021.105808>
- Waters Corporation, 2003. Column Dimensions & Related HPLC Parameters.
- Waters Oasis Sample Extraction SPE Products : Waters [WWW Document], n.d. URL https://www.waters.com/waters/en_GB/Waters-Oasis-Sample-Extraction-SPE-Products/nav.htm?cid=513209&locale=en_GB (accessed 6.9.20).
- Watson, N.E., Parsons, B.A., Synovec, R.E., 2016. Performance evaluation of tile-based Fisher Ratio analysis using a benchmark yeast metabolome dataset. *Journal of Chromatography A* 1459, 101–111. <https://doi.org/10.1016/j.chroma.2016.06.067>
- Weatherall, 1990. In search of a cure. Oxford University Press.
- Wong, J.W.C., Fang, M., 2000. Effects of lime addition on sewage sludge composting process. *Water Research* 34, 3691–3698. [https://doi.org/10.1016/S0043-1354\(00\)00116-0](https://doi.org/10.1016/S0043-1354(00)00116-0)
- World Health Organisation, 2020. WHO | 2. Anatomical Therapeutic Chemical (ATC) Classification [WWW Document]. WHO. URL http://www.who.int/medicines/regulation/medicines-safety/toolkit_atc/en/ (accessed 8.6.20).
- World Health Organisation, 2018. WHOCC - Structure and principles [WWW Document]. Structure and Principles. URL https://www.whocc.no/atc/structure_and_principles/ (accessed 8.6.20).
- Wu, J., Hu, R., Yue, J., Yang, Z., Zhang, L., 2009. Determination of fecal sterols by gas chromatography–mass spectrometry with solid-phase extraction and injection-port derivatization. *Journal of Chromatography A* 1216, 1053–1058. <https://doi.org/10.1016/j.chroma.2008.12.054>
- Xiang, J., Wu, M., Lei, J., Fu, C., Gu, J., Xu, G., 2018. The fate and risk assessment of psychiatric pharmaceuticals from psychiatric hospital effluent. *Ecotoxicology and Environmental Safety* 150, 289–296. <https://doi.org/10.1016/j.ecoenv.2017.12.049>
- Xie, C.Z., 2009. Environmental Impacts of Effluent Containing EDTA from Dairy Processing Plants (Thesis). The University of Waikato.

- Xu, J., Wu, L., Chen, W., Chang, A.C., 2008. Simultaneous determination of pharmaceuticals, endocrine disrupting compounds and hormone in soils by gas chromatography–mass spectrometry. *Journal of Chromatography A* 1202, 189–195.
<https://doi.org/10.1016/j.chroma.2008.07.001>
- Xu, Li, X., Hu, X., Yin, D., 2017. Distribution and relevance of iodinated X-ray contrast media and iodinated trihalomethanes in an aquatic environment. *Chemosphere* 184, 253–260.
<https://doi.org/10.1016/j.chemosphere.2017.05.048>
- Xu, Xu, Y., Wang, H., Guo, C., Qiu, H., He, Y., Zhang, Y., Li, X., Meng, W., 2015. Occurrence of antibiotics and antibiotic resistance genes in a sewage treatment plant and its effluent-receiving river. *Chemosphere* 119, 1379–1385.
<https://doi.org/10.1016/j.chemosphere.2014.02.040>
- Yang, Y.-Y., Toor, G.S., Wilson, P.C., Williams, C.F., 2017. Micropollutants in groundwater from septic systems: Transformations, transport mechanisms, and human health risk assessment. *Water Research* 123, 258–267. <https://doi.org/10.1016/j.watres.2017.06.054>
- Yang, Y.-Y., Toor, G.S., Wilson, P.C., Williams, C.F., 2016. Septic systems as hot-spots of pollutants in the environment: Fate and mass balance of micropollutants in septic drainfields. *Science of The Total Environment* 566–567, 1535–1544. <https://doi.org/10.1016/j.scitotenv.2016.06.043>
- Yebra, M.C., 2012. A Green Analytical Method Using Ultrasound in Sample Preparation for the Flow Injection Determination of Iron, Manganese, and Zinc in Soluble Solid Samples by Flame Atomic Absorption Spectrometry [WWW Document]. *Journal of Analytical Methods in Chemistry*. <https://doi.org/10.1155/2012/298217>
- Yilmaz, Arslan, S., 2009. GC–MS Determination of Atenolol Plasma Concentration after Derivatization with *N*-methyl-*N*-(trimethylsilyl)trifluoroacetamide. *Chroma* 70, 1399.
<https://doi.org/10.1365/s10337-009-1325-3>
- Yilmaz, B., Arslan, S., 2010. Development and Validation of GC-MS Method for Determination of Metoprolol in Human Urine. *Journal of Chromatographic Science* 48, 613–617.
<https://doi.org/10.1093/chromsci/48.8.613>

- Yilmaz, E., Soylak, M., 2020. Chapter 5 - Type of green solvents used in separation and preconcentration methods, in: Soylak, M., Yilmaz, E. (Eds.), *New Generation Green Solvents for Separation and Preconcentration of Organic and Inorganic Species*. Elsevier, pp. 207–266. <https://doi.org/10.1016/B978-0-12-818569-8.00005-X>
- Yu, Y., Wu, L., 2012. Analysis of endocrine disrupting compounds, pharmaceuticals and personal care products in sewage sludge by gas chromatography–mass spectrometry. *Talanta* 89, 258–263. <https://doi.org/10.1016/j.talanta.2011.12.023>
- Yu, Y., Wu, L., 2011. Comparison of four extraction methods for the analysis of pharmaceuticals in wastewater. *Journal of Chromatography A* 1218, 2483–2489. <https://doi.org/10.1016/j.chroma.2011.02.050>
- Zenker, A., Cicero, M.R., Prestinaci, F., Bottoni, P., Carere, M., 2014. Bioaccumulation and biomagnification potential of pharmaceuticals with a focus to the aquatic environment. *Journal of Environmental Management* 133, 378–387. <https://doi.org/10.1016/j.jenvman.2013.12.017>
- Zhang, M.-J., Chou, J., Sun, Z.-W., Zhao, J.-H., Guo, J., Yu, J.-Y., Gao, S.-Q., Tang, Y.-S., Liu, L.-Y., 2021. Gas chromatography/mass spectrometry analysis of organic acid profiles in human serum: A protocol of direct ultrasound-assisted derivatization. *Rapid Communications in Mass Spectrometry* 35, e9149. <https://doi.org/10.1002/rcm.9149>
- Zhang, X., Zhu, X., Wang, C., Zhang, H., Cai, Z., 2016. Non-targeted and targeted metabolomics approaches to diagnosing lung cancer and predicting patient prognosis. *Oncotarget* 7, 63437–63448. <https://doi.org/10.18632/oncotarget.11521>
- Zheng, W., Wiles, K.N., Holm, N., Deppe, N.A., Shipley, C.R., 2014. Uptake, Translocation, and Accumulation of Pharmaceutical and Hormone Contaminants in Vegetables, in: *Retention, Uptake, and Translocation of Agrochemicals in Plants*, ACS Symposium Series. American Chemical Society, pp. 167–181. <https://doi.org/10.1021/bk-2014-1171.ch009>
- Zimmerman, J.B., Anastas, P.T., 2015. Chemistry. Toward substitution with no regrets. *Science* 347, 1198–1199. <https://doi.org/10.1126/science.aaa0812>

-
- Zuin, V.G., Eilks, I., Elschami, M., Kümmerer, K., 2021. Education in green chemistry and in sustainable chemistry: perspectives towards sustainability. *Green Chem.* 23, 1594–1608. <https://doi.org/10.1039/D0GC03313H>
- Zuo, Y., Zhang, K., Lin, Y., 2007. Microwave-accelerated derivatization for the simultaneous gas chromatographic–mass spectrometric analysis of natural and synthetic estrogenic steroids. *Journal of Chromatography A* 1148, 211–218. <https://doi.org/10.1016/j.chroma.2007.03.037>